



**Maynooth  
University**

National University  
of Ireland Maynooth

# Exploring the Hydroclimatology of Floods: From Detection to Attribution

Shaun Harrigan BA, MSc

**Thesis Submitted for the Degree of Doctor of Philosophy**

Irish Climate Analysis and Research Units (*ICARUS*),  
Department of Geography,  
Maynooth University, National University of Ireland

May 2016

**Head of Department:**

Dr. Jan Rigby

**Research Supervisor:**

Dr. Conor Murphy

# Table of Contents

**Abstract**

**Acknowledgments**

**List of Figures**

**List of Tables**

<b>1</b>	<b>Introduction</b> .....	<b>1</b>
1.1	Background and rationale .....	1
1.2	Research gaps, aim and objectives.....	3
1.3	Thesis structure .....	5
<b>2</b>	<b>Literature Review and Research Gaps</b> .....	<b>7</b>
2.1	Introduction.....	7
2.2	Understanding the link between climate and floods.....	7
2.2.1	Changes in precipitation .....	8
2.2.2	Changes in floods .....	13
2.2.3	The hydroclimatic perspective.....	14
2.3	Climate variability and atmospheric circulation in the North Atlantic .....	19
2.3.1	Synoptic-scale atmospheric circulation patterns.....	20
2.3.2	Large-scale climate variability of atmospheric circulation .....	23
2.4	Hydroclimatological links: Approaches and evidence.....	25
2.5	Identification of research gaps.....	31
<b>3</b>	<b>Classification of Extreme Rainfall Regions</b> .....	<b>33</b>
3.1	Introduction.....	33
3.2	Precipitation data .....	36
3.2.1	Station selection.....	37
3.2.2	Data quality control.....	41
3.2.3	Infilling and bridging rainfall time-series .....	42
3.3	Methods .....	43
3.3.1	Extreme value theory and circular statistics.....	45
3.3.2	Variable selection.....	48

3.3.3	Principal component analysis and cluster analysis .....	52
3.4	Results .....	54
3.4.1	PCA results .....	54
3.4.2	Cluster analysis results .....	58
3.5	Climatology of extreme precipitation for final Extreme Rainfall Regions (ERRs) .....	62
3.6	Discussion .....	64
3.7	Chapter summary .....	66
<b>4</b>	<b>Detection of Spatio-temporal Changes in Extreme Precipitation and Floods .....</b>	<b>68</b>
4.1	Introduction.....	68
4.2	The Irish Reference Network (IRN) of streamflow stations .....	69
4.3	Extraction of extreme precipitation and flood indices .....	77
4.3.1	Extreme precipitation indices .....	79
4.3.2	Flood indices .....	80
4.4	Methods .....	87
4.4.1	Tests for change detection.....	88
4.4.2	Study design .....	92
4.5	Results .....	93
4.5.1	Fixed period trends .....	93
4.5.2	Temporal variability analysis.....	101
4.5.3	Persistence of trends .....	106
4.6	Discussion .....	106
4.7	Chapter summary .....	109
<b>5</b>	<b>Synoptic and Large-scale Climate Drivers of Floods .....</b>	<b>111</b>
5.1	Introduction.....	111
5.2	Hydroclimatic data .....	114
5.2.1	Flood indices .....	114
5.2.2	Weather type classifications .....	116
5.3	Methods .....	117

5.3.1	Flood classification .....	117
5.3.2	Annual and seasonal flood-index.....	120
5.3.3	Linkages with large-scale climate.....	120
5.4	Results .....	121
5.4.1	Expected frequency of LWTs.....	121
5.4.2	Flood occurrence by LWT and region .....	122
5.4.3	Reconstructed annual and seasonal flood occurrence.....	127
5.4.4	Large-scale climate links .....	134
5.5	Discussion .....	140
5.5.1	Objective 5.1: Which synoptic weather types are associated with floods at the annual and seasonal scale? .....	140
5.5.2	Objective 5.2: Reconstruction of flood occurrence for earlier periods..	142
5.5.3	Objective 5.3: Investigating relationships with large-scale climate drivers .....	143
5.6	Chapter summary .....	146
<b>6</b>	<b>Attribution of Detected Changes in Streamflow Using Multiple Working Hypotheses.....</b>	<b>148</b>
6.1	Introduction.....	148
6.2	Study area and hypotheses of hydrological change.....	152
6.2.1	The Boyne catchment .....	152
6.2.2	Overview of potential drivers of hydrological change.....	152
6.3	Data and Methods.....	159
6.3.1	Hydroclimatic data .....	159
6.3.2	Hydrological modelling .....	160
6.3.3	Trend and change point analysis .....	162
6.4	Results .....	164
6.4.1	Hydrological modelling .....	164
6.4.2	Trend and change point analysis .....	169
6.5	Discussion .....	172

6.5.1	Attribution of change in Boyne streamflow .....	172
6.5.2	Confidence in attribution .....	175
6.5.3	Towards more rigorous attribution .....	176
6.6	Chapter summary .....	177
<b>7</b>	<b>Discussion, Conclusions, and Future Work .....</b>	<b>179</b>
7.1	Introduction.....	179
7.2	Summary of main research findings.....	180
7.2.1	Thesis Objective 1: Extreme Rainfall Regions (Chapter 3).....	180
7.2.2	Thesis Objective 2: Detection of Spatio-temporal changes in extremes (Chapter 4) .....	180
7.2.3	Thesis Objective 3: Synoptic and Large-scale drivers of floods (Chapter 5) .....	182
7.2.4	Thesis Objective 4: Attribution of detected changes in streamflow (Chapter 6) .....	183
7.3	Synthesis of cross-cutting themes.....	184
7.3.1	The importance of observations.....	184
7.3.2	Scale considerations.....	186
7.3.3	From Detection to Attribution .....	188
7.4	Priorities for future work.....	189
7.4.1	Seasonal hydrological forecasting.....	189
7.4.2	Long-term projections of flood risk .....	191
7.5	Final Remarks .....	192
	<b>References</b>	<b>194</b>
	<b>Appendix I</b>	<b>217</b>
	<b>Appendix II</b>	<b>221</b>

## Abstract

Uncertainties in projected future flood risk and challenges of detecting signals of change from observations highlight the need to advance process understanding through linking hydrological extremes to large-scale climate drivers. In Ireland, recent years have highlighted vulnerability to flooding yet little research has been undertaken exploring hydroclimatic signatures of change in extremes at different scales, in part due to a lack of quality assured data for relevant variables. This is an important research gap given Ireland's sentinel position on the Atlantic margin of northwest Europe and is addressed within this thesis. The Island of Ireland (IoI) is classified into 3 Extreme Rainfall Regions (ERRs) reflecting distinct extreme precipitation climatologies, thus furthering understanding of physical flood-producing mechanisms. A comprehensive statistical trend analysis is performed on extreme precipitation and flood indices under a standard statistical framework. Results show a robust increasing trend in extreme precipitation magnitude, frequency, duration, and intensity. Similar results are found for flood indices at longer time-scales but limited station density prohibits stronger conclusions. Atmospheric drivers of flood occurrence are reconstructed back to 1872 using an objective weather classification scheme and used to identify four flood rich periods: 1.) 1870s to 1890s; 2.) late-1900s to mid-1930s, 3.) a short spell in the 1980s, and 4.) late-1990s onwards. The recent flood rich period is not unprecedented at the centennial time-scale. Moving towards attribution, the North Atlantic Oscillation (NAO) is found to modulate flood propensity, with strongest influence in the west and northwest. At the catchment scale the utility of an attribution framework based on the method of multiple working hypotheses is posited using the Boyne catchment as an exemplar. Results show the complexity of attributing hydroclimatic change at the catchment scale where the system is influenced by internal and external change. This work advances understanding of hydroclimatic flood processes and establishes new datasets that together will be important for better managing current and future flood risk and opens prospects for new management tools in Ireland, especially seasonal hydrological forecasting.

## Acknowledgments

First, I thank my PhD supervisor Dr. Conor Murphy for creating the opportunity for me to do research, long before this PhD. It's been an incredible journey and I thank you for your support and encouragement no matter what time of the day or night, especially in the final weeks of writing this PhD. I am truly grateful for the research mentorship of Prof. Rob Wilby. His expertise and discussion has been instrumental to all aspects of this work. I particularly appreciate his warm hosting of my visits to Loughborough which I gained so much from.

Thanks to Dr. Jan Rigby and Prof. Peter Thorne for making the department and ICARUS such a fantastic and supportive environment for postgraduates, this extends to Prof. John Sweeney too. I was always made feel like a colleague and your advice was critical for my career development. Special thanks to Peter for the weekly PhD comics digest that always lighted the mood!

Thanks also to Dr. Mari Tye for her discussion on classification of Extreme Rainfall Regions (Chapter3) and to Prof. Chris Brunsdon for advice on geostatistical techniques.

This research was funded by the Irish Research Council (IRC) under the 'Embark' scholarship.

To all my friends in ICARUS, past and present, for making the PhD experience enjoyable. The lunchtime topics of conversation were much to be desired days, but always a good laugh! Sharing ideas, skills, and discussing research with you greatly influenced this PhD.

To all my family and friends who always took my mind off research when needed. To Dad, my interest in trying to understand how the world works and seeing the bigger picture no matter how stressful things get is from you, and to Mum for always being at the other end of the phone making sure everything was grand - This PhD would not have been possible without your hard work which gave me the opportunity to go to university in the first place.

Emer, what can I say you have been there with me through it all and have grounded me at every stage. Your love and support gave me the strength to finish this but it is only the beginning of our exciting new journey.

## List of Figures

Figure 1.1: Schematic of thesis structure and chapters with arrows highlighting inter-relationships. MWH is the abbreviation for Multiple Working Hypotheses. ....	5
Figure 2.1: Definition of Flood Risk (Adapted from IPCC, 2012). ....	8
Figure 2.2: Hypothetical example of the importance of considering rainfall intensity when dealing with hydrological extremes in a warming climate. Stations A and B have the same monthly amount of rainfall, but intensity and frequency are very different (a.), Source: (Trenberth, 2011). Schematic of the sequence involved in how climate change is expected to alter atmospheric moisture content, evaporation, and precipitation (b.), Source: (Trenberth, 1998). ....	10
Figure 2.3: Fraction of total variance in decadal mean precipitation projections explained by internal natural climate variability (orange), model uncertainty (blue) and scenario uncertainty (green), for Global DJF mean (left) and British-Irish Isles DJF mean (right). Source: (Hawkins and Sutton, 2011; available at accompanying interactive website in which this figure was generated: <a href="http://climate.ncas.ac.uk/research/uncertainty/index.html">http://climate.ncas.ac.uk/research/uncertainty/index.html</a> .....	13
Figure 2.4: Summary of direction of changes in observed floods across Europe based on studies using different not directly comparable change analysis methods and time periods. Arrows represent directional majority from reviewed studies and blank areas with no/inconclusive studies due to insufficient data (e.g. Italy) and inconclusive change signal (e.g. Sweden), Source: (Hall et al., 2014). ....	15
Figure 2.5: Apparent linear trend in short time-series and (b.) decadal/multi-decadal periods of flood rich/poor episodes, Source: (Hall et al., 2014). ....	17
Figure 2.6: Annual number of peer-reviewed publications within the Web of Science database containing in the title 'climate' and 'flood*' between 1970-2015 (total = 661), last checked: (13/12/2015). ....	18
Figure 2.7: Drivers of flood risk change, dynamic flood risk, and dynamic flood risk management, Source: (Merz et al., 2014). ....	18
Figure 2.8: Spatial patterns of climate modes in Table 2.1. Adapted from Box 2.5 in Hartmann et al. (2013). ....	22
Figure 2.9: Composite integrated Total Column Water Vapor between 00:00 and 18:00 UTC 19 <sup>th</sup> November 2009 showing an atmospheric river associated with extreme precipitation that affected the November 2009 floods in Ireland (Cork and Galway) and the UK (Cumbria) (A.), and A general distribution of areas of AR occurrence (red contours) with land areas with reported cases of ARs linked to extreme precipitation and floods (white contours), Source: (Gimeno et al., 2014).....	28
Figure 3.1: UK Extreme Precipitation Regions identified from a principal component analysis of extreme precipitation measures by Jones et al. (2014a) with HadUKP (Alexander and Jones, 2001) regions inset. ....	35
Figure 3.2: Precipitation stations retained from automatic application of A-list criteria with most prominent clusters and gaps circled in blue and black, respectively. See Appendix I for details on stations added and removed. ....	38
Figure 3.3: Flow chart of semi-objective rules for removing (adding) stations from (to) clusters (gaps).....	39
Figure 3.4: Final station selection (94 A-List stations and 32 Gap stations from the B- & C-List). Station metadata in Appendix II. ....	39
Figure 3.5: Histograms of station details: a.) distance to nearest station (km), b.) elevation (m a. s. l.), c.) distance to coast (km), and d.) percentage of record missing for each of the 126 final precipitation stations. ....	40
Figure 3.6: Total precipitation (mm) per day of the week from 1973-2011. Boxplots summarise totals for each of the 126 final precipitation stations, with the red line representing the median, and boxes the interquartile range (IQR); whiskers extend to the most extreme data point, which is no more than 1.5 times the IQR from the box, and black circles are outliers beyond this range. ....	42
Figure 3.7: Diagram of methodological analysis: Step 1 selection of variables; Step 2 Selection of Principal Components (PCs) and conversation of rotated PCs to 5 km grids with kriging (PCg); Step 3 Cluster	

Analysis with just PC1 is C1 while PC1 and 2 is denoted C2; k = 2 to 5 are the number of clusters, and Step 4 is mapping results and examine the impact of methodological decision of final ERR delineation.	44
Figure 3.8: Schematic of calculation of timing variables, the mean timing of extreme precipitation events (red dots) is represented as the mean vector ( $\theta$ , $\theta_{\text{bar}}$ ) and the variability (i.e. the seasonality) as $r$ , $r_{\text{bar}}$ .	48
Figure 3.9: Scatterplot matrix for all 17 extreme rainfall variables.	51
Figure 3.10: Measures of extreme rainfall variables in set 2 for each of the 126 stations (excluding 'height' and 'coast'). Areas of low (< 100 m) medium (100-300 m) and high (300-1000 m) elevation are marked in white, light grey, and dark grey, respectively.	52
Figure 3.11: Scree plot of Principal Components (PCs) for the 11 variables in Set 2.	56
Figure 3.12: Loadings dot plots for the first 4 rotated PCs from Set 2.	57
Figure 3.13: Spatially interpolated (Kriging on 5 km grids) rotated PC scores for PCs 1-4 for set 2. PC1.) describes magnitude; PC2.) reflects differences in extreme distribution tail behaviour and variability; PC3.) proximity to the coast, and PC4.) seasonality, timing, and persistence of events.	58
Figure 3.14: Total k-means within cluster sum of squares (TWCSS) for Set 2 using rotated PCs 1- 4.	59
Figure 3.15: Scatterplot of clusters (k = 3) for set 2 using rotated PCs 1-4 (left: station based scores, right: gridded scores).	60
Figure 3.16: Sensitivity of selection of sets (rows) and rotated PCs 1-4 (columns) keeping number of clusters stationary (k-means with k = 3).	60
Figure 3.17: Maps of objectively identified homogeneous extreme rainfall regions for set 2 using PC1-4 and k from 2-5. Sensitivity of selection of number of clusters from k = 2 to 5 keeping PCs and Set stationary (all rotated PCs 1-4 used for Set = 2).	61
Figure 3.18: Final classification of Extreme Rainfall Regions (ERRs) with precipitation stations used for classification and Irish Reference Network (IRN) streamflow catchments that will be used in following chapters.	63
Figure 3.19: Variance of kriged estimates for rotated PC1 scores for Set 2 shown in Figure 3.13.	65
Figure 4.1: Maps of the 29 non-nested IRN catchments used in the analysis, 6 Physical Catchment Descriptors (PCDs), QMED-DMF, and RBMED.	74
Figure 4.2 Scatterplot matrix of 8 FSU/FEH PCDs, QMED based on DMFs, and RBMED using Spearman's Rho correlation.	76
Figure 4.3: Scatterplot of ALTBAR and RBMED ( $\rho = 0.81$ ). Catchments with areas < 650 km <sup>2</sup> and an average altitude > 150 m a. s. l. are highlighted in red.	76
Figure 4.4: Example of the plots generated for visual inspection of the POT procedure to ensure proper peaks were being extracted at an acceptably high threshold for the most (least) flashy catchments on the top (bottom). The red circles are the maximum independent peaks in each cluster, grey circles dependent peaks lower than the maximum but above the final threshold $T_i$ (shown in the grey dotted horizontal line), and black circles flow values below the threshold. Key statistics were also generated to aid interpretation and included in the legend in the top right of each plot (count is the number of iterations the algorithm needed to reach the target peak count). Note that the POT series for St27002 is actually a POT2.5 series (i.e. 80 peaks generated instead of 96).	86
Figure 4.5: Heatmaps of results from the Shapiro-Wilk test for normality (left) and the detrended ACF for positive lag-1 serial correlation (right) on all extreme precipitation (top) and flood (bottom) indices. Red (grey) values are (are not) statistically significant at the 5 % level.	91
Figure 4.6: Magnitude and direction of trends for short fixed period (1978-2009) for extreme precipitation indices. Blue triangles represent increasing trends and red decreasing trends, with magnitude proportional to size. Magnitude of frequency indices calculated from logistic regression odd ratios, while the rest are based on TSArel. Significant trends (5 % level) shown by white triangles and derived from the MK and logit tests.	96
Figure 4.7: As Figure 4.6 but for short period (1978-2009) for flood indices with catchment boundaries plotted in yellow.	97
Figure 4.8: As Figure 4.6 but for long period (1956-2009) for extreme precipitation.	100

Figure 4.9: As Figure 4.6 but for the long period (1956-2009) for flood indices with catchment boundaries plotted in yellow. ....	101
Figure 4.10: Standardised and LOESS smoothed extreme precipitation indices for all 94 A-list stations. Light grey lines are individual stations, solid red lines are the 5 <sup>th</sup> and 95 <sup>th</sup> percentiles across all stations, solid black line the mean, and blue lines the regional mean per ERR (Colours as Fig. 3.18). Grey vertical lines represent the start date of short and long set period. Note data for longer stations extend to water year 1942 and all series end in 2009. ....	102
Figure 4.11: As in Figure 4.10 but for flood indices. Exception is too few time-series pre-1956 to calculate mean and 5 <sup>th</sup> and 9 <sup>th</sup> percentiles and ERR-SW is only represented by one catchment so merged into ERR-CU for calculation of regional mean as described in Chapter 5. ....	103
Figure 4.12: Persistence plots for full available time-series of extreme precipitation indices end in water year 2009. Blue lines represent MKZs statistics for varying start years for individual stations across lol with shade of blue per ERR (Colour as in Fig. 3.18). Dashed red lines are the threshold for statistically significant trends at the 5 % level with MKZs above (below) these indicating significant increasing (decreasing) trends since the corresponding start date. The vertical grey lines mark the start year of fixed periods. ....	104
Figure 4.13: As in 4.12 but for flood indices. Exception is ERR-SW is only represented by one catchment so this is given same colour as ERR-CU as described in Chapter 5. ....	105
Figure 5.1: Histogram of percentage of POT3 events that occur during the summer half year between water years 1978-2009. ....	115
Figure 5.2: Map of contribution of summer floods per IRN station. Larger (smaller) circles represent greater (lesser) contribution to total POT3 events from the summer half year. The flashiness of each catchment is also mapped using RBMED. ....	115
Figure 5.3: Expected frequencies of each of the 27 Lamb Weather Types (LWTs) between Water Years (WY) 1978-2009, for annual (grey bars), winter (October to March; blue bars), and summer (April to September; red bars). ....	121
Figure 5.4: Comparison between 'day 0' and '3 day centred' methods for classifying flood-producing LWTs for (a.) annual, (b.) winter half year, and (c.) summer half year based on percentage of associated POT3 floods over the water year 1978-2009 period. ....	123
Figure 5.5: Flood loadings for each LWT and ERR for a.) annual, b.) winter half year, and c.) summer half year. Black lines are average flood loadings for the Island of Ireland (lol), dark blue Coastal & Upland ERR (CU), and light blue Inland & East ERR (IE). Grey lines are flood loadings for individual stations and dashed red line represents when a LWT has a loading equal to the expected frequency (i.e. flood loading = 1); values above (below) are flood rich (poor). ....	125
Figure 5.6: Spatial distribution of flood loadings for individual catchments for the top 5 LWTs associated with 75 % of POT3 floods. Circles increase (decrease) in size for catchments with greater (lower) flood loadings. Catchments are coloured according to RBMED (as in Fig. 4.1). ....	126
Figure 5.7: Mean Sea Level Pressure (MSLP) fields (in hPa) at 12:00 UTC from ERA-Interim reanalysis at 0.75° × 0.75° resolution on the day before, day of (08/01/2005), and day after the most widespread flooding across the Island of Ireland (almost 80 % of catchments). ....	128
Figure 5.8: Total Column Water (TCW) fields (in kg m <sup>-2</sup> ) at 12:00 UTC from ERA-Interim reanalysis at 0.75° × 0.75° resolution on the day before, day of (08/01/2005), and day after the most widespread flooding across the Island of Ireland (almost 80 % of catchments). ....	129
Figure 5.9: Annual (a.), winter (b.), and summer (c.) relationships between F-index and average number of observed POTs per active station per year. Open circles show data used during calibration (1978-2009) with solid circles during evaluation (1956-1977). ....	131
Figure 5.10: Annual F-Index using annual 1978-2009 flood loadings for ERR-IE (top), ERR-CU (middle), and lol (bottom) applied to yearly LWT frequencies from 1872-2015 (water years), forming a 144-year flood reconstruction (black line). The F-Index has been standardised by its long-term mean and standard deviation. Red line is LOESS smoothed with a span = 15 years. Values above (below) 0 are rich (poor) with +/- 1 standard deviation as dashed grey line. ....	132
Figure 5.11: As for Figure 5.10 but for the winter half year. ....	133

Figure 5.12: As for Figure 5.10 but for the summer half year. ....	134
Figure 5.13: Correlations between DJF NAO and flood indices over water years 1978-2009. Size of positive (blue triangles) and negative (red triangles) correlations are shown according to strength ( $Rho$ is the Pearson correlation $\rho$ ) with statistically significant correlations (at the 5 % level) as inner white triangles. ....	136
Figure 5.14: Pearson correlations between synoptic (LWT variables), large-scale climate indices (NAO and AMO), and annual (AFI) and winter (WHFI) F-Index variables (a.). The same time-series are Loess smoothed with 15 year span in (b.). Blue (red) represents positive (negative) correlations with those statistically significant and the 5 % level denoted with a star. All variables are for the winter half year except for NAO* (DJF) and AFI* (Oct to Sep). ....	138
Figure 5.15: Detrended and smoothed (DS) winter half year NAO and detrended, standardised, and smoothed (DSS) W- and SW-type frequency (a.). Smoothed AMO (already detrended) with units °C, DS winter half year NAO, and DSS A- and C-type frequency (b). Linear detrending was performed with trend estimated using the Theil-Sen Approach (Section 4.4.1), standardisation by long-term mean and standard deviation, and smoothing by Loess with span = 15 years. All series cover water years 1872-2015. ....	139
Figure 6.1: Observed annual mean flows in the Boyne for 1941-1995. Solid red line is the median of the period before and after the 1978 change point detected by Kiely (1999). ....	151
Figure 6.2: Boyne catchment showing major urban areas, streamflow and precipitation stations. ....	153
Figure 6.3: Number of major watercourses per year in which arterial drainage was completed in the Boyne. The cumulative length (km) completed is shown by the red line. ....	157
Figure 6.4: Objective functions (a) NSE, (b) PBIAS and (c) MAE for HYSIM, HyMOD and NAM for calibration (Cal: 1952-1959), evaluation (Eval: 1960-1969) and post 1970 (Post70: 1970-2009) periods. Each bar represents the median score for behavioural simulations with error bars giving the maximum and minimum range. ....	165
Figure 6.5: Annual (a) mean and (b) cumulative volume of reconstructed and observed flow for 1952-2009. The period of drainage works is shown by the shaded grey area. Behavioural simulations for each model structure are colour coded. ....	166
Figure 6.6: Monthly (left) mean and (right) cumulative volume of reconstructed and observed flow for 1952-2009 for the summer half year (April to September). Colour code as in Fig. 6.5. ....	167
Figure 6.7: As in Fig. 6.6 but for the winter half year (October to March). ....	168
Figure 6.8: Mann-Kendall tests for monotonic trend in precipitation and flow indicators. MKZs values above (below) 5% significance line ( $ MKZs  > 1.96$ ) indicate significant increasing (decreasing) trends. Boxplots summarise MKZs values for 328 reconstructed time-series with the black line representing the median, box the interquartile range (IQR), whiskers extend to the most extreme data point which is no more than 1.5 times the IQR from the box, and grey circles are outliers beyond this range. ....	170
Figure 6.9: Pettitt test for change points in selected indicators. Solid red lines represent the threshold for significant change points at the 5 % level with p-values below (above) indicating a significant (non-significant) change point for corresponding year of change on the x-axis. ....	172
Figure 6.10: Observed and median of 328 reconstructed series for March mean flow. Solid red line is the observed median flow before (1952-1975) and after (1976-2009) the detected change point; dash red is the reconstructed median flow for the same periods. ....	174

## List of Tables

Table 2.1: Established indices of climate variability with regional surface climate impacts. Adapted from IPCC AR5 chapters 3 (Hartmann et al., 2013) and 14 (Christensen et al., 2013). .....	21
Table 2.2: Selection of papers assessing hydroclimatological links considering the British-Irish Isles in the past decade. ....	29
Table 3.1: Number of precipitation stations retained after applying criteria on data period, record length, and completeness. ....	37
Table 3.2: Pool of 17 precipitation variables used in PCA. Variables 1-15 were calculated between calendar years 1973-2011. ....	49
Table 3.3: Selection of 3 sets of extreme rainfall variables: Set 1 (Full 17), Set 2 (Redundancy removed), and Set 3 (Minimum number, i.e. 1 per category). ....	51
Table 3.4: Unrotated and rotated loadings for the first 4 Principal Components (PCs) for each of the 11 variables in Set 2. Proportion of variance of the entire dataset explained by each PC is given in italics and variables with greatest loading in bold. Loading values < 0.1 are left blank to aid interpretability. ....	56
Table 3.5: Statistics of 5 precipitation characteristics for each of the 3 ERRs. Central tendency is given by the median with an estimate of the range given by the lower and upper quartiles in brackets. Units as Table 3.2. ....	64
Table 4.1: Station details with flood relevant Physical Catchment Descriptors (PCDs) for 29 IRN catchments. ....	72
Table 4.2: Extreme precipitation (Core ETCCDI precipitation indices) and flood indices used in assessment of trends. ....	82
Table 4.3: Direction of change and proportion of statistically significant (5 % level) trends for short fixed period (1978-2009) extreme precipitation indices. Direction and significance tested using Mann-Kendall (MKZs) and magnitude tested with the relative Theil-Sen Approach ( $TSA_{rel}$ ). Logistic regression Odds Ratios (OR) used for both magnitude and significance of frequency indices. Magnitude of change is based on the median of the test statistics with spread (+/- bounds) given by interquartile range. ....	95
Table 4.4: As in Table 4.3 but for flood indices. ....	95
Table 4.5: As in Table 4.3 but for long fixed period (1956-2009) for extreme precipitation indices. ....	99
Table 4.6: As in Table 4.3 but for long fixed period (1956-2009) for flood indices. ....	99
Table 5.1: Top 10 floods with largest spatial extent (% catchments from $n = 29$ ) from stations reporting a POT3 flood within a 3 day window. 'Date' is the date of the centre day where in most cases the majority of floods were recorded. LWT and G are the Lamb Weather Type and G-index associated with floods over each 3 day window. Bold are very severe gales ( $G > 50$ ), underlined are severe gales ( $G > 40$ ), and Italics are gales ( $G > 30$ ). ....	127
Table 5.2: Flood Index evaluation and calibration based on Pearson correlation. Bold are statistically significant at the 5 % level with a null hypothesis of $\rho = 0$ . ....	130
Table 6.1: Working hypotheses (WHs) for drivers of change in the Boyne catchment. The table provides an overview of potential influence of each WH and a preliminary assessment and justification for inclusion/exclusion in further investigation (Roman = not analysed further; Italic = not analysed further but justification based on limited evidence; Bold = Warrants further investigation). ....	155
Table 6.2: Stations and correction factors used to obtain catchment average precipitation. ....	160

# 1 Introduction

---

## 1.1 Background and rationale

Floods are one of most costly natural hazards in terms of socio-economic impacts across the globe. This has been particularly the case in Ireland in the past decade. The November 2009 flood that affected mainly Cork and Galway in Ireland (and Cumbria in the UK) broke hydrological and meteorological records. The estimated maximum 24 hr precipitation return period was 1 in 480 years for a gauge in the Lake District in the UK, while the same gauge at the time of writing this introduction (6<sup>th</sup> December 2015) recorded an even more severe event estimated at a return period of 1300 years due to storm “Desmond” passing over the British-Irish Isles on the 4<sup>th</sup> and 5<sup>th</sup> of December 2015 (CEH, 2015). This led to devastating floods in Ireland and the UK in the same areas affected just 6 years previously. This therefore poses the question whether this recent cluster of floods is purely random chance, or are underlying drivers changing the probability of occurrence of these events (e.g., van Oldenborgh et al., 2015, submitted)?

It is expected that anthropogenic climate change will intensify the hydrological cycle as the world continues to warm as basic thermodynamics tells us that a warmer atmosphere can hold more moisture (IPCC, 2013). Evidence shows this will lead to increased frequency and magnitude of extremes, such as heavy precipitation (Groisman et al., 1999), floods (Milly et al., 2002), and droughts (Prudhomme et al., 2014). However, there is much uncertainty in projections of future flood risk with the most recent comprehensive assessment stating “there continues to be a lack of evidence and thus low confidence regarding the sign of trend in the magnitude and/or frequency of floods on a global scale” (Hartmann et al., 2013: pp 214). This poses a great challenge for climate change adaptation and flood risk management.

In an attempt to reconcile this apparent mismatch, Merz et al. (2014) offers some perspective moving forward. They argue that flood research has traditionally taken too narrow a view; floods are often perceived as random local events occurring within a stationary climate system. Instead, a much broader inter-disciplinary approach is

needed that brings together the fields of hydrology and climatology – the concept of hydroclimatology. Recent advancements have shown that at the global scale flood risk is modulated by natural large-scale climate drivers, such the El Niño-Southern Oscillation (ENSO) (Ward et al., 2014), and may have a much more dominant influence than climate change, at least for the near-term.

The most important mode of natural climate variability in the vicinity of the British-Irish Isles is the North Atlantic Oscillation (NAO). The NAO has been linked with increased mean and extreme precipitation (Kiely, 1999; Leahy and Kiely, 2011), and mean streamflow (Kiely, 1999; Murphy et al., 2013a) in Ireland, but few studies have yet to assess the role of the NAO in modulating high flows and floods. Furthermore, there is a dearth of research on assessment of extreme precipitation in Ireland, and virtually no study on hydroclimatic extremes considers both Ireland and Northern Ireland together. A major barrier to progress in this area has been the limited availability of observed precipitation and streamflow datasets at the appropriate spatio-temporal resolution for detection of climate-driven variability and change.

*Detection* is defined by the IPCC (2013) as demonstrating that changes in a system's behaviour are *statistically significant* beyond what can be explained by internal (natural) variability alone. Statistical detection of change is by far the most common approach taken by previous research when evaluating whether or not climate change has affected the hydrological cycle. However, in the field of hydroclimatology there is a growing body of literature that promotes caution when interpreting results from detection only studies. For example, Wilby (2006) demonstrates that the climate change signal is relatively weak compared to natural variability thus requiring very large magnitudes of change in streamflow (often > 50 %) in order to become statistically detectable. Moreover, even when a robust change is detected it is a non-trivial task to establish the most likely driver(s) of change. This is because streamflow is the integrated response to all drivers, climate and internal, natural and human induced, and so separating the response of each component is challenging. The process of determining the *relative contribution of multiple factors* that may be responsible for detected changes, and *assigning a level of confidence* is the domain of *Attribution* (IPCC, 2013). However, Merz et al. (2012) argue that given the complex interplay of climate variability and change, individual catchment characteristics, and

confounding impacts of human disturbances within catchments (such as urbanisation, dam regulation, and river engineering), more effort and scientific rigour are needed to attribute trends in flood time-series.

This thesis focuses on advancing understanding of drivers of changes in floods on the Island of Ireland from a hydroclimatic perspective. There are many gaps in knowledge on *how* (detection) and *why* (attribution) floods have changed within observations, and thus a better understanding of the physical flood-producing processes will reduce uncertainty in both climate and hydrological models, and critically, will provide more observational evidence. Given the immense socio-economic impacts of flooding it is imperative that a fuller scientific understanding of extreme precipitation and floods is achieved so that this knowledge can be exploited for improved management of flood risk in future.

## 1.2 Research gaps, aim and objectives

A more detailed literature review on the above topics was undertaken in Chapter 2 and the following 4 key **gaps in knowledge** were identified in Section 2.5:

- **Research Gap 1:** Lack of basic data for assessment of extremes at appropriate spatio-temporal variability on the Island of Ireland and hence fundamental understanding of extreme precipitation climatology is limited.
- **Research Gap 2:** Few studies internationally examine spatio-temporal patterns of change in a range of characteristics (e.g. frequency and magnitude) in both extreme precipitation and flood indices under a standard statistical framework. Further, even fewer use streamflow data that can be considered limited from the influence of artificial catchment disturbances and be used for purposes of detection of climate variability and change over decadal time-scales. The lack of a flood Peaks-Over-Threshold database is also identified as a major data gap impeding progress.
- **Research Gap 3:** Understanding drivers of floods from a hydroclimatic perspective, that is, exploring the underlying climatological drivers of floods at large spatial scales (e.g. synoptic to hemispheric) and long temporal scales (centennial scale) has not been undertaken for the Island of Ireland before, and

thus remains a significant research gap in a sentinel location on the Atlantic fringe of Europe.

- **Research Gap 4:** Attribution of hydrological change at the catchment scale, where ultimately decision making and management takes place, has been identified internationally as one of the grand challenges of hydrology due to the many competing influences on streamflow from human disturbance to climate variability and change. A more scientifically rigorous approach to attribution is needed whereby the influence of many plausible drivers is considered.

In light of these research gaps, the overarching **aim** of this thesis is to explore spatio-temporal changes in physical flood hazard on the Island of Ireland taking a hydroclimatic perspective to better understand *how* (detection) and *why* (attribution) floods have changed over multi-decadal time-scales. These research gaps are addressed with 4 main **thesis objectives**:

- **Thesis Objective 1:** Classify extreme rainfall regions for the Island of Ireland to explore the fundamental climatology of extreme precipitation (Chapter 3).
- **Thesis Objective 2:** Assess spatio-temporal changes in extreme precipitation and floods for a number of characteristics (Chapter 4).
- **Thesis Objective 3:** Explore the relationship between large-scale atmospheric circulation and variability and change in floods (Chapter 5).
- **Thesis Objective 4:** Advance approaches in attributing drivers of change at the catchment scale by considering both external and internal drivers of change under a multiple working hypotheses framework (Chapter 6).

These objectives could only be undertaken once 2 key **thesis data objectives** were completed:

- **Thesis Data Objective 1:** Establish a network of station-based precipitation observations appropriate for the analysis of extreme precipitation (Chapter 3).
- **Thesis Data Objective 2:** Extract a flood Peaks-Over-Threshold database from near natural catchments for the Island of Ireland appropriate for the analysis of changes in flood frequency (Chapter 4).

### 1.3 Thesis structure

These 4 thesis objectives each relate to one of the core thesis analysis chapters (Fig. 1.1) and in themselves have more specific **chapter objectives** or **chapter research questions** outlined in their respective introduction section. Chapter 2 provides a literature review that sets the context for the entire thesis as well as identifying the above research gaps (Section 1.4 and Section 2.5). The extreme precipitation dataset and classification of Extreme Rainfall Regions are presented in Chapter 3. Chapter 4 examines extreme precipitation and flood indices for evidence of climate-driven change, after derivation of a new Peaks-Over-Threshold (POT) database (Section 4.3.2.1). The synoptic and large-scale climate drivers of floods are explored in Chapter 5, with a more rigorous attribution of detected changes, taking both climate and internal drivers into account, demonstrated for the Boyne catchment in Chapter 6. Finally, Chapter 7 discusses the main research findings before offering two key priorities for future work.

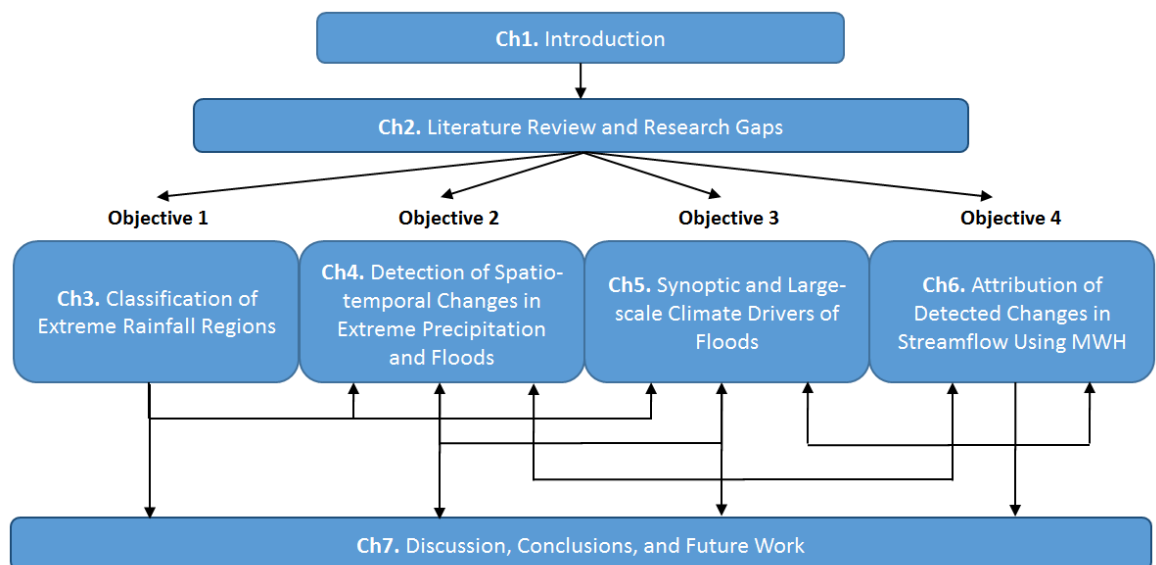


**Figure 1.1: Schematic of thesis structure and chapters with arrows highlighting inter-relationships. MWH is the abbreviation for Multiple Working Hypotheses.**

During the course of this 3 year PhD project I was involved in the following peer-reviewed publications to varying degrees. Many of the ideas and components of this PhD stemmed from these and collaboration with co-authors:

- Murphy et al. (2013a) and Murphy et al. (2013b): I was 1 of 2 research assistants on the '*HydroDetect*' project that developed the Irish Reference Network (IRN) of streamflow stations which is heavily used in Chapters 4 and 5.
- Merz et al. (2014): This large team paper was initiated from the EGU topical meeting "Floods and Climate: Understanding and exploiting the link between floods and climate" in October 2012 in Potsdam. I contributed to ideas throughout and writing of minor sections of the manuscript. Perspectives from this paper (set out in Chapter 2) are exercised throughout this thesis.
- Harrigan et al. (2014): This is a direct product from this thesis and is published as Chapter 6.
- Matthews et al. (2015): I was involved in discussion of ideas and writing of the paper. Many of the results of this paper are used throughout for aiding interpretation of findings here (closely connected to Chapter 5).
- Wilby et al. (2015): I was involved in discussion of ideas and writing of the paper. Potential links between atmospheric drivers of floods *and* droughts were highlighted in Section 7.4.1 as an interesting avenue for future work.

## 2 Literature Review and Research Gaps

---

### 2.1 Introduction

This chapter places relevant literature in context and identifies key research gaps which this research aims to address. First, justification for studying climate-flood links is put forward before a review of literature exploring hydroclimatic links is undertaken to establish (i) the advantages and disadvantages of different approaches of linking climate and floods and (ii) the current strength of evidence on the links between climate and floods. The literature reviewed is necessarily selective given that the topic of flood hydroclimatology encompasses broad fields of hydrology, climatology and atmospheric science, and is strongly regionally dependent. Hence, this literature review is not limited to but focuses primarily on:

- **Literature:** Recent advancements in hydroclimatic links (past ~10 years)
- **Spatial domain:** North Atlantic and vicinity of the British-Irish Isles (BI)
- **Variables:** High flows, floods, and extreme precipitation

Section 2.2 discusses literature on the connection between climate and floods; Section 2.3 outlines important modes of large-scale climate variability in the North Atlantic; Section 2.4 reviews previous research on hydroclimatological links before key research gaps are identified in Section 2.5.

### 2.2 Understanding the link between climate and floods

Flooding is one of the most costly natural hazards in the world to both economy and society and has been a prominent feature in Ireland recently as introduced in Chapter 1. Therefore, in order to reduce their impact, flood risk must be managed through planning, policy, and insurance measures. Flood risk is defined here as the interaction of hazard (probability and intensity of flooding), exposure (elements at risk e.g., people and their assets), and vulnerability (susceptibility or propensity of elements at risk to be adversely affected) (IPCC, 2012 (Special Report on Extreme Events (SREX)); UNISDR, 2013). This framework is outlined in Figure 2.1. While acknowledging that overall flood risk will change if any one of the three components change, and therefore an overall assessment of flood risk must consider them together, this thesis is concerned with the

change in physical flood hazard and the driving climatic and hydrological mechanisms only.

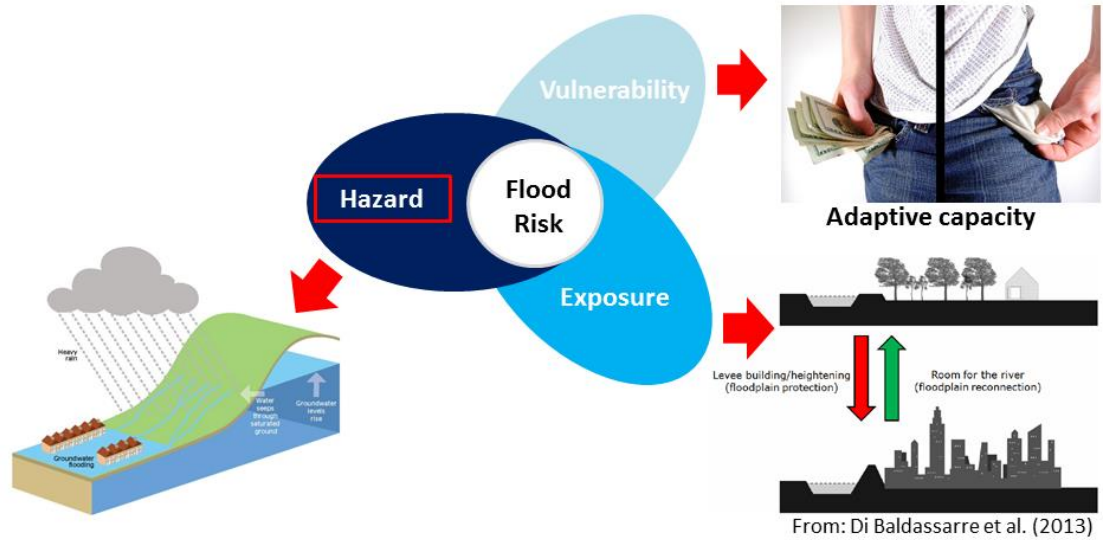


**Figure 2.1: Definition of Flood Risk (Adapted from IPCC, 2012).**

Anthropogenic greenhouse gas induced climate change is expected to intensify the hydrological cycle (Huntington, 2006), leading to increased frequency and magnitude of extremes, such as heavy precipitation (Groisman et al., 1999), floods (Milly et al., 2002), and droughts (Prudhomme et al., 2014). This physical relationship can be explained theoretically by the Clausius-Clapeyron (CC) relationship that shows an almost exponential increase in water vapour concentration with increasing atmospheric temperature at about 6-7 % K<sup>-1</sup> near the surface (Hegerl et al., 2015). However, the chain of causality from increased atmospheric temperature to water vapour concentration, to rainfall and floods is not straightforward and many considerations are needed as outlined below.

### 2.2.1 Changes in precipitation

Global mean precipitation is increasing at a rate of 2-3 % K<sup>-1</sup> (Hegerl et al., 2015), but this is not uniform across the planet. It has been summarised that rainfall is increasing at latitudes and seasons that currently have high rainfall and decreasing in dry regions (Collins et al., 2013). This is known as the 'wet get wetter, dry get drier' paradigm (Chou et al., 2009). However, it is vital to distinguish between changes over the ocean

and land. Enhancement of Precipitation minus Evaporation (P-E), the net water flux into the surface, has been observed over the ocean (e.g., Held and Soden, 2006), and confirmed independently from examination of changes in salinity (Durack et al., 2012). Over land (where moisture is limited), this simplifying summary has been challenged. Greve et al. (2014) show that between 1948 and 1968 only ~ 10 % of the land area confirms the 'wet get wetter, dry get drier' paradigm. Using a CMIP5-based assessment of projected changes in 21<sup>st</sup> century mean annual P-E, Greve and Seneviratne (2015) found ~ 70 % of all land areas will not experience significant changes.

The relationship between warmer atmospheric temperature and increased intensity of precipitation is more robust for extremes (i.e., precipitation occurring within an extratropical cyclone or convective system). According to Trenberth et al. (2003), as these storms are fuelled mostly by low-level moisture convergence, precipitation rates when it rains (precipitation intensity) should increase by about the same rate as the moisture increase (6-7 % K<sup>-1</sup> with warming). Additionally, feedbacks of additional latent heat release are expected to further intensify storms, particularly convective events, though this will be most notable in sub-daily precipitation extremes (Westra et al., 2014). For example, around 70 % of the moisture in an extratropical cyclone comes from moisture already in the atmosphere at the start of the storm, while the rest comes from surface evaporation (Trenberth, 1998). This implies there must be a decrease in light and moderate rains, and/or a decrease in the frequency of rain events which leads to the prospect of fewer but more intense precipitation events (see Figure 2.2a). Essentially, more intense precipitation leads to more floods, while longer dry periods between precipitation events leads to more droughts (Collins et al., 2013). It is this physical understanding of how precipitation *characteristics* are likely to change in a warming world (see Figure 2.2b for a conceptual summary), rather than just total amounts or averages, that is imperative for assessing hydrological extremes of floods and droughts.

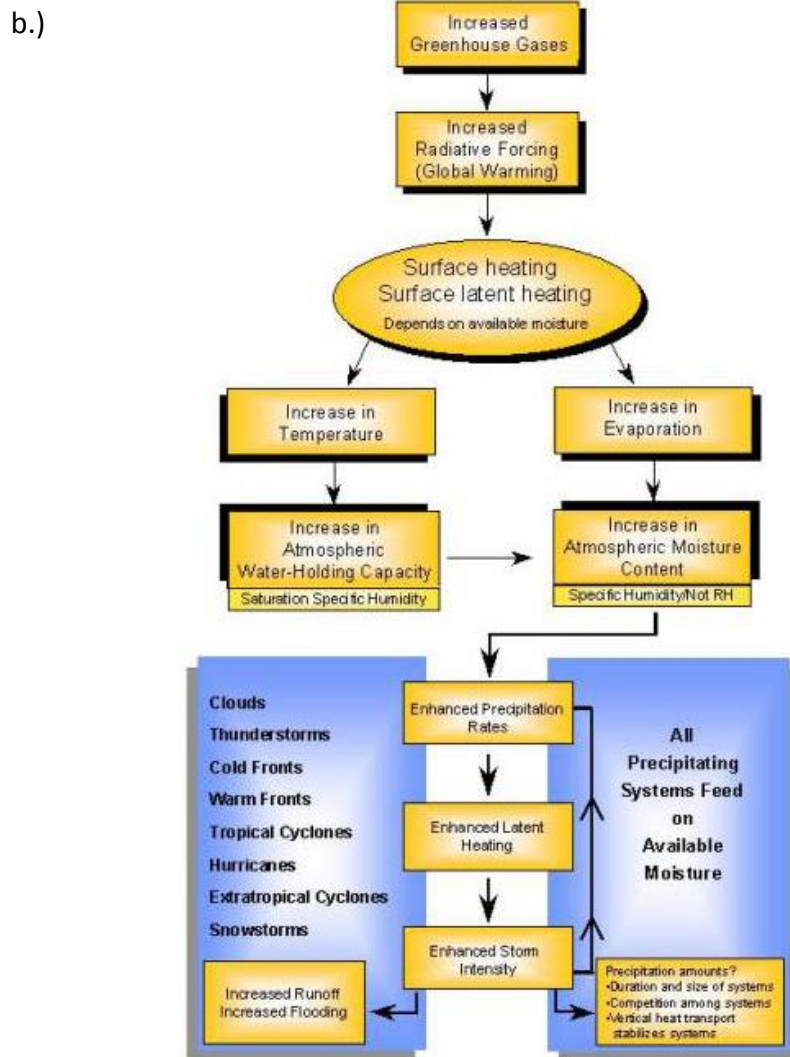
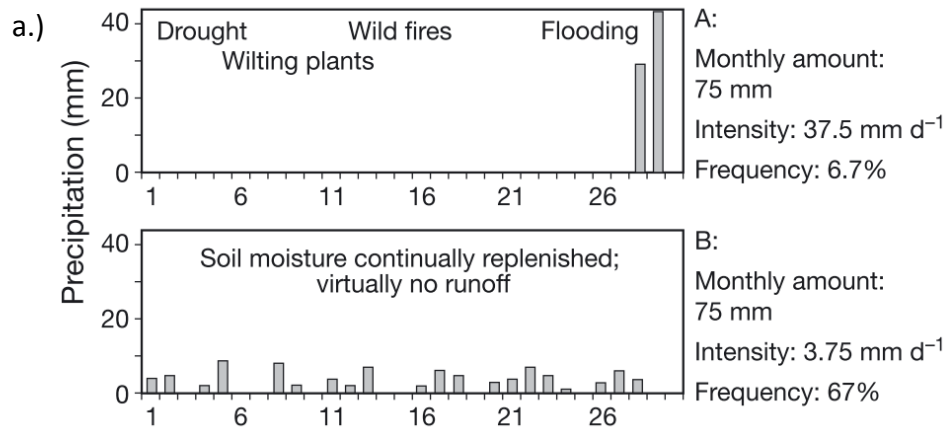


Figure 2.2: Hypothetical example of the importance of considering rainfall intensity when dealing with hydrological extremes in a warming climate. Stations A and B have the same monthly amount of rainfall, but intensity and frequency are very different (a.), Source: (Trenberth, 2011). Schematic of the sequence involved in how climate change is expected to alter atmospheric moisture content, evaporation, and precipitation (b.), Source: (Trenberth, 1998).

Projected 21<sup>st</sup> Century changes in extreme precipitation are more robust than mean changes for some regions (Fischer et al., 2013), again due to the fact that increases in atmospheric water vapour are expected to increase the intensity of individual precipitation events, but have less impact on their frequency (Collins et al., 2013). This is particularly the case in higher latitudes where a warmer climate allows storm systems in the extratropics to transport more water vapour poleward, without requiring large changes in wind strength. This has contributed to the IPCC in both the SREX (Seneviratne et al., 2012) and AR5 (Collins et al., 2013) to conclude a very likely (90-100 % probability) increase in the intensity and frequency in heavy precipitation in particular in the high latitudes and tropical regions, and in winter in the northern mid-latitudes, with high confidence by the end of the century (see IPCC, 2012; SREX Box SPM.2 for description of uncertainty language used in IPCC reports).

Despite this robust finding, precipitation is notoriously more difficult to model than temperature due to its high spatial variability and the fact that the current generation of Global Climate Models (GCMs) and Regional Climate Models (RCMs) have typical grid resolutions of between 60-300 km and 10-50 km, respectively, and thus need to parameterise key rainfall generating processes such as convection (Kendon et al., 2014). While convective-permitting models (~1 km grid resolution), as used for short-duration weather forecasting, have been used for long-term climate change projections (e.g. Kendon et al., 2014), these simulations are largely experimental. Therefore, it remains imperative that observations are used for the basis of evidence of changing extreme precipitation.

Observed evidence for the theory of increasing precipitation extremes at the CC rate has been shown by Westra et al. (2013) in a global analysis of annual maximum daily precipitation time-series (RX1day) from 8326 land-based stations with more than 30 years of record over the period 1900-2010. Statistically significant increasing trends were detected (at the 5 % level) at the global scale with mean intensity of extreme precipitation increasing in line with global mean near-surface temperature at a rate of between 5.9 % and 7.7 % K<sup>-1</sup>. However, while this study uses the most comprehensive and high-quality global dataset for precipitation extremes available (HadEX2; Donat et al., 2013), there is a very uneven distribution of stations with North America and Europe dominating coverage. While such large-scale studies are necessary to get a

global picture of changing precipitation extremes, little understanding of regional and local changes is gained, which is imperative for assessments of impacts.

At the scale the British-Irish Isles (BI), many studies have also identified increases in observed precipitation extremes. Osborn et al. (2000) found an intensification of daily precipitation in the UK in winter with a decrease in summer over the period 1961-1995, highlighting a decline in light and medium events and an increase in the heaviest events. Maraun et al. (2008) extended this analysis both temporally by updating time-series to 2006, and spatially by increasing the number of stations used from 110 to 689, and find consistent results. Using a regional frequency analysis approach, Fowler and Kilsby (2003) found that multi-day, prolonged heavy rainfall events increased, but are confined to the northern and western parts of the UK. An updated study by Jones et al. (2013a) found that extreme precipitation events having a 1 % probability of occurrence increased to 10 % in some parts of Scotland, but highlighted evidence of oscillations likely driven by natural climate variability in their estimates. In Ireland, 75 % of the extreme rainfall events (ranked 20 events) between 1940-1996, occurred in the more recent (post-1975) period (Kiely, 1999). Again, this finding was supported by Leahy and Kiely (2011) with an additional 10 years of data. However, there was no clear spatial pattern as only 13 precipitation stations were used.

Many of the above studies highlight the importance of considering natural climate variability when interpreting trends in extreme precipitation time-series. This is because multi-annual/decadal features, as a result of natural variability generated within the climate system, are difficult to separate from the long-term climate change forcing and often dominate the signal in shorter time-series (Hegerl et al., 2015). The role of natural climate variability has been shown to be a limiting factor in climate predictability (Deser et al., 2012), but the amplitude of variability varies considerably across the globe. For example, in Figure 2.3 for winter mean precipitation (after Hawkins and Sutton, 2011), the degree of natural variability at smaller scales such as the British-Irish Isles (right panel) is much greater than for the global scale (left panel). Although changes in extreme precipitation are more robustly detectable than mean precipitation due to a higher signal-to-noise ratio (Hegerl et al., 2004), the importance of recognising the high degree of natural variability at regional scales still prevails.

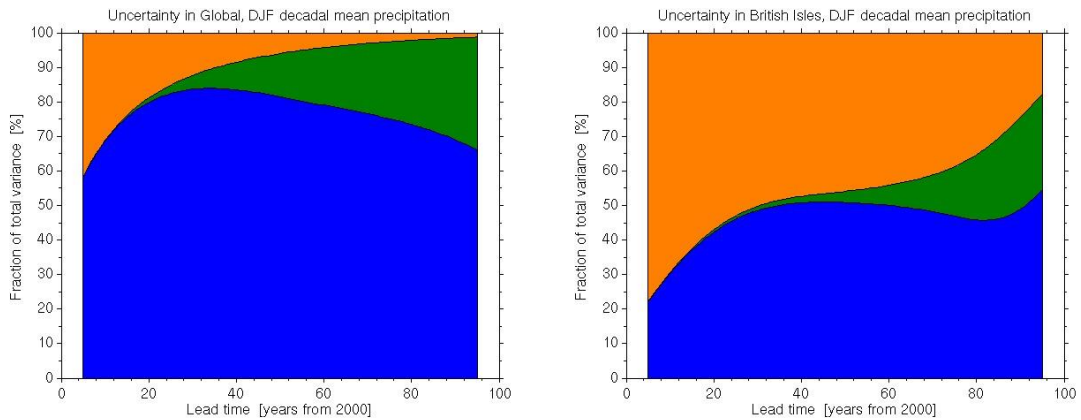


**Figure 2.3: Fraction of total variance in decadal mean precipitation projections explained by internal natural climate variability (orange), model uncertainty (blue) and scenario uncertainty (green), for Global DJF mean (left) and British-Irish Isles DJF mean (right). Source: (Hawkins and Sutton, 2011; available at accompanying interactive website in which this figure was generated: <http://climate.ncas.ac.uk/research/uncertainty/index.html>).**

### 2.2.2 Changes in floods

It is reasonable to assume that enhanced extreme precipitation would increase flood hazard. Indeed, state-of-the-art projections of future flood risk by Hirabayashi et al. (2013) show a large increase in flood frequency (i.e., the return period of the 100-year flood decreases) across large areas of South Asia, Southeast Asia, Northeast Eurasia, eastern and low-latitude Africa, and South America using 11 of the GCMs that participated in CMIP5 forced by the most extreme Representative Concentration Pathway (RCP), RCP8.5. For large parts of the British-Irish Isles, Hirabayashi et al. (2013) project that the 100-year flood may become the 25-75-year flood by the end of the century. Yet, evidence for increasing flood hazard in streamflow observations at global to regional scales is limited.

The conclusion from IPCC AR5 regarding changes in flood observations is that “there continues to be a lack of evidence and thus low confidence regarding the sign of trend in the magnitude and/or frequency of floods on a global scale” (Hartmann et al., 2013: pp 214). This is similar to the statement on observed flood changes in the SREX and Kundzewicz et al. (2013) where there was limited to medium evidence to assess climate-driven changes at the regional scale, as well as low agreement in this evidence (Seneviratne et al., 2012). Even the medium confidence given to the statement that projected future increases in heavy precipitation would contribute to rain-generated

local flooding in some catchments or regions is very uncertain and based on physical reasoning rather than robust evidence from observational and/or modelling studies.

It is clear that a general statement cannot be made on observed changes in global floods. Even concentrating on Europe, a comprehensive review of recent studies on observed flood changes by Hall et al. (2014) finds considerable disparity in even the direction of trends between countries, but some broad patterns emerge as summarised in Figure 2.4. Floods have increased during the period of available streamflow observations in regions along the Atlantic fringes of western Europe, such as Ireland, the UK, northern Spain and France, as well as within some areas of western central Europe; this is in contrast to detected decreases in regions in the Mediterranean and Eastern Europe.

It is clear from the above literature that definitive conclusions on the changing nature of floods are not yet possible. Simulated precipitation from current generation climate models is inherently uncertain and robust increases in extreme precipitation are not necessarily detected in hydrological records. A fuller understanding of the physical processes driving floods, both climatic and hydrological, need to be considered together in an effort to resolve this apparent mismatch and is the topic of the next section.

### 2.2.3 The hydroclimatic perspective

Statistical trend detection, on its own, reveals very little about the drivers of floods. It is imperative to understand *why* floods in certain regions are increasing while others are decreasing (the goal of trend attribution), and if these trends will continue under future climate change. In order to advance trend attribution, a more detailed understanding of the physical processes governing floods is needed, such as:

- **Establishing the predominant physical flood-generating mechanism:** Floods can be rainfall or snow melt fed, or a mixture of both. The seasonality of floods will also help identify the drivers (Merz and Blöschl, 2003). For example, are floods driven by short duration local-scale convection in summer or long-duration synoptic-scale storms in winter?



**Figure 2.4: Summary of direction of changes in observed floods across Europe based on studies using different not directly comparable change analysis methods and time periods. Arrows represent directional majority from reviewed studies and blank areas with no/inconclusive studies due to insufficient data (e.g. Italy) and inconclusive change signal (e.g. Sweden), Source: (Hall et al., 2014).**

- **Understanding the role of local hydrology:** Even within a single country the local hydrology will determine how different catchments ‘filter’ precipitation depending on unique catchment characteristics, such as: underlying geology, soil type, vegetation, basin size, shape, slope, and elevation. For example, a small steep sloped upland catchment will have a flashy rainfall-runoff response, whereas a large, lowland shallow sloped groundwater dominated catchment, will have a much more dampened response.
- **Taking account of confounding factors:** The extent of development of the land-surface by humans is such that it is becoming increasingly difficult to find completely natural or “pristine” catchments (Stahl et al., 2010). Urbanisation, deforestation, agriculture, and river regulation for water resources and flood control, are just a few examples of this land-use change. Substantial human alterations within a catchment and/or stream network will introduce artificial changes to streamflow response and will make it difficult, if not impossible, to

separate climatic and non-climatic driven changes within observed streamflow observations.

This 'catchment perspective' (Garner et al., 2015) is needed for understanding drivers of changes in floods as individual catchments will respond to atmospheric inputs differently depending on their physiographic characteristics and modulated by artificial disturbances (e.g., dam regulation, flood control structures). However, there is an apparent contrast between traditional hydrological approaches and emerging perspectives to tackle estimation of flood risk as outlined in Merz et al. (2014):

- **Randomness:** Traditional approaches view floods as completely random events. This contrasts the view that floods depend on a causal network of processes in the atmosphere, catchments, and river systems; that a fraction of flood variability is described by deterministic processes.
- **Spatial Reference:** Traditional views describe floods fully by processes on a catchment scale, whereas, the view that floods occur within the spatial framework of large-scale circulation patterns and global climate mechanisms is emerging.
- **Natural variability of floods:** On one hand, flood characteristics are seen as stationary, on the other, they change in time due to climate variability at different scales.
- **Temporal perspective:** The majority of flood research is based on the very recent past and limited by availability of high-resolution (daily/sub-daily) streamflow observations which are often < 50 years in length. However, this can lead to misleading trends and not reflect the longer term picture. Figure 2.5 demonstrates the idea that floods can cluster in time resulting in multi-annual/decadal flood rich/poor periods.

The contrast between traditional approaches and emerging perspectives can be explained by recognising the need for interdisciplinary approaches, linking the fields of hydrology and climatology, to tackle the problem of changing flood hazard. Climate change, climate variability, and human disturbance in catchments (e.g. land-use change and river regulation) have been shown to invalidate the assumption of stationarity (Milly et al., 2008; Milly et al., 2015). Understanding the

evolution of floods in the past, and how they will change in future needs consideration of both hydrological and climatological processes – the concept of hydroclimatology (Langbein, 1967). Researchers have long realised the need to study hydrological events within their climatological context, from both a physical and statistical perspective at local to global scales (Kilmartin, 1980). It was Hirshboeck (1988) that extended this to extreme hydrological events, arguing that studying floods within their climatological context provides a means of combining the origins of physical drivers of flood variability with the statistical properties of the time-series, which allows improved process understanding of floods and quantitative assessment of its variability.

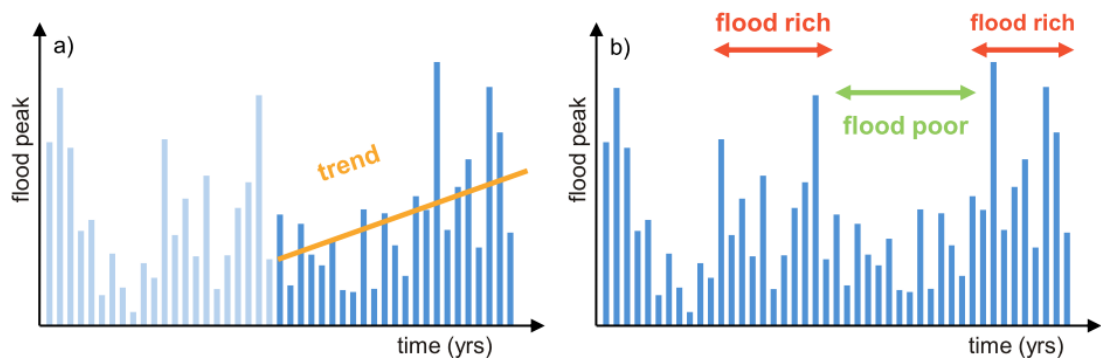


**Figure 2.5: Apparent linear trend in short time-series and (b.) decadal/multi-decadal periods of flood rich/poor episodes, Source: (Hall et al., 2014).**

One area in which a hydroclimatic perspective is particularly valuable is in the attribution of changes in streamflow. Merz et al. (2012) claim that most studies of statistically detected change in floods fall into the category of ‘soft’ attribution: they typically employ qualitative reasoning and/or correlation based techniques to show consistency between changes detected and typically a single driver (e.g. climatic change), with little effort to reliably quantify the assumed cause-effect relationship, and even less effort to falsify alternative candidate drivers. Attribution of change is an area that clearly would benefit from taking a hydroclimatic perspective. For example, if a change in streamflow is detected in a particular catchment, it will be important to know if it is caused by changing climate patterns, or if the change is internal to the catchment, perhaps by human disturbance. Without knowing the driver of change

(attribution) statistical detection is of limited benefit both in terms of practical decision making purposes, but also for scientific advancement.

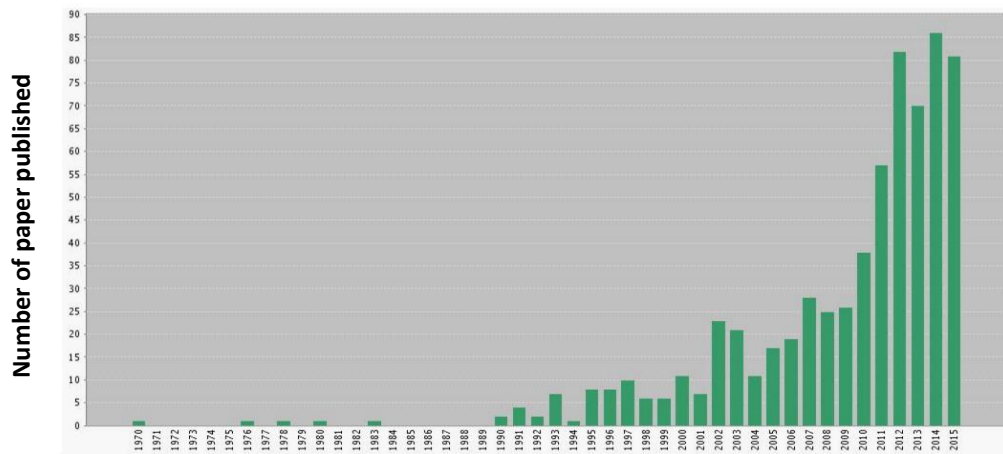


Figure 2.6: Annual number of peer-reviewed publications within the Web of Science database containing in the title ‘climate’ and ‘flood\*’ between 1970-2015 (total = 661), last checked: (13/12/2015).

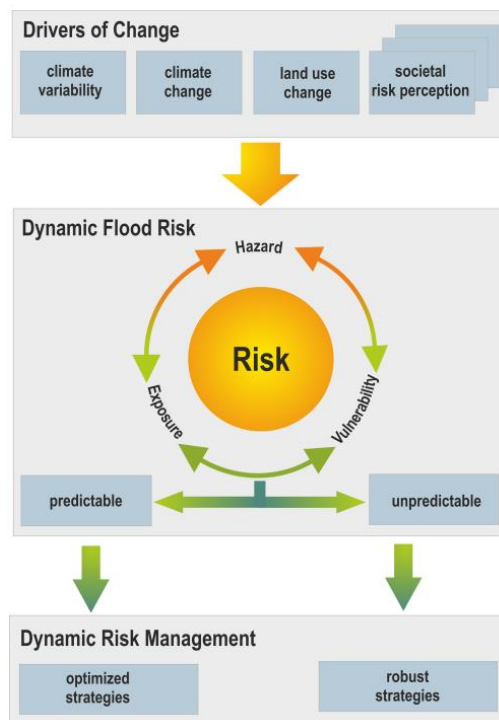


Figure 2.7: Drivers of flood risk change, dynamic flood risk, and dynamic flood risk management, Source: (Merz et al., 2014).

The hydroclimatic perspective has however not been widely adopted, but its value has been recognised as demonstrated by an increase in research interest, summarised by the increase in year-to-year published literature on climate and floods from ‘Web of

Science' (Fig. 2.6). Set in the wider context of climate, there is potentially a structured and deterministic proportion of observed climate variability linked to flooding that can be exploited in flood risk management strategies such as dynamic flood risk management (Fig. 2.7). However, there remain many open research questions. While large-scale climate phenomenon (or natural climate variability), such as the El Niño-Southern Oscillation (ENSO), have been shown to have global influences on flooding (Ward et al., 2014), it is region specific. Some regions in the world will have clear dominant modes of climate variability, while others may not. It is therefore important to first establish the role of large-scale climate variability and atmospheric circulation in modulating flood risk for specific regions, here the Island of Ireland and BI more generally, where the climate is controlled by the North Atlantic Ocean.

### **2.3 Climate variability and atmospheric circulation in the North Atlantic**

Many of the studies on changes in observed precipitation and floods from section 2.2 found evidence of multi-annual/decadal oscillations rather than simple linear trends within time-series, connected with well know patterns of climate variability. These preferred patterns of global atmospheric circulation can modulate the location and strength of storm tracks and poleward fluxes of heat, moisture and momentum, and thus can impact surface climate from large distances and hence are known as teleconnections (Trenberth et al., 2007). Many indices of these modes of variability have been created by various researchers and institutions using, for example, observations of Sea Level Pressure (SLP) and Sea Surface Temperatures (SSTs). The hydroclimatology of western Europe has been shown to be affected by a number of widely studied teleconnections which are introduced below with their associated indices in Table 2.1 and spatial patterns in Figure 2.8. It must however be reiterated that western Europe has one of the most variable climates of any land area on Earth, and it is often hard to trace the origins of a given event back to a particular source (Woollings, 2010). Nevertheless, an important factor about this region is that long records of observed surface climate variables at high spatial resolution exist so climate variability and atmospheric circulation is well understood.

### 2.3.1 Synoptic-scale atmospheric circulation patterns

**Extratropical cyclones (ETCs)** are a key feature in the mid-latitudes. In the northern hemisphere, the sharp contrast between cold polar air masses and warm tropical maritime air over the western Atlantic, warmed by the powerful poleward flow of water in the Gulf Stream is a favoured site for cyclogenesis. The north-western Atlantic breeds storms which drive across the high north Atlantic to arrive in their maturity in the Western approaches of Europe (McIlveen, 2010). In areas where extratropical cyclonic storms contribute most to the overall precipitation climatology (such as in the British-Irish Isles), the more important the expected increase in their projected intensity due to anthropogenic climate change is likely to be (Hawcroft et al., 2012). According to Hawcroft et al. (2012), the contribution of storm associated precipitation (extratropical cyclones) to total precipitation in BI is between 70-80% in both winter (DJF) and summer (JJA). The recycling ratio (i.e. ratio of P coming from local E versus from advection into the region) of BI is one of the lowest on the planet (< 10% in Trenberth, 1999, < ~20% in Van der Ent et al., 2010), emphasising the importance of moisture transport systems in delivering precipitation to BI. Understanding future changes in the most intense winter cyclones, how they are connected to large-scale modes of variability, and whether they have a strong influence on flood occurrence are important research questions.

**Blocks/blocking highs** are often larger than cyclones and the air is slow moving, almost stationary. They can persist for several weeks, preventing the normal eastward procession of mid-latitude depressions, thus giving the name blocking high (McIlveen, 2010). In winter, precipitation deficits can occur from the blocking of cyclones, and can lead to the supply of cold polar air into the region for long periods of time (e.g., 2012 winter blocking in Europe). In summer, they also block summer depressions (less rain) and lead to unusually high temperatures from a lack of clouds. For example, in July and August 1976 BI lay under a block which came at the end of a period of more than a year in which precipitation had been consistently well below normal because of unusually high incidence of blocking. With reservoirs not fully restocked from the preceding dry winter, and the prolonged excessive evaporation over precipitation in the hot, dry summer, led to one of the most severe droughts on record (McIlveen, 2010; Marsh et al., 2007).

**Table 2.1: Established indices of climate variability with regional surface climate impacts. Adapted from IPCC AR5 chapters 3 (Hartmann et al., 2013) and 14 (Christensen et al., 2013).**

Climate Phenomenon	Index Name	Index Definition	Regional Climate Impacts	Primary Reference(s)
<b>El Niño-Southern Oscillation (ENSO)</b>	NIÑO1+2	SSTa averaged over [10°S–0°, 90°W–80°W]	Global impact on interannual variability in global mean temperature. Influences severe weather and tropical cyclone activity worldwide. El Niño presents different teleconnection patterns that induce large impacts in numerous regions from polar to tropical latitudes	Rasmusson and Wallace (1983), Cane (1986)
	NIÑO3	Same as above but for [5°S–5°N, 150°W–90°W]		
	NIÑO4	Same as above but for [5°S–5°N, 160°E–150°W]		
	NIÑO3.4	Same as above but for [5°S–5°N, 170°W–120°W]		Trenberth (1997)
	SOI	Standardized difference of SLPsa: Tahiti minus Darwin		Trenberth (1984); Ropelewski and Jones (1987)
<b>North Atlantic Oscillation (NAO)</b>	Azores-Iceland NAO Index	SLPsa difference: Lisbon/Ponta Delgada minus Stykkisholmur/ Reykjavik	Influences the N. Atlantic jet stream, storm tracks and blocking and thereby affects winter climate over the N. Atlantic and surrounding landmasses. The summer NAO (SNAO) influences Western Europe and Mediterranean basin climates in the season	Hurrell (1995)
	PC-based NAO Index	Leading PC of SLPa over the Atlantic sector		
	Gibraltar – South-west Iceland NAO Index	Standardized for each calendar month SLP a difference: Gibraltar minus SW Iceland / Reykjavik		Jones et al. (1997)
<b>Atlantic Ocean Multi-decadal Variability (AMO)</b>	Atlantic Multi-decadal Oscillation (AMO) index	10-year running mean of linearly detrended Atlantic mean SST a [0°–70°N]	Influences air temperatures and rainfall over much of the Northern Hemisphere; in particular, North America and Europe. It is associated with multi-decadal variations in Indian, East Asian and West African monsoons, the North African Sahel and northeast Brazil rainfall, the frequency of North American droughts and Atlantic hurricanes	Enfield et al. (2001)
	Revised AMO index	As above, but detrended by subtracting SSTa [60°S–60°N] mean		Trenberth and Shea (2006)

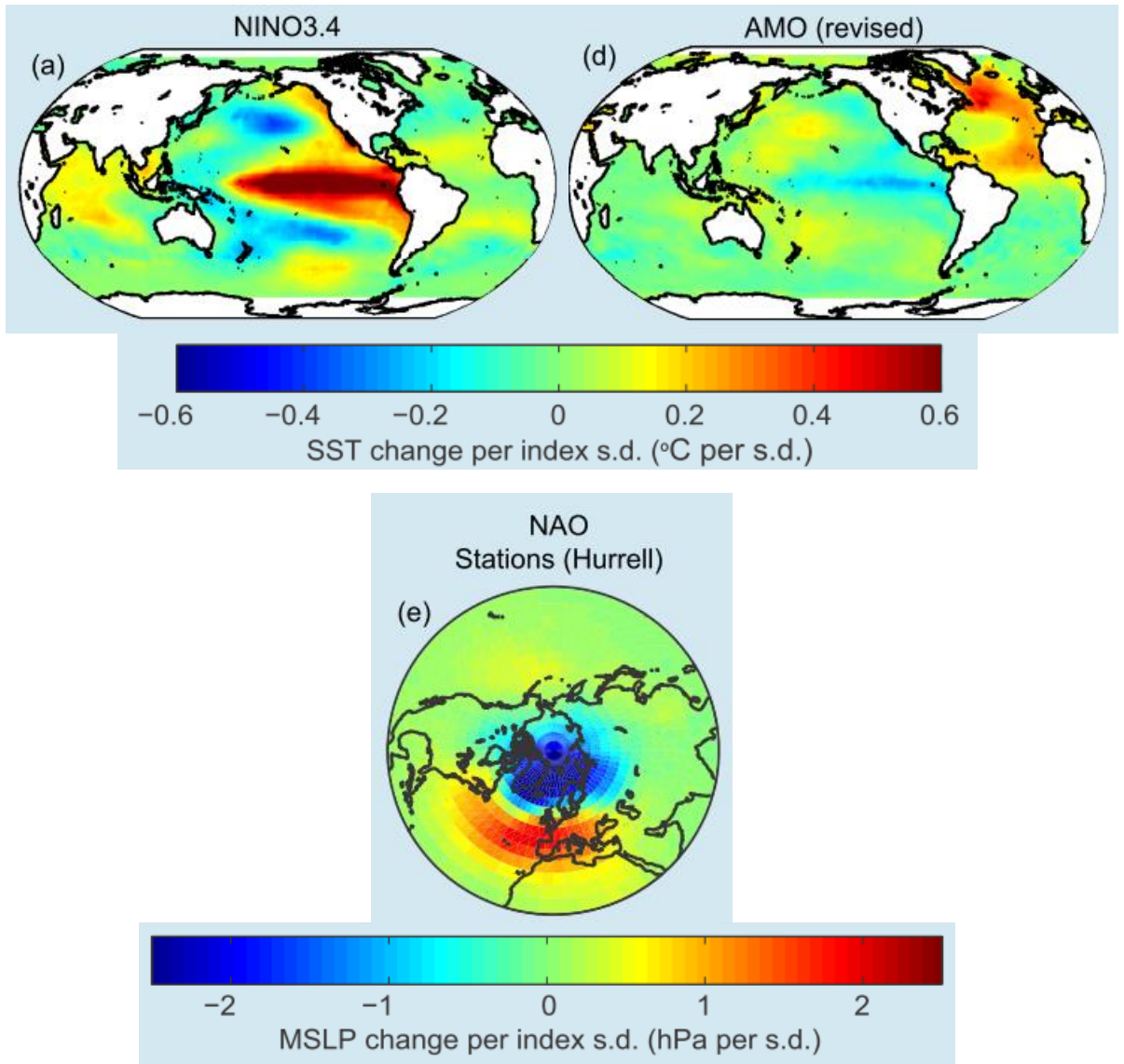


Figure 2.8: Spatial patterns of climate modes in Table 2.1. Adapted from Box 2.5 in Hartmann et al. (2013).

**Atmospheric circulation pattern** classification has a rich history in synoptic climatology, though the focus of classifications has changed from mere description of atmospheric states to their use as a tool for understanding and interpretation of atmospheric processes and examining the linkages between circulation and surface climate variables (Huth et al., 2008). The most significant atmospheric circulation patterns or features within the British-Irish Isles have been classified subjectively (or manually) by Lamb (1972). The catalogue of daily circulation types (CTs) is known as Lamb Weather Types (LWTs). The catalogue was originally created by defining the

direction of air flow and (anti)cyclonicity. An objective scheme to classify the daily circulation according to the Lamb weather typing scheme was developed by Jenkinson and Collison (1977) by setting numerical criteria for the direction, strength, and vorticity of airflow. A comparison of the subjective and objective LWT schemes was undertaken by Jones et al. (1993) and found that a decline in westerly days noted in the subjective catalogue was not reproduced in the objective catalogue. A new series has now been produced using long-term reanalysis data (Jones et al., 2013b). Seven main categories of synoptic pattern are recognised for each day of the year: the anticyclonic (A), easterly (E), southerly (S), westerly (W), northwesterly (NW), northerly (N) and cyclonic (C) types. Remaining days are classified into 19 hybrid combinations of the main types, such as cyclonic westerly (CW) or northeasterly (NE) types. Chapter 5 discusses synoptic classification schemes in more detail.

### 2.3.2 Large-scale climate variability of atmospheric circulation

While it has been established that the most important mechanism for delivery of extreme precipitation into the BI are Extratropical cyclones (ETCs) and an important condition for 'blocking' entry to BI are anticyclones, such circulation patterns are themselves influenced by particular modes of low-frequency climate variability in the North Atlantic. The most widely studied modes are described below.

**North Atlantic Oscillation (NAO):** The main mode of climate variability in the North Atlantic is the NAO and Arctic Oscillation (Kingston et al., 2006). The NAO is a large-scale meridional oscillation in atmospheric mass between the two semi-permanent centres of action in the North Atlantic, near the Icelandic low and Azores high (Hurrell and van Loon, 1997). The AO (Arctic Oscillation) is an annular seesaw of atmospheric mass between polar regions north of 60° and the surrounding regions near 45°N (Kingston et al., 2006). According to Huth (2007) the AO is a statistical artefact so the NAO, which is more physically interpretable, should be given the preferred description and interpretation of Northern Hemisphere SLP variability. The state of the NAO is described by several indices (summarised in Table 2.1). According to Kingston et al. (2006) during a high (positive) NAO state in winter, northwest Europe experiences increased intensity of westerlies across the Atlantic, with atmospheric moisture transport switching to a more South-westerly-North-easterly axis (Hurrell, 1995) thus

influencing the storm track strength (i.e. number of depressions) and position (i.e. the median route taken by that winter's storms), leading to above average precipitation and increased streamflow in northern Europe, with drier than normal conditions in Mediterranean Europe (the opposite is the case for a low or negative NAO).

**Atlantic Multi-decadal Variability (AMO):** The AMO is a prominent mode of multi-decadal variability which consists of spatially coherent changes in North Atlantic SSTs which have oscillated between cold and warm phases with a range of  $\sim 0.4$  °C with two major cold phases from the 1900s to mid-1920s and from the 1960s to mid-1990s with a cycle of  $\sim 65$ -80 years (Enfield et al., 2001). McCarthy et al. (2015a) shows that ocean circulation is primarily driven by the first mode of Atlantic atmospheric forcing, the NAO, through circulation changes between the sub-tropical and subpolar gyres—an area known as the intergyre region. This then affects the heat content of the North Atlantic over decadal time-scales and consequently the phases of the AMO. This demonstrates the complex ocean-atmosphere relationship in the North Atlantic whereby the ocean integrates the NAO forcing and returns it to the atmosphere as the AMO (McCarthy et al. 2015a).

The effect of the Atlantic Ocean is particularly substantial for European maritime land masses such as the British-Irish Isles. Sutton and Dong (2012) find the anomalously wet summers during the 1990s in northern Europe were driven by the substantial warming of the North Atlantic Ocean. McCarthy et al. (2015b) show that during a warm phase AMO (positive AMO) Irish summer temperature and precipitation is higher than average. Casanueva et al. (2014) show that the AMO index is strongly positively correlated with extreme precipitation (but not mean precipitation) across all seasons in Europe. This study was only based on data from 1950-2010, which does not even cover one full AMO cycle, nor do they go into detail on spatial patterns of this relationship. Thus it remains an open research question whether extreme precipitation and floods are related with the AMO in Ireland, and if so, details of the physical chain of causality need to be determined.

**El Niño-Southern Oscillation (ENSO):** The irregular reversal of the Walker Circulation every few years, called the Southern Oscillation, is linked to the El Niño phenomenon. El Niño occurs when dramatically warmer than average SSTs occur over the central and

eastern equatorial Pacific region and colder waters in the western Pacific, causing a huge release of heat from the Pacific Ocean into the atmosphere, which can disrupt weather patterns globally. There is evidence of a teleconnection between mid-latitude circulation in the Northern Hemisphere and the ENSO warm and cold extremes (Fraedrich, 1990). Ward et al. (2014) found that ENSO exerted a significant influence on annual floods (between 1958-2000) in river basins covering a third of the world's land surface, particularly during La Niña (cold phase) – but the pattern over Ireland and the UK is not clear. Wilby (1993) found associations between strong ENSO phases and the synoptic climatology of the British-Irish Isles. However, it is not well understood what influence, if any, ENSO has on extreme precipitation and floods in the vicinity of BI. Any assessment would need to consider the physical connection between ENSO phases and large-scale systems that deliver flood-generating precipitation, if any.

#### **2.4 Hydroclimatological links: Approaches and evidence**

This section focuses on recent papers (past decade) that explore hydroclimatological links focusing on/including the British-Irish Isles (Ireland and/or UK). Criteria for including papers were that they must specifically assess links between large-scale climate (e.g. NAO, Mean Sea Level Pressure (MSLP), Weather Type classifications (WTs), or atmospheric moisture) and hydrology and are summarised in Table 2.2. Research in this area can be separated into 3 categories depending on the scale of the hydrological regime investigated: Category 1.) Mean monthly/seasonal streamflow; Category 2.) High flows/floods; and Category 3.) Most extreme floods.

Most common among studies exploring mean monthly/seasonal streamflow changes is correlation or regression analysis linking streamflow and the NAO. Murphy et al. (2013a) found strong positive correlations between the NAO and mean winter streamflow and the maximum 30 day flow for the Island of Ireland with strongest correlation in the west. Burt and Howden (2013) also found strongest NAO links in the northwest of the UK (western Wales, northwest England, and western Scotland). They also find that the influence of the positive NAO is amplified in higher altitude catchments due to 'double orographic enhancement'. Lavers et al. (2010a) also find strong positive correlations between the NAO and monthly mean streamflow for a basin in Wales (highest  $\rho = 0.69$  for December), but show that higher correlations are

possible using monthly MSLP instead ( $\rho > |0.8|$  possible) suggesting that static NAO indices might not capture the dynamic movement of NAO centres of action. Lavers et al. (2010b) extend this analysis to 10 basins and highlight the role catchment characteristics have in modulating climate-flow links. More flashy catchments (i.e. more surface water dominated than groundwater in upland areas) have stronger climate-flow relationships.

Two studies examining high flow/flood indices in Table 2.2 assessed links with the NAO. Hannaford and Marsh (2008) find strongest NAO-flow relationships across the UK for winter runoff and PQ10 (high flow prevalence above 90<sup>th</sup> percentile) than for MAX10 (extended duration maximum consecutive 10-day flow) or Peaks-Over-Threshold (POT) floods, indicating that the NAO signal is most pronounced in indices that describe the wetness of the winter period, than for single/multi-day events. Again, positive correlations were strongest in north western areas of the UK. In contrast, Macdonald et al. (2010) did not find statistically significant correlation between flood frequency (POT) and the NAO aggregated over Wales. Perhaps averaging over such a large area conceals more relationships. For example, when considering 6 sub-regions of Wales classified by flood seasonality, they do find positive correlation between westerly types (aggregating SW-, W-, and NW-types from the Lamb Weather Type catalogue) in 2 of the 6 regions, both located in northern Wales, but conclude overall that weather type frequencies are a poor predictor of annual flood occurrence. However, they do suggest weak correlation is likely due to combining multiple weather types together.

The remaining papers concerned with high flow/flood indices take a different approach than correlation with the NAO. These studies investigate which atmospheric patterns are most associated with flood events. Prudhomme and Geneviev (2011) examined if WTs could be linked to flooding at the European scale using 73 different WT catalogues developed within the COST733 action (Harmonisation and applications of weather type classifications for European regions) and found that some WTs occurred more frequently before and during a flood than in any other period, so could be classed as flood-producing. However, there was no single WT that could explain flooding at the European scale, instead there were large spatial differences highlighting that flood generating mechanisms are regionally different and depend on

season. For a single catchment (Eden catchment 2400 km<sup>2</sup>) in northwest England, Pattison and Lane (2012) found just 5 out of 27 LWTs accounted for 82 % of floods. When considering the whole of Britain, Wilby and Quinn (2013) found that the same 5 LWTs account for 68 % of flood occurrence, and just 3 (Cyclonic, Westerly, and Southerly components) were linked with the most widespread winter floods across Britain.

The third category of study identified is for the most extreme floods in terms of magnitude. The atmospheric conditions responsible for the largest floods have been found to be related to Atmospheric Rivers (ARs). ARs are narrow bands of strong moisture transport within the warm sector of extratropical cyclones (Zhu and Newell, 1994; Allan et al., 2015) and are thought to be responsible for the majority of poleward water vapour transport in the mid-latitudes (Gimeno et al., 2014; see Fig. 2.9). For example, Lavers et al. (2011) find that the 10 largest winter half year flood events in 4 basins in Britain occurred under ARs, but ARs are not necessarily associated with smaller floods. This finding was extended by Lavers et al. (2012) who found 40-80 % of winter annual maximum flows are associated with ARs in 9 basins across western Britain. There is however some debate about the formation of ARs. Dacre et al. (2014) argue that ARs are formed within an extratropical cyclone ahead of the cold front through convergence of local sources of water vapour, and that 'filaments' of high water vapour content are actually the footprints left behind as these systems move polewards, rather than a direct and continuous feed of moist air from the sub-tropics (as the term 'Atmospheric River' suggests).

Each of the 3 approaches above have relative advantages and disadvantages depending of the aim of the study. While many studies within Category 1 (mean monthly/seasonal analysis) claim the positive relationship between NAO and streamflow would have implications for flood risk, this might not always be the case as shown by category 2 studies which reveal that the strength of NAO-flood relationship depends on the particular indicator used and is weaker at the event level and more spatially confined to Atlantic facing upland areas in BI. ARs take a back-trajectory approach and consider the actual moisture supply mechanism directly, which has many advantages when the most extreme floods are of interest. However, this approach relies on high spatio-temporal resolution data from the satellite era (~ late

1970s), hence atmospheric moisture cannot be adequately estimated before then due to the lack of high-quality global-scale observations (Hurrell, 1995). In contrast, Sea Level Pressure (SLP) has been more routinely observed at a sufficient resolution since the late 19<sup>th</sup> Century for many parts of the globe. This is particularly the case in the vicinity of the British-Irish Isles (BI). These data have been used to create long-running catalogues of weather types (e.g., Jones et al., 2013b) and used by Wilby and Quinn (2013) to reconstruct flood occurrence back to the 1870s (Category 2).

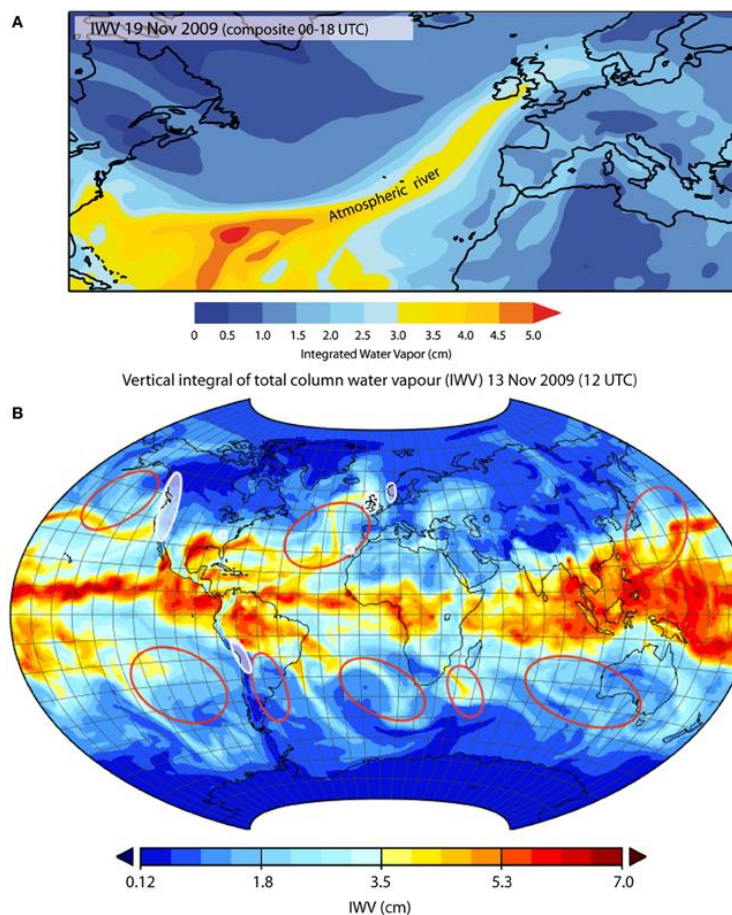


**Figure 2.9: Composite integrated Total Column Water Vapor between 00:00 and 18:00 UTC 19<sup>th</sup> November 2009 showing an atmospheric river associated with extreme precipitation that affected the November 2009 floods in Ireland (Cork and Galway) and the UK (Cumbria) (A.), and A general distribution of areas of AR occurrence (red contours) with land areas with reported cases of ARs linked to extreme precipitation and floods (white contours), Source: (Gimeno et al., 2014)**

**Table 2.2: Selection of papers assessing hydroclimatological links considering the British-Irish Isles in the past decade.**

No.	Reference	Region (basins)	Period (metrics)	Atmospheric data	Methods	Key Findings
<b>Category 1.) Mean monthly / seasonal streamflow scale</b>						
1	Lavers et al. (2010a)	Wales (1: RHN)	Jan 1976-Dec 2001 (Monthly mean flow and total basin-averaged precipitation)	Reanalysis (ERA-40: 11 variables); NAO (Monthly fixed CRU)	Correlation analysis (Spearman's rank); 5% level	Stronger correlations (negative) with MSLP (some $\rho >  0.8 $ ) than NAO (max $\rho = 0.69$ ) for flow
2	Lavers et al. (2010b)	Eng, Scot, Wales (10: RHN)	Jan 1976-Dec 2001 (Monthly mean flow and total basin-averaged precipitation)	Reanalysis (ERA-40: 5 variables); NAO (Monthly fixed CRU)	Correlation analysis (Spearman's rank); 5% level	More flashy basins have stronger climate-flow link, particularly in winter for western Britain
3	Burt and Howden (2013)	UK (86)	Multiple periods between 24 and 181 years (Seasonal [DJF, MAM, JJA, SON] total flow and total precipitation)	NAO (Seasonal [DJF, MAM, JJA, SON] fixed CRU)	Regression analysis (Ordinary least squares); multiple significance levels	Increase in flow with elevation amplified when NAO is strongly positive: 'double orographic enhancement'
4	Murphy et al. (2013a)	Ireland and NI (43: RHN)	1976-2009 (Winter [DJF] and summer [JJA] mean flow and MAX30 [Oct-Sep])	NAO (Winter [DJF] fixed Hurrell, NCAR)	Correlation analysis (Spearman's rank); 5% level	Strongest significant positive correlations ( $\rho > 0.8$ ) found between winter mean flow and NAO in NW and SW
<b>Category 2.) High flow / flood scale</b>						
5	Hannaford and Marsh (2008)	UK (87: RHN)	1969-2003 (Winter [DJFM] runoff [mm], MAX10, PQ10 and annual flood frequency [POT])	NAO (Winter [DJFM] fixed CRU)	Correlation analysis (Pearson); significance not tested	Stronger positive correlations ( $\rho > 0.6$ ) between NAO and winter runoff and PQ10 in upland NW than for MAX10 and POT

6	Macdonald et al. (2010)	Wales (40)	Jun-May 1973-2002 (Annual flood seasonality [Mean day of flood] and flood frequency [POT])	Objective LWT catalogue; NAO (Annual [Jun-May] and winter [DJF] fixed CRU)	Correlation analysis (Pearson); 5% and 10% level	No significant correlation exists ( $\rho = 0.21$ ) nationally between flood frequency and NAO
7	Prudhomme and Geneviev (2011)	Europe (488)	1957-2002 (Event level flood occurrence [POT])	73 Circulation Type Catalogues (CTCs) derived from mainly ERA-40 reanalysis MSLP fields	Exploratory analysis (Measures CT occurrence prior to (1-30 days)/during flood)	Some circulation patterns (e.g. cyclonic westerly type), at river basin scale, have positive frequency anomalies with flood occurrence
8	Pattison and Lane (2012)	Eng (1)	Gauged records: 1976-2007 WY (Flood frequency [POT] and flood magnitude [POT and AMAX])	Objective LWT catalogue [1880-2007] (NCEP/NCAR MSLP)	Exploratory analysis (Calculate percentage of floods occurring on days of each LWT)	5 flood-producing LWTs accounted for 82% of extreme flood events between 1976 to 2007
9	Wilby and Quinn (2013)	Eng, Scot + Wales (114)	Gauged records: 1961-2000 WY (flood frequency [POT] and magnitude [AMAX])	2 Objective LWT catalogues (NCEP/NCAR MSLP [1880-2007] and 20CR [1871-2011])	Exploratory analysis (Flood index: A LWT is flood rich if ratio of observed to expected frequency exceeds 1)	5 weather types accounted for ~68% of recorded POT between 1961-2000. Flood frequency, but not magnitude can be reconstructed with moderate skill
<b>Category 3.) Extreme Flood scale - Atmospheric Rivers</b>						
10	Lavers et al. (2011)	Eng, Scot + Wales (4)	1970-2010 WY (Top 10 winter maximum series [Oct-Mar] flood events)	2 Reanalysis (ERA-Interim and 20CR: Specific humidity and zonal and meridional wind)	Exploratory analysis (ARs coincide with floods)	10 largest winter floods in each basin related to ARs; ARs are not necessarily associated with smaller winter floods
11	Lavers et al. (2012)	Eng, Scot + Wales (9)	1980-2010 WY (Flood frequency for winter maximum series [Dec-Mar] and AMAX using POT-1)	5 Reanalysis (NCEP, ERA-Interim, 20CR, MERRA, NCEP/NCAR: specific humidity, zonal and meridional wind and MSLP)	Exploratory analysis (Calculate percentage of floods occurring 1-3 days post/during an AR)	Percentage of winter POT-1 floods associated with ARs ranged from approximately 40-80% in each basin

**Abbreviations:** CRU (Climatic Research Unit, University East Anglia), NI (Northern Ireland), Eng (England), Scot (Scotland), NAO (North Atlantic Oscillation index), NCAR (National Center for Atmospheric Research), NCEP (National Centers for Environmental Prediction), ERA-40 (European Centre for Medium-Range Weather Forecasts (ECMWF) reanalysis product), RHN (Reference Hydrometric Network), MSLP (Mean Sea Level Pressure), LWTs (Lamb Weather Types), MAX30 (extended duration maximum consecutive 10-day flow), WY (Water Year).

## 2.5 Identification of research gaps

This literature review has identified the following research gaps in relation to advancing understanding on the hydroclimatology of floods for the Island of Ireland which this thesis aims to fill, as outlined in Section 1.2:

- **Research Gap 1:** While there have been numerous studies assessing changes in mean precipitation conditions in Ireland there is a general lack of understanding of extreme precipitation. This knowledge gap is addressed in this thesis. In Chapter 3 extreme rainfall regions are established for the Island of Ireland and in Chapter 4 trends in indicators representing extreme precipitation are assessed for evidence of variability and change.
- **Research Gap 2:** Across the international literature there are relatively few studies that take a hydroclimatic perspective by assessing/detecting change in extreme precipitation and floods together. Such studies are critical in furthering understanding of the changes between these variables and establishing consistency with expected anthropogenic climate change. In this thesis the same study design is used to assess changes in indices of extreme precipitation and flooding using high quality datasets (Chapter 4) to assess precisely these aspects.
- **Research Gap 3:** To understand the drivers of change in precipitation and floods multi-decadal time-scales must be considered, together with increased understanding of how large-scale climate variability affects these relationships. Given the importance of understanding flood occurrence over the longest period possible, this research makes use of a weather classification product (Jones et al., 2013b) based on long-term mean SLP (MSLP) data from the 20th Century reanalysis (20CR) project (Compo et al., 2011) to reconstruct flood occurrence over the last 144 years (Chapter 5). The relationship between key flood indices and synoptic circulation with large-scale modes of climate variability is also explored in Chapter 5.
- **Research Gap 4:** The literature review also identifies the need for cross-scale approaches in understanding hydroclimatic links – ranging from the large-scale to understanding the role of catchment characteristics in modulating climate variability and change. This aspect is addressed throughout Chapters 4 and 5

where attention is given to exploring how catchment physiographic features filter atmospheric drivers and extreme precipitation. It is evident from the literature that few studies consider the challenge of attributing detected changes in 'real world' catchments where management decisions are necessary at the catchment scale and where confounding factors such as land-use change can complicate such tasks. Chapter 6 seeks to advance approaches to attribution of detected changes in catchments that are affected by human activity.

Based on these identified research gaps, the overall thesis aims and objectives were established and presented in Section 1.2. The next chapter tackles the first of the 4 core thesis objectives identifying an appropriate precipitation dataset for analysing extremes and subsequently classification of Extreme Rainfall Regions (Chapter 3).

## 3 Classification of Extreme Rainfall Regions

---

### 3.1 Introduction

In hydrological assessments it is common practice to group streamflow stations into regions for simplifying interpretation. This is often done using agency boundaries, such as Water Framework Directive (WFD) River Basin Districts (RBDs) as in Murphy et al. (2013a) or UK Environment Agency boundaries in (Wilby and Quinn, 2013). However, it is argued here that it does not make sense to use a grouping scheme that has no physical bearing to the processes governing floods. Therefore, the objective of this chapter is to classify the Island of Ireland (IoI) into a number of Extreme Rainfall Regions (ERRs) reflective of similar extreme precipitation characteristics to aid interpretation and understanding of extreme precipitation and hence floods.

The Island is characterised by low-intensity and long-duration rainfall with Atlantic airstreams interacting with the topography in Atlantic facing coastal regions meaning precipitation is observed on over 220 days of the year compared to only 150 in the low-lying east (Sweeney, 2014). Frontal precipitation from Atlantic storms (the main delivery mechanism) interacts with a land surface dominated by shallow slopes and poorly drained soils to produce a flood hydrology dominated by long-rain floods (Merz and Blöschl, 2003), rather than flash floods (Convective/short-duration rainfall, e.g. southeast England) or snowmelt floods (flooding mainly in spring or summer due to large snow cover, e.g. Scandinavia). While the precipitation climatology of Ireland is well understood, the climatology of extreme precipitation, more relevant for flood generation, is less so.

Classification of ERRs has been undertaken in many countries. For example, Frei and Schär (2001) when studying trends in extreme precipitation frequency in Switzerland divided the region into 3 due to the strong influence of the Alps on precipitation with summertime convection dominating heavy precipitation in the north and over the Alps, while precipitation south of the ridge is dominated by orographic enhancement from moist southerly airflow. Agel et al. (2015) examined the extreme precipitation climatology of the northeast US and found two distinct sub-regions, with an inland

region having extreme precipitation peaking in summer, and a coastal region dominated by more intense precipitation peaking later in the year. In both these examples, and others, interpretation of findings from trend analysis and atmospheric association was improved from grouping individual precipitation stations into similarly responding regions. Although these studies show the utility of grouping extreme precipitation stations into regions, they do not do this formally using climatological classification methods. Classification in climatology has a rich history. There are several types of climatological classification such as weather classification (chapter 5) and precipitation regionalisation (focus in this chapter), in which studies divide a geographical area into sub-regions with similar precipitation characteristics (Huth et al., 2008).

The UK is one of the best examples internationally of application of climatological classification. Five homogeneous rainfall regions covering England and Wales were initially identified by Wigley et al. (1984) using Principal Components Analysis (PCA) based on monthly totals. Gregory et al. (1991) then extended this, using the same PCA approach, to include Scotland and Northern Ireland, producing 9 UK regions (see Fig. 3.1 inset) of spatially coherent precipitation variability from 63 precipitation sites (7 evenly distributed sites within each of the 9 regions). These are the 9 regions currently used to produce the UK regional precipitation series (HadUKP; Alexander and Jones, 2001).

While the HadUKP regions represent mean precipitation variation well, Jones et al. (2014a) argue that regions which are defined from mean characteristics will not necessarily reflect the spatial characteristics of extreme precipitation climatology; it may not therefore be appropriate to use the HadUKP regions for regional assessment of extreme precipitation. Jones et al. (2014a) consequently filled this research gap in the UK by developing 14 new regions using data at the daily time-scale that better represent temporal, orographic and atmospheric drivers affecting extreme precipitation (see Fig. 3.1).



**Figure 3.1: UK Extreme Precipitation Regions identified from a principal component analysis of extreme precipitation measures by Jones et al. (2014a) with HadUKP (Alexander and Jones, 2001) regions inset.**

For identification of the original HadUKP mean rainfall regions, Wigley et al. (1984) used 55 precipitation stations spanning 1861-1970 based on PCA using monthly precipitation anomalies at produce monthly, seasonal, and annual principal component patterns. For identification of Extreme Rainfall Regions (ERRs), Jones et al. (2014a) used 223 stations of daily precipitation totals with a minimum record length of 40 years, spanning the period 1856-2010 with minimum start date 1961. PCA was used to identify a set of parameters which best compute regional differences in extreme precipitation following the approach of Dales and Reed (1989). Cluster analysis, using the k-means method, was then applied to this subset of data to group stations with similar extreme precipitation responses.

However, to date no study has identified ERRs for Ireland. **Thesis Objective 1** addresses this research gap using precipitation data from across the island of Ireland (including precipitation data from Northern Ireland). A major obstacle to ERR

classification was availability of an appropriate dataset covering both Ireland and Northern Ireland with the necessary high spatial density required for analysis of extremes. In addressing these gaps this chapter has the following objectives:

- **Thesis Data Objective 1:** To compile a dataset of daily precipitation stations suitable for analyses of extreme precipitation.
- **Chapter Objective 3.1:** To classify Extreme Rainfall Regions (ERRs) for the island of Ireland.

Investigating the spatial homogeneity of extreme precipitation will improve physical understanding of extreme precipitation in Ireland, allowing greater understanding of the role of physiographic controls on precipitation (elevation and coastal effects), areas that receive the most precipitation, and the seasonality of extreme precipitation events. This in itself will give greater insight to rain-generated floods. However, the classification of ERRs will be used in Chapter 4 to better interpret trends in extreme precipitation and flood time-series, and in the development of the flood index in Chapter 5.

### 3.2 Precipitation data

A 1 km precipitation grid is available for Ireland from 1941-2012 (Walsh, 2012a; Walsh, 2012b). However, Zhang et al. (2011) state that gridding daily extreme observations and the use of monthly rather than daily observations smooth's over a lot of important information which characterises the behaviour of extremes. Also, there will be more wet days in gridded data than point observations due to spatial averaging of the former. Hence, point-based daily precipitation data were used for the analysis of extreme precipitation. Data were obtained for Ireland from Met Éireann for 1841 stations. For Northern Ireland, data for 34 stations were obtained from the UK Met Office Integrated Data Archive System (MIDAS) held at the Centre for Environmental Data Analysis (CEDA) Available: <http://www.ceda.ac.uk/>, last accessed 29/01/2015). A number of steps were completed before analysis was undertaken, such as selection of appropriate stations, data quality control, and infilling gaps in the record. The following sections outline data preparation steps taken.

### 3.2.1 Station selection

#### 3.2.1.1 Data period, length, and completeness

Not all the 1875 stations were appropriate for use in this study. Criteria were devised and applied to the full dataset to filter out inappropriate stations (See Table 3.1). Three levels of criteria were established: A-List (Most strict - optimised for most recent, longest record length, and least percentage of record missing, while retaining sufficient station density); B-List (Relaxed - Criteria were relaxed to include more stations in-case needed) and, C-List (Minimum tolerable - Criteria were further relaxed to allow for stations to be included, if needed, in locations where no stations were available from A and B lists).

**Table 3.1: Number of precipitation stations retained after applying criteria on data period, record length, and completeness.**

Criteria	No. Original	No. Knocked Out
A-List = 122		
Recent (end year $\geq$ 2011)	1875 to 543	1332
Record length (start year $\leq$ 1973 [min 39 Yrs])	543 to 172	371
Percent missing ( $\leq$ 5%)	172 to 122	50
B-List = 175		
Recent (end year $\geq$ 2009)	1875 to 576	1299
Record length (start year $\leq$ 1980 [min 30 Yrs])	576 to 206	370
Percent missing ( $\leq$ 10%)	206 to 175	31
C-List = 393		
Recent (end year $\geq$ 2000)	1875 to 735	1140
Record length ( $\geq$ 25 Yrs [not strict start year])	735 to 410	325
Percent missing ( $\leq$ 20%)	410 to 393	17

#### 3.2.1.2 Spatial distribution

It is important to have an even as possible spatial distribution of stations across the island as the statistical methods used (PCA and cluster analysis) are biased in areas with station clusters (too dominant in analysis) or gaps (underweighted in analysis) (Wilks, 2011). It is clear that such biases would be introduced to the analysis if only stations from the A-List were used (Fig. 3.2). Hence, a list of rules were established and applied systematically to remove A-List stations from clusters and add B- and C-List

stations to gaps in station density in a semi-objective manor (Fig. 3.3). Details of stations added to gaps 1-7 and removed from clusters 1-3 are provided in Appendix I. Of the 122 A-List stations, 28 were trimmed from clusters 1-3 (retaining 94) while 32 B- and C-List stations were added to the gaps in the network leaving the final station selection at 126 (see Fig. 3.4 with station metadata in Appendix II).

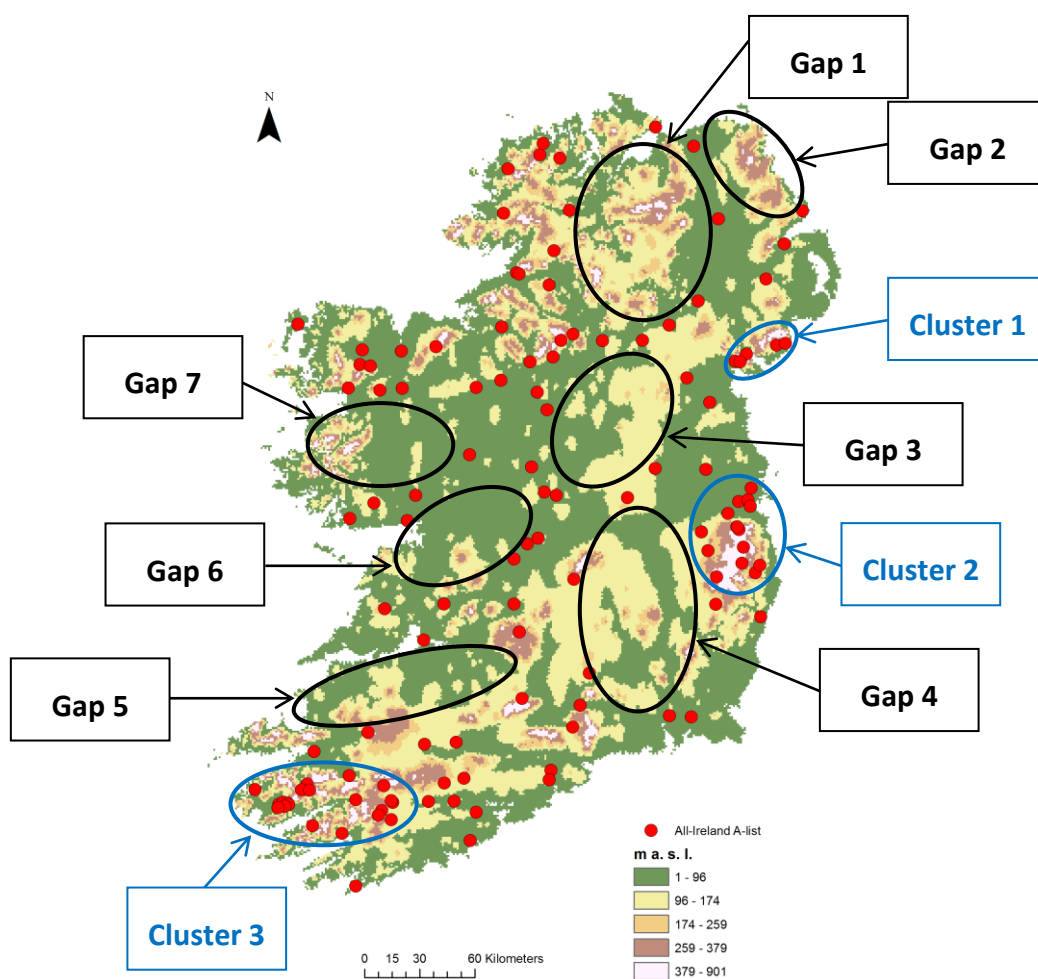


**Figure 3.2: Precipitation stations retained from automatic application of A-list criteria with most prominent clusters and gaps circled in blue and black, respectively. See Appendix I for details on stations added and removed.**

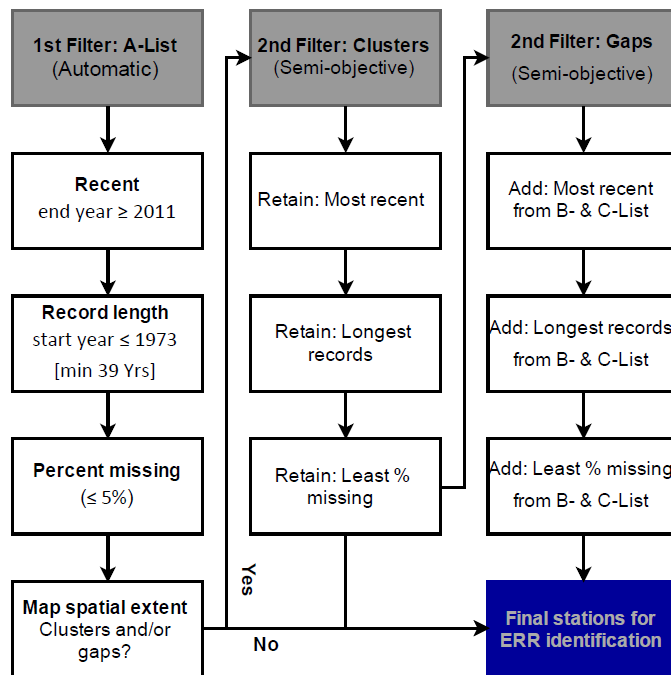


Figure 3.3: Flow chart of semi-objective rules for removing (adding) stations from (to) clusters (gaps).

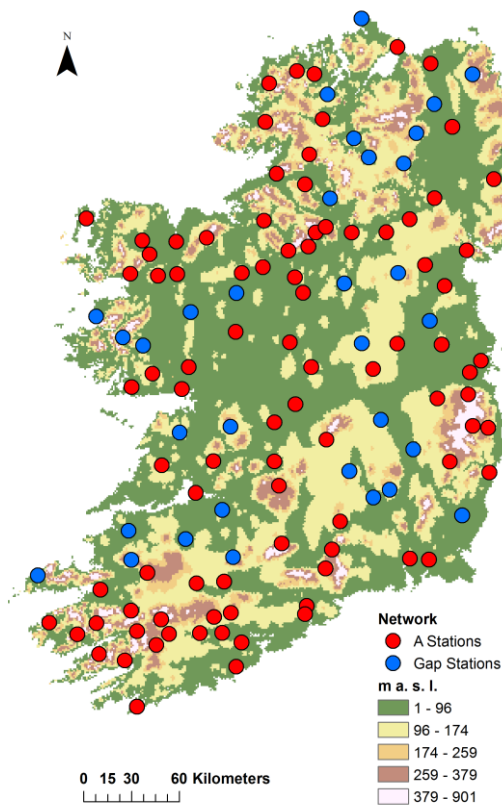
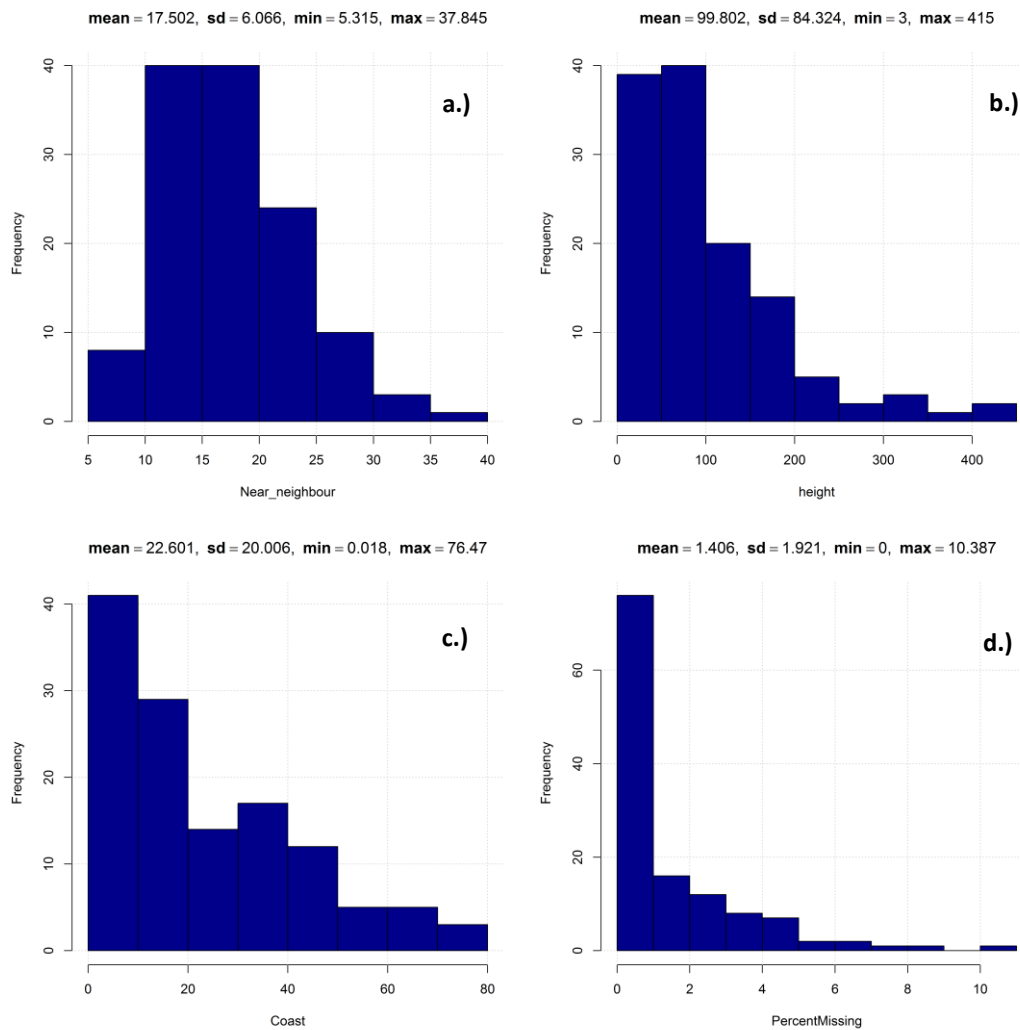


Figure 3.4: Final station selection (94 A-List stations and 32 Gap stations from the B- & C-List). Station metadata in Appendix II.



**Figure 3.5: Histograms of station details: a.) distance to nearest station (km), b.) elevation (m a. s. l.), c.) distance to coast (km), and d.) percentage of record missing for each of the 126 final precipitation stations.**

For the final selection of stations Figure 3.5 shows histograms of station details. It is important to have a high density network to capture the spatial variability of extreme precipitation. The mean inter-station distance within the network is 17.5 km, with a maximum of 38 km. Orography has a large influence on extreme precipitation and therefore effort was made to ensure stations at higher elevation were included, although it is acknowledged that in general precipitation at high elevations is poorly monitored throughout the globe and hence underestimated. More than 30 stations are at elevations between 100 and 200 m, and 14 between 200 and 415 m. Ireland receives its moisture from surrounding sea's: the Irish Sea to the East, Celtic Sea to the

South, and the North Atlantic Ocean from the southwest to northern coast, with only minimal contribution from precipitation recycling (van der Ent et al., 2010). This influence should be well captured as 50 % of stations are located within 20 km of the coast. The inclusion of 32 B- and C-List stations did not introduce many stations with large quantities of missing data. On average, stations have less than 1.5 % missing, with the least complete station having 10.4 % of its record missing.

### 3.2.2 Data quality control

Both datasets have undergone basic quality control (QC) from their respective measurement agencies. However, 3 further checks/modifications were undertaken here:

- 1.) **Pre-processing raw data:** Raw precipitation data from the MIDAS database needs pre-processing before use due to the presence of duplicate values for a single day. Each row in the downloaded time-series is given a version number (1 means it has been quality controlled, 0 means it has not and was therefore assigned missing here). However, there are many cases where a single date has multiple quality controlled precipitation values. In some cases the precipitation value is the same, so it does not matter which row is taken, but in others the precipitation value is considerably larger. In these instances the BADC system has overwritten an entry, which can introduce duplicates. The most recent of these was taken as the value (as recommended by the Met Office).
  
- 2.) **Match dates between agencies:** While both agencies record 24 hour precipitation totals at 09:00 UTC each day, Met Éireann assign that value to the previous day (i.e. the day with the majority of time recording – 15 hours), while the UK Met Office assign the value to the day of recording (9 hours). This means the associated dates of the data are different by one day. This has a significant effect when assessing the day in which very heavy precipitation occurred. For example, a simple correlation of daily time-series from 1941-1973 between two neighbouring sites on the border of Ireland and Northern Ireland (Met Éireann, St538 and UK Met Office, St16478) shows a Pearson correlation of  $\sim 0.13$  without modifying the dates and  $\sim 0.78$  when the dates are modified to

match. Here, all the time-series from Northern Ireland are modified (by one day) to match those of Met Éireann.

**3.) Day-of-the-week analysis:** Before automated precipitation recorders, measurements were recorded by a manual observer. The nature of precipitation measurement is such that if the rain gauge was not emptied on a daily basis, the amount of rainfall would accumulate (for example, if measurements were not taken over the weekend, then rainfall totals on Monday's would be systematically higher). Precipitation for each day in the week between 1973-2011 was totalled for each of the final 126 stations (see Appendix 2) and summarised in the boxplot in Figure 3.6. There is no obvious systematic bias between days of the week and therefore this issue does not exist for the stations used in this analysis.

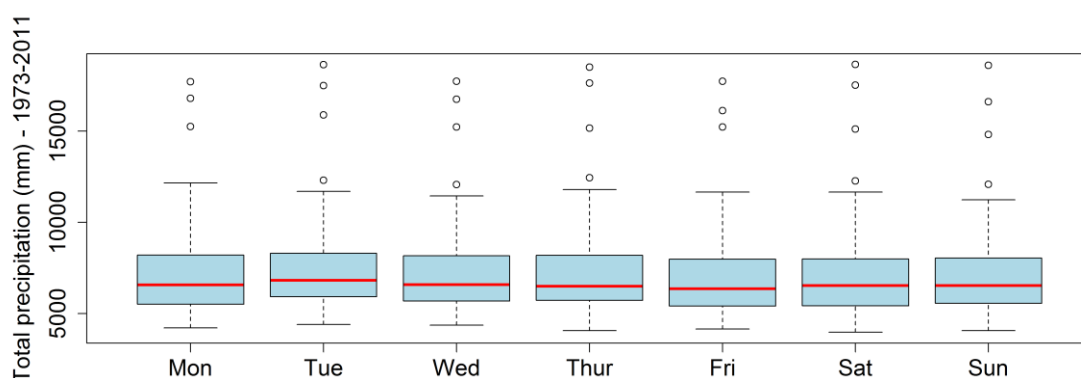


**Figure 3.6: Total precipitation (mm) per day of the week from 1973-2011. Boxplots summarise totals for each of the 126 final precipitation stations, with the red line representing the median, and boxes the interquartile range (IQR); whiskers extend to the most extreme data point, which is no more than 1.5 times the IQR from the box, and black circles are outliers beyond this range.**

### 3.2.3 Infilling and bridging rainfall time-series

To ensure accuracy of estimated statistics, particularly the calculation of indices involving 'number of days of rain', a complete data record for the period is needed. The relatively stringent percentage missing data criteria for A-List stations ( $\leq 5\%$ ) minimises the influence of temporal gaps on the calculation of variables. However, the inclusion of 32 B- and C-List stations introduced 7 stations with more than 5% missing. Furthermore, the network was optimised for longest possible length (at least 39 years

from 1973 to 2011) of records, however, inclusion of B- and C-List stations means some stations do not cover the entire 1973 to 2011 period.

To minimise both these issues, network wide infilling and bridging was undertaken. The 1 km daily precipitation from Met Éireann (Walsh, 2012a; Walsh, 2012b) has a temporal coverage of 1941-2012 and spatially covers the entire Island of Ireland. All the underlying point based precipitation stations used here, were also used to produce the gridded product, so the 1 km grid box containing the station is essentially a weighted average between the point based station and its neighbours (see Walsh (2012a) for more detail). Here, if a daily precipitation value is missing in the point-based time-series, then the equivalent value from the corresponding 1 km grid box is used. Also, if a station in the network does not have data covering a section of the 1973 to 2011 period, then the equivalent time-series slice from the corresponding grid box is directly bridged to the start (if the start date is > 1973) or to the end (if the end date is < 2011). Despite it being highlighted above that a grid estimate should not be used as a point-based measurement when dealing with extreme precipitation; it is argued here that having an estimate of missing precipitation is more reliable than leaving gaps in the record when extracting variables.

### 3.3 Methods

There are four main steps in the classification of extreme rainfall regions here as summarised in Figure 3.7. First, a pool of 17 variables describing a range of extreme precipitation characteristics was extracted for each infilled and bridged precipitation time-series. Second, Principal Component Analysis (PCA) was used to reduce the dimensionality of the pooled variables, identifying the most important components of variability within the dataset. Third, extreme rainfall regions were classified from cluster analysis on PCA scores and geographical location. Fourth, maps of the classified regions were produced.

The nature of classification in climatology is such that there is no universally identified method (Huth, 2008). Hence, there is no 'correct' classification of precipitation regions. The methodology used here is statistically based and thus many subjective decisions have to be made. For example, the number of principal components to retain (e.g. first 2 or 4 PCs), or number of clusters (e.g.  $k$  from 2 to 5) to select when applying the  $k$ -

## ERR Method – Sensitivity Testing

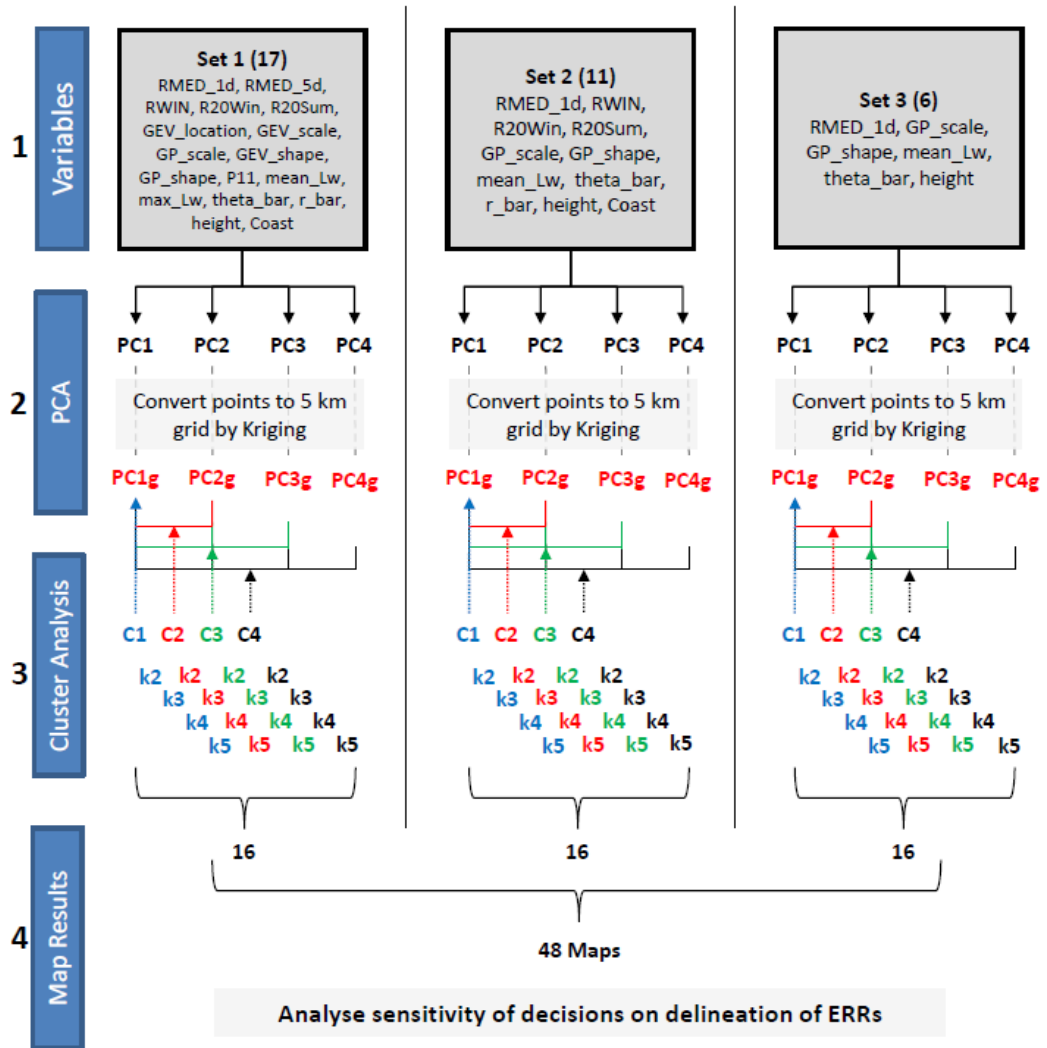


Figure 3.7: Diagram of methodological analysis: Step 1 selection of variables; Step 2 Selection of Principal Components (PCs) and conversion of rotated PCs to 5 km grids with kriging (PCg); Step 3 Cluster Analysis with just PC1 is C1 while PC1 and 2 is denoted C2;  $k = 2$  to 5 are the number of clusters, and Step 4 is mapping results and examine the impact of methodological decision of final ERR delineation.

means algorithm. The only way to measure the influence of these subjective decisions on the final outcome, here delineation of ERRs, is to perform a sensitivity analysis at each key stage of analysis. The sensitivity of those decisions tested is shown in Figure 3.7. Most critically, this classification procedure cannot be treated as a completely black-box experiment; it must be supplemented with physical understanding of processes governing extreme precipitation.

### 3.3.1 Extreme value theory and circular statistics

The statistics of extreme values involves the description of the behaviour of

$$M_n = \max\{X_1, \dots, X_n\},$$

where  $X_1, \dots, X_n$  is a sequence of independent random variables having a common distribution. Here,  $X_i$  represents values of daily total precipitation, and  $M_n$  is the maximum value over  $n$  number of observations in a single year ( $n = 365$  or  $366$ ) so the block maximum,  $M_n$ , becomes the annual maximum of a time-series and a collection of  $M_n$  is known as the annual maximum series (AMAX). Here, 1-day AMAX of daily precipitation. The AMAX follow a generalized extreme value (GEV) distribution (see Coles, 2001), given by:

$$G(x; \mu, \sigma, \xi) = \exp \left\{ - \left[ 1 + \xi \left( \frac{x - \mu}{\sigma} \right) \right]^{-1/\xi} \right\}, \quad 1 + \xi \left( \frac{x - \mu}{\sigma} \right) > 0.$$

**Equation 3.1**

where  $-\infty < \mu < \infty$ ,  $\sigma > 0$  and  $-\infty < \xi < \infty$ . The location parameter  $\mu$  determines the position of the distribution, the scale parameter  $\sigma$  the width, and the shape parameter  $\xi$  the tail. For  $\xi < 0$ , the tail has a finite upper value (Weibull distribution), for  $\xi > 0$ , the tail is long with a power law decay (Fréchet distribution) and in the limit  $\xi \rightarrow 0$ , the tail has exponential decay (Gumbel distribution).

Observations of extremes for most systems are by definition rare; hence data to derive distributions are limited. An advantage with climate and hydrological systems is that they are observed often at regular intervals. In such cases where daily observations exist, threshold models can be used, also known as Peaks-Over-Threshold (POT) or Partial Duration Series. Let  $X_1, X_2, \dots$  be a sequence of independent and identically distributed (*iid*) random variables and extreme events are defined as those of the  $X_i$  that exceed some high threshold. The POT follow a Generalized Pareto (GP) distribution (see Coles, 2001), given by:

$$H(y; \tilde{\sigma}, \xi) = 1 - \left( 1 + \frac{\xi y}{\tilde{\sigma}} \right)^{-\frac{1}{\xi}}, \quad y > 0 \text{ and } \left( 1 + \frac{\xi y}{\tilde{\sigma}} \right) > 0.$$

**Equation 3.2**

where  $u$  is the station specific threshold (here 99<sup>th</sup> percentile of wet days ( $\geq 1$  mm), P99) and  $\tilde{\sigma} = \sigma + \xi(u - \mu)$  the scale parameter. The GEV and GP distributions are related through the shape parameter  $\xi$ . The 'extRemes' package in R (Gilleland and Katz, 2011) was used to fit both extreme value distributions with parameters estimated using the Maximum Likelihood Estimation (MLE) (i.e. find maximum of Likelihood Function numerically by seeking the probability distribution that makes the observed data most likely).

Assumptions may be violated if data are not *iid* (trends or serial correlation). This is particularly important for POT as extreme precipitation or flood events can last for multiple days thereby more than one observation will exceed the threshold for the same event. This can be resolved by declustering the original data so that exceedances should be separated by at least  $m$  days (runs-declustering; see Section 4.3.2.1 for more detail of this method). Following Jones et al. (2014a), each precipitation event was separated by an interval of at least 2 days to ensure only independent events were considered (As a rule of thumb, the lifetime of large extratropical cyclones is 1-2 days (Trenberth et al., 2003)). The maximum of the cluster will be included in the POT rather than individual cluster members.

A GEV or GPD can show a change in any of the mean (location), variance (scale), or kurtosis (shape i.e. tail behaviour) parameters without a change in the others. The shape parameter is of particular interest to the examination of extremes as a value  $< 0$  (light/short tailed) is evidence that the original distribution of the data has a fixed upper limit,  $\rightarrow 0$  has exponential decay (e.g. normal distribution), and  $> 0$  (heavy/long tailed) comes from a long tailed distribution and is important as it implies more 'extreme' extremes are possible.

Circular statistics were used to identify timing characteristics of extreme precipitation following Institute of Hydrology (1999). The Julian day of extreme precipitation occurrence (here defined as POT P99 events) is converted to a directional variable then the directional mean and variance is calculated (see Fig. 3.8 for a schematic). The Julian day of extreme precipitation occurrence ( $JD_i$ ) can be converted to an angular value ( $\theta_i$ ) using:

$$\theta_i = JD_i \frac{2\pi}{ND}$$

**Equation 3.3**

where  $ND$  is the number of days in a year ( $ND = 365$  or  $366$  for a leap year). The 31<sup>st</sup> of May is used as the start-of-year (after Black and Werritty, 1997) to avoid a discontinuity in numerical date values during the main seasons of extreme precipitation/flooding. The directional mean,  $\bar{\theta}$ , is calculated as the addition of unit vectors:

$$\bar{\theta} = \tan^{-1} \left( \frac{\bar{y}}{\bar{x}} \right)$$

**Equation 3.4**

where:

$$\bar{x} = \frac{1}{N} \sum_{i=1}^N \cos(\theta_i) \qquad \bar{y} = \frac{1}{N} \sum_{i=1}^N \sin(\theta_i)$$

**Equation 3.5**

The mean direction ( $\bar{\theta}$ ) represents a directional measure of a sample consisting of dates of extreme precipitation occurrence.  $\bar{\theta}$  can be converted to a mean day of extreme precipitation,  $MDEP$ , adapted from Cunderlik et al (2004):

$$MDEP = \bar{\theta} \left( \frac{ND}{2\pi} \right)$$

**Equation 3.6**

In addition, the measure of dispersion (variability) of the individual dates around the mean is defined as (Bayliss and Jones, 1993):

$$\bar{r} = \sqrt{\bar{x}^2 + \bar{y}^2}, \qquad 0 \leq \bar{r} \leq 1$$

**Equation 3.7**

The variable  $\bar{r}$  represents a dimensionless dispersion measure. A value close to one signifies that all events in the sample are closely grouped about the mean direction (strong seasonality) while a value closer to zero signifies greater variability in the occurrence of events (weak seasonality) (Cunderlik et al., 2004).

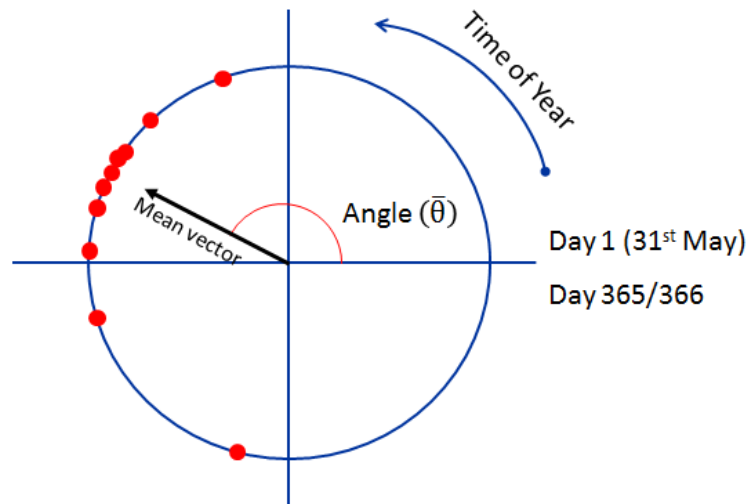


Figure 3.8: Schematic of calculation of timing variables, the mean timing of extreme precipitation events (red dots) is represented as the mean vector ( $\bar{\theta}$ , theta\_bar) and the variability (i.e. the seasonality) as  $\bar{r}$ , r\_bar.

### 3.3.2 Variable selection

There is no standard definition of ‘extreme precipitation’. Some studies define it as very rare events, such as the precipitation event that occurs once every 50 or 100 years. Observed precipitation datasets are rarely longer than 100 years, so only few of these very rare events will be observed. Extreme Value Theory (EVT), as discussed above, can also be used to make inferences on longer return period amounts in shorter records. However, here ‘moderate extremes’ that occur at least once a year (Zhang et al., 2011) are examined. Given the focus on flooding in this thesis, the selection of precipitation variables used to classify extreme rainfall regions is based on *characteristics* of extreme precipitation, as it is the characteristics that are often more important than total amount for flood generation (Trenberth et al., 2003). A pool of 17 extreme precipitation variables derived from 6 categories describing key precipitation characteristics and physiographic controls are used for PCA: 1.) Magnitude, 2.) Variance, 3.) Tails of extreme distributions, 4.) Persistence, 5.) Timing, and 6.) Physiographic controls (Table 3.2). Selection of magnitude, timing, variance, and tails

of extreme value distributions variables were informed by Jones et al. (2014a), persistence from (Wilby et al., 1998), as well as two physiographic variables (elevation and distance to coast).

**Table 3.2: Pool of 17 precipitation variables used in PCA. Variables 1-15 were calculated between calendar years 1973-2011.**

Variable	Details	Units
<i>Magnitude</i>		
1. RMED-1d	Median of all 1-day AMAX	mm
2. RMED-5d	Median of all 5-day AMAX	mm
3. RWIN	Mean Winter total wet-day rainfall	mm
4. R20win	Number of very heavy rainfall days ( $\geq 20$ mm) in Winter (Oct-Mar)	days
5. R20sum	Number of very heavy rainfall days ( $\geq 20$ mm) in Summer (May-Aug)	days
6. GEV_location	GEV parameter*	-
<i>Variance</i>		
7. GEV_scale	GEV parameter*	-
8. GP_scale	GP parameter*	-
<i>Tails of extreme distributions</i>		
9. GEV_shape	GEV parameter*	-
10. GP_shape	GP parameter*	-
<i>Persistence</i>		
11. P11	Probability of wet-day conditional on the previous day being wet	-
12. mean_Lw	Mean wet-spell length in days, which is directly related to P11	days
13. max_Lw	Median annual maximum wet-spell length	days
<i>Timing</i>		
14. theta_bar	Mean time-of-year of POT, starting 31 <sup>st</sup> May	Angle ( $\bar{\theta}$ )
15. r_bar	Dispersion of individual dates of POT (i.e., Seasonality)	-
<i>Physiographic</i>		
16. height	Elevation of each station	m a.s.l.
17. Coast	Minimum distance to coast	km

**Note:** Details of variables marked with (\*) can be found in Section 3.3.1; Wet-day is defined as  $\geq 1$  mm of precipitation to remove potential bias introduced from under-reporting of small rainfall amounts (Zhang et al., 2011).

Figure 3.9 shows Pearson correlations between each of the 17 extreme rainfall variables. Several variables are very strongly correlated and are thus redundant. For example, RMED\_1d and RMED\_5d have a correlation coefficient of 0.97 while RMED\_1d and GEV\_location are essentially the same ( $\rho = 0.99$ ). The aim of PCA is to eliminate this redundant information; however, having too many strongly related variables describing a single aspect of precipitation will also introduce bias. The effect

of the initial pool of variables on the final classification of regions is examined by performing the analysis on different combinations of variables as summarised in Table 3.3. Set 1 includes all 17 variables, Set 2 has the obvious redundant variables removed, leaving 11. For example, RMED\_1d is used instead of RMED\_5d and GEV\_location while the scale and shape parameters from the GP distribution are preferred over the GEV given they are estimated from a larger sample (POT) than GEV (AMAX) and are likely to provide more reliable parameter estimates (Coles, 2001). Set 3 includes only 1 variable from each of the six categories.

The spatial variability of each variable in Set 2 is mapped in Figure 3.10. Coastal and upland areas are wetter (RWIN), and receive higher annual maximum precipitation (RMED\_1d) and more days of very heavy rainfall in winter (R20win) and summer (R20sum), particularly in the southwest with several stations recording annual maximum values of over 90 mm on average which is around three times higher than for low lying inland areas. The variability of extreme rainfall magnitude in these wetter areas is also larger (GP\_scale) while the timing of these events occur later in the year (thea\_bar values between 2.5 and 3.4 which equates to 23<sup>rd</sup> October and 14<sup>th</sup> December, respectively). Some inland stations receive their large rainfall events between the end of August and beginning of September (theta\_bar values between 1.36 and 1.8 which equates to 18<sup>th</sup> August and 8<sup>th</sup> September, respectively). The persistence of rainfall in general is greater for stations along the western seaboard, with wet-day spell lengths of between 6 and 9 days on average, which is over twice as high as most stations in the midlands and east. Surprisingly, the variability in event magnitude (GP\_scale) is not correlated with variability in timing, i.e. seasonality (r\_bar) ( $\rho = 0.04$ ). In general, the seasonality of extreme precipitation in Ireland is low with the highest r\_bar value only 0.56 with a mean of 0.38. There does not appear to be strong spatial pattern in the shape parameter (GP\_shape). 63% of stations have values > 0 (heavy tailed) with the largest of these occurring around the Wicklow Mountains in the east. It was expected that areas along the western seaboard would have had heavier tails than in the east, however this was not the case. Jones et al. (2014a) also found it difficult to interpret the spatial distribution of the shape parameter in the UK. Perhaps this could be due to the difficulty in estimating this parameter (there was by far more estimation uncertainty in GP\_shape compared to GP\_scale) or that the nature of

coastal precipitation in Ireland is dominated by low intensity long duration events (Sweeney et al., 2014).

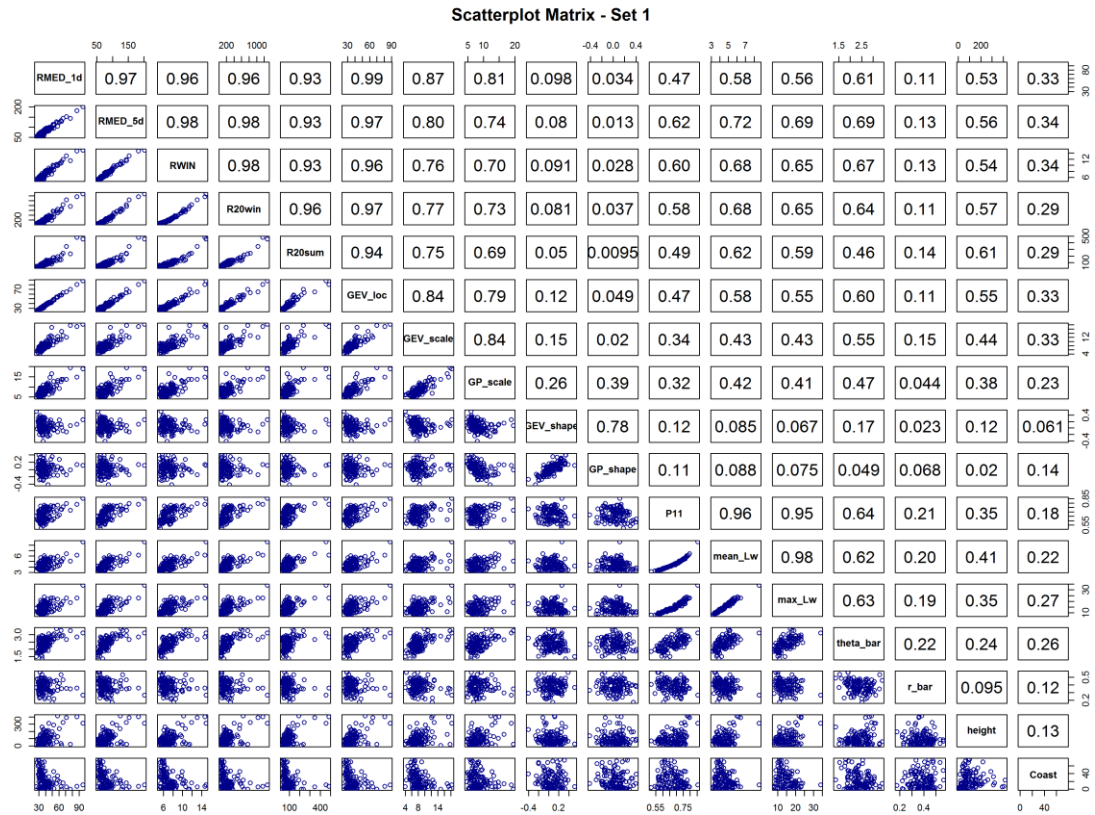
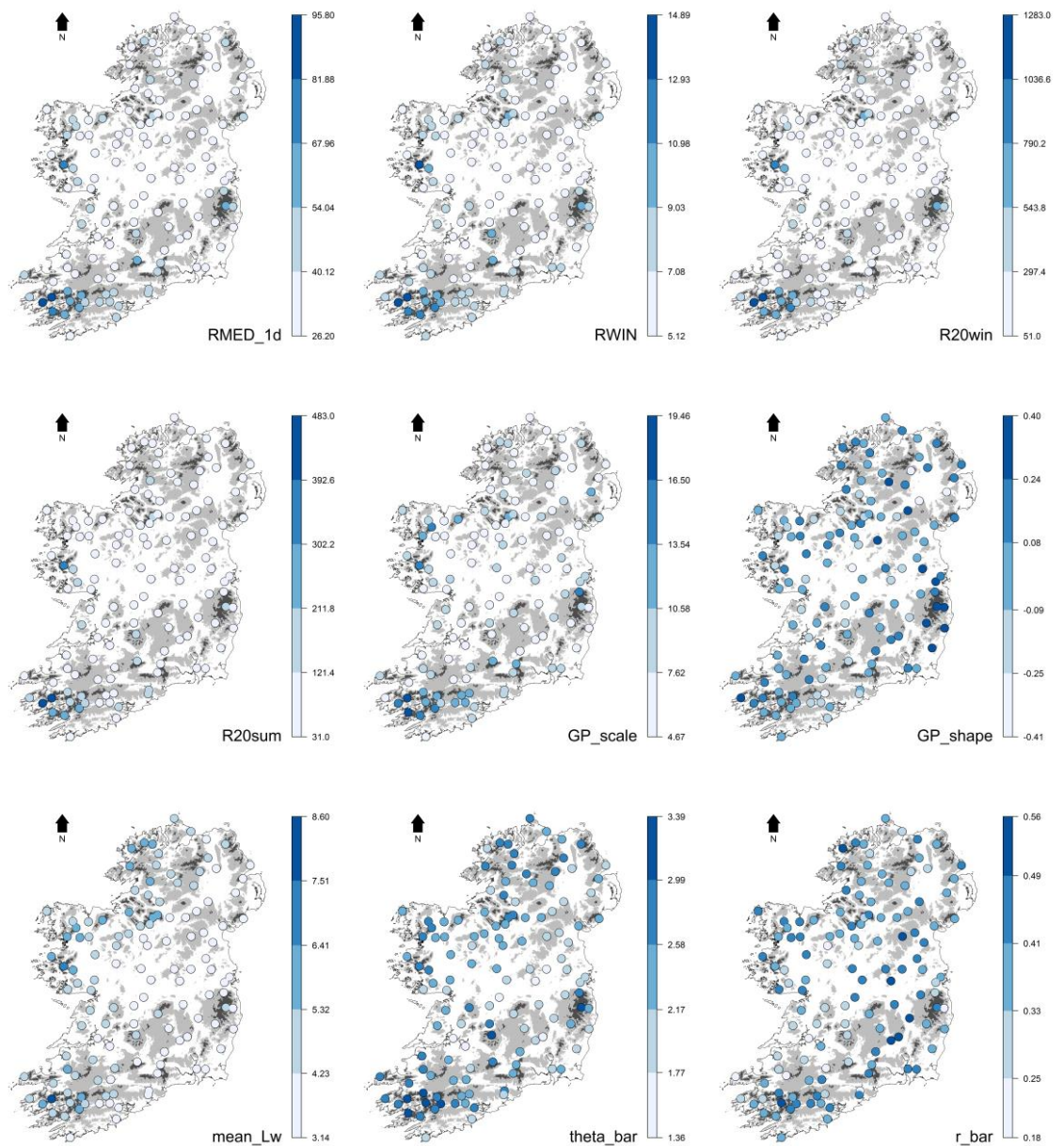


Figure 3.9: Scatterplot matrix for all 17 extreme rainfall variables.

Table 3.3: Selection of 3 sets of extreme rainfall variables: Set 1 (Full 17), Set 2 (Redundancy removed), and Set 3 (Minimum number, i.e. 1 per category).

Variable Category	Set 1 (full) [17]	Set 2 (Redundant) [11]	Set 3 (minimum) [6]
Magnitude	RMED_1d; RMED_5d; RWIN; R20win; R20sum; GEV_location	RMED_1d; RWIN; R20win; R20sum	RMED_1d
Variance	GEV_scale; GP_scale	GP_scale	GP_scale
Tails	GEV_shape; GP_shape	GP_shape	GP_shape
Persistence	P11; mean_Lw; max_Lw	mean_Lw	mean_Lw
Timing	theta_bar; r_bar	theta_bar; r_bar	theta_bar
Physiographic	height; Coast	height; Coast	height



**Figure 3.10:** Measures of extreme rainfall variables in set 2 for each of the 126 stations (excluding 'height' and 'coast'). Areas of low (< 100 m) medium (100-300 m) and high (300-1000 m) elevation are marked in white, light grey, and dark grey, respectively.

### 3.3.3 Principal component analysis and cluster analysis

One of the most widely used methods for exploring the spatial and temporal variation and structure within large multivariate datasets is Principal Component Analysis (PCA); also referred to as Empirical Orthogonal Function (EOF) Analysis. This is done by reducing a dataset containing a large number of variables to one with fewer new variables. These new variables are linear combinations of the original ones which represent the maximum possible fraction of variability contained in the original data (Wilks, 2011). The main reason why PCA is needed before application of Cluster

Analysis is that if variables are very similar, they will be given too much weight during clustering, thereby overemphasising the importance of those variables – PCA overcomes this limitation.

Despite the aim of objectively, rather than subjectively, classifying extreme rainfall regions, there is still an unavoidable number of methodological decisions must be made in application of PCA: 1.) The correlation matrix, rather than covariance matrix, was used as the variables are all measured in different units (Jolliffe, 1990); 2.) The truncation of the number of PCs is largely subjective, with the most common method specifying a sufficiently large target variance of the original data captured by the PCs (say between 70 to 90 %), but balanced on physical interpretability as PCs become more complex moving from the first (Jolliffe, 1993); and 3.) Huth et al. (2007) argue that rotating PCs can improve physical interpretation of results; this is especially the case if the joint variability of PCs rather than individual variability is of interest (as is the case here with ERRs). So where some unrotated components are difficult to interpret because many of their loadings are reasonably large in size, rotation attempts to force most loadings towards zero and the remainder towards unity, thereby making the rotated components easier to interpret (Jolliffe, 1993). Rotation was performed using VARIMAX rotation.

Cluster Analysis with the k-means algorithm was used to objectively group stations with similar rotated PC scores. A drawback with the k-means algorithm is that the number of clusters must be defined *a priori*. As stated above, there is no correct number of rainfall regions, although by physical reasoning, if there are too few then many extreme precipitation generating mechanisms would be lumped together, while if too many the aim of classification (i.e. purpose-made simplification of reality (Huth et al., 2008)) would not be achieved. Following Jones et al. (2014a) a sensitivity analysis on the number of clusters  $k$  is performed, here, between 2 and 5. The k-means algorithm measures similarity in Euclidean distance and aims to minimise the within-cluster sum of squares (WCSS) (Wilks, 2011). While it is expected that stations near each other will have similar extreme precipitation characteristics, it is possible for stations in opposite parts of the Island to be part of the same cluster.

An additional source of subjectivity in this process is deciding where to draw the lines on the map separating clusters as data are point-based and hence boundaries arbitrary. To overcome this, PC scores were interpolated using ordinary kriging on a 5 km grid prior to Cluster Analysis. Kriging is particularly well suited to applications using precipitation data as it gives closer stations greater weight from implementation of a semi-variogram model (here using the Matérn model as in Brunson and Comber, 2015). So instead of a sample of 126 (point-based stations), a sample of 3465 (5 km interpolated grids) is used meaning that the division between clusters is less ambiguous. This step appears as an apparent contradiction and would have been avoided if the 1 km precipitation grid (introduced above) was used instead. However, it is argued that interpolating a more reliable extreme precipitation estimate in space (i.e. Estimate extreme from station based observation then apply kriging), is more appropriate than using extremes estimated from smoothed series (i.e. 1 km gridded product) that may not properly capture extreme events in the first place.

### **3.4 Results**

#### **3.4.1 PCA results**

Results concentrate on those from set 2 as seen above this is the most reasonable set to use as it removes obvious redundancy while retaining a good range of variables covering each of the 6 categories. However, the sensitivity of the set used is further tested below. For set 2, the first (unrotated) principal component (PC) explains 53 % of variability in the original dataset. The remaining PCs explain considerably less with 75 % and 84 % captured within the first 3 and 4 PCs, respectively. The selection of the number of PCs is subjective but the approach here is to select a subset that explains a sufficient degree of variance then test the impact on the number of remaining PCs on the final delineation of ERRs supplemented with physical reasoning. The scree plot in Figure 3.11 shows the dramatic decrease in proportion of variance explained after PC1 and a smaller decrease after PC4. Therefore, PCs 1-4 were retained and subject to VARIMAX rotation in order to simplify the PC loadings to aid interpretation.

Table 3.4 shows loadings for the first 4 unrotated and rotated PCs but description and interpretation here focuses on the rotated PCs summarised visually in the dot plots in Figure 3.12. PC1 summarises primarily the magnitude of extreme precipitation with

negative PC1 values representing stations with higher precipitation magnitude. However, 10 of the 11 set 2 variables all contribute in the same direction as PC1, albeit with lesser weight, and because PC1 is so dominant suggests that there is relatively simple structure to extreme precipitation in Ireland. For example, height, GP\_scale, mean\_Lw, and theta\_bar are all strongly correlated to PC1 in the same direction as the magnitude variables. Physical interpretation of PC1 becomes apparent when the interpolated PC1 scores are mapped (Fig. 3.13). Areas with increasingly negative scores tend to be in upland areas near the coast, have larger extreme precipitation magnitude, are more variable, have maximum precipitation occurring later in the year, and have more persistent rainfall spells than areas with high positive PC scores that tend to be more inland.

PC2 appears to represent an interaction between extreme precipitation tail behaviour (GP\_shape) and variance (GP\_scale). More negative PC2 scores are related to stations with a heavier tailed distribution, while more positive PC2 scores represent lighter tails. PC2 summarises variance inversely to tail behaviour. More negative (positive) PC2 scores represent stations with lower (higher) extreme precipitation variance. When mapped the areas of the Kerry/Cork Mountains have the highest variance (as expected) but with lighter/bounded tails. Interestingly, (as noted above) when interpolated the eastern seaboard north and south of the Wicklow Mountains have the lowest precipitation variance but have the heaviest tails, which suggests that while on average the variance of precipitation is not as large as other regions, the potential for very 'extreme' extremes is greater.

PC3 and PC4 represent just 10 % and 9 % of the total variability respectively. PC3 summarises proximity to coast. There is not a simple linear relationship between elevation and coast on the Island of Ireland. Despite the majority of the upland areas being located close to the coast, some of the lowest lying areas also are near the coast. PC4 summarises seasonality, timing of maximum precipitation, and persistence of wet spells. Interesting patterns emerge when PC4 is mapped. The most southwest region is characterised as having low seasonality (r\_bar) with maximum precipitation occurring later in the year (theta\_bar) and more persistent wet spells (mean\_Lw). This is in contrast to inland and eastern regions (exception of the Wicklow Mountains) where

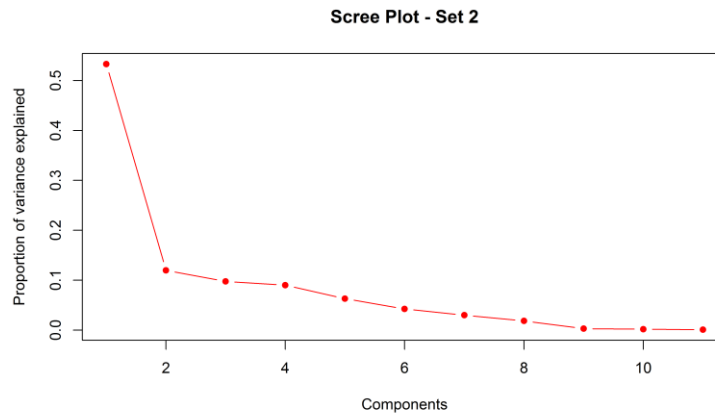
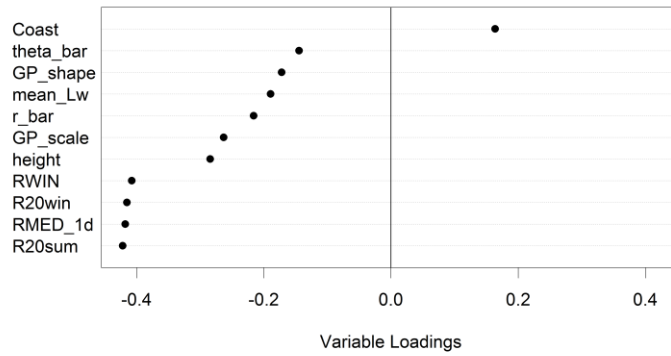


Figure 3.11: Scree plot of Principal Components (PCs) for the 11 variables in Set 2.

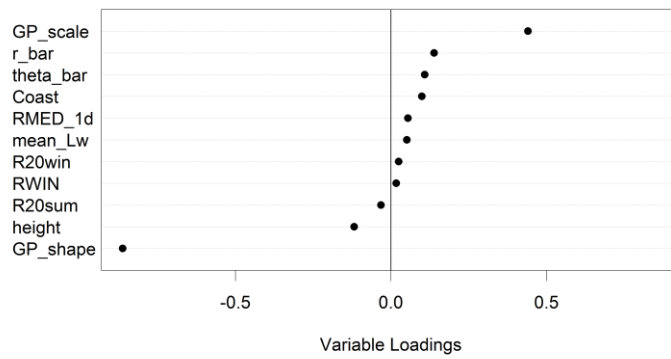
Table 3.4: Unrotated and rotated loadings for the first 4 Principal Components (PCs) for each of the 11 variables in Set 2. Proportion of variance of the entire dataset explained by each PC is given in italics and variables with greatest loading in bold. Loading values < 0.1 are left blank to aid interpretability.

Variable	PC1	PC2	PC3	PC4
<i>Unrotated - Set 2</i>				
RMED_1d	<b>-0.397</b>			
RWIN	<b>-0.402</b>			
R20win	<b>-0.404</b>			
R20sum	<b>-0.386</b>			
GP_scale	<b>-0.323</b>	-0.283	0.288	
GP_shape		<b>0.633</b>	<b>-0.512</b>	-0.344
mean_Lw	<b>-0.304</b>			0.241
theta_bar	<b>-0.288</b>	0.167	0.190	0.247
r_bar		<b>-0.387</b>		<b>-0.793</b>
height	-0.247	-0.245	<b>-0.576</b>	
Coast	0.141	<b>-0.524</b>	<b>-0.506</b>	0.271
<i>Rotated - Set 2</i>				
RMED_1d	<b>-0.418</b>			
RWIN	<b>-0.407</b>			
R20win	<b>-0.415</b>			
R20sum	<b>-0.422</b>			
GP_scale	-0.263	<b>0.441</b>		
GP_shape	-0.172	<b>-0.862</b>		
mean_Lw	-0.189			<b>0.341</b>
theta_bar	-0.144	0.109	0.167	<b>0.384</b>
r_bar	-0.216	0.139		<b>-0.848</b>
height	-0.284	-0.118	<b>-0.601</b>	
Coast	0.164	0.100	<b>-0.765</b>	
<i>Proportion of variance</i>	<i>0.53</i>	<i>0.12</i>	<i>0.10</i>	<i>0.09</i>
<i>Cumulative proportion</i>	<i>0.53</i>	<i>0.65</i>	<i>0.75</i>	<i>0.84</i>

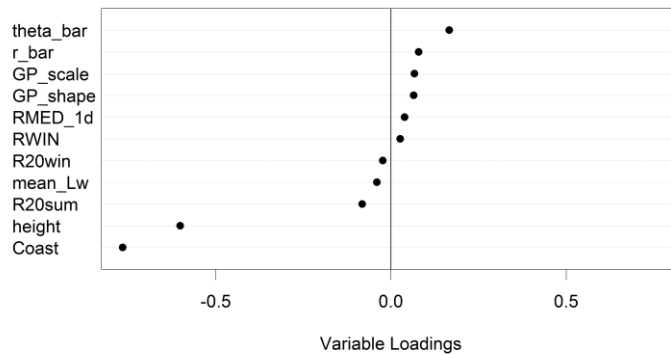
**Loadings Plot for PC1 - Set 2 - rotated**



**Loadings Plot for PC2 - Set 2 - rotated**



**Loadings Plot for PC3 - Set 2 - rotated**



**Loadings Plot for PC4 - Set 2 - rotated**

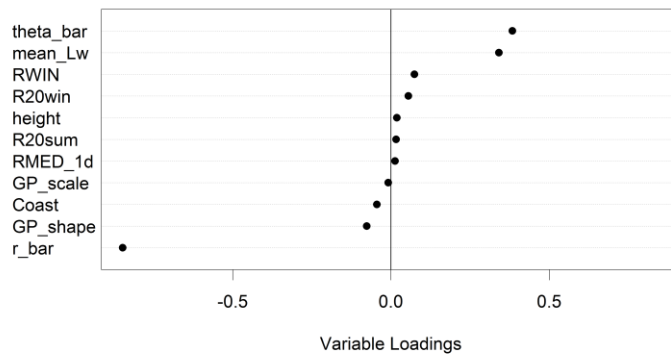


**Figure 3.12: Loadings dot plots for the first 4 rotated PCs from Set 2.**

seasonality is highest, extreme precipitation occurring earliest in the year with shorter wet spells mean lengths.

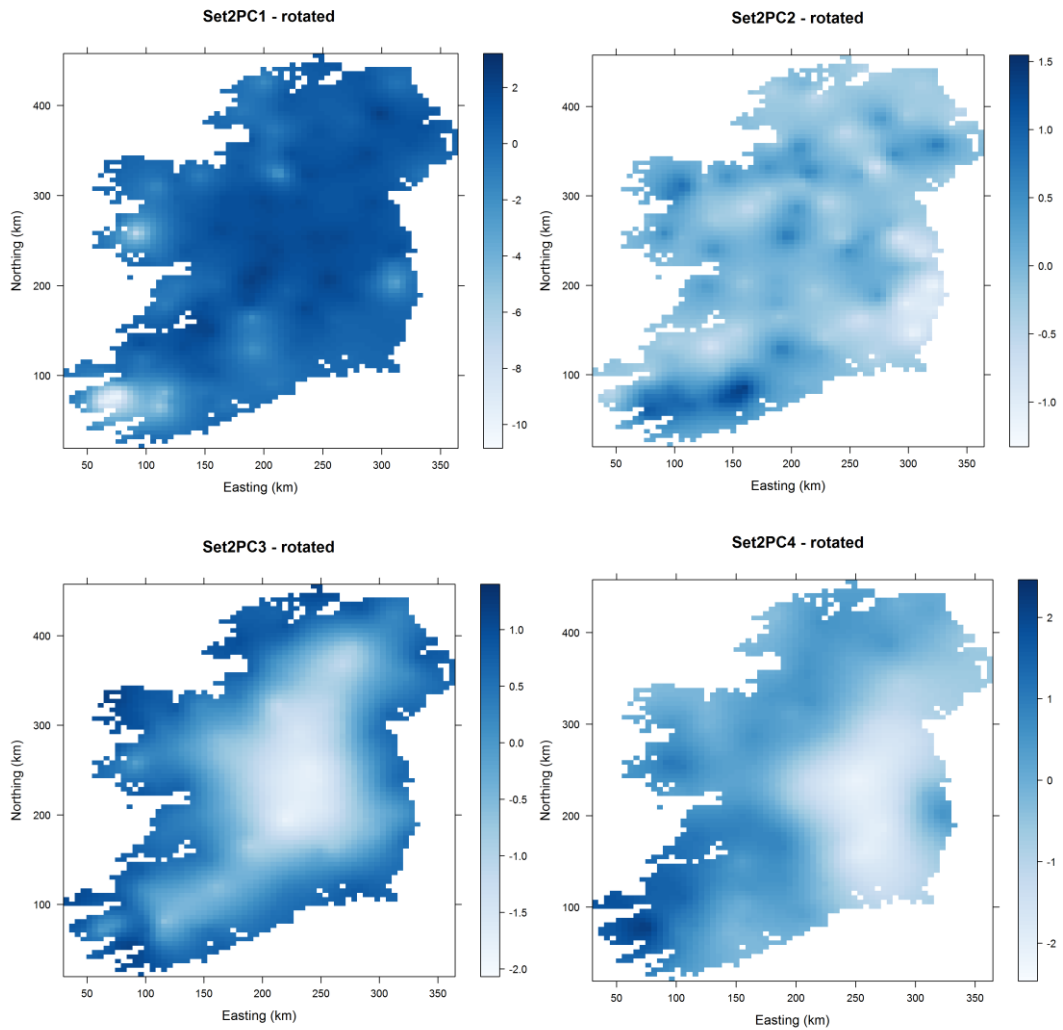


**Figure 3.13: Spatially interpolated (Kriging on 5 km grids) rotated PC scores for PCs 1-4 for set 2. PC1.) describes magnitude; PC2.) reflects differences in extreme distribution tail behaviour and variability; PC3.) proximity to the coast, and PC4.) seasonality, timing, and persistence of events.**

### 3.4.2 Cluster analysis results

The total within cluster sum of squares (TWCSS) for each  $k$  clusters used is shown in Figure 3.14. Similar to the scree plot above the recommended choice of number of clusters is to select a number at the 'elbow' of the plot. Following this guidance, the selection of  $k$  should be 3 or 4. Scatterplots of clusters using  $k = 3$  is shown in Figure 3.15 for station-based PC scores (left) and rotated gridded PC scores (right) for the first four rotated PCs. Notice that each cluster is not a distinct cluster in the strictest sense,

rather k-means provides a method to objectively classify PC scores that are most similar.

Figure 3.16 shows the sensitivity of selection of Sets 1-3 and rotated gridded PCs 1-4 keeping the number of clusters stationary (k-means with  $k = 3$ ). In all cases the patterns are dominated by PC1 (similar pattern between sets). The wet southwest mountainous region is given its own cluster, with a small area in the mountains of Galway. In general, a second cluster is given to the Atlantic facing upland coastal regions, and third the central plain of the Island. There are some differences between cluster extents when more PCs are retained. For example, the upland coastal cluster increases in extent up to PC3 and PC4 in all sets. In Set 2, the upland and coastal cluster also extends across the south eastern seaboard joining the Wicklow Mountains. Overall, the reasonably similar pattern regardless of Set (particularly for Set 1 and 2) used shows that PCA does an appropriate job of reducing the original dataset to while keeping fundamental structure. Similar patterns is evident for PC1 (magnitude) and PC2 (variance and tail behaviour, however the addition of PC3 (proximity to coast) and

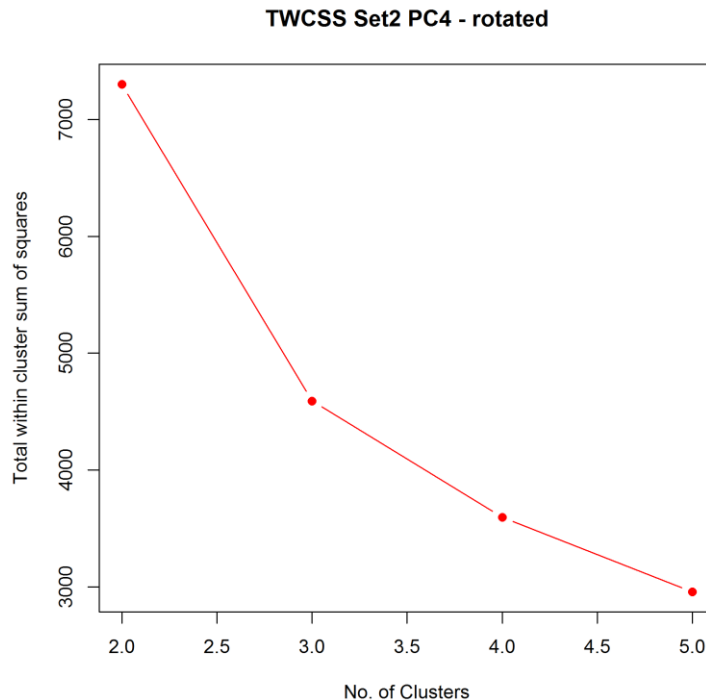


Figure 3.14: Total k-means within cluster sum of squares (TWCSS) for Set 2 using rotated PCs 1- 4.

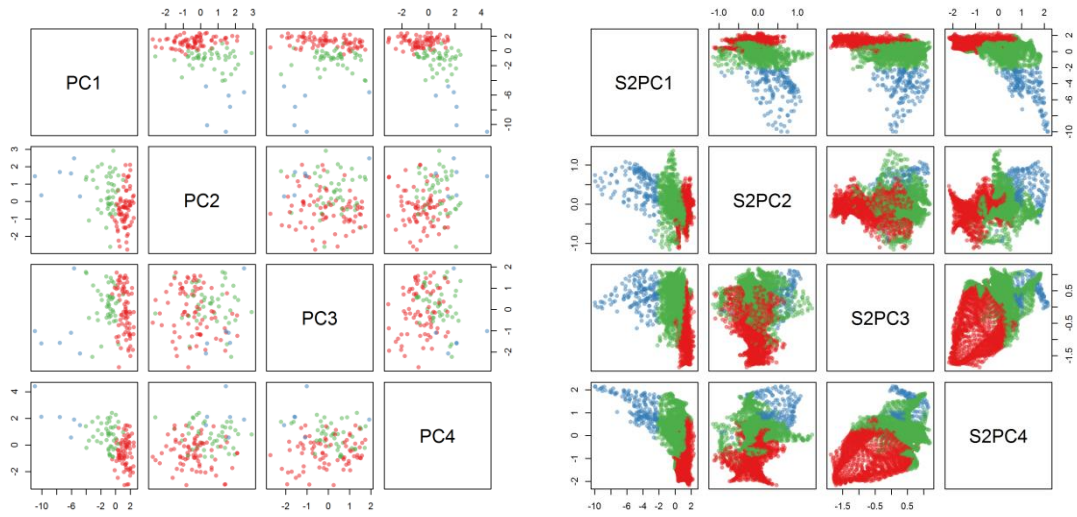


Figure 3.15: Scatterplot of clusters ( $k = 3$ ) for set 2 using rotated PCs 1-4 (left: station based scores, right: gridded scores).

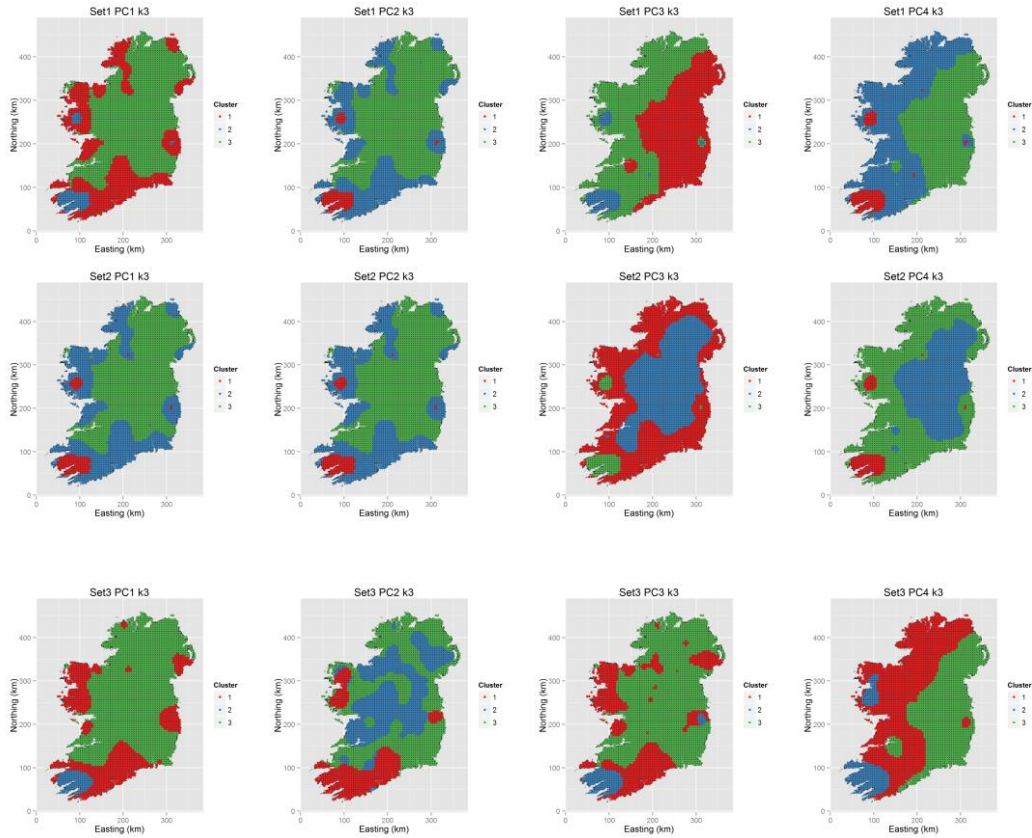
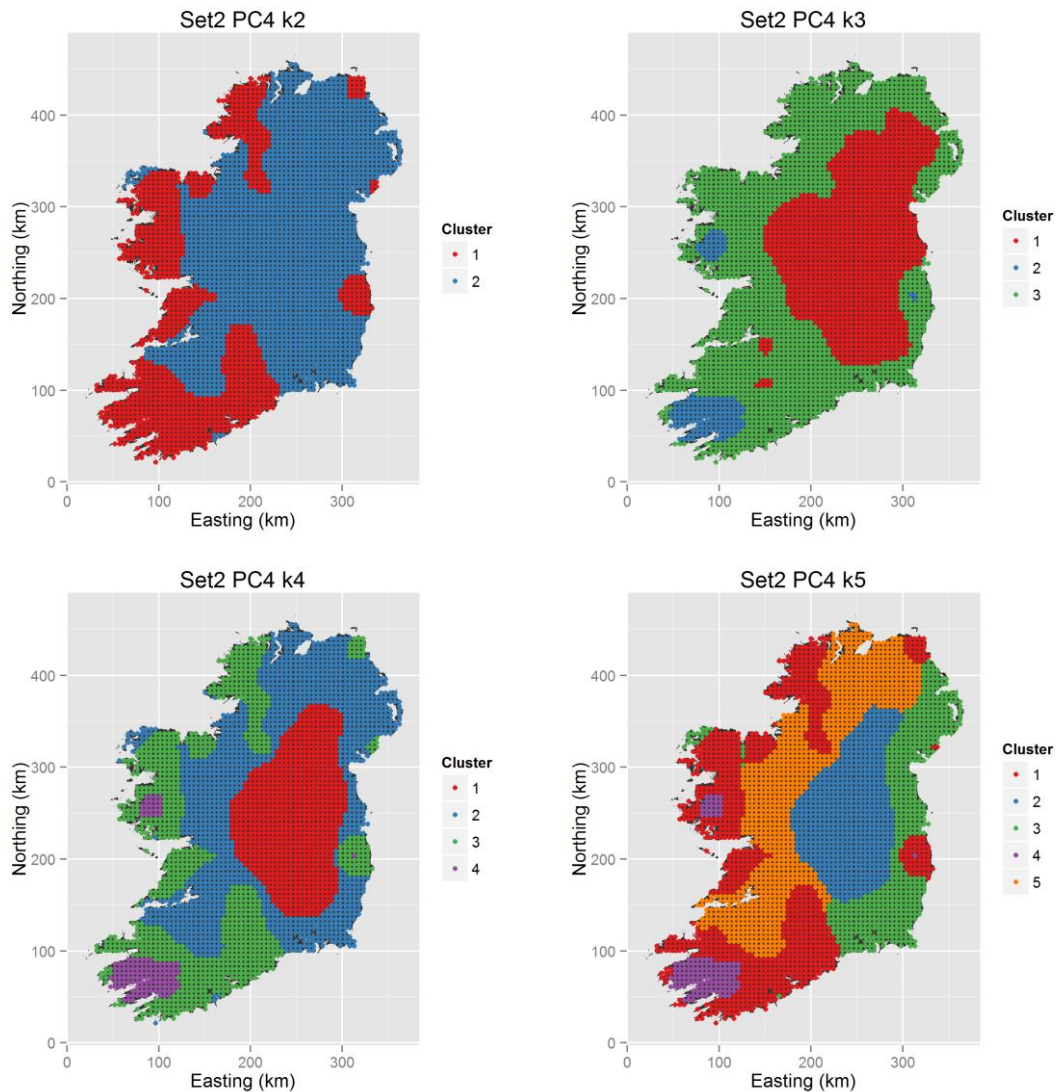


Figure 3.16: Sensitivity of selection of sets (rows) and rotated PCs 1-4 (columns) keeping number of clusters stationary (k-means with  $k = 3$ ).



**Figure 3.17: Maps of objectively identified homogeneous extreme rainfall regions for set 2 using PC1-4 and  $k$  from 2-5. Sensitivity of selection of number of clusters from  $k = 2$  to 5 keeping PCs and Set stationary (all rotated PCs 1-4 used for Set = 2).**

PC4 (seasonality, timing, and persistence) extends the sizes of the middle cluster between the most extreme precipitation in the southwest to the inland areas. This suggests that while the majority of extreme precipitation variability can be explained by PC1, there are important components that are not captured unless PC3 and PC4 are included. Therefore, the final classification of ERRs is based on clustering the first 4 rotated PCs, using set 2, balancing inclusion too many/too few variables.

The sensitivity of the choice of  $k$  using Set 2 and rotated PCs 1-4 is shown in Figure 3.17. It is clear that the choice of number of clusters has the largest impact on classification of ERRs. A prominent feature independent of the number of  $k$  used is the

mountainous areas in the southwest, Wicklow Mountains, and mountainous areas in the west and northwest for  $k = 2$ . For  $k = 3$ , the mountains in the southwest and Galway are assigned their own cluster, and the two remaining clusters are assigned to coastal and upland, and the central plain.  $k = 4$  breaks the coastal and upland cluster apart from more mountainous areas, while  $k = 5$  assigns the eastern seaboard its own cluster. The strongest feature that is consistently given its own cluster is the area in the southwest and a small mountainous area in Galway. The influence of orography on extreme precipitation is extremely strong here. Ireland is bowl-shaped, with the majority of mountainous regions on the coast, and the classification of ERRs reflect this. Rainfall regions based on 2 clusters is arguably too simplistic, whereas 4 and 5 clusters too complex. A 3 cluster solution is chosen here, balancing physical interpretation and simplicity, where, 1.) the most mountainous areas have the most extreme precipitation regime, 2.) there is a distinct extreme precipitation signature for upland and coastal areas, particularly in the Atlantic facing coastline, and 3.) the central plain is less effected by orography and much of the moist air traveling from the Atlantic has precipitated out before reaching it. A final test examined if the final ERRs (i.e. Set 2, rotated PCs 1-4, and  $k = 3$ ) were sensitive to use of rotated PCs compared to unrotated. It was found that VARIMAX rotation had minimal effect on the final boundary divisions; rather it provided simplicity in terms of physical interpretation of each of the PCs.

### 3.5 Climatology of extreme precipitation for final Extreme Rainfall Regions (ERRs)

The final classification of 3 spatially coherent Extreme Rainfall Regions (ERRs) is given in Figure 3.18:

- **Southwest (ERR-SW):** Smallest region ( $3430 \text{ km}^2$ ) with 10 precipitation stations and just a single IRN catchment. Largest average elevation (189 m a. s. l.) and standard deviation (146 m a. s. l.).
- **Coastal and Upland (ERR-CU):** Largest region ( $48,610 \text{ km}^2$ ) with 72 precipitation stations and contains 16 IRN catchments. Second largest average elevation (117 m a. s. l.) and standard deviation (105 m a. s. l.).

- **Inland and East (ERR-IE):** Second largest region (31,863 km<sup>2</sup>) with 44 precipitation stations and contains 12 IRN catchments. Lowest average elevation (93 m a. s. l.) and standard deviation (57 m a. s. l.).

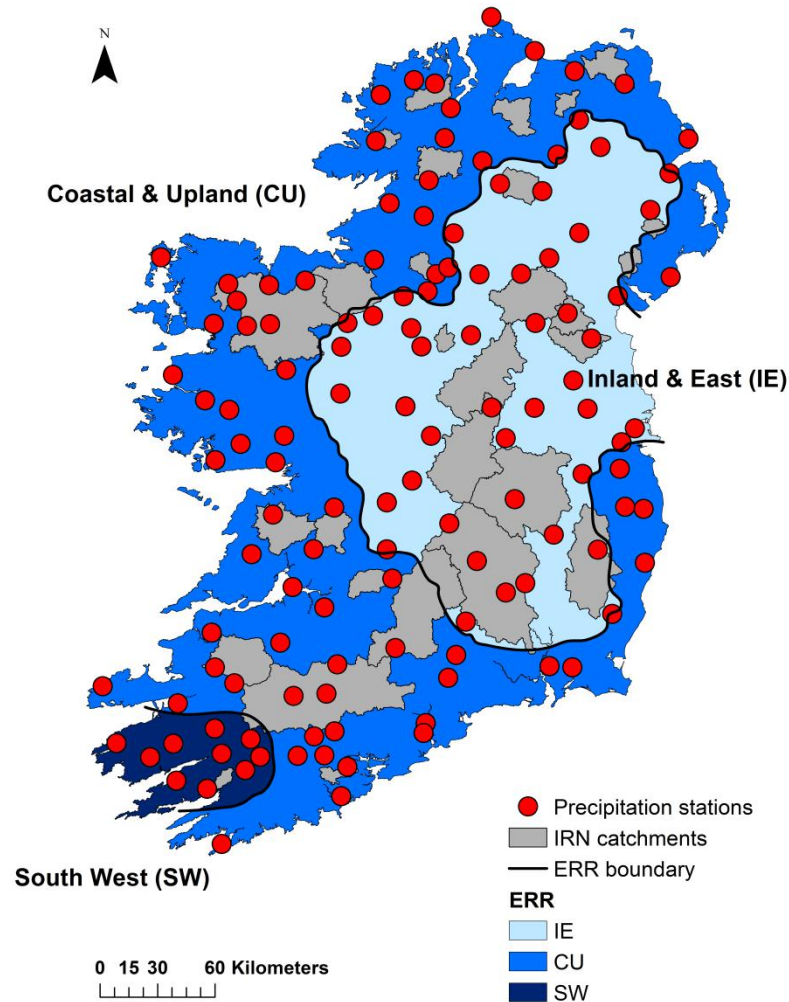


**Figure 3.18: Final classification of Extreme Rainfall Regions (ERRs) with precipitation stations used for classification and Irish Reference Network (IRN) streamflow catchments that will be used in following chapters.**

It is important to bear in mind that these new regions are a classification of the general extreme precipitation climatology, and will by definition mask some known smaller scale features such as the rain shadow in the lee of the Cork/Kerry Mountains and the higher precipitation totals in small mountainous areas in Galway and Wicklow that have been combined into the ERR-CU.

**Table 3.5: Statistics of 5 precipitation characteristics for each of the 3 ERRs. Central tendency is given by the median with an estimate of the range given by the lower and upper quartiles in brackets. Units as Table 3.2.**

Extreme precipitation characteristics		ERR-SW n = 10	ERR-CU n = 72	ERR-IE n = 44
Magnitude	RMED_1d	63.6 (56.8, 74.4)	39.1 (34.8, 43.6)	32.0 (30.8, 34.05)
	RMED_5d	130.2 ( 125.2, 144.6)	81.3 ( 73.0, 89.4)	61.85 ( 59.7, 67.1)
Variance	GP_scale	13.2 (11.2, 14.6)	8.0 (7.2, 9.6)	6.9 (6.1, 7.9)
Tails	GP_shape	0.026 (-0.008, 0.106)	0.050 (-0.093, 0.130)	0.036 (-0.057, 0.157)
Persistence	mean_Lw	5.1 (5.0, 5.9)	4.7 (4.1, 5.2)	3.8 (3.5, 4.2)
Timing	theta_bar	3.0 (2.9, 3.2)	2.4 (2.2, 2.7)	2.2 (1.9, 2.3)

Statistics of core extreme precipitation characteristics for each of the three regions is shown in Table 3.5. Analysis of Variance (ANOVA) and the Tukey multiple comparisons of means (at the 5 % level) are used to test if extreme precipitation characteristics are statistically different between each ERR. All extreme precipitation characteristics are shown to be statistically different between each region, except for the extreme tail parameter (GP\_shape), which is not surprising given the large range in values for each region (Table 3.5). Median maximum precipitation magnitude for ERR-SW (63.6 mm) is twice that of ERR-IE (32 mm) with almost twice the variance. The median wet-day spell length (mean\_Lw) for ERR-SW is 5.1 days in comparison to 4.7 for ERR-CU, and 3.8 for ERR-IE. Median timing of maximum precipitation in ERR-SW is the 20<sup>th</sup> November (theta\_bar = 3), 16<sup>th</sup> October in ERR-CU (theta\_bar = 2.4), and 6<sup>th</sup> October in ERR-IE (theta\_bar = 2.2), with 27 % of stations in ERR-IE having maximum precipitation between 17<sup>th</sup> August and 17<sup>th</sup> of September. The degree of extreme precipitation in late summer and early autumn could to an extent be due to the Island being at the receiving end of Atlantic hurricanes which have become deep mid-latitude depressions (Sweeney, 2014). The magnitude of maximum 5-day precipitation (RMED\_5d) is also given for each region given the importance of multi-day heavy precipitation to flood-generation, with median values of over 130 mm for stations in ERR-SW.

### 3.6 Discussion

Compilation of an appropriate dataset of daily precipitation stations for the analysis of extremes (Thesis Data Objective 1) allowed for a major research gap, that of

classification of Extreme Rainfall Regions (ERRs) for the Island of Ireland, to be filled (Chapter Objective 3.1) using a comparable methodology to Jones et al. (2014a). In this chapter, 3 ERRs were identified reflecting different extreme precipitation characteristics for a mountainous region in the southwest (ERR-SW), coastal and upland areas (ERR-CU), and for inland and east (ERR-IE) parts of the Island. Extreme precipitation characteristics, such as magnitude, variance, and timing of maxima, as well as mean wet-day spell are statistically significantly different between each ERR, thereby providing an evaluation of the success of the PCA and Cluster Analysis.

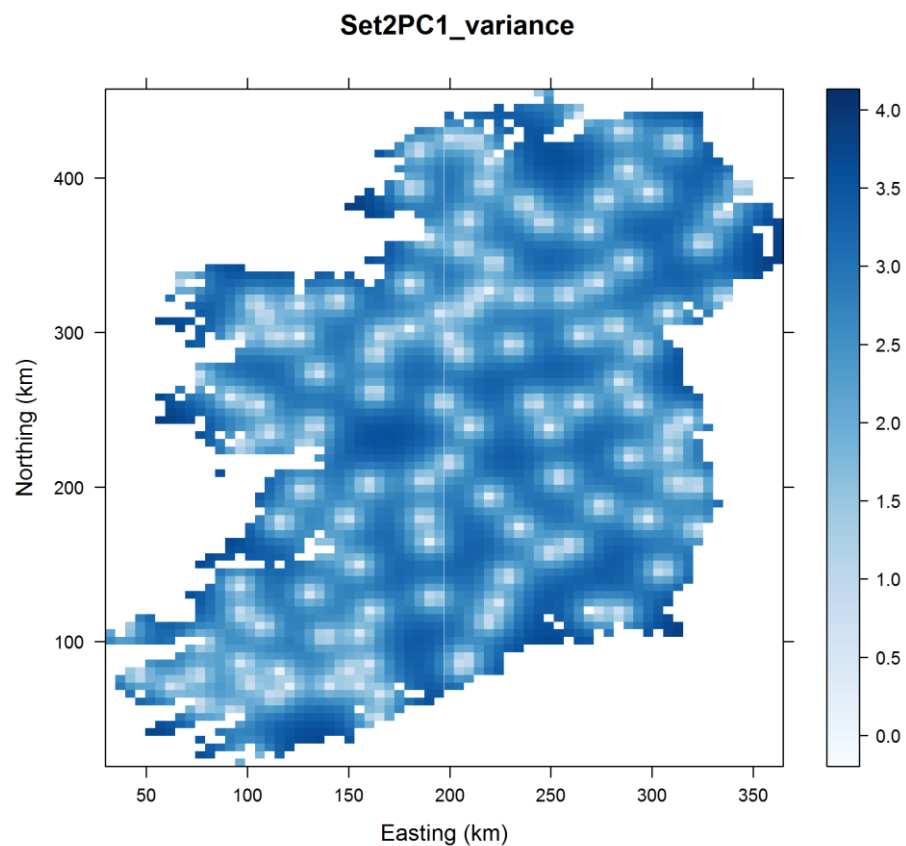


**Figure 3.19: Variance of kriged estimates for rotated PC1 scores for Set 2 shown in Figure 3.13.**

While effort was made to include dense a network as possible without unduly compromising data quality, some areas simply did not have records available that met the minimum criteria for A- B-, or C-Lists. Therefore for areas with stations gaps (such as the Sperrin Mountains), classification is more uncertain. A distinct advantage of kriging is that it is possible to obtain variances of the interpolated estimates and thus give an indication of the reliability of the estimates. Gaps in station density, particularly

in mountainous areas, would result in higher kriged variances and hence less reliability. Fig. 3.19 shows the variances of kriged rotated PC1 scores for set 2 as an indication of uncertainty. As expected the area over the Sperrin Mountains in Northern Ireland north towards the Inishowen Peninsula is underrepresented as is an area east of Belfast to the Ards Peninsula and a significant area of east Galway.

Despite these limitations, these results make an important contribution to understanding the spatial variability of extreme precipitation across the Island of Ireland. For example, Jones et al. (2014a) lumped all of Northern Ireland as a single ERR in their study. As data from Ireland was not included in the analysis of Northern Ireland, it was not possible to assess if edge effects had a significant influence. With the benefit of data from both sides of the border results here show that Northern Ireland does not respond as a single unit in terms of extreme precipitation climatology. There is a distinct difference between more upland areas that are found closer to the coast (ERR-CU) and that of flatter inland and eastern areas (ERR-IE). The lack of availability of a high density, daily station-based precipitation database that is quality controlled and infilled meant that comparable analyses across the Island of Ireland, and the greater British-Irish Isles (BI), could not be undertaken. While data from Ireland has contributed to European gridded products such as E-obs (Haylock et al., 2008), it has not been possible to include a dataset deemed appropriate for analyses of extremes, until now. Ireland is at the fringe of the Atlantic and is first landfall for Atlantic storm systems that have considerable socio-economic impacts, and is therefore a sentinel location for tracking hydroclimatic variability and change in Europe, and for understanding atmosphere-ocean dynamics in the Atlantic basin as a whole.

### **3.7 Chapter summary**

This chapter has provided the precipitation dataset necessary to complete Chapter Objective 3.1, classification of ERRs. The classification of ERRs will be used throughout this thesis to improve interpretability of physical processes governing extreme precipitation on Iol. They will also be used extensively in Chapter 5 for grouping synoptic drivers of floods as it is argued that a physically meaningful grouping of regions (extreme precipitation here given floods are rain-fed in Iol), rather than

political or agency boundaries, is a more appropriate unit of analysis. Finally, many studies in the application of PCA and/or Cluster Analysis do not extensively assess the sensitivity of subjective methodological decisions. It has been shown here that while some decisions are insensitive, selection of number of PCs to retain and selection of final number of clusters requires careful consideration, tailored to the aims of the study, and supported by physical interpretability at each stage. It is recommended where there is no single accepted standard for making these decisions (e.g. how many PCs to retain), the simpler more physically realistic decision is best.

The compiled precipitation dataset provides the foundation for detection of spatio-temporal changes in extreme precipitation and is the purpose of Chapter 4 with a focus on understanding floods.

## 4 Detection of Spatio-temporal Changes in Extreme Precipitation and Floods

---

### 4.1 Introduction

The globe has warmed by 0.85 [0.65 to 1.06] K over the period 1880-2012 (IPCC, 2013), and as outlined in Chapter 2, the hydrological cycle is expected to have intensified as a result. To date, there has been limited research confirming if extreme precipitation and/or floods in Ireland have also changed in line with other regions of the globe, and to the author's knowledge no study has considered both observed extreme precipitation and floods together, considering both Ireland and Northern Ireland. Statistical change or trend detection is the most widely used method for assessing *how* observed hydroclimatic time-series have changed and is the focus of this chapter. However, change detection cannot answer *why* any detected changes have occurred, i.e. to understand the drivers of change (this is the focus of Chapters 5 and 6). It is very difficult to determine the cause of a change in a streamflow time-series, compared to precipitation, as many climatic and non-climatic factors may influence streamflow at multiple scales. In fact, one of the main reasons for the IPCC to reduce confidence in statements on changes in observed floods is due to the confounding influence of human disturbance within catchments on any detected signal (Chapter 2). To limit this problem only catchments that are classed as 'near natural' from a reference network of streamflow stations in Ireland (Murphy et al., 2013a) are used. Data from reference networks have greater quality assurance and have been specifically designed to exclude catchments with large degrees of known human influence (e.g. urbanisation or water abstraction), and therefore are considered more suitable for identifying climate-driven changes in streamflow. This chapter aims to assess spatio-temporal changes in extreme precipitation and floods on the Island of Ireland (**Thesis Objective 2**) with the following chapter research questions:

- **Chapter Research Question 4.1:** How have extreme precipitation and flood characteristics (magnitude, duration, and frequency) changed in time and space?

- **Chapter Research Question 4.2:** Is there evidence of decadal climate variability (DCV) within extreme precipitation and/or flood indices, and if so, how might this affect interpretation of any detected trends in light of what is expected from climate change?

Previous studies in Ireland were unable to examine changes in flood *frequency* as there is no national Peaks-Over-Threshold (POT) database available. The need for a flood POT database was identified in Chapters 1 and 2 as a major thesis data objective and needs to be completed before the above research questions can be answered:

- **Thesis Data Objective 2:** Extract a flood Peaks-Over-Threshold (POT) database from near natural catchments for the Island of Ireland appropriate for the analysis of changes in flood frequency and links to atmospheric drivers.

With a fit-for-purpose network of precipitation stations for the analysis of extremes (Chapter 3) and streamflow from a reference network (Sect 4.2), extreme indices were extracted (Section 4.3) and a comprehensive trend analysis undertaken using a range of widely used statistical methods (described in Section 4.4). Results from this analysis are presented in Section 4.5 and discussed in Section 4.6.

## 4.2 The Irish Reference Network (IRN) of streamflow stations

Over the past 15 years a growing number of countries have invested in Reference Hydrometric Networks (RHNs) (Whitfield et al., 2012), to collect streamflow data that is minimally impacted by confounding human influences (Stahl et al., 2010). RHNs provide a more reliable basis for detecting climate variability and change and are increasingly employed in trend analyses (e.g., Lins and Slack, 1999; Douglas et al., 2000; Zhang et al., 2001; Burn and Hag Elnur, 2002; Yue and Wang, 2002; Hannaford and Marsh 2008; Hannaford and Buys, 2012). In addition, RHNs facilitate more focused and strategic investment in monitoring, increased understanding of hydrological change and a heightened awareness of the importance of long streamflow series for contextualising trends from recent decades.

As part of the *HydroDetect* project (Murphy et al., 2013a; Murphy et al., 2013b), the Irish Reference Network (IRN) of streamflow stations was identified by screening the national hydrometric network against a set of criteria based on best international RHN

standards, most notably the UK Benchmark Network and is described in detail in Murphy et al. (2013a) and Murphy et al., (2013b). The key criteria for streamflow stations to be included in the IRN include:

- Good and consistent hydrometric data quality (particularly at extreme flow ranges), as determined by hydraulic conditions at each site (stable control and accurate rating curves) and by expert judgement from hydrometric agencies.
- Near natural flow regime - zero or stable water abstractions and discharges (impact less than 10% of flow at or in excess of the low flow parameter Q95, i.e. the 5<sup>th</sup> percentile).
- Long record length (minimum 25 years).
- Limited land-use influence ( $\leq 2.5$  % of catchment area developed). Stations subject to arterial drainage were excluded where possible, otherwise post-drainage records were used if spatial coverage was lacking.
- Stations must be representative of Irish hydrological conditions and climatic regions with good geographical coverage, ensuring that stations from each of the eight Water Framework Directive (WFD) River Basin Districts (RBDs) are included.

In some circumstances it was necessary for rules to be relaxed in order to capitalise on the existing network. For example, stations that have good hydrometric quality across the full flow regime are difficult to obtain (Hannaford and Marsh, 2008) particularly in terms of quality ratings at high and low flow extremes. Avoidance of arterial drainage was particularly challenging given such widespread installation across the island to improve agricultural land drainage and reduce flood risk. This has resulted in the deepening and widening of river channels to improve their discharge conveyance resulting in changes in catchment response (Bhattarai and O'Connor 2004). For Irish conditions Lynn (1981) notes an acceleration of catchment response to rainfall, with increased intensity of flood peaks and more rapid recessions post-drainage. This would clearly confound detection and attribution of trends. Where a station was found to be drained, the post drainage record was included for consideration and close attention paid to the comparison of trends from other non-drained stations to check for consistency. Only where there were no obvious inconsistencies with trends identified

for non-drained stations were these stations included in the IRN. While attention was paid to ensuring homogeneity of records, a lack of metadata on land-use change means that such influences cannot be entirely ruled out. Similar challenges have been noted by Hannaford and Marsh (2008).

Stations from Northern Ireland that are part of the UK Benchmark Network (Bradford and Marsh, 2003; Hannaford and Marsh, 2006) were also included to facilitate an all-Island analysis. Thirty-five stations were identified for inclusion in the IRN plus a further 8 from the UK Benchmark Network (Murphy et al., 2013a; Murphy et al., 2013b). However, not all stations were used in this analysis. First, all IRN catchments that are nested (i.e. a smaller catchment contained within a larger catchment area) were removed as this could lead to misleading results through, for example, 'double counting' any statistically significant trends. This dropped the available stations from 43 to 32 non-nested catchments. Second, both the number and length of records for streamflow stations is much less than for precipitation, so selection of common periods to assess changes in both extreme precipitation and floods is limited to the number and length of record of streamflow stations. Only stations with greater than 30 years of data were selected for the analysis. This reduced the number of streamflow stations to 29.

Table 4.1 provides details of the 29 IRN station sub-set used here (note: the use of IRN henceforth also includes Northern Irish UK Benchmark catchments). The average record length is 41 years (minimum of 32 years and longest 63 years), with an average catchment size of 661 km<sup>2</sup> (smallest 64.8 km<sup>2</sup> and largest 2418.3 km<sup>2</sup>). All stations have data up to the end of 2009. Missing data is an important consideration for analysis of trends. Stations within the IRN sub-set have on average ~3.8 % of record missing. Stations have been infilled, where possible, using a hydrological modelling approach (see Murphy et al. (2013a) for details). The exceptions are the Northern Irish stations as it was not necessary due to the limited degree of missing data (< 1 %), and St26029 and St27002 (both < 2.5 % missing) due to the inability to fit an acceptable hydrological model to these stations. Visual inspections of St26019 and St27002 were made to ensure calculation of flood indices was not heavily impacted.

**Table 4.1: Station details with flood relevant Physical Catchment Descriptors (PCDs) for 29 IRN catchments.**

Station	Station name	River	Easting	Northing	Org.	ERR	Start Year	AREA (km <sup>2</sup> )	QMED (m <sup>2</sup> s <sup>-1</sup> )	SAAR (mm)	ALTBAR (m a. s. l.)	FLATWET	FARL	BFI	RBMED
6013	Charleville Weir	Dee	304411	290763	OPW	IE	1977	309.1	25.97	873	82	0.60	0.971	0.617	0.165
6014	Tallanstown Weir	Glyde	295298	297888	OPW	IE	1977	270.4	21.47	928	82	0.62	0.927	0.634	0.112
12001	Scarawalsh	Slaney	298380	145014	OPW	IE	1956	1030.8	133.05	1167	160	0.54	0.999	0.716	0.179
14019	Levitstown	Barrow	270623	187609	OPW	IE	1955	1697.3	99.21	862	93	0.58	1	0.624	0.149
15006	Brownsbarn	Nore	261699	139098	OPW	IE	1973	2418.3	260.02	942	137	0.58	0.999	0.633	0.183
16009	Caher Park	Suir	205297	122870	OPW	CU	1955	1582.7	157.05	1079	140	0.59	0.998	0.667	0.140
18002	Ballyduff	Blackwater	196410	99140	OPW	CU	1956	2333.7	331.27	1201	166	0.62	0.999	0.622	0.215
19001	Ballea	Owenboy	170971	63276	OPW	CU	1973	103.3	19.15	1176	99	0.66	1	0.64	0.199
21002	Coomhola	Coomhola	99825	54901	EPA	SW	1976	64.8	42.30	2580	245	0.68	0.982	0.373	0.753
23002	Listowel	Feale	99700	133295	OPW	CU	1961	646.8	200.23	1346	197	0.63	1	0.312	0.511
25002	Barrington's Br.	Newport	167908	154908	OPW	CU	1954	221.6	40.57	1298	189	0.59	0.999	0.542	0.337
25006	Ferbane	Brosna	211536	224406	OPW	IE	1956	1162.8	76.50	936	87	0.63	0.955	0.708	0.129
25030	Scarriff	Graney	164180	184277	OPW	CU	1973	280	42.05	1185	135	0.61	0.85	0.542	0.146
26009	Bellantra Bridge	Black	212848	289416	OPW	IE	1973	90.5	11.43	1019	91	0.68	0.936	0.538	0.353
26021	Ballymahon	Inny	216107	256987	OPW	IE	1977	1098.8	64.75	945	88	0.66	0.807	0.828	0.068
26029	DOWRA	Shannon	199064	326947	EPA	CU	1976	116.9	45.82	1759	217	0.70	0.988	0.463	0.628
27002	Ballycorey	Fergus	134431	180323	OPW	CU	1955	511.4	34.61	1337	71	0.62	0.835	0.697	0.061
34001	Rahans	Moy	124367	317782	OPW	CU	1975	1974.8	178.66	1323	80	0.73	0.825	0.776	0.083
35005	Ballysadare	Ballysadare	166832	329046	OPW	CU	1947	639.7	70.47	1198	99	0.71	0.898	0.609	0.146
36010	Butlers Bridge	Annalee	240817	310466	OPW	IE	1972	771.7	66.47	968	122	0.66	0.861	0.632	0.129
38001	Clonconwal Ford	Owenea	176584	392714	OPW	CU	1973	111.2	40.76	1752	183	0.70	0.922	0.285	0.555
39006	Claragh	Leannan	220215	420084	EPA	CU	1978	245.1	47.99	1527	132	0.70	0.842	0.329	0.180
201005	Camowen	Camowen Terr.	246071	373048	NI	IE	1973	276.6	58.01	1144	157	0.64	0.989	0.514	0.391
201008	Castlederg	Derg	226512	384216	NI	CU	1977	335.4	117.30	1558	176	0.62	0.914	0.504	0.508
202002	Drumahoe	Faughan	246411	415098	NI	CU	1977	273.1	61.30	1219	188	0.61	1	0.426	0.425
203028	Whitehill	Agivey	288337	419362	NI	CU	1973	100.5	27.95	1270	181	0.61	0.999	0.404	0.550
204001	Seneirl Bridge	Bush	294191	436250	NI	CU	1973	299.2	52.96	1116	119	0.61	0.992	0.561	0.354
205008	Drumiller	Lagan	323635	352493	NI	IE	1975	84.6	21.80	1015	168	0.53	0.992	0.403	0.427
206001	Mountmill Bridge	Clanrye	308536	331026	NI	IE	1975	120.3	17.91	975	96	0.53	0.972	0.568	0.270

**Note:** Org.: monitoring organisation; ERR: Extreme Rainfall Region; SAAR calculated between 1961-1990; FLATWET, FARL, BFI, and RBMED are dimensionless.

As discussed in the previous chapter, the objective of deriving ERRs (Extreme Rainfall Regions) was borne from the need to understand the climatic drivers of floods. However, it is also recognised that streamflow is controlled by many more factors than just climate, and every catchment will translate inputs of precipitation into streamflow differently depending on physiographic characteristics. Figure 4.1 maps 6 flood relevant Physical Catchment Descriptors (PCDs) along with median flood magnitude (QMED) and streamflow flashiness (RBMED). The PCDs have been derived for catchments in Ireland as part of the recent Flood Studies Update (FSU; OPW, 2014) and the UK Flood Estimation Handbook (FEH; Institute of Hydrology, 1999) for Northern Ireland. PCDs for Ireland and Northern Ireland were derived from two separate projects, hence 4 of the 6 PCDs (SAAR, FLATWET, FARL, and BFISOILS) were based on similar, but not necessarily the same, data and methods. Figure 4.2 shows the relationship (based on the non-parametric Spearman's rho correlation coefficient,  $\rho$ ) between each of the six PCDs, QMED, and RBMED. Details on the calculation of these variables and their relevance to understanding floods are summarised below:

**General descriptors - Catchment area (AREA), median flood magnitude (QMED), mean altitude (ALTBAR), and Standard-period Average Annual Rainfall (SAAR):** Catchment area (AREA in km<sup>2</sup>) and mean catchment altitude (ALTBAR in m a. s. l.) were calculated using a 90m Digital Elevation Model (DEM) for the Island of Ireland. QMED is the median of the annual maximum streamflow calculated using Daily Mean Flows (DMFs) rather than instantaneous (15-min) peak flow data as only 22 of the 29 stations have instantaneous peak flows available. QMED is the magnitude of the 1 in 2 year flood, and as expected is very strongly positively correlated to catchment area ( $\rho = 0.83$ ), that is, larger floods occur in larger catchments. SAAR is the Standard-period Average Annual Rainfall over the catchment for 1961-1990 in mm and catchments at higher altitude (ALTBAR) receive considerably more precipitation ( $\rho = 0.6$ ) due to the effect of orography. For example, St21002 is the only catchment situated within the most extreme ERR in the southwest (ERR-SW) and has the largest SAAR (2580 mm) and ALTBAR (245 m a. s. l.)

**Catchment wetness (FLATWET):** Prior catchment wetness provides antecedent conditions for flooding, and determines how receptive soils are to absorbing precipitation by infiltration. This is captured using the FLATWET index (PROPWET used

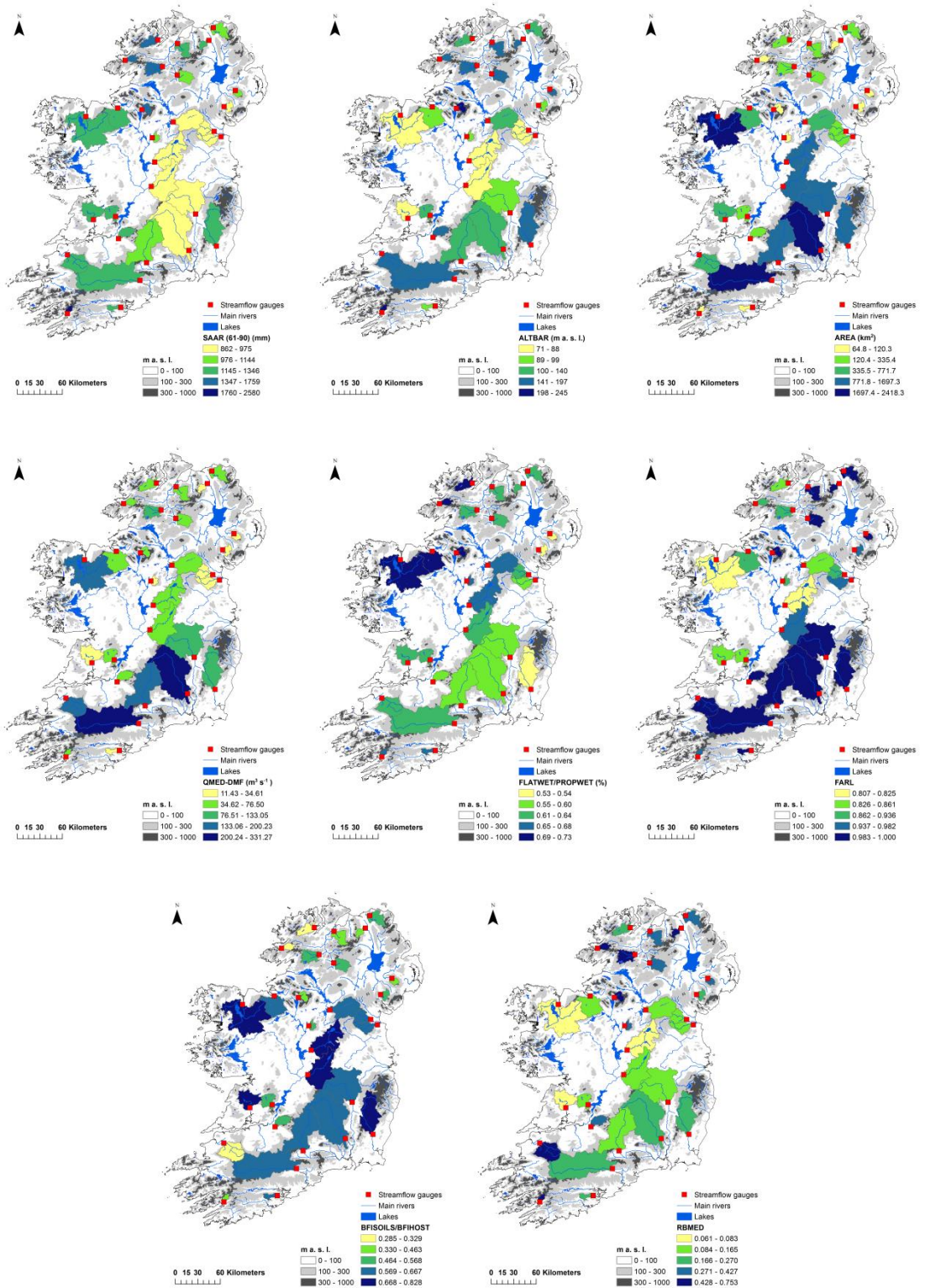


**Figure 4.1: Maps of the 29 non-nested IRN catchments used in the analysis, 6 Physical Catchment Descriptors (PCDs), QMED-DMF, and RBMED.**

for Northern Irish stations) derived using Soil Moisture Deficit (SMD) data. The index is defined as the proportion of time for which soils can be expected to be typically quite wet, and values represent the broad variation in soil wetness across the Island. While

moderately positively correlated to SAAR ( $\rho = 0.47$ ), it is not influenced by orographic precipitation (i.e. no correlation with ALTBAR,  $\rho = -0.055$ ), lending to the 'FLAT' in the naming of 'FLATWET'. There is a clear spatial pattern to catchment wetness with the driest (FLATWET < 55 %) catchments distributed along the eastern seaboard, compared to catchments in the western half of the country that receive more reliable frontal precipitation and lower evapotranspiration rates. For example, while St12001 is within the coastal and upland ERR (ERR-CU) and receives a high annual precipitation receipt, it is located in the east so the prevailing SMD is larger and will inhibit flood generation more of the time.

**Streamflow flashiness (RBMED), base flow index (BFISOILS), and flood attenuation by reservoirs and lakes (FARL):** A catchments streamflow regime reflects all the components affecting a catchment such as the climate, topography, geology, soils, vegetation, catchment size (as shown above), as well as many non-natural influences. Flashiness is defined as the frequency and rapidity of short term changes in streamflow (Baker et al., 2004). This means catchments that translate precipitation quickly to streamflow are 'flashier' than those that tend to filter the inputs into the slower groundwater pathways and/or are attenuated by reservoirs and lakes. The baseflow index (BFI) is a widely used measure of catchment permeability. It is measured on a scale between 1 and 0 with a value close to 1 indicating a highly permeable catchment in which baseflow fed from groundwater is the dominant contributor to streamflow (low flashiness) and a value  $\sim 0.3$  represents an impervious surface dominated catchment that will produce a more immediate rainfall-runoff response (high flashiness). Soil information was used during the FSU and FEH projects to generalise the BFI index for extrapolation to ungauged catchments (BFISOILS and BFIHOST, respectively). There are many ways of performing baseflow separation (defining the proportion of streamflow between peaks that is not attributed to storm precipitation), and no single accepted standard. However, when observations are available a remarkably simple measure of streamflow flashiness is the Richards-Baker Flashiness Index (RB Index; Baker et al., 2004). It is calculated by dividing the pathlength of flow oscillations for a time interval (i.e., the sum of the absolute values of day-to-day changes in DMF) by total streamflow during that time interval. Here, the RB Index was calculated on DMFs for each Water Year (1<sup>st</sup> October – 30<sup>th</sup> September) over the

period 1978-2009. The median over this period is taken to give a single measure of streamflow flashiness (RBMED).

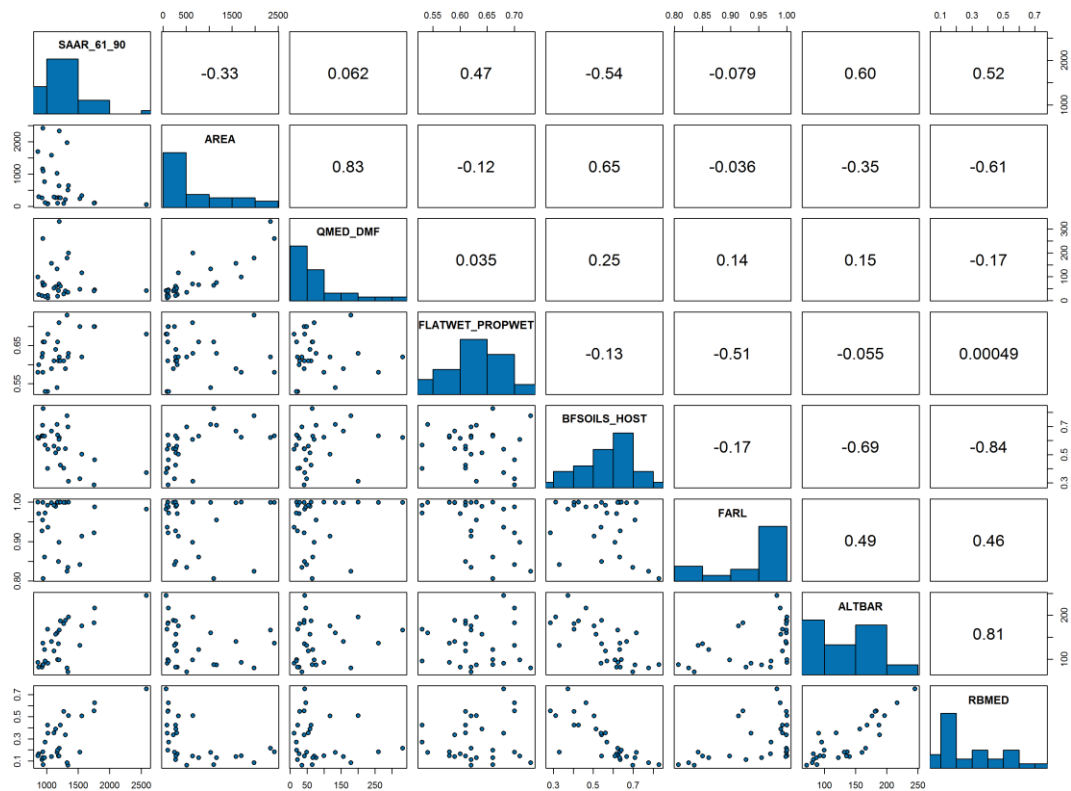


Figure 4.2 Scatterplot matrix of 8 FSU/FEH PCDs, QMED based on DMFs, and RBMED using Spearman's Rho correlation.

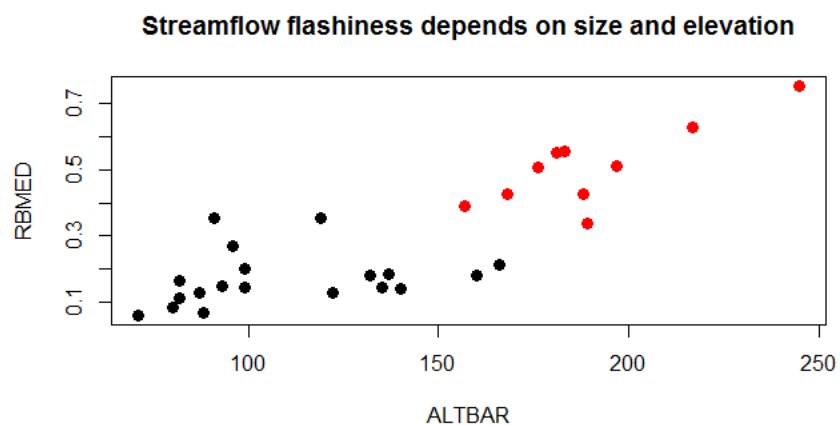


Figure 4.3: Scatterplot of ALTBAR and RBMED ( $\rho = 0.81$ ). Catchments with areas  $< 650 \text{ km}^2$  and an average altitude  $> 150 \text{ m a. s. l.}$  are highlighted in red.

The relationship between RBMED and BFI is physically consistent as they are very strongly negatively correlated ( $\rho = -0.84$ ). Catchments with a high BFI have lower

flashiness values. Interestingly, RBMED is also very strongly positively correlated with ALTBAR ( $\rho = 0.81$ ) and strongly positively correlated with SAAR ( $\rho = 0.52$ ), suggesting that floods in flashy catchments are driven by orography. There does appear however to be a physical threshold for streamflow flashiness based on catchment size, rather than a linear relationship. Catchments with an area above the average ( $661 \text{ km}^2$ ) have an RBMED  $< 0.25$ , whereas smaller than average catchments have an RBMED between 0.061 and 0.753. Hence, large catchments located even within ERR-CU (e.g. St34001), or at high elevations, do not have a flashy response; essentially large precipitation inputs are dampened with increased catchment area. It is not obviously clear then what controls the degree of flashiness in less than average sized catchments. With further investigation it was found that high streamflow flashiness (RBMED  $> 0.4$ ) occurred only in smaller ( $< 650 \text{ km}^2$ ) upland (ALTBAR  $> 150 \text{ m a. s. l.}$ ) catchments (Figure 4.3). Finally, catchments with reservoir and lake attenuation (FARL) tend to be wetter (FLATWET), lowland catchments (ALTBAR) with less flashy streamflow response (RBMED).

### 4.3 Extraction of extreme precipitation and flood indices

The choice of index, spatial and temporal scale of aggregation, statistical design, and the account taken of confounding factors, all require thorough justification in a detection study (Fowler and Wilby, 2010). As discussed in Chapter 2, determining if changes are occurring in mean precipitation and streamflow is of limited relevance for flooding. Therefore, the precipitation and streamflow indices extracted here capture important aspects of *extremes* within the hydroclimatic regime. Critically, the underlying data in which these extreme indices were extracted was carefully considered. The daily precipitation dataset for the Island of Ireland, as introduced in Chapter 3, was used. Only the 94 A-list stations were selected as these have limited missing data ( $< 5 \%$ ), cover the recent period (up to the end of minimum 2009), and have longest temporal coverage (minimum start year 1973). Streamflow (DMFs) from the 29 IRN sub-set introduced in Section 4.2 were used along with instantaneous (15-minute) annual maximum peak flow data (IAMAX) available for 22 of those catchments.

Data quality and homogeneity of station time-series are important considerations for trend analysis. For precipitation, basic quality control was undertaken by Met Éireann

and the UK Met Office, however, additional quality checks and infilling were made in Section 3.2. For streamflow, only quality assured stations within the IRN are used to limit the impact of artificial disturbances. Testing for and the removal of non-climatic breaks, such as changes in instrumentation practices, station movement, or changes in the surrounding environment, in climate (and other environmental) time-series is the aim of homogenisation (Toreti et al., 2011). This is a currently a very active area of research. For example, a major COST (European Cooperation in Science and Technology) action (HOME; COST-ES0601) has been undertaken to advance the homogenisation of climate series and as an outcome developed standardised methods and software for homogenising climate and environmental datasets (HOMER for monthly and HOM/SPLIDHOM for daily time-series (HOME, 2013)). These procedures have been successfully applied to long-term monthly precipitation in Ireland but relied on detailed station metadata for justification of corrections (Noone et al., 2015). For this study, this level of detailed metadata is not available for the majority of precipitation stations. Thus, it is argued that in the absence of metadata a ‘black box’ homogenisation procedure is not scientifically justified as it is inherently difficult, particularly when dealing with daily precipitation data and extremes, to know with reasonable certainty that a detected break is truly a result of an inhomogeneity (e.g. station shift), instead of a climatic fluctuation, or statistical artefact. The challenge of attributing a change point to any single cause using streamflow time-series, even with extensive metadata, is demonstrated in Chapter 6. In the absence of a full network homogenisation, these datasets are deemed the best available in terms of quality, spatio-temporal coverage, and at the appropriate resolution for examining changes in extremes.

As mentioned previously, indices of extreme events used here (both precipitation and floods) are acknowledged to be “moderate extremes” rather than very rare events (such as 1-in-100 year flood). The trade-off is such that these extreme events are severe enough to be socially and scientifically important, yet not so rare that an insufficient number of events be extracted from the relatively short length of precipitation and streamflow time-series (Wilby et al., 2014). Additionally, all indices are extracted using the water year (1<sup>st</sup> October – 30<sup>th</sup> September) as the calendar year begins and ends during the main flood season in Ireland and cuts the flood series (and

extreme precipitation series as seen in Chapter 3) at an inappropriate time. The convention used is that the date which the water year ends is given as the year; so for example, a flood occurring on the 12<sup>th</sup> December 1990 will be assigned to the water year 1991. In the climatological community the convention is to use calendar years for the extraction of extreme precipitation indices. It is therefore important that a common standard is used here when extracting extreme indices from precipitation and streamflow data for comparability, hence, the water year will be used for both.

#### 4.3.1 Extreme precipitation indices

The Expert Team on Climate Change Detection and Indices (ETCCDI) was established in 1999 to compile an internationally agreed suite of indices of climate extremes from daily precipitation and temperature data (Zhang et al., 2011). The explicit definitions for 27 core indices are available here: [http://etccdi.pacificclimate.org/list\\_27\\_indices.shtml](http://etccdi.pacificclimate.org/list_27_indices.shtml). While user friendly software is available (RClimDex; available at <http://etccdi.pacificclimate.org/software.shtml>) for extraction of indices, it was not used here. Instead the indices were calculated separately and adapted for extraction on water years. Checks were made to ensure consistency with the RClimDex software. Twelve ETCCDI recommended indices are derived from daily precipitation data. The indices include key precipitation characteristics imperative for assessment of changing hydroclimate regimes including changes in magnitude, duration, intensity, and frequency of precipitation events. These have been divided into 5 different categories by Alexander et al. (2006):

**Percentile-based indices** include occurrence of very wet days (R95p), and extremely wet days (R99p) which represent the magnitude of precipitation falling above the 95<sup>th</sup>/99<sup>th</sup> percentiles respectively and include, but are not limited to, the most extreme precipitation events in a water year.

**Absolute indices** represent the magnitude of the maximum precipitation values within a water year. The maximum 1-day precipitation amount (RX1day) is one of the most important and readily available measures of extreme rainfall (Westra et al., 2013), while the maximum 5-day precipitation amount (RX5day) is more flood relevant as high cumulative multi-day precipitation leads to antecedent conditions particularly favourable to flooding (Mayes et al., 2006).

**Threshold indices** are defined as the number of days in which a precipitation value falls above a fixed threshold including the number of heavy precipitation days > 10 mm (R10mm) and number of very heavy precipitation days > 20 mm (R20mm). Changes in these indices indicate a change in frequency of extreme precipitation and therefore are of great importance for understanding changes in flood frequency.

**Duration indices** define periods of excessive wetness or dryness, such as longest consecutive spell of wet days (CWD) and longest consecutive spell of dry days (CDD) in each water year.

**Other indices** include annual precipitation total (PRCPTOT), the simple daily intensity index (SDII), and annual contribution from very wet days (R95pTOT). These do not fit in the above categories but are important to include. PRCPTOT is needed to calculate R95pTOT, which is another flood relevant indicator. Theoretically, increasing atmospheric temperature will lead to increases in precipitation intensity so both SDII and R95pTOT are used as indicators of this.

Precipitation indices were derived for two set periods: A 32 year short period (1978-2009) from 94 stations, and a 54 year long period (1956-2009) from 58 stations. The choice of set periods was restricted by spatio-temporal availability of streamflow data. Thirty-six daily precipitation stations have > 65 years and will be used in Section 4.5.2 for contextualising both set periods in the longer-term. A wet day is defined here as  $\geq 1$  mm and the common 20 year base period used to define thresholds for percentile-based indices was 1981-2000. The use of a base period is common practice in climatology as it allows comparison of indices across stations with different record lengths, and for easy updating as new data become available (Zhang et al., 2011). More detailed description of extreme precipitation indices is contained in Table 4.2.

### 4.3.2 Flood indices

Unlike precipitation, there is no internationally accepted suite of flood indices. Streamflow is a flux ( $\text{m}^3 \text{s}^{-1}$ ) and hence is much more difficult to measure continuously. Instead, the water level (stage) is recorded and converted to a flow measurement using a rating curve. Before digitisation in 2008, an autographic recorder and

arithmetic graph paper were used to continuously record water level in time in Ireland. This data was then digitised at 15-minute intervals, converted to a flow rate, then provided to the end user as a single value per day, the daily mean flow (DMF). However, DMF data are not first preference for studying floods as the time-scale in which a catchment responds to heavy rainfall may be too short to capture the flood peak (Institute of Hydrology, 1999). Instead, separate projects to digitise sub-daily instantaneous (15-minute) peak flow have been undertaken in Ireland and the UK for purposes of flood frequency estimation (Flood studies Report; Institute of hydrology, 1975). From these data two key flood indices were extracted at the time on water years: the Instantaneous (15-min) annual maximum peak flow (IAMAX) for both Ireland and UK, and the instantaneous (15-min) peaks-over-threshold flow (POT) dataset for the UK only. Internationally, DMFs are far more readily available than peak flow data. The majority of flood studies use the annual maximum daily mean flow (AMAX), and if available IAMAX. There are noticeably few papers that use POTs based on DMFs (see Petrow and Merz, 2009) for a summary of flood trend studies), and even fewer that use an instantaneous POT database. Hannaford and Marsh (2008) and Prosdocimi et al. (2014) are notable recent exceptions from the UK.

POT data (either from DMFs or sub-daily data) offer a distinct advantage compared to AMAX or IAMAX; in flood quiescent periods an AMAX value will be included but will not truly represent a flood. Instead, a POT database will include only the highest streamflow events, regardless of when they occur (Svensson et al., 2005). A major research objective of this thesis is therefore to extract a POT database from DMFs using a common method across the Island of Ireland following international standards (and described in detail in Section 4.3.2.1). Flood indices extracted here capture the magnitude and frequency of flooding, as well as duration of high flows and are broken into 4 categories:

**Percentile-based index** is the annual prevalence of high flows above the 90<sup>th</sup> percentile (PQ10). The convention in hydrology is to refer to flows above the 90<sup>th</sup> percentile as Q10, which is the flow that was equalled or exceeded for 10% of the specified time, and is a widely used high flow measure.

**Table 4.2: Extreme precipitation (Core ETCCDI precipitation indices) and flood indices used in assessment of trends.**

Label	Index Name	Precipitation/flood characteristic	Index Definition	Units
<i>Extreme precipitation indices</i>				
RX1day	Annual maximum 1-day precipitation	Magnitude (absolute)	Annual maximum 1-day precipitation	mm
RX5day	Annual maximum 5-day precipitation	Magnitude (absolute)	Annual maximum consecutive 5-day precipitation	mm
SDII	Simple daily intensity	Intensity	The ratio of annual total precipitation to the number of wet days ( $\geq 1$ mm)	mm/day
CDD	Consecutive dry days	Duration	Annual maximum number of consecutive days when precipitation $< 1$ mm	days
CWD	Consecutive wet days	Duration	Annual maximum number of consecutive days when precipitation $\geq 1$ mm	days
R95p	Very wet days	Magnitude (percentile-based)	Annual total precipitation from days $> 95$ th percentile, where 95 <sup>th</sup> percentile calculated on wet days during 1981-2000 period	mm
R99p	Extremely wet days	Magnitude (percentile-based)	Annual total precipitation from days $> 99$ th percentile, where 99 <sup>th</sup> percentile calculated on wet days during 1981-2000 period	mm
PRCPTOT	Total wet-day precipitation	Magnitude (amount)	Annual total precipitation from days $\geq 1$ mm	mm
R95pTOT	Annual contribution from very wet days	Magnitude (contribution)	$(R95p / PRCPTOT) * 100$	%
R1mm	Number of wet days	Frequency (threshold)	Annual count when precipitation $\geq 1$ mm	days
R10mm	Number of heavy precipitation days	Frequency (threshold)	Annual count when precipitation $\geq 10$ mm	days
R20mm	Number of very heavy precipitation days	Frequency (threshold)	Annual count when precipitation $\geq 20$ mm	days

---

*Flood indices*

IAMAX	Annual maximum instantaneous (15-min) flow	Magnitude	Annual maximum instantaneous (15-min) flow	$m^3 s^{-1}$
AMAX	Annual maximum 1-day mean flow	Magnitude	Annual maximum 1-day mean flow, from daily mean flows (DMFs)	$m^3 s^{-1}$
MAX10	Annual maximum 10-day flow	Magnitude	Annual maximum consecutive 10-day flow, from daily mean flows (DMFs)	$m^3 s^{-1}$
CQ10	Annual maximum consecutive days above Q10	Duration	Annual maximum consecutive days above Q10, where Q10 is calculated during 1981-2000 period	days
POT3F*	Annual flood frequency (3 per year)	Frequency (threshold)	Annual Peaks-Over-Threshold, with on average 3 peaks per year (see Section 4.3.2.1) for more details on calculation	days
POT3F_WH*	Winter flood frequency	Frequency (threshold)	POT3F events occurring during winter half year (Oct-Mar)	days
POT3F_SH*	Summer flood frequency	Frequency (threshold)	POT3F events occurring during summer half year (Apr-Sep)	days
PQ10	Annual number of days above Q10	Frequency (Percentile-based)	Annual number of days above Q10, where Q10 is calculated during 1981-2000 period	days

---

**Note:** (\*) The POT3 series for three stations have 2.5 rather than 3 peaks per year on average (stations: 26021, 27002, and 34001); Q10 is the 90<sup>th</sup> percentile of daily mean flow.

**Absolute indices** include the AMAX and IAMAX (where available). These are the most widely used measures for assessing changes in the magnitude of flooding. Annual maximum 10-day flow from DMFs (MAX10) is also extracted as it is a commonly used measure of extended-duration high flows (Hannaford and Marsh, 2008).

**Threshold indices** include the newly derived POT database for the Island of Ireland, which identifies on average 3 independent peaks per water year (POT3F). POT3F events are also subset by season half years: winter (POT3F\_WH) and summer (POT3F\_SH). This facilitates the first comprehensive assessment of changes in flood frequency for Ireland.

**Duration index** is Annual maximum consecutive days above Q10 (CQ10) and measures periods of excessive high flow.

The above flood indices were derived for the two set periods, short (1978-2009) using 29 stations (22 for IAMAX), and long (1956-2009) using 8 stations (9 for IAMAX). The 90<sup>th</sup> percentile threshold used in PQ10 and CQ10 was calculated over the 1981-2000 base period. Full details are contained in Table 4.2, with the next sub-section dedicated to the full description of the new POT database.

#### **4.3.2.1 A new POT flood database for Ireland**

The extraction of the POT flood database follows Svensson et al. (2005). The POT series consist of independent DMFs that exceed a threshold selected to include only relatively large events. As the purpose of the POT database here is on flood occurrence, peaks in the DMFs can be considered indicative of the occurrence of those from instantaneous flow peaks, but will not capture the instantaneous peak magnitude (Svensson et al., 2015) and so lack of an instantaneous POT database is not a major limitation in this study. Compared to precipitation, peaks in streamflow tend to cluster in time more severely adding an additional level of complexity. This happens due the nature in which a catchment converts precipitation to streamflow and the difficulty in identifying independent peaks is related to individual catchment characteristics. For example, a groundwater dominated catchment will have a larger BFI and hence streamflow will be less flashy. This increased permeability will act as a filter, thereby, slowing the release of a heavy input of precipitation to streamflow leading to a cluster

of high flow events. Only the true peak i.e. the maximum within this cluster is of interest. Further, erroneous peaks can occur shortly after streamflow drops below the threshold if it rains, thereby counting the primary event twice.

There are several ways of dealing with clusters of extremes that occur in natural systems. One of the most common, and straightforward, is runs declustering (Coles, 2001). In this method, a cluster is identified as beginning with the first value that exceeds the threshold, and ending once  $r$  values fall below the threshold, where  $r$  is the chosen (or possibly estimated) run length. In hydrology, the selection of run length  $r$  differs depending on the catchment characteristics. Svensson et al. (2005) devised a simple rule of thumb after visual inspection of time-series:  $r \geq 5$  days for catchments with areas  $< 45,000 \text{ km}^2$ ;  $r \geq 10$  days for catchments between  $45,000 \text{ km}^2$  and  $100,000 \text{ km}^2$ , and  $r \geq 20$  days for catchments  $> 100,000 \text{ km}^2$ . However, it is difficult to generalise these rule of thumb as this study only used 21 catchments worldwide. It is therefore necessary to visually check time-series to ensure proper peaks are being identified. For example, Petrow and Merz (2009) used visual inspection to conclude that  $r = 10$  days was sufficient for the majority of German catchments, while Mallakpour and Villarini (2015) allow only one peak within an  $r = 15$  day period for the central United States. Two POT flood datasets were extracted for each of the 29 IRN catchments for the short period (1978-2009), and for the full length of available data. The magnitude of the threshold was set so that *on average* 3 independent POT events (i.e. POT3) were selected per year. This allows for only the medium and largest floods to be included (Institute of Hydrology, 1999). An iterative procedure was used for deriving the POT flood database:

**Step 1:** Set the highest possible threshold - For  $n$  years of record, the highest possible threshold  $T_i$  will be the  $i^{\text{th}}$  largest DMF, where  $i$  is  $3 \times n$ .

**Step 2:** Extract only independent peaks above  $T_i$  using runs declustering (Coles, 2001) from the 'extRemes' package in R (Gilleland and Katz, 2011). From visual inspection of hydrographs, it was found that an  $r = 5$  days included too many erroneous peaks, and that a more conservative value of  $r = 10$  days was more suitable.

**Step 3:** Repeat Step 1 and 2 by systematically lowering  $T_i$  until  $3 \times n$  (or up to + 5) independent peaks are identified. The ‘up to + 5’ peak tolerance is included for reasons outlined below.

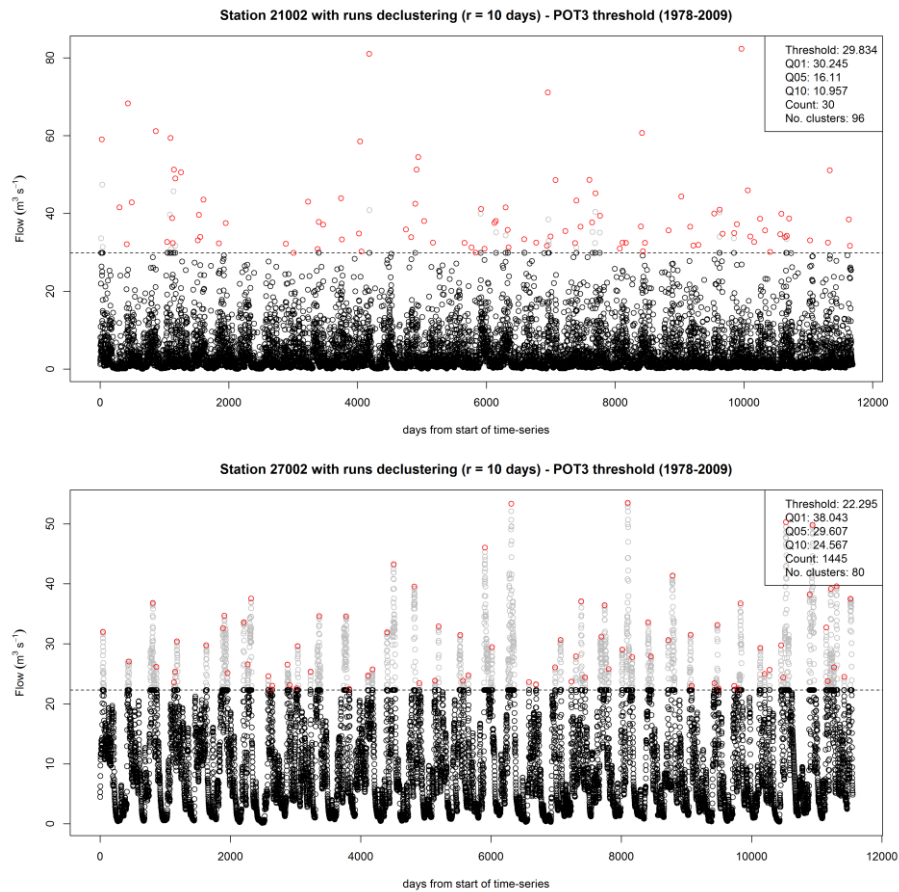


**Figure 4.4:** Example of the plots generated for visual inspection of the POT procedure to ensure proper peaks were being extracted at an acceptably high threshold for the most (least) flashy catchments on the top (bottom). The red circles are the maximum independent peaks in each cluster, grey circles dependent peaks lower than the maximum but above the final threshold  $T_i$  (shown in the grey dotted horizontal line), and black circles flow values below the threshold. Key statistics were also generated to aid interpretation and included in the legend in the top right of each plot (count is the number of iterations the algorithm needed to reach the target peak count). Note that the POT series for St27002 is actually a POT2.5 series (i.e. 80 peaks generated instead of 96).

In practice, a fully automatic implementation of the POT identification procedure is not recommended as it was found that requiring exactly  $3 \times n$  independent peaks is too strict for two reasons: 1.) In several cases the POT algorithm continued to lower the threshold  $T_i$  to a level that was much too low (e.g. below the average annual mean flow value). It was found that reducing the strictness of the exact number of independent peaks to  $3 \times n (+ 5)$  eliminated this problem. For example, when

extracting the POT3 for St205008 during the 32 year short period, the threshold that equalled exactly 96 independent peaks was below the median of DMFs. However, by allowing a small tolerance, in this case 97 independent peaks, a sufficiently high threshold was achieved ( $> 95\%$  percentile, i.e. Q05), and 2.) In some catchments, 3 independent peaks per year, large enough to be classified as a flood, simply did not exist. For three catchments (St27002, St26021, and St34001), a POT3 database was not possible. From further investigation, it was found that these three catchments are also the three with the least flashy streamflow according to RBMED (Table 4.1 and Fig. 4.1). This is because they are large low-lying catchments with floods being attenuated by reservoirs or lakes (lower FARL value from Fig. 4.1). Therefore, only 2.5 independent peaks on average per year could be identified for these catchments. This issue has also been found by Svensson et al. (2005) and rather than leaving them out of the analysis, it was decided to keep these stations in the study, but to bear in mind the difference in number of peaks when interpreting results.

The greatest lesson learned from extraction of the POT flood database was the importance of visually inspecting output from the automatic POT procedure. Figure 4.4 shows the plots that were generated for each station. The plot on the top is for St21002, which is the flashiest (largest RBMED), where 3 independent peaks per year could easily be identified and the threshold is almost as large as the Q01 value. In comparison, St27002 is the least flashy, and only a POT2.5 series could be identified with a reasonably high threshold (i.e.  $> Q15$ ). Note, a general finding here is that the POT3 threshold for 21/29 stations was  $> Q05$ ,  $> Q10$  for 6/29 stations, and  $> Q15$  for 2/29 stations. Notwithstanding the above pragmatic issues, a much richer analysis of floods in Ireland can be achieved from the extraction of this new POT flood database.

#### **4.4 Methods**

Three tasks were undertaken using the extracted extreme precipitation and flood indices: 1.) Trend analysis using fixed periods; 2.) Assessment of temporal representativeness of fixed periods in light of likely influence of Decadal Climate Variability (DCV) highlighted in Chapter 2; and 3.) Investigation of dependency of trends on period of record for the full available time-series. Statistical methods are described below before more details of the study design are outlined.

#### 4.4.1 Tests for change detection

Evidence for monotonic trends was assessed using the Mann-Kendall (MK) test (Mann, 1945; Kendall, 1975), a non-parametric rank-based method that is widely applied in analyses of streamflow (e.g. Hannaford and Marsh 2008; Villarini et al., 2011b; Murphy et al., 2013a) and precipitation (e.g. Villiarini et al., 2011a; Guerreiro et al., 2014). The standardized MK statistic (MKZs) follows the standard normal distribution with a mean of zero and variance of one. A positive (negative) value of MKZs indicates an increasing (decreasing) trend. Statistical significance was evaluated with probability of Type I error set at the 5 % significance level. A two tailed MK test was chosen, hence the null hypothesis of no trend (increasing or decreasing) is rejected when  $|MKZs| > 1.96$ .

The MK test requires data to be independent (i.e. free from serial correlation) as positive serial correlation increases the likelihood of Type 1 errors or incorrect rejection of a true null hypothesis (Kulkarni and von Storch, 1995). All indicators were, therefore, checked for positive lag-1 serial correlation at the 5% level using the autocorrelation function (ACF). The existence of a trend influences the correct estimate of serial correlation (Yue et al., 2002). Therefore to avoid the possibility of detecting significant serial correlation, when in fact none may exist, original time-series were detrended to form a 'trend-removed' *residual* series before the ACF was applied. The linear trend  $\beta$  used to detrend the original time-series was estimated using the robust Theil-Sen approach (TSA; Theil, 1950; Sen, 1968). This is the median of all pairwise slopes in the time-series:

$$\beta = \text{Median} \left( \frac{X_j - X_i}{j - i} \right) \forall i < j.$$

Equation 4.1

where  $X_i$  and  $X_j$  are sequential data values of the time-series in the years  $i$  and  $j$ . The TSA is more suitable for use with hydroclimatic data compared to linear regression as it is a robust non-parametric method that is less sensitive to outliers (Helsel and Hirsch, 2002).

Pre-whitening was used to remove statistically significant positive lag-1 serial correlation from time-series. The conventional pre-whitening approach (Kulkarni and

von Storch, 1995) was however found to artificially remove part of the magnitude of the trend hence a modified Trend Free Pre-Whitening (TFPW) technique was applied (Yue et al., 2002). This has been implemented before to deal with serially correlated data when using the Mann-Kendall test (e.g. Yue et al., 2002; Petrow and Merz, 2009). Steps involved with the TFPW procedure are described in detail by Yue et al. (2002). In summary, the trend (estimated using TSA) is first removed, the lag-1 positive serial correlation is removed, and then the trend is added back to the time-series producing a blended TFPW time-series including the original trend but without serial correlation. In this study, trend tests were only applied to the TFPW time-series when statistically significant serial correlation existed; otherwise they were applied to the original time-series.

Trend magnitudes were also estimated from the TSA in order to corroborate and map trends detected by the MK method. To facilitate a relative comparison, the trends  $TSA_{rel}$  (%) for each time-series were expressed as a percentage over the period of record of  $n$  years relative to the mean  $\mu$  for the period, where  $\beta$  is the TSA slope:

$$TSA_{rel} = \left( \frac{\beta \times n}{\mu} \right) \times 100$$

**Equation 4.2**

and has also been used by Stahl et al. (2012).

For indices involving counts (i.e. frequency indices, such as R10mm and POT3F), the MK test is often not suitable for formal statistical testing as there can be extensive ties in such time-series (e.g. repeated zeros in POT3F for flood poor years), and linear regression is inappropriate because of non-normal residuals and variable variance common in count data. However, logistic regression (Logit) provides a suitable alternative for trend analysis of count records and was applied to the assessment of extreme precipitation first by Frei and Schär (2001) and is used here. The concept is based on a binomial process whereby threshold exceedances are considered “successful” trials and is a class of generalized linear models (McCullagh and Nelder, 1989). The magnitude of the trend in logistic regression  $\beta_{Logit}$  is expressed as an odds ratio (OR) which represents the change in probability of occurrence of rare events

between the beginning and end of the period and is an exponential function of the period length  $n$ :

$$OR = \exp(\beta_{Logit} \times n)$$

**Equation 4.3**

An OR = 1 is interpreted as no change in the probability of occurrence of extreme precipitation or floods over the time period (i.e.,  $\beta = 0$ ), an OR = 2 is a doubling in probability of occurrence, while an OR = 0.5 means the probability of extreme event occurrence has halved over the period of record. Statistical significance of the estimated trend parameter can be inferred from p-value testing against the null hypothesis ( $\beta = 0$ ) where p-values represent the probability of accepting the null hypothesis. Test results are given for a two-tailed test with a significance level of 5 % as well as the trend magnitude (odds ratio) itself.

To examine the degree to which hydroclimatic time-series violate key statistical testing assumptions of being normally distributed and independent, the Shapiro-Wilk test for normality and the detrended ACF procedure were applied to all time-series. Figure 4.5, shows the results for the short period in graphical form. Red indicates when either of these tests is significant at the 5 % level. Clear is the extensive violation of the assumption of normality. This should be expected as hydroclimatic data rarely conform to normality and for example, RX1day has been shown to fit an extreme value distribution in Chapter 3. Less prevalent is the violation of independence (i.e. presence of positive serial correlation). However, for rigorousness it is incorporated here from the implementation of TFPW.

There is much debate on the over-reliance of statistical significance testing in hydroclimatology. For example, Cohn and Lins (2005) and Clarke (2010) highlight common misuses of statistics in hydroclimatic studies, while Busuioc and von Storch (1996) recommend that statistical tests are not viewed as strict confirmatory tools when dealing with environmental data. Focus here is on the direction and strength of changes and not entirely on statistical significance relative to arbitrary p-value thresholds (Nicholls, 2001).

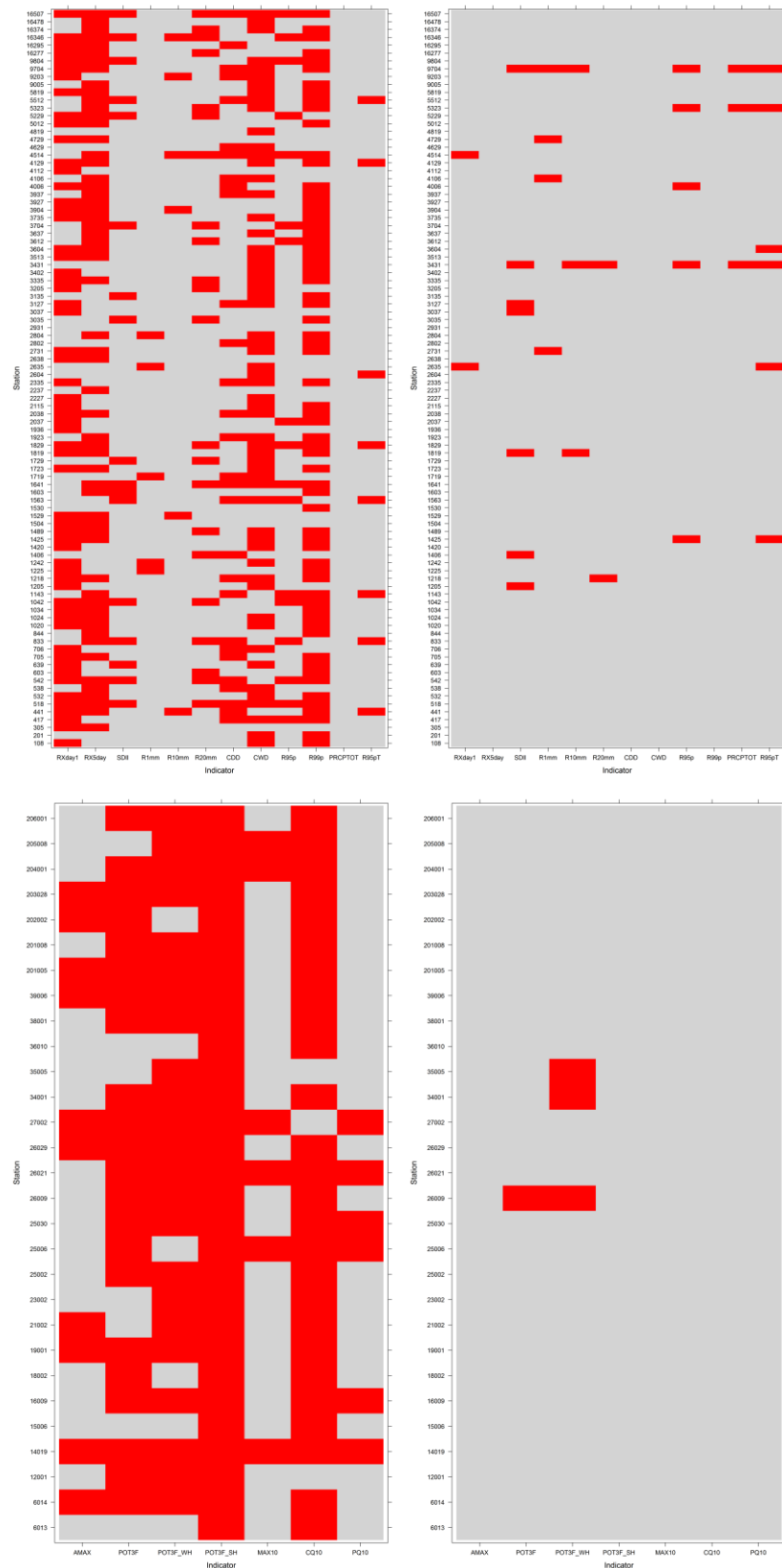


Figure 4.5: Heatmaps of results from the Shapiro-Wilk test for normality (left) and the detrended ACF for positive lag-1 serial correlation (right) on all extreme precipitation (top) and flood (bottom) indices. Red (grey) values are (are not) statistically significant at the 5 % level.

## 4.4.2 Study design

### 4.4.2.1 Fixed period analysis

Two fixed periods (short: 1978-2009 and long: 1956-2009) were chosen by optimising record length and temporal coverage. The short period includes the best spatial distribution while retaining a reasonable, but still relatively short, length of record (32 years). Longer records are critical for contextualising trends from shorter periods, so a less dense longer period is also used covering 54 years. Both these periods were limited by the availability of long streamflow time-series in comparison to precipitation. The key advantage with selecting fixed periods is that strength and direction of changes in both space and time can be compared directly between all extreme precipitation and flood indices.

### 4.4.2.2 Temporal variability analysis

The disadvantage with selecting fixed periods is that there is a compromise in the use of all available temporal information. Many stations have longer records than those selected during set periods, and due to the importance of this information, effort was made to use them to gain further insight to the temporal evolution of changes, where possible. Following a similar approach to Hannaford et al. (2013), raw time-series were first standardised by their mean and standard deviation calculated over the 1981-2000 base period, to allow for comparability regardless of record length of the full time-series, referred to a STD series. Locally weighted regression smoothing (LOESS) was then applied to filter short-term variability from the STD series. LOESS is a flexible non-parametric smoothing method that has many advantages over the widely used method of moving averages. LOESS is different to moving averages in that instead of using a fixed amount of time before and after the moment of interest (i.e., an 11 year moving average using 5 years either side of the moment of interest), the LOESS smoothing window, known as the span, uses a fixed proportion of the data points, which are nearest in time to the moment of interest and the smoothness is based on a weighted least-squares regression with points closer to the moment of interest given greater weight. A key advantage to LOESS is that a fit is produced for the entire time-series, rather than having the start and end periods cut off as is the case with using a moving average; although it can still be influenced by outliers at the beginning and end of a

time-series. The level of smoothing is controlled by the user defined span parameter. Here the span was set to include 15 years of data and as it is calculated as a proportion of the data, needs to be adjusted for record length (i.e.,  $\text{span} = 15/n$ ). Hannaford et al. (2013) found that a span including ~15 years of data best characterised the decadal-scale fluctuations within STD series, whereas a span of ~7 years resulted in too much fine-scale variation, and a span of ~22 years too much smoothing. The STD and LOESS smoothed time-series from each station for each index were then plotted together to characterise decadal-scale variability within extreme precipitation and floods indices across the Island of Ireland.

#### **4.4.2.3 Persistence of trends**

While using fixed periods is necessary for a comparative analysis, much temporal information is not used, particularly for precipitation indices. For example, all 94 A-list precipitation stations are available for the short period (1978-2009), 62 % of these have data for the long period (1956-2000), 36 % for the period 1945-2009, and 21 % for the longest available period 1942-2009. Making full use of available record length, dependency of trends on period of record was examined by systematically reducing the start year of analysis from the whole record to a minimum of 20 years following the approach of Wilby (2006). For each indicator, the MKZs statistic was derived first for the full record (e.g. 1942-2009), then 1943-2009, and so on until 1990-2009 to give sample sizes ranging between 68 (for the longest record) and 20 years. By plotting MKZs values for each iteration of start years a fuller appreciation of the evolution of trend can be achieved as well as an indication of the persistence of any statistically significant trends throughout the period of record. Note that this is an exploratory tool for examining the robustness of trends found in shorter periods rather than a formal test.

### **4.5 Results**

#### **4.5.1 Fixed period trends**

##### **4.5.1.1 Short period (1978-2009)**

For the short period, increasing trends in extreme precipitation indices are more prevalent than decreasing, except for CWD and R1mm (Table 4.3). In terms of indices

measuring magnitude, RX5day, percentile-based indices (R95p and R99p), and percentage contribution from very wet days to total precipitation (R95pTOT) all show stronger magnitudes of increasing trends than RX1day. Both R95p and R95pTOT have a median increase of ~15 % ( $TSA_{rel}$ ) over the period 1978-2009, with over 75 % of stations having increasing trends. Although the strength of increasing changes is less than for magnitude indices, intensity (SDII) has the highest number of stations with statistically significant increasing trends (16 %). Precipitation duration (CDD and CWD) has not changed much over this time period. Changes in precipitation frequency based on logistic regression, differs between indicators. More decreases than increases were found for R1mm with a median OR < 1 (0.96). In comparison, 11.7 % of stations for both R10mm and R20mm are statistically significant with R20mm showing stronger increases in frequency (OR = 1.19) than R10mm (1.07). There does not appear to be any clear spatial patterns of change (Fig. 4.6) within any of the Extreme Rainfall Regions (ERRs) identified in Chapter 3.

For flood indices during the short period, IAMAX and AMAX show very similar direction, magnitude (Table 4.4), and spatial pattern (Fig. 4.7) of changes. There is no dominant direction of change, but in comparison to precipitation, there is a clear spatial pattern with decreases in the north and along the eastern seaboard, and increases in the west and midlands. The strength of decreasing (increasing) trends is greatest in the north (west); several stations have magnitudes of change > 30 %. MAX10, a measure of extended-duration high flows, has increased at almost 70 % of stations (20.7 % statistically significant) with a median magnitude of change of 6.63 %. Increases in MAX10 occurred throughout the Island except for the northeast and smaller southerly catchments. Changes in the duration of high flows (CQ10) are mostly increasing with no dominant spatial pattern. Flood frequency at the annual scale (POT3F) does not show a principal direction of change, rather there is a marked east/west pattern of decreasing/increasing changes, by a factor of between 1.5 and 2 or even greater at a few stations. When assessed on a seasonal basis, the changes in annual flood frequency can be explained by changes in winter flood occurrence (POT3F\_WH), with very similar direction, strength, and spatial pattern of change. The pattern of changes in summer flood occurrence (POT3F\_SH) are opposite to POTF and POTF\_WH (i.e., decreases in west and increase in east), but while the strength of

changes are large (by a factor > 2), none are statistically significant indicating a high degree of variability in time-series. PQ10 shows changes in-line with POT3F and POTF\_WH.

**Table 4.3: Direction of change and proportion of statistically significant (5 % level) trends for short fixed period (1978-2009) extreme precipitation indices. Direction and significance tested using Mann-Kendall (MKZs) and magnitude tested with the relative Theil-Sen Approach (TSA<sub>rel</sub>). Logistic regression Odds Ratios (OR) used for both magnitude and significance of frequency indices. Magnitude of change is based on the median of the test statistics with spread (+/- bounds) given by interquartile range.**

Indicator	<i>n</i>	Stat.	Positive (sig.) %	Negative (sig.) %	Stat.	Magnitude (+/- bounds) %
RXday1	94	MKZs	56.4 (5.3)	43.6 (3.2)	TSA <sub>rel</sub>	2.47 (-9.78, 11.49)
RX5day	94	MKZs	62.8 (11.7)	37.2 (4.3)	TSA <sub>rel</sub>	5.91 (-4.32, 15.82)
SDII	94	MKZs	71.3 (16)	28.7 (6.4)	TSA <sub>rel</sub>	3.20 (-0.13, 6.54)
CDD	94	MKZs	60.6 (1.1)	39.4 (0.0)	TSA <sub>rel</sub>	0.00 (0.00, 9.91)
CWD	94	MKZs	50.0 (1.1)	50.0 (4.3)	TSA <sub>rel</sub>	0.00 (-11.94, 11.43)
R95p	94	MKZs	76.6 (11.7)	23.4 (4.3)	TSA <sub>rel</sub>	15.43 (1.65, 29.28)
R99p	94	MKZs	68.1 (13.8)	31.9 (5.3)	TSA <sub>rel</sub>	7.79 (-4.95, 47.56)
PRCPTOT	94	MKZs	62.8 (3.2)	37.2 (3.2)	TSA <sub>rel</sub>	1.92 (-2.41, 5.81)
R95pTOT	94	MKZs	74.5 (12.8)	25.5 (5.3)	TSA <sub>rel</sub>	14.23 (1.68, 27.77)
R1mm	94	OR	39.4 (1.1)	60.6 (5.3)	OR	0.96 (0.89, 1.04)
R10mm	94	OR	71.3 (11.7)	28.7 (4.3)	OR	1.07 (0.98, 1.17)
R20mm	94	OR	71.3 (11.7)	28.7 (5.3)	OR	1.19 (0.97, 1.42)

**Table 4.4: As in Table 4.3 but for flood indices.**

Indicator	<i>n</i>	Stat.	Positive (sig.) %	Negative (sig.) %	Stat.	Magnitude (+/- bounds) %
IAMAX	22	MKZs	50.0 (9.1)	50.0 (13.6)	TSA <sub>rel</sub>	-1.22 (-8.27, 5.58)
AMAX	29	MKZs	44.8 (10.3)	55.2 (10.3)	TSA <sub>rel</sub>	-1.47 (-11.71, 8.84)
MAX10	29	MKZs	69.0 (20.7)	31.0 (3.4)	TSA <sub>rel</sub>	6.63 (-2.87, 18.5)
CQ10	29	MKZs	72.4 (6.9)	27.6 (0.0)	TSA <sub>rel</sub>	0.00 (0.00, 18.12)
POT3F	29	OR	37.9 (3.4)	62.1 (6.9)	OR	0.93 (0.74, 1.19)
POT3F_WH	29	OR	37.9 (0.0)	62.1 (6.9)	OR	0.86 (0.80, 1.17)
POT3F_SH	29	OR	55.2 (0.0)	44.8 (0.0)	OR	1.04 (0.74, 1.39)
PQ10	29	OR	44.8 (0.0)	55.2 (6.9)	OR	0.96 (0.88, 1.19)

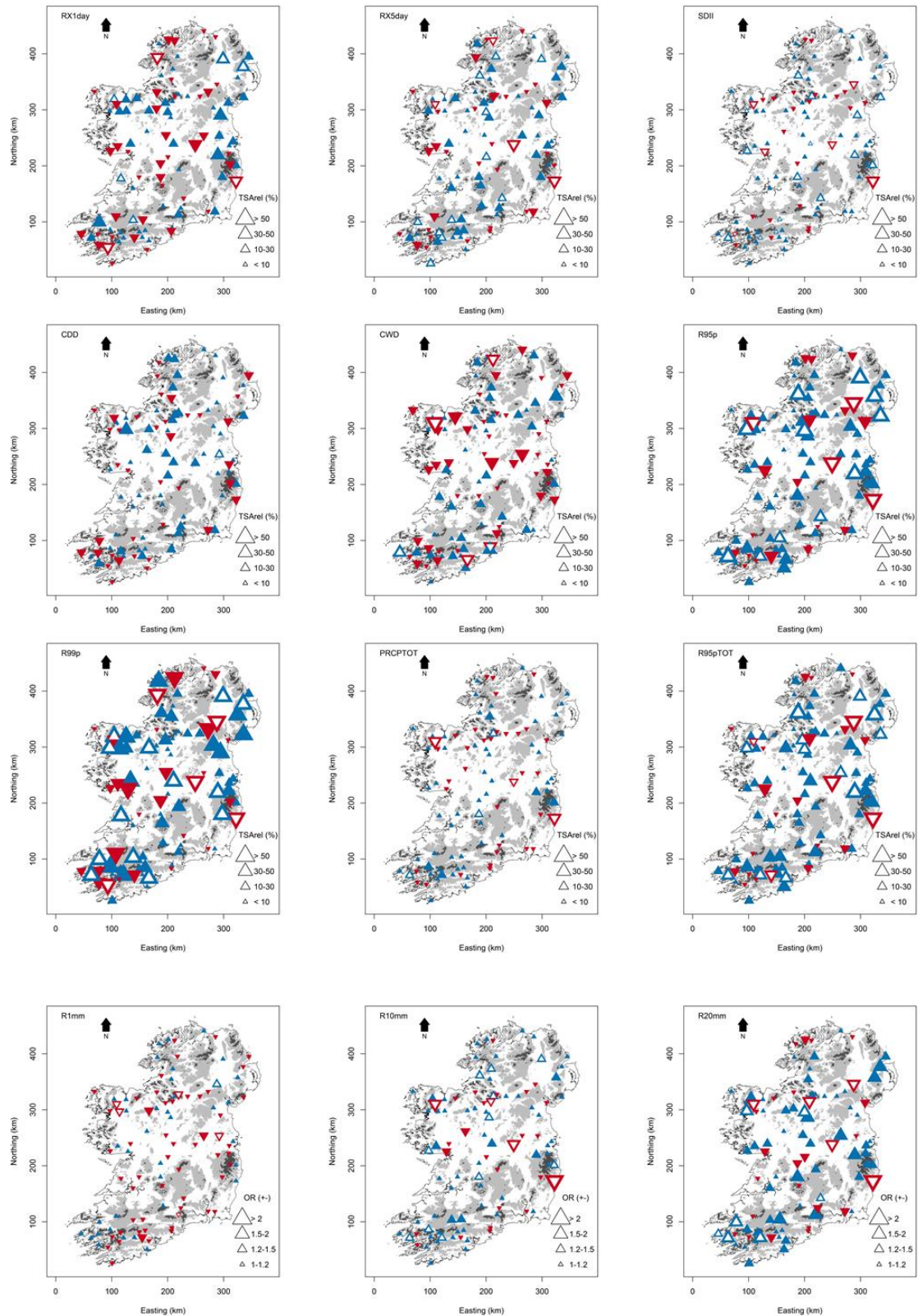


**Figure 4.6: Magnitude and direction of trends for short fixed period (1978-2009) for extreme precipitation indices. Blue triangles represent increasing trends and red decreasing trends, with magnitude proportional to size. Magnitude of frequency indices calculated from logistic regression odd ratios, while the rest are based on TSAreI. Significant trends (5 % level) shown by white triangles and derived from the MK and logit tests.**

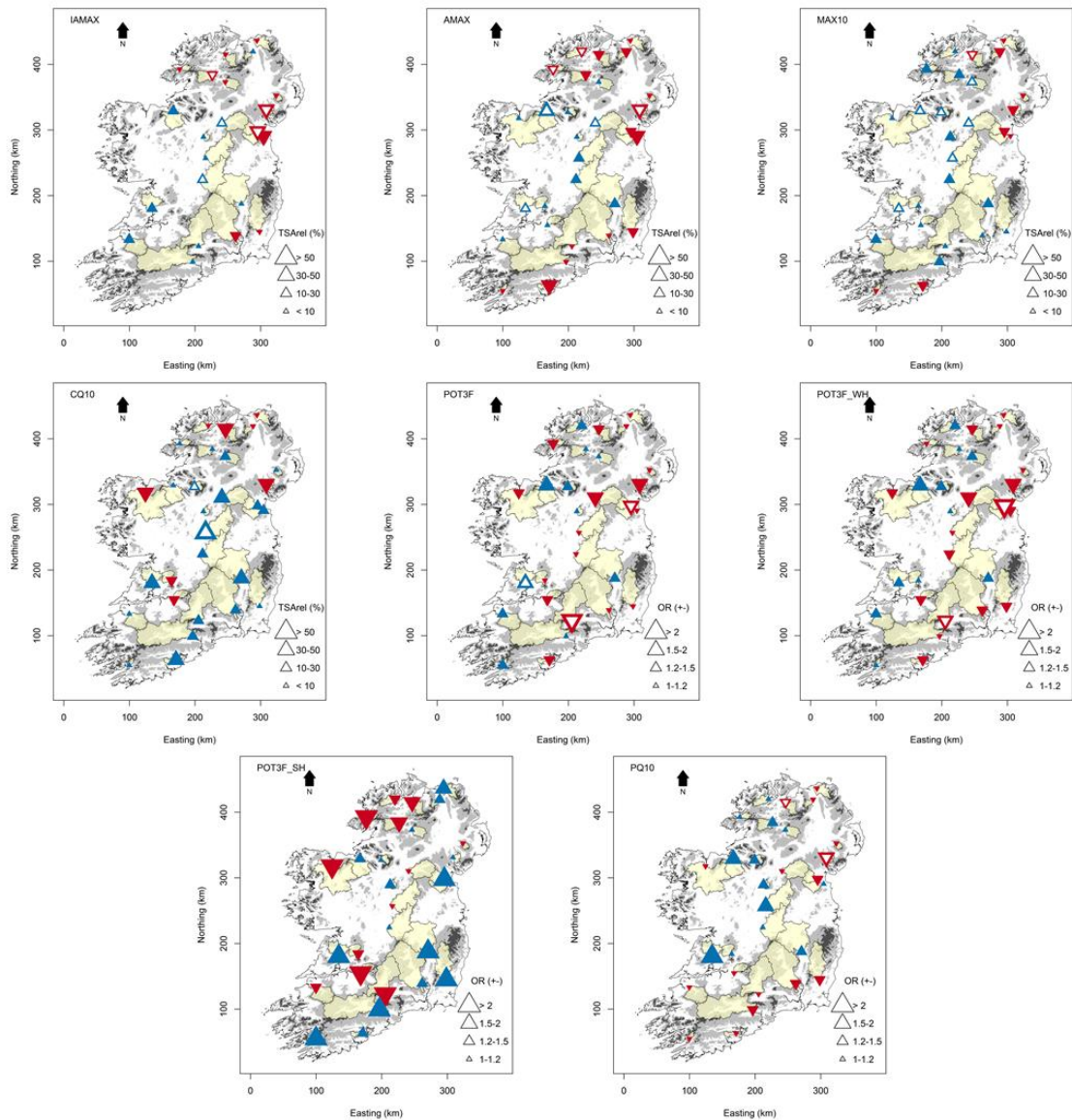


**Figure 4.7:** As Figure 4.6 but for short period (1978-2009) for flood indices with catchment boundaries plotted in yellow.

#### 4.5.1.2 Long period (1956-2009)

The number of precipitation stations drops to 58 for the long period leaving gaps in coverage in Northern Ireland and the southeast. Nevertheless, there is a clear increasing signal in extreme precipitation indices across the Island (Fig. 4.8). For indices describing the magnitude of extremes, R95p has the largest median increase in trend magnitude ( $TSA_{rel} = 21.61\%$ ), followed by RX5day ( $TSA_{rel} = 10.64\%$ ) from Table 4.5. Although both have over 20% of stations with statistically significant increases, over 80% of stations show increases in RX5day across Iol. Over 65% of stations show an increase in RX1day with 8.6% statistically significant. There is a notable difference

between the spatial distribution of trends for RX1day and RX5day. Decreasing trends are observed within ERR-SW and in the northwest of ERR-CU for RX1day, whereas statistically significant increasing trends are found for longer-duration RX5day events in these same locations. Remarkably, more than 40 % of stations show statistically significant increases in precipitation intensity (SDII) with a median magnitude of change of 6.98 %. Wet-day duration (CWD) has increased with over 30 % of stations being statistically significant. This is in contrast to duration of dry days (CDD) where little widespread change has been observed. Over 43 % of stations show statistically significant increases in PRCEPTOT, but the pattern of increasing trends in R95pTOT follows R95p in terms of spatial patterns, with most significant changes in the ERR-SW and ERR-CU. Similarly, changes in precipitation frequency are dominated by increases. The probability of occurrence of extremely wet days (R20mm) has increased by a median of factor of 1.25 over this period with over 75 % of stations showing increases (27.6 % statistically significant). Although increases in very wet day occurrence (R10mm) are not as strong, 50 % of stations have statistically significant increases.

Results for flood indices are presented differently in Table 4.6 compared to above as reporting the percentage of stations with changes with a sample of only 8 or 9 is misleading, so the actual number of stations showing trends is reported instead. The reduction of station density for long records is much more severe than for precipitation with large portions of the west, north, and north east not represented and thus inferences on spatial changes between ERRs cannot be made. Nevertheless, many stations that showed decreases during the short period have increased over 1956-2009, with increases dominating (minimum of 6 out of 8 stations) across all flood indices. Changes in AMAX and IAMAX are very similar, although the magnitude of change is greater for IAMAX (median  $TSA_{rel}$  of 16.75 %, compared to 11.61 %). Strong increasing trends (median  $TSA_{rel}$  of 18.81 %) are observed for MAX10 with all 8 stations showing increases, 2/8 statistically significant. Largest increases are seen for high flow duration (CQ10), with a median increase of almost 50 % with 4/8 stations statistically significant. In general, the probability of occurrence of floods has also increased over this period. The probability of occurrence of Q10 events (PQ10) increased more than POT3F events, with 3/8 compared to 1/8 and an OR = 1.47 and OR = 1.18, respectively. Similar to the short period, changes in annual flood occurrence match changes in

winter (POT3F\_WH) rather than summer (POT3F\_SH). Although 1/8 stations had a statistically significant increasing change for both POT3F\_WH and POT3F\_SH, the median probability of occurrence was greater for POT3F\_SH (OR = 1.92). However, two stations showed decreases in probability of occurrence of summer floods of similar magnitude. It is worth noting that two stations in particular showed consistent increases across several indices, both located in ER-CU. St27002 showed statistically significant increases in 5 out of 8 indices, and 7 out of 8 indices for St35002.

**Table 4.5: As in Table 4.3 but for long fixed period (1956-2009) for extreme precipitation indices.**

Indicator	<i>n</i>	Stat.	Positive (sig.) %	Negative (sig.) %	Stat.	Magnitude (+/- bounds) %
RXday1	58	MKZs	65.5 (8.6)	34.5 (0.0)	TSA <sub>rel</sub>	6.21 (-2.52, 11.2)
RX5day	58	MKZs	82.8 (22.4)	17.2 (1.7)	TSA <sub>rel</sub>	10.64 (2.67, 16.99)
SDII	58	MKZs	75.9 (41.4)	24.1 (5.2)	TSA <sub>rel</sub>	6.98 (1.39, 11.31)
CDD	58	MKZs	74.1 (3.4)	25.9 (0.0)	TSA <sub>rel</sub>	0.00 (0.00, 9.49)
CWD	58	MKZs	75.9 (27.6)	24.1 (1.7)	TSA <sub>rel</sub>	14.38 (0.00, 25.79)
R95p	58	MKZs	70.7 (20.7)	29.3 (1.7)	TSA <sub>rel</sub>	21.61 (-2.38, 34.76)
R99p	58	MKZs	70.7 (8.6)	29.3 (1.7)	TSA <sub>rel</sub>	1.90 (0.00, 34.39)
PRCPTOT	58	MKZs	74.1 (43.1)	25.9 (3.4)	TSA <sub>rel</sub>	10.96 (1.47, 15.51)
R95pTOT	58	MKZs	72.4 (19.0)	27.6 (1.7)	TSA <sub>rel</sub>	7.73 (-1.76, 26.97)
R1mm	58	OR	65.5 (25.9)	34.5 (6.9)	OR	1.08 (0.95, 1.18)
R10mm	58	OR	74.1 (50.0)	25.9 (3.4)	OR	1.21 (0.99, 1.37)
R20mm	58	OR	75.9 (27.6)	24.1 (1.7)	OR	1.25 (1.01, 1.47)

**Table 4.6: As in Table 4.3 but for long fixed period (1956-2009) for flood indices.**

Indicator	<i>n</i>	Stat.	Positive (sig.) %	Negative (sig.) %	Stat.	Magnitude (+/- bounds) %
IAMAX	9	MKZs	7/9 (3/9)	2/9 (0/9)	TSA <sub>rel</sub>	16.75 (10.14, 19.39)
AMAX	8	MKZs	7/8 (2/8)	1/8 (0/8)	TSA <sub>rel</sub>	11.61 (7.97, 18.82)
MAX10	8	MKZs	8/8 (2/8)	0/8 (0/8)	TSA <sub>rel</sub>	18.81 (14.94, 23.46)
CQ10	8	MKZs	8/8 (4/8)	0/8 (0/8)	TSA <sub>rel</sub>	47.45 (26.23, 64.67)
POT3F	8	OR	7/8 (1/8)	1/8 (0/8)	OR	1.18 (1.08, 1.48)
POT3F_WH	8	OR	7/8 (1/8)	1/8 (0/8)	OR	1.24 (1.14, 1.39)
POT3F_SH	8	OR	6/8 (1/8)	2/8 (0/0)	OR	1.92 (1.17, 2.52)
PQ10	8	OR	8/8 (3/8)	0/8 (0/8)	OR	1.47 (1.23, 2.19)

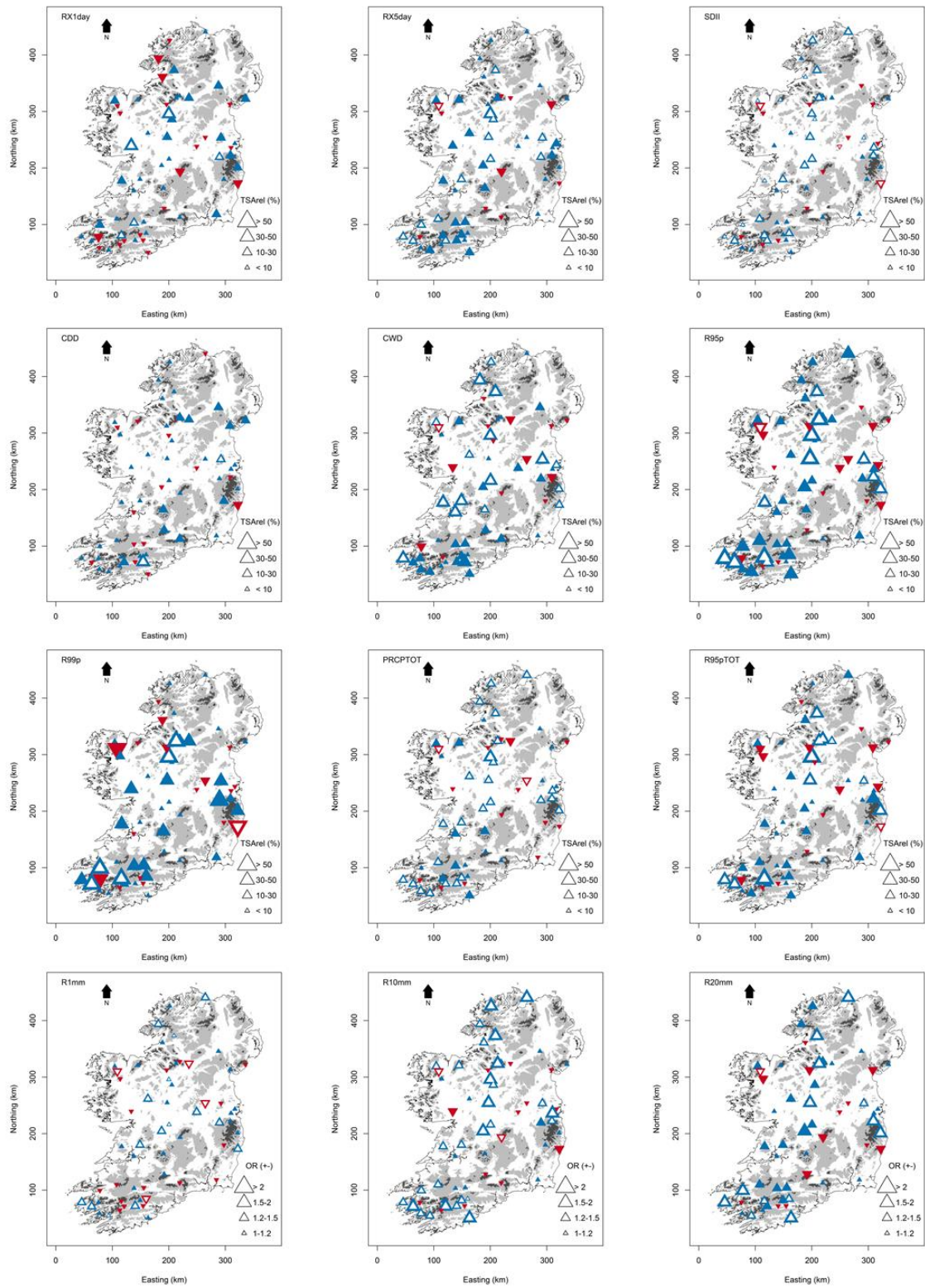


Figure 4.8: As Figure 4.6 but for long period (1956-2009) for extreme precipitation.

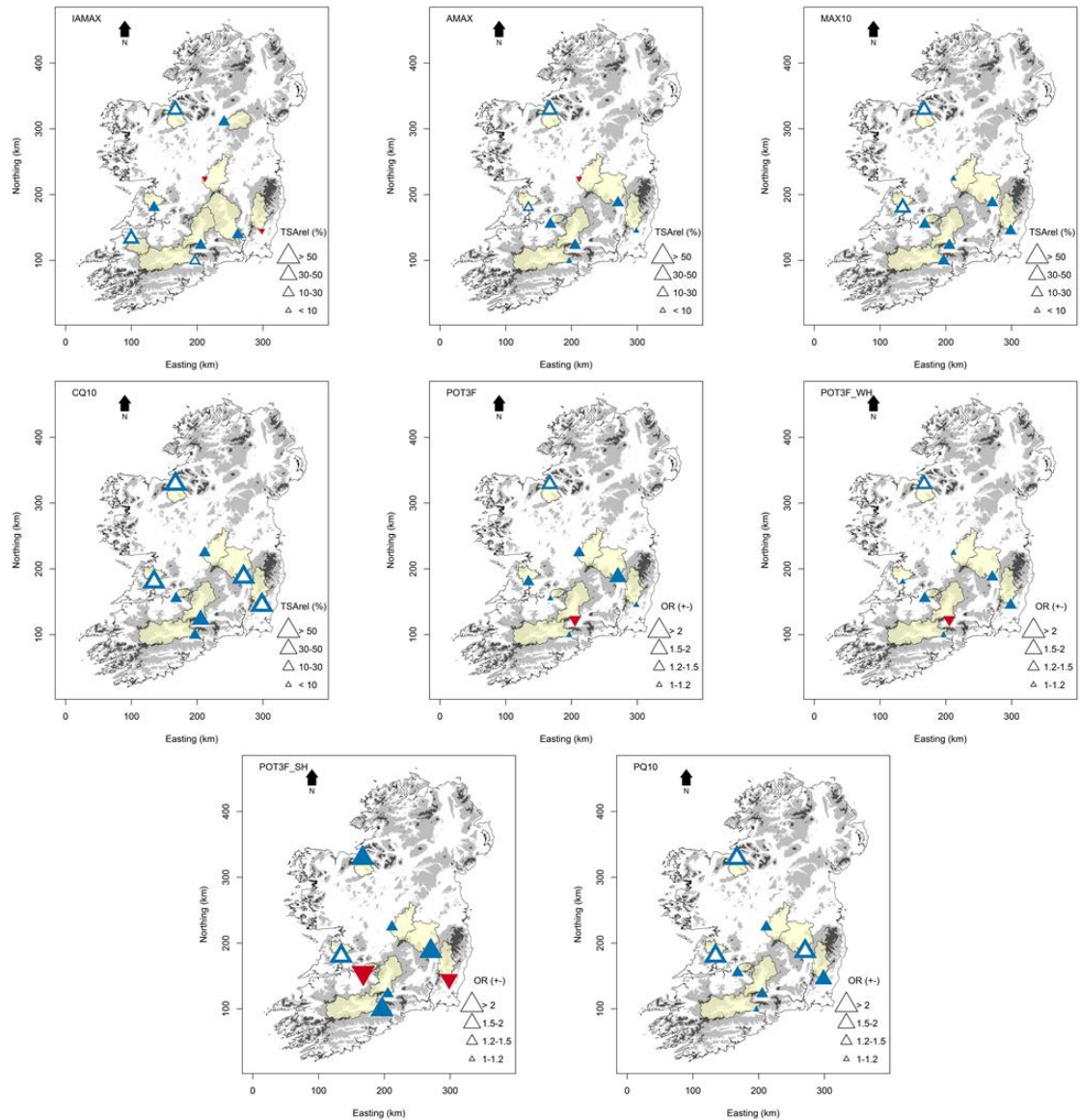
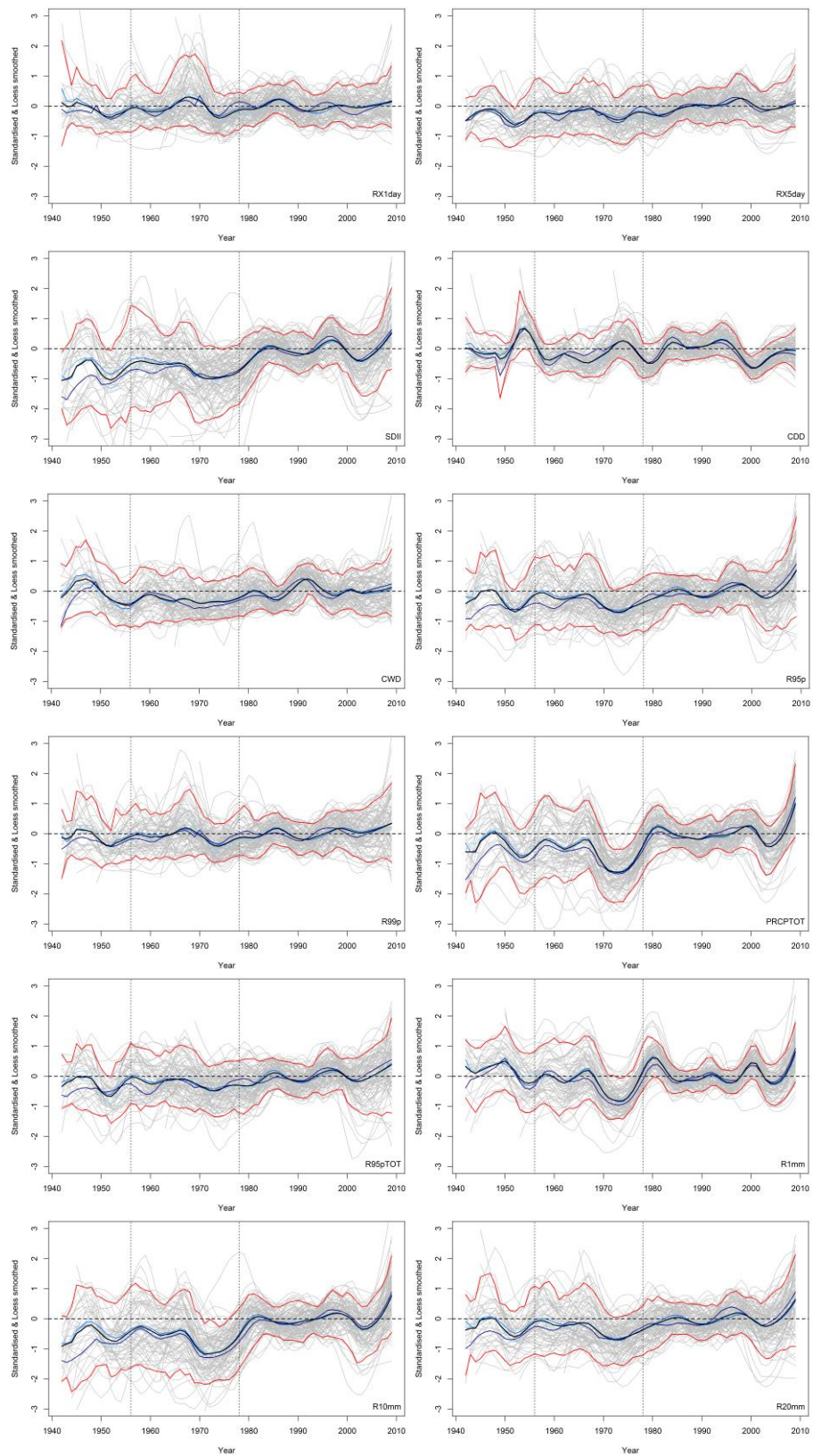


Figure 4.9: As Figure 4.6 but for the long period (1956-2009) for flood indices with catchment boundaries plotted in yellow.

#### 4.5.2 Temporal variability analysis

Fixed period assessments allow for a relative comparison of direction, magnitude, and spatial patterns in trends between extreme precipitation and flood indices. Evident was the large differences in changes between the short and long period. Figures 4.10 and 4.11 gives greater insight to why such differences exist in the context of decadal-scale variability.

For precipitation, immediately apparent is the widespread spatio-temporal consistency of decadal-scale oscillations across all indices (Fig. 4.10). A much fuller understanding of patterns observed in the fixed periods is gained. The most prominent feature is the



**Figure 4.10: Standardised and LOESS smoothed extreme precipitation indices for all 94 A-list stations. Light grey lines are individual stations, solid red lines are the 5<sup>th</sup> and 95<sup>th</sup> percentiles across all stations, solid black line the mean, and blue lines the regional mean per ERR (Colours as Fig. 3.18). Grey vertical lines represent the start date of short and long set period. Note data for longer stations extend to water year 1942 and all series end in 2009.**

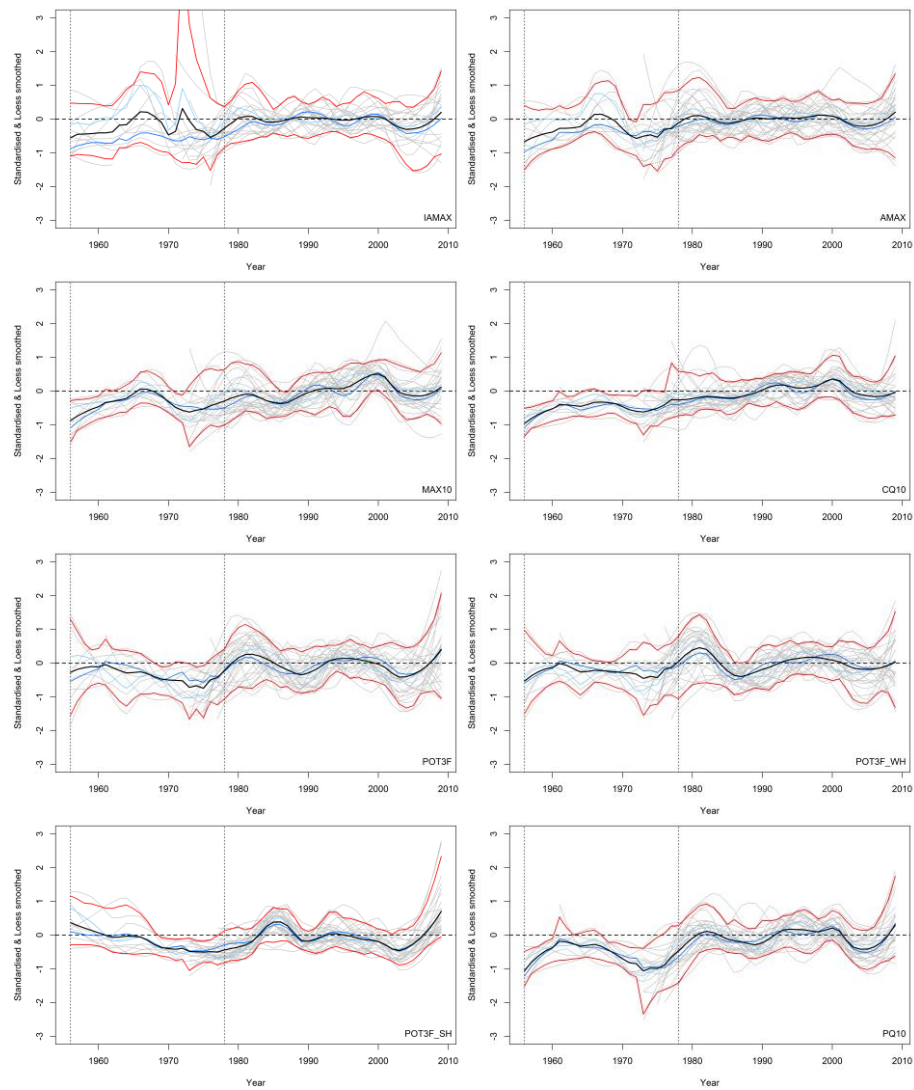


**Figure 4.11:** As in Figure 4.10 but for flood indices. Exception is too few time-series pre-1956 to calculate mean and 5<sup>th</sup> and 9<sup>th</sup> percentiles and ERR-SW is only represented by one catchment so merged into ERR-CU for calculation of regional mean as described in Chapter 5.

large fluctuation from dryer to wetter conditions between the mid-1970s and mid-1980s, relative to the 1981-2000 baseline. While the focus here is on extreme precipitation and floods, PRECPTOT reflects this oscillation most clearly, with notable increases in dry day durations (CDD) during the mid-1970s. This has been at the expense of a reduction of extreme precipitation magnitude (RX1day, RX5day, R95p, and R95pTOT), intensity (SDII), wet day duration (CWD), and frequency of wet days (R1mm), very wet days (R10mm), and extremely wet days (R20mm). Since the mid-1970s, precipitation has increased with a marked above-average period post the mid-2000s. Again, this period of variability is strongly reflected across the majority of indices. Fluctuations in RX1day, RX5day, R99p and CWD are less pronounced than

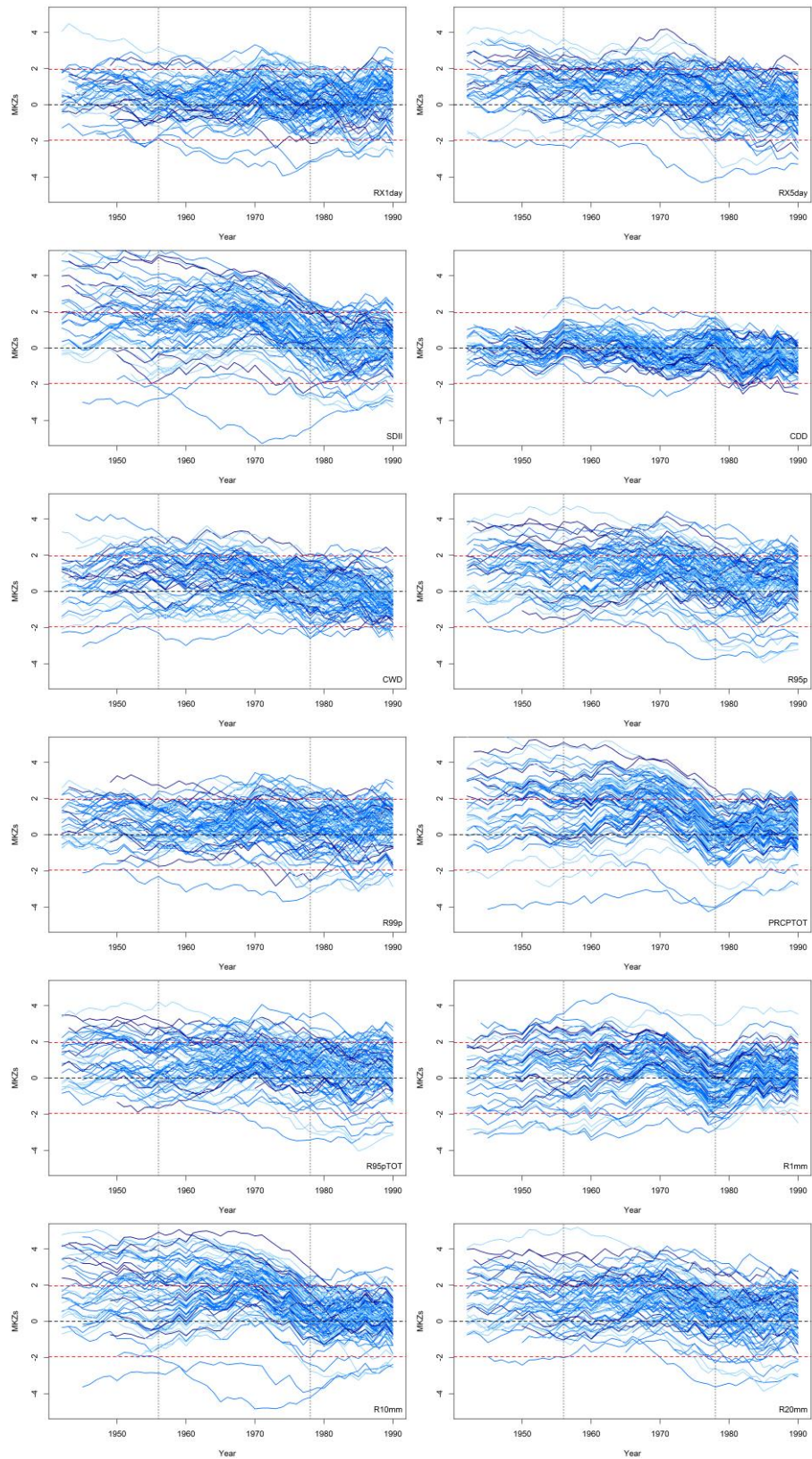


**Figure 4.12: Persistence plots for full available time-series of extreme precipitation indices end in water year 2009. Blue lines represent MKZs statistics for varying start years for individual stations across IOL with shade of blue per ERR (Colour as in Fig. 3.18). Dashed red lines are the threshold for statistically significant trends at the 5 % level with MKZs above (below) these indicating significant increasing (decreasing) trends since the corresponding start date. The vertical grey lines mark the start year of fixed periods.**

others. Time-series pre mid-1970s are systematically below 1981-2000 baseline values in most indices.

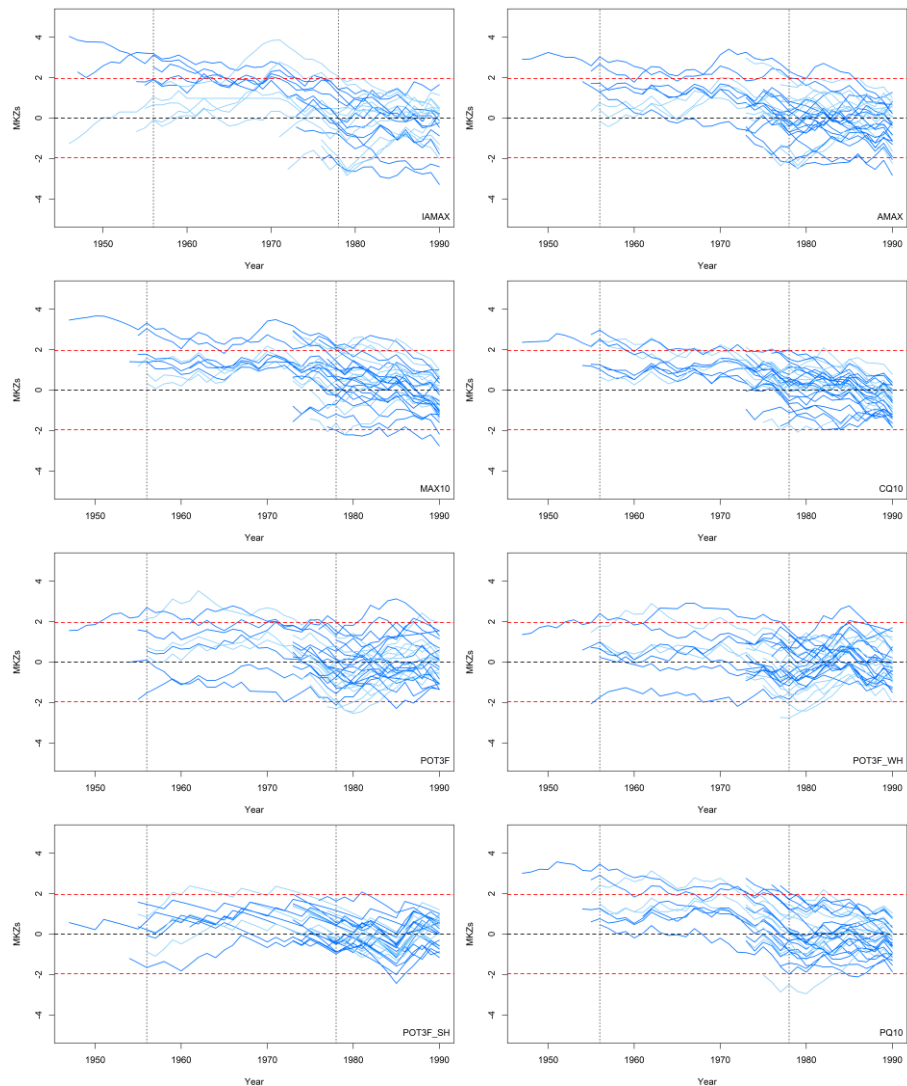


**Figure 4.13:** As in 4.12 but for flood indices. Exception is ERR-SW is only represented by one catchment so this is given same colour as ERR-CU as described in Chapter 5.

Despite fewer stations than precipitation, flood indices reveal corresponding decadal-scale fluctuations consistent across the entire Island (Fig. 4.11). Again, the mid-1970s to mid-1980s oscillation is most prominent with averages transitioning from below to above 1981-2000 baseline values, for flood frequency indices in particular. MAX10 and CQ10 time-series, while still showing decadal scale variability, have widespread clear gradual increases over the period, supporting findings from the fixed period analysis. The increase in extreme precipitation post mid-2000s is also shown for flood indices, although most marked in frequency indices.

### 4.5.3 Persistence of trends

The prevalence of this decadal-scale variability clearly has implications for the interpretation and generalisation of trends from the two fixed periods. Therefore the dependency of trends on period of record, and hence persistence of any statistically significant trends, was assessed for both extreme precipitation (Fig. 4.12) and flood (Fig. 4.13) indices. Evident is the inability of the short fixed period to capture the longer term signal. For both extreme precipitation and flood indices, those that showed increasing trends over the short fixed period, have more stations with statistically significant trends as record length increases. These plots show the importance of considering the longest record length and testing the robustness of trends in shorter records to the period used in analysis.

## 4.6 Discussion

The aim of this chapter was to assess the spatio-temporal changes in both extreme precipitation and flood indices for the Island of Ireland (IoI), based on observed station-based datasets fit-for-purpose for examination of extremes for the first time. Two key research questions were asked: Chapter Research Question 4.1 - How have extreme precipitation and flood characteristics (magnitude, duration, and frequency) changed in time and space, and are changes similar in direction, magnitude, and spatial distribution? Chapter Research Question 4.2 - Is there evidence of decadal climate variability (DCV) within extreme precipitation and/or flood indices, and if so, how might this affect interpretation of any detected trends in light of what is expected from climate change? A much more in-depth understanding of changes in floods was achieved by the completion of Thesis Data Objective 2, the development of a POT flood database for Ireland, allowing the analysis of flood frequency as well as magnitude.

Results show that there is robust evidence of an increase in extreme precipitation in-line with climate change expectations outlined in Chapter 2. The most widely reported index of extreme precipitation magnitude, RX1day, had 8.6 % of stations reporting a statistically significant increase which is in-line with the global average (Westra et al., 2013). However, stronger increases were found for extended-duration events (RX5day) which have more important implications for flooding as it signals greater multi-day

accumulations of precipitation, more important for creating flood favourable antecedent conditions (Mayes et al., 2006). While duration of wet days (CWD), and frequency of extreme precipitation events are also increasing (R10mm and R20mm), and are also flood relevant, according to Trenberth et al. (2003) it is precipitation intensity (SDII) that is expected theoretically to reveal increases in-line with the Clausius-Clapeyron (CC) relation. It is found here that precipitation intensity has increased at a similar rate to the CC rate of  $7\% \text{ K}^{-1}$  (i.e., median increase of 6.98 % between 1956 and 2009 with spread from the interquartile range of 1.39 % and 11.31 % with annual average temperature for the Irish grid box (52.5 N 7.5 W) increasing by approximately 0.94 K over the same period using data from CRUTEM4 (Jones et al., 2012)). To what extent Decadal Climate Variability (DCV) has modulated this increase was however not tested explicitly, but there is evidence of strong decadal-scale variability within extreme precipitation time-series.

For the short period (1978-2009), where spatial coverage of both precipitation and streamflow stations is generally representative of the whole Island, there was a clear spatial pattern to changes in flood indices compared to precipitation. This highlights the added complexity brought about by the interaction of the climate and hydrology of the land-surface and makes interpretation of the drivers of change in floods more of a challenge. For longer records, albeit from a much reduced sample, changes in flood magnitude, frequency, and high flow duration were consistent with increasing trends in extreme precipitation characteristics, becoming stronger with increasing record length. Further, extreme precipitation in longer series show strongest increasing changes is the southwest (ERR-SW) and coastal and upland (ERR-CU) regions, suggesting the driver of change in extreme precipitation, in general, does not have as strong an influence in the low-lying inland and east region (ERR-IE). However, such conclusions cannot be made for changes in flood indices due to the limited number of long record stations at an appropriate spatial density. The lack of long-term streamflow stations is a major limitation in the understanding flood variability and change in Ireland.

The reason for so few long-term streamflow stations is due to the more stringent criteria that stations within the Irish Reference Network (IRN) are subjected to. However, spatial coverage was compromised for good reason. The credibility of

statements on changes in flood indices in the context of climate variability and change is increased with use of data from Reference Hydrometric Networks (RHNs) such as the IRN. This is imperative given the many influences that can confound signals of change within catchments. For instance, Legates et al. (2005) call into question the findings of (Labat et al., 2004) who claim their study is the “first experimental data-based evidence demonstrating the link between global warming and the intensification of the global hydrological cycle” (Labat et al., 2004, pg 631). One of the primary concerns was the use of data from heavily disturbed catchments i.e. large catchments ( $\sim 100,000 \text{ km}^2$ ) with substantial proportions urbanised and even regulated by dams upstream of the gauging site. Data from the IRN are an integral part of the ongoing movement within the hydroclimate community to minimise these confounding anthropogenic influences by promoting the development and use of RHNs. In this case, the use of a fit-for-purpose network of streamflow stations was prioritised over spatial density, but is argued that this is the more important of the two in the context of understanding what is driving changes in floods. The challenge of attribution of change at the catchment scale given the interaction of both climatic and human disturbance is the topic of Chapter 6.

Spatial density is perhaps more important for the understanding of changes in extreme precipitation given its much higher spatial variability. In Ireland, the vast majority of studies have primarily focused on mean precipitation changes, and even those that assess changes in extreme precipitation used data from the synoptic network that has very limited coverage in terms of capturing regional variations in extremes. For example, Kiely (1999) used just 8 stations, Sheridan (2001) 12 stations, McElwain and Sweeny (2007) 11, and Leahy and Kiely (2011) 13 stations. Moreover, none of these studies include data from Northern Ireland and therefore makes drawing conclusions on changes in the northwest of Ireland and within border counties, a challenge. The inclusion of 94 precipitation stations here significantly adds to the station density thereby increasing confidence in findings of spatio-temporal changes in extreme precipitation across Ireland.

While Ireland is included in many large European and global studies on changing precipitation extremes, these studies mostly use gridded rather than station-based data. For example, the HadEX2 (Donat et al., 2013) gridded product for extremes is

interpolated onto a  $3.75^\circ \times 2.5^\circ$  grid would clearly not capture the more subtle spatial patterns found over Iol that are relevant for the assessment of floods. Additionally, Casanueva et al. (2014) performed a European wide assessment of trends in extreme precipitation using a higher resolution gridded daily precipitation product from the E-OBS data set (version 5.0) with a resolution of  $0.5^\circ \times 0.5^\circ$ , for the period from 1950 to 2010 (Haylock et al., 2008). They used R95pTOT but did not find changes as strong as those detected here. For the long period, almost 20 % of stations here show statistically significant increasing trends with a median increase of 7.73 % and interquartile range of -1.76 to 26.97), compared to only moderate changes found by Casanueva et al. (2014). It is however acknowledged that Casanueva et al. (2014) performed their analysis on a seasonal basis so a full comparative assessment using consistent methodology is needed for a conclusive comparison, but it calls into question the appropriateness of using (relatively) coarse gridded datasets for the assessment of extremes particularly with regards to understanding flooding. More effort needs to be made to ensure such products capture changing patterns of extreme precipitation characteristics.

Finally, the persistence plots (Fig. 4.12 and 3.13) have proved a useful graphical tool for identification of stations with suspect homogeneity issues. Despite stringent quality controls by data providers, there are many factors that could introduce an inhomogeneity into a time-series, such as station relocation, change in instrumentation or observer practices at the site, and changes to site surroundings such as growth of trees or construction of nearby buildings. For example, in Figure 4.12 for PRCPTOT a single series (St2635, Derryhillagh) situated in ERR-CU in Mayo shows a persistent statistically significant decreasing trend (i.e. line with most negative trend in the plot) which disagree with the temporal evolution of all other stations and therefore calls into question the homogeneity of this time-series that requires further investigation.

#### **4.7 Chapter summary**

The above findings support the hypothesis that the hydrological cycle is intensifying. However, structured decadal-scale variability is dominant in the temporal evolution of the majority of extreme precipitation and flood indices, and is coherent across the

entire Island. This suggests that the mechanism responsible for delivering extreme precipitation varies considerably in-time and a simple linear trend should not be assumed. The limited availability of long streamflow stations is a major limitation in the understanding of changes in floods and their drivers. Chapter 5 aims to reconstruct flood occurrence for earlier periods by first establishing the atmospheric drivers of floods.

## 5 Synoptic and Large-scale Climate Drivers of Floods

---

### 5.1 Introduction

Floods in Ireland have been shown to respond similarly in both space and time (Chapter 4) suggesting that floods are governed by common large-scale atmospheric drivers. Section 2.4 reviewed studies that assessed linkages between large-scale climate and flooding, each with relative advantages and disadvantages. For example, Atmospheric Rivers (ARs) have been linked with the most extreme flood events in UK (Lavers et al., 2011) and US (Lavers and Villarini, 2013a) and can track moisture delivery to a region at high spatio-temporal resolution, but depend on data from the satellite era (~ late 1970s). Hence atmospheric moisture cannot be adequately estimated before then due to the lack of high-quality global-scale observations (Hurrell, 1995). In contrast, Sea Level Pressure (SLP) has been more routinely observed at a sufficient resolution since the late 19<sup>th</sup> Century for many parts of the globe. This is particularly the case in the vicinity of the British-Irish Isles (BI). Given the importance of understanding flood occurrence over the longest period possible, the approach used here makes use of long-term mean SLP (MSLP) data from the 20<sup>th</sup> Century reanalysis (20CR) project (Compo et al., 2011).

One of the most common methods of classifying atmospheric circulation patterns from SLP fields is identification of a catalogue of weather types (WTs), also referred to as circulation patterns, that simplify and summarise atmospheric circulation for a particular region at a particular instant in time (Huth et al., 2008). Two of the most widely used catalogues of WTs are the Grosswetterlagen types (Hess and Brezowsky, 1952) for central Europe and the Lamb WTs (LWTs) for BI (Lamb, 1972). These manual methods have developed over time to automatic objective methods since the advance of computing resources and availability of gridded reanalyses datasets and are continuing to prove useful in a diverse range of applications including high-impact weather events such as analyses of extreme temperature episodes, floods, and droughts (Ramos et al., 2015).

One of the earliest applications of WTs to flooding was by Duckstein et al. (1993) who investigated the occurrence of daily WTs prior to floods in Arizona and found evidence of flood-producing WTs. Bárdossy and Filiz (2005) found in the majority of cases just 2 of 10 WTs were related to the largest floods for two catchments in France and Spain. Petrow et al. (2009) found that 5 of the 30 Grosswetterlagen WTs accounted for 62 % of maximum streamflow events in the west of Germany in winter, but highlighted that the relationship varied spatially and seasonally with different WTs dominating for winter floods compared to summer floods in some regions. Prudhomme and Geneviev (2011) examined if WTs could be linked to flooding at the European scale using 73 different WT catalogues developed within the COST733 action (Harmonisation and applications of weather type classifications for European regions) and found that some WTs occurred more frequently before and during a flood than in any other period, so could be classed as flood-producing. However, there was no single WT that could explain flooding at the European scale, instead there were large spatial differences highlighting that flood generating mechanisms are regionally different and depend on season. For a single catchment (Eden catchment 2400 km<sup>2</sup>) in northwest England, Pattison and Lane (2012) found just 5 out of 27 LWTs accounted for over 80 % of extreme flood events (cyclonic (27.3 %), westerly (15.9 %), southwesterly (15.9 %), cyclonic westerly (15.9%), and cyclonic southwesterly (6.8 %)). When considering the whole of Britain, Wilby and Quinn (2013) found that the same 5 LWTs account for 68 % of flood occurrence, and just 3 (Cyclonic, Westerly, and Southerly components) were linked with the most widespread winter floods across Britain.

Once flood-producing WTs are identified, a flood index can be developed that reconstructs atmospheric drivers of flood occurrence over multi-decadal time-scales as demonstrated by Wilby and Quinn (2013), hereafter WQ2013, using an objective LWT scheme extended to 1871 using 20CR (Jones et al., 2013b). To date such an approach has not been undertaken for Ireland or Northern Ireland and WQ2013 note that further research is needed to determine whether disaggregating the flood index to a seasonal scale can improve the approach.

Additionally, synoptic conditions themselves have been shown to be governed by large-scale climate drivers. For example, Burt et al. (2015) found a statistically significant positive correlation between westerly LWT frequency and one of the most

important modes of large-scale climate variability in western Europe, the North Atlantic Oscillation (NAO) (Hurrell, 1995). Several studies have demonstrated that a positive phase of the NAO has a potential to increase flood risk in Ireland (Kiely, 1999) and the UK (Hannaford and Marsh, 2008; Burt and Howden, 2013) as increased intensity of westerlies force moisture transport across the Atlantic to a more southwest-northeast axis bringing more intense storms and hence above average precipitation (Kingston et al., 2006). However, for Ireland Kiely (1999) uses annual and monthly mean streamflow indices to assess the NAO-streamflow relationship, and to the authors knowledge no study has yet to assess the relationship between the NAO and flood indices such as Peaks-Over-Threshold or Annual Maximum Flow (from Section 4.3.2) across the Island of Ireland to determine if the NAO has an influence at the higher range of the flow regime.

The Atlantic Ocean has also been shown to be an important driver of hydroclimatic variability in Europe over decadal time-scales. Knight et al. (2006) find patterns of increased extratropical cyclonicity and precipitation over parts of the Atlantic during a warm phase Atlantic Multidecadal Oscillation (AMO) increasing precipitation in northwest Europe in summer (JJA). Summer precipitation in Europe was also found to be wetter (drier) than normal during warm (cold) phases of the AMO by Sutton and Dong (2012). The last AMO cool phase is thought to have been responsible for the dramatic reduction in summertime precipitation in Ireland (McCarthy et al., 2015b). However, the influence of the AMO on the hydroclimate during winter months is not as clear. On one hand, a reduction in winter MSLP during a warm phase might lead to more cyclonic activity, but increases in precipitation in Knight et al. (2006) only occurred in concentrated areas over the North Atlantic Ocean and with only a limited spatial extent over land in Europe.

In light of these research gaps (**Thesis Objective 3**) this chapter addresses the following **chapter objectives**:

- **Chapter Objective 5.1:** Identify which synoptic weather types are associated with floods at the annual and seasonal scale.

- **Chapter Objective 5.2:** Reconstruct flood occurrence for earlier periods using a long running reanalysis product of mean sea level pressure to explore decadal-/multi-decadal-scale variability.
- **Chapter Objective 5.3:** Investigate the relationship between flood-producing synoptic weather types, flood indices and large-scale climate indices that are expected to modulate flooding in Europe.

Section 5.2 outlines the flood indices and atmospheric datasets used; Section 5.3 describes the methods in which there are three main components following each of the research objectives: i.) classification of synoptic drivers of floods, ii.) development of a flood Index for the Island of Ireland, and iii.) examination of how floods and their synoptic drivers are related to larger-scale climate drivers such as the North Atlantic Oscillation (NAO); Section 5.3 displays results which are discussed in Section 5.5 in light of previous work in this area.

## 5.2 Hydroclimatic data

### 5.2.1 Flood indices

The Peaks-Over-Threshold (POT) flood database extracted in Section 4.2.3.1 for 29 catchments in the Irish Reference Network (IRN) was used. The threshold is such that three independent peaks, on average, are identified (i.e. POT3) during each water year (1<sup>st</sup> October to 30<sup>th</sup> September) from daily mean flows (DMFs). All 29 catchments have data covering the period 1978-2009 (water years), with 8 catchments having data between 1956-2009. While the POT3 database is dominated by winter floods, a notable amount (18 %) of POT3 events occur during the summer half year (April to September) (Fig. 5.1) and therefore it will be important to determine if the atmospheric drivers of floods are the same for winter and summer events. It was expected that catchments situated in the Inland and East Extreme Rainfall Region (ERR-IE) would have a higher fraction of summer POT3 events than the rest of the country due the higher proportion of convective precipitation to total precipitation, compared to coastal locations (Logue, 1984). However, Fig 5.2 shows that this is not the case. In fact, the highest contribution of POT3 floods from summer is for small upland catchments, as summarised by higher median Richard-Baker hydrological flashiness index (RBMED) values (from Section 4.2). There is a strong positive linear

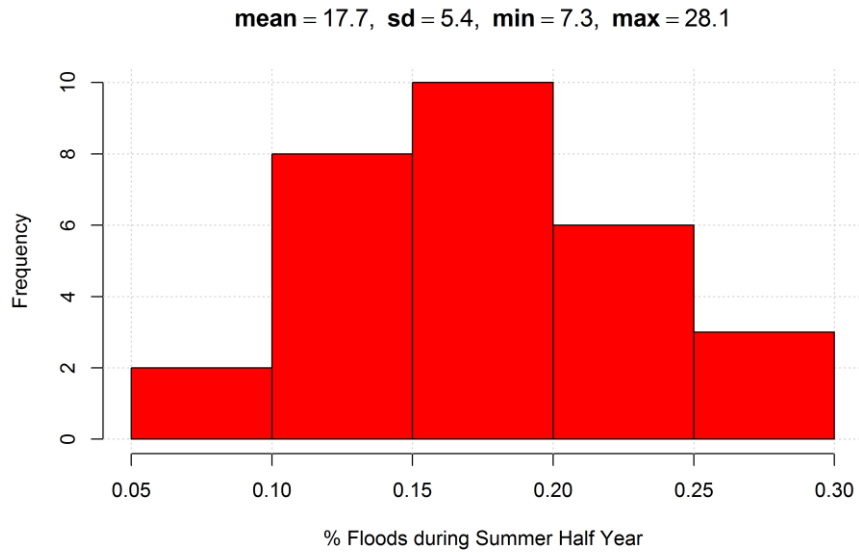


Figure 5.1: Histogram of percentage of POT3 events that occur during the summer half year between water years 1978-2009.

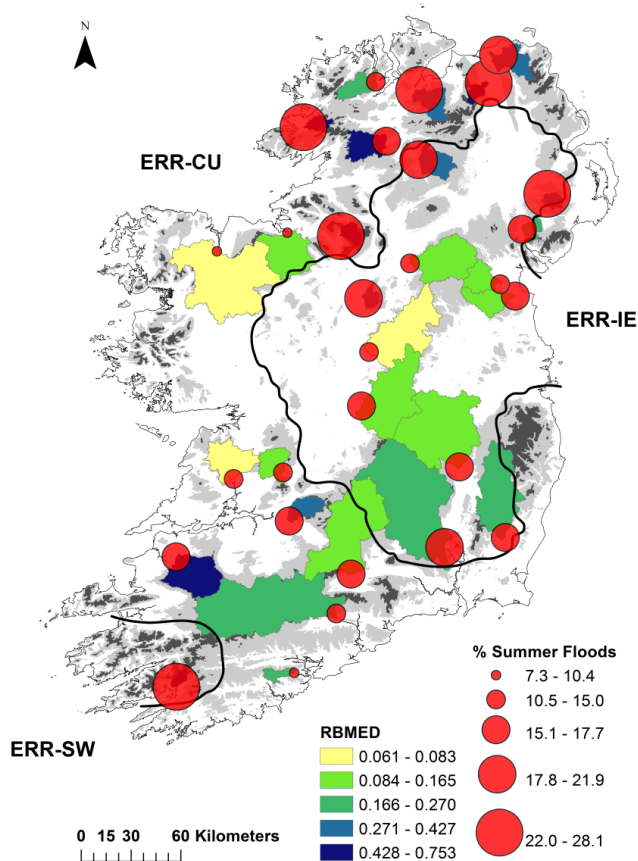


Figure 5.2: Map of contribution of summer floods per IRN station. Larger (smaller) circles represent greater (lesser) contribution to total POT3 events from the summer half year. The flashiness of each catchment is also mapped using RBMED.

relationship between RBMED and percentage of POT3 floods during summer ( $\rho = 0.78$ ). This makes sense as reduced soil moisture in summer means larger groundwater dominated catchments will not translate inputs of heavy rainfall to floods as often compared to flashy (small  $< 650 \text{ km}^2$  and upland  $> 150 \text{ m. a. s. l.}$ ) catchments.

### 5.2.2 Weather type classifications

By far the most widely used weather type classification for the British-Irish Isles (BI) is the Lamb Weather Type (LWT) scheme. The original LWT catalogue was a subjective classification of daily atmospheric flow across the BI by Lamb (1972). Jenkinson and Collison (1977) developed an objective scheme using gridded MSLP but was discontinued in 2007 (Jones et al., 2013b). More recently, the objective LWT scheme was applied by Jones et al. (2013b) to MSLP from the National Centers for Environmental Prediction (NCEP) Reanalysis by (Kalnay et al., 1996) from 1948 to present, and extended to 1871 using the 20CR product and is used here (available: <http://www.cru.uea.ac.uk/cru/data/lwt/>). This approach makes use of three basic variables describing atmospheric circulation at the surface within the BI domain extracted from a 'snapshot' of MSLP at 12:00 UTC: direction of mean flow (D), the strength of mean flow (F), and the vorticity (Z). The rules to define 27 LWTs are given in the Appendix of Jones et al. (2013b). Seven main categories are recognised: the anticyclonic (A), easterly (E), southerly (S), westerly (W), northwesterly (NW), northerly (N), and cyclonic (C) types. The remaining are classified into 19 hybrid combinations of the main types (e.g. cyclonic southerly (CS)) and an unclassified category (U).

The distinct advantage of this new long-term LWT catalogue is the length of record at daily resolution. Given the relatively short length of streamflow data, the possibility of reconstructing flood occurrence back to the 1870s is an attractive approach to contextualise shorter-term variations as shown in Chapter 4. Nevertheless, the quantity and quality of MSLP observations assimilated into 20CR is known to be more limited in the early part of the record (Wang et al., 2013), but Matthews et al. (2015) shows that the BI domain is one of the most stable through time in no small part due to the rich history of pressure observations from ship logbooks in this part of the world (Küttel et al., 2009).

Persistent periods of above/below average sea surface temperatures (SSTs) are described using the Enfield et al. (2001) detrended Atlantic Multidecadal Oscillation (AMO) index (available: <http://www.esrl.noaa.gov/psd/data/timeseries/AMO/>). Atlantic SSTs have oscillated between cold and warm phases with a range of  $\sim 0.4$  °C with two major cold phases from the 1900s to mid-1920s and from 1960s to mid-1990s with a cycle of  $\sim 65$ -80 years (Enfield et al., 2001). While flood series are too short (only cover half a cycle) to test for influence of the AMO, LWT series are sufficiently long to examine if LWT frequencies are governed by Atlantic SST anomalies.

## 5.3 Methods

### 5.3.1 Flood classification

Individual flood events (POT3) for each of the 29 catchments were classified by objective LWTs. However, establishing the flood-producing LWT is not always straightforward as the weather system that caused the flood does not necessarily occur on the same day as the flood was recorded at the gauge. This can happen for two reasons: 1.) individual catchment characteristics determine how an input of precipitation is translated to streamflow: Catchments with low flashiness will have a longer time-to-concentration, thereby introducing a more lagged flood response, compared to small upland flashy catchments. Therefore the flood-producing storm may have passed over the catchment on the previous day but there is a delay before peak streamflow is recorded. 2.) There is a temporal mismatch in the way floods and LWTs are captured. LWTs are extracted daily at 12:00 UTC, whereas the POT3 database is derived from daily mean flows (DMFs) over a 24 hour period. This period is also not standard across different hydrometric agencies. In Ireland, DMFs are recorded between 00:00 and 00:00 UTC (personal communication with hydrometric division of the Office of Public Works (OPW)) whereas for the UK 09:00 to 09:00 UTC is used (Marsh and Hannaford, 2008).

There are several scenarios where extracting the LWT on the concurrent day of a flood may be inaccurate. For example, say a large storm passed over Ireland between the 20<sup>th</sup> and 21<sup>st</sup> of November lasting 24 hours (10:00 UTC on first day to 10:00 UTC the second day). It is easily possible that peak streamflow in a given catchment could have occurred on either the 20<sup>th</sup> or 21<sup>st</sup> (as the storm occurred across two periods of 24

hour streamflow measurement cycles). Antecedent conditions are less important for flashy catchments and hence they might report peaks on the 20<sup>th</sup>, while less flashy catchments will report a peak on the 21<sup>st</sup>. Similarly, if the flood-producing storm event happened over the later part of the day (i.e., post 12:00 UTC), it would not be recorded on that day within the LWT catalogue and may actually be captured on the day after the flood (at 12:00 UTC on the 22<sup>nd</sup>). Lastly, slower moving extratropical storms associated with most extreme precipitation in Ireland can take more than 24 hours to pass overhead. The only way to truly capture the exact synoptic event that produced flooding is to manually examine each individual flood event in the database along with detailed historical meteorological summaries and charts. However, over the water years 1978-2009 there were almost 3000 individual flood events recorded within the POT3 database and so would be impractical.

A simple method was therefore used to objectively identify the more likely flood-producing atmospheric condition by examining the LWT that occurred on the concurrent day of flood (day 0), the previous day (day – 1), and the day following the recorded flood (day + 1) and select the LWT with the highest Jenkinson Gale Index (G), also calculated as part of the Jones et al (2013b) LWT catalogue. G makes use of two of the three basic variables (F and Z) and is higher for days with more *intense* circulation (and assumed to be more likely to produce most extreme precipitation amounts):  $G = [F^2 + (0.5Z)^2]^{1/2}$ , with a gale defined when  $G > 30$ , severe gale when  $G > 40$ , and a very severe gale when  $G > 50$ . If G is higher for the LWT on day -1 or day + 1, then that LWT is instead recorded as the flood-producing type. This approach is referred to as the 3 day centred approach (3 day) and for comparability with WQ2013 the LWT on the concurrent day was also extracted (day 0). Admittedly, while it seems physically impossible for a system occurring the day after a flood to have caused the flood itself, conceptually it is plausible in the case that a precipitation event occurs after 12:00 UTC on the concurrent day and is instead captured in the day following the flood.

Using the method of WQ2013 over the period 1978-2009 (Water Years), a given LWT was considered flood rich if the ratio of observed to expected frequencies exceeds 1, or flood poor if less than 1. The expected frequency  $Ef$  is the percentage of all days (between 1978-2009) falling into that LWT category regardless of whether or not a

flood occurred. The observed frequency  $Of$  is the percentage of those days under the same LWT with a flood (using both the day 0 and 3 day centred approaches introduced above). For example, the expected frequency of the C-type is 13.3 % at the annual time-scale while floods at St6013 occur 39.6 % (when using the day 0 approach) and 55.2 % (when using the 3 day centred approach) of the time under this LWT resulting in a ratio of 2.98 and 4.15 respectively, hence this LWT is regarded as a flood rich type for this catchment at this time-scale.

These LWT-flood ratios are termed flood loadings and have been calculated for each catchment at annual (October to September), winter (October to March), and summer (April to September) time-scales ( $T$ ), and pooled for the entire Island of Ireland (Iol), and per Extreme Rainfall Region (ERR-CU and ERR-IE). Note, there is only one catchment (St21002) within the southwest ERR (ERR-SW), so this is instead pooled within the ERR-CU leaving 17 catchments within this ERR, and 12 within ERR-IE. Flood loadings are calculated as a vector of weights  $\omega$  for time-scale  $T$ , each of the  $n = 27$  LWTs  $i$ , and  $m$  catchments in regions  $j$  by:

$$\omega_{Tij} = \frac{1}{m} \sum_{j=1}^m \frac{Of_{Ti}}{Ef_{Ti}}$$

**Equation 5.1**

where the flood loading per region (e.g. Iol or CU) is simply the average of flood loadings across  $m$  catchments within that region. The relative weight (i.e., flood loading  $\omega_{Tij}$ ) attached to each region will be different depending on local weather influences, and is also tested on a seasonal scale to examine if the atmospheric drivers of flooding are similar throughout the year. A flood loading of 2 for a C-type means floods occur twice as often as would be expected under that particular LWT and hence would be classed as flood rich. Distinction is made between flood-producing and flood rich LWTs. A flood-producing LWT is one that has been physically associated with any single observed flood event; whereas more specifically a flood rich LWT is one that has a flood loading above 1 (i.e. the expected frequency of the LWT is also taken into consideration). The role of antecedent conditions was also tested by calculating

observed frequencies from lag = 0 to lag = 30, and similar to WQ2013 observed and expected frequencies converged after about two weeks (not shown).

### 5.3.2 Annual and seasonal flood-index

Flood loadings were combined with the annual frequencies of LWTs by WQ2013 to produce an annual flood-Index (F-Index) that gives a measure of flood occurrence dependent upon if a particular year had a high/low frequency of flood rich LWTs. Here, the F-Index in year  $y$  ( $F_{Tyj}$ ) was calculated for annual, winter half year, and summer half year time-scales  $T$  using flood loadings ( $\omega_{Tij}$ ) from Equation 5.1 calibrated over the 1978-2009 period for lol, ERR-CU, and ERR-IE regions  $j$ :

$$F_{Tyj} = \sum_{i=1}^n LWT_{Tyi} \times \omega_{Tij}$$

Equation 5.2

where  $LWT_{Tyi}$  is the frequency of the  $n$  LWTs  $i$  in year  $y$  at time-scale  $T$ . The ability of the F-Index to reconstruct flood occurrence was assessed by applying flood loadings during calibration (1978-2009) and LWT frequencies during a 22 year independent evaluation period (1956-1977) to hindcast observed POT events. There are at least 8 active streamflow stations from 1956 which represent the best spatio-temporal coverage available. Five of these catchments reside within the ERR-CU and 3 within the ERR-IE. From Chapter 4 it was shown that the north of the Island is not represented within this longer term network of stations and must be taken into account when interpreting results. The skill of the F-Index at the annual (Ann), winter half year (WH), and summer half year (SH) time-scale for the entire lol is tested during the evaluation period by Pearson correlation with a null hypothesis of no linear relationship ( $\rho = 0$ , at the 5 % level) between the average number of POT frequencies per active stations and the F-Index.

### 5.3.3 Linkages with large-scale climate

The NAO and AMO are used for two tasks: 1.) To examine the relationship between the DJF NAO and flood indices using Pearson correlation (at the 5 % level) over the 1978-2009 period to test if the NAO is associated with flood frequency (POT3,

POT3\_WH), magnitude (AMAX, MAX10), high flow prevalence (PQ10), and high flow duration (CQ10); 2.) The most important flood-producing LWTs for the winter half year (i.e. when > 80 % of floods occur) are correlated with both the winter half year NAO (ONDJFM NAO) and DJF NAO, and the winter half year AMO. It is recognised that the AMO is not strictly a ‘large-scale climate’ mode but considered here due to its known influence in modulating large-scale climate variability in Europe.

## 5.4 Results

### 5.4.1 Expected frequency of LWTs

The most frequent LWTs (regardless of flooding) over the 1978-2009 period is the A-type (20.8 %), C-type (13.3 %), W-type (10.3 %), and SW-type (9.7 %) (Fig. 5.3). The A-type and C-type are more common in summer (23.2 and 14.2 % respectively) than in winter (18.4 and 12.5 % respectively), whereas W- and SW-types occur more in winter (12.3 and 12.1 % respectively) compared to summer (8.3 and 7.3 % respectively).

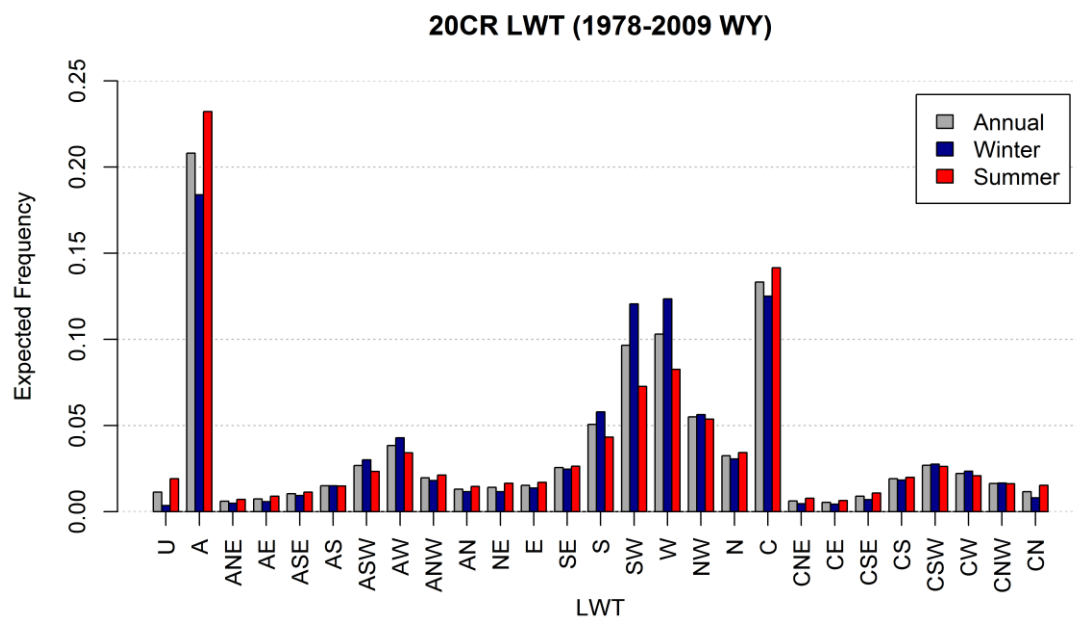


Figure 5.3: Expected frequencies of each of the 27 Lamb Weather Types (LWTs) between Water Years (WY) 1978-2009, for annual (grey bars), winter (October to March; blue bars), and summer (April to September; red bars).

Matthews et al. (2015) also find cyclones occur more during summer (using a different cyclone metric) than in winter in the BI domain (50°- 60°N, 16°W - 6°E). However, it must be noted that summer cyclones are much less intense than in winter, and hence

storminess (cyclone frequency  $\times$  cyclone intensity) actually peaks around November (Matthews et al., 2015). Interestingly, this coincides with the average timing of maximum precipitation in Ireland (from Chapter 3).

#### 5.4.2 Flood occurrence by LWT and region

Across the Island of Ireland at the annual-scale, 5 LWTs accounted for 75 % for observed POT3 floods during the water year period 1978-2009. In order of importance: C (41.2 %), SW (12.3 %), W (10 %), S (7.1 %), and CSW (4.4 %) based on the 3 day centred method of classification (Fig. 5.4a). In comparison, classification based on the LWT on concurrent day of flood (day 0) reveals similar flood-producing LWTs, but gives much reduced dominance to the C-type (34.3 %). Assuming the 3 day centred approach gives more accurate classification of the flood-producing LWT, then this would mean classification based on the day 0 method associates floods with a non-flood producing LWT. However, it is tested below whether or not the day 3 method improves the skill of the F-Index. For the winter half year (Fig. 5.4b), the same 5 LWTs are also the top 5 and account for 77 % of POT3\_WH events. For the summer half year (Fig. 5.4c), the same 5 LWTs account for 67 % of POT3\_SH floods with the C-type even more dominant (45.5 %) and the W- and SW-types less important (4.5 % and 5.6 % respectively). CS- (6 %) and CN-types (4.9 %) replace W- and CSW-types in the top 5 and bring the number of summer floods accounted for from 67 % to 69 %, highlighting that the C- (most dominant) and S-types (second most dominant, 7 %) are associated with the majority of summer floods.

To determine if these flood-producing LWTs are flood rich the expected frequency of each LWT regardless of whether or not a flood occurred is taken into account (i.e., a LWT with a flood loading  $> 1$  is considered flood rich). For example, 2.3 % of all floods occurred under an A-type (using the 3 day method), but the expected frequency of an A-type is 20.8 % so therefore this LWT is classed as flood poor (with a flood loading of just 0.11 for the Island of Ireland as a whole). Figure 5.5 shows the flood loadings for each of the 27 LWTs at the annual and seasonal time-scale for the Island of Ireland and sub-regions using the 3 day centred approach. At the annual scale (Fig. 5.5a), almost all cyclonic types (pure and hybrid) are flood rich, with the exception of CNE- and CE-types for the ERR-CU (and hence lol overall). S- and SW-types are also flood rich, albeit

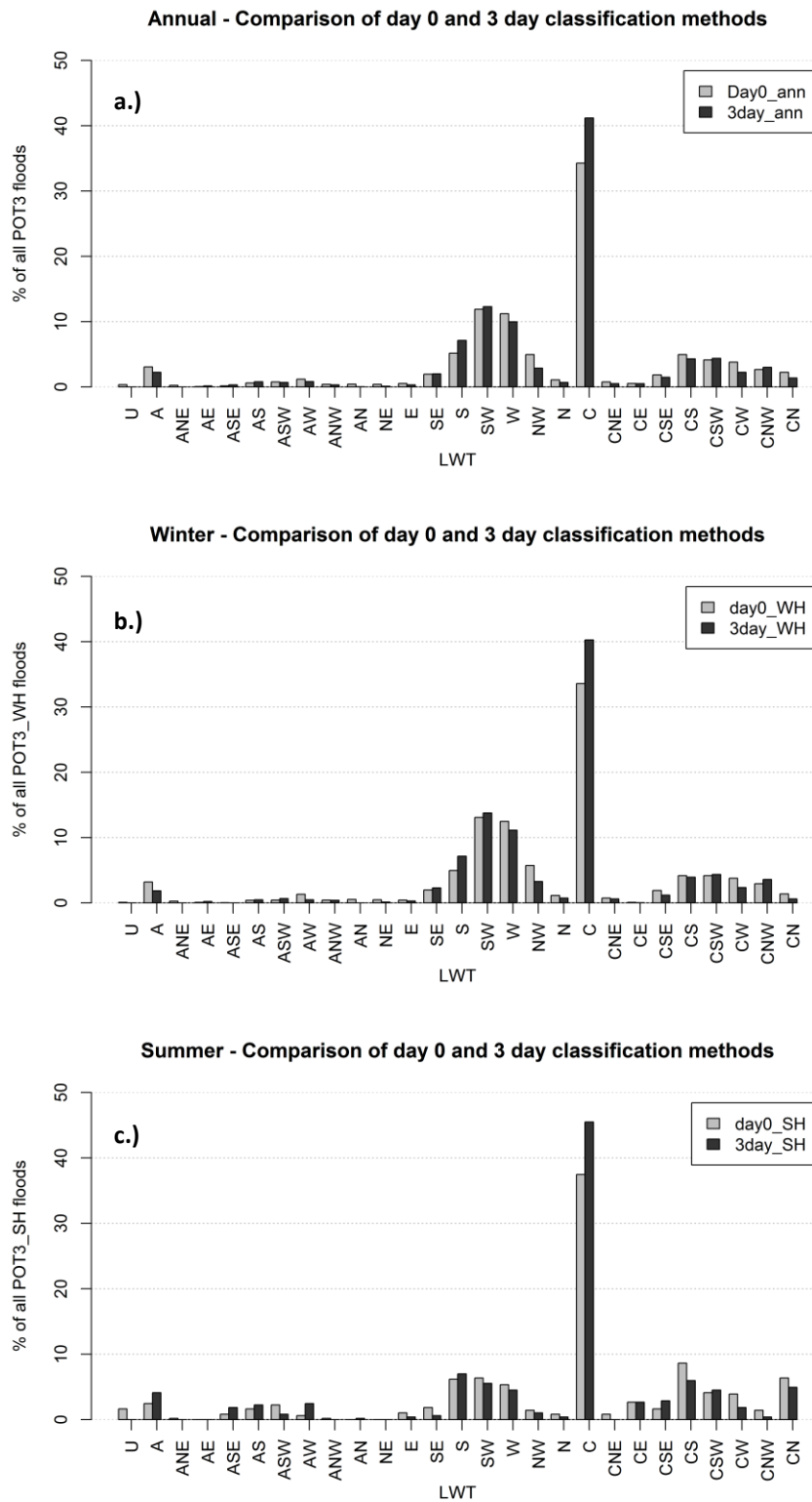


**Figure 5.4: Comparison between 'day 0' and '3 day centred' methods for classifying flood-producing LWTs for (a.) annual, (b.) winter half year, and (c.) summer half year based on percentage of associated POT3 floods over the water year 1978-2009 period.**

with a lower weight. Even though the W-type is the third most important flood-producing LWT, it is not a flood rich LWT for annual at the scale of IoI or ERR-IE because it also has a high expected frequency, but is for ERR-CU.

Flood loadings for the winter half year are very similar to annual (Fig. 5.5b), but there are some differences for summer (Fig. 5.5c). Cyclonic types are more dominant than for annual and winter, although with some notable differences between ERR-CU and ERR-IE sub-regions. Cyclonic types have a greater weighting in ERR-IE (with a flood loading of almost 4), whereas LWTs with a southerly component (S-, AS-, and ASE-types) are flood rich in catchments within ERR-CU. However, it must be noted that because there are fewer floods during the summer half year (18 % of POT3 events), even if a single flood occurs under a LWT with a low expected frequency, the observed frequency may be artificially high. This can be seen by some flood loadings > 10 for individual stations in Figure 5.5c.

The spatial distribution of flood loadings for the top 5 LWTs associated with the majority (75 %) of floods at the annual time-scale are shown in Figure 5.6. Notable is the more subtle spatial variation even within the same ERR. The C-type affects floods in the ERR-IE mostly but in particular catchments in the northeast of the Island with some having flood loadings above 4. SW- and W-types have a stronger influence in ERR-CU, in the northwest in particular. The S-type, as expected, has highest flood loadings for catchments along the southern coast; four having loadings > 2.5: St21002 (Coomhola in Kerry/Cork boarder), St19001 (Owenboy in Cork), St18002 (Blackwater in Cork), and St12001 (Slaney covering much of Wexford, Carlow, and southern Wicklow).

To find out which circulation patterns were responsible for the most widespread flooding (i.e. spatial extent of a single flood event), days were ranked in terms of how many stations reported a flood, within a 3 day window, and the top 10 most widespread flood events examined in more detail (Table 5.1). Similar to above the 3 day centred approach was preferred for ranking stations reporting most floods for a single day as it was found that in a significant number of cases the true extent of an event was not captured if the previous or following days were not considered. For example, between the 08/12/2007 and 10/12/2007 23 catchments (~ 80 % of stations) reported a POT event across the Island (ranked joint first most widespread). However,

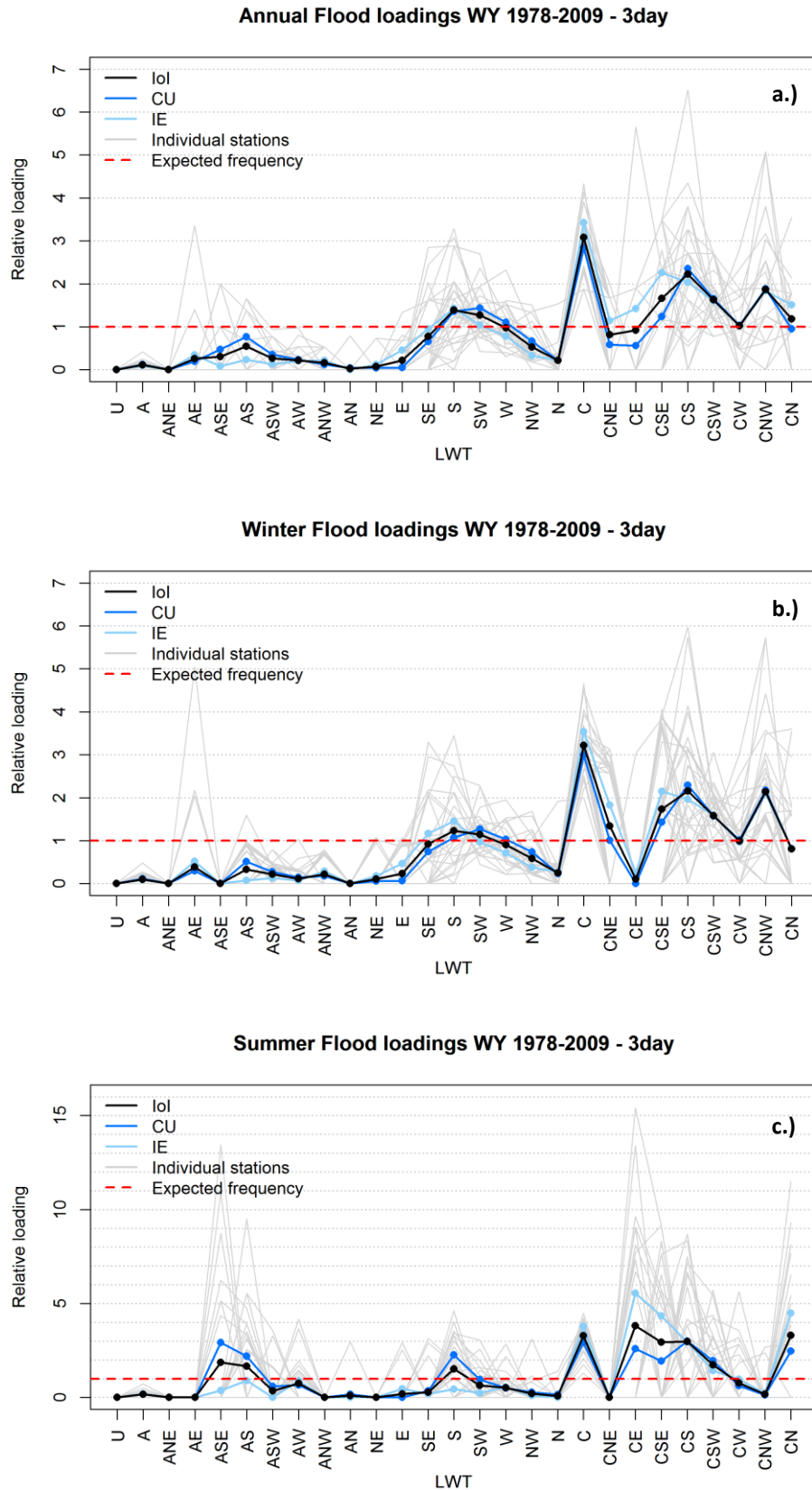
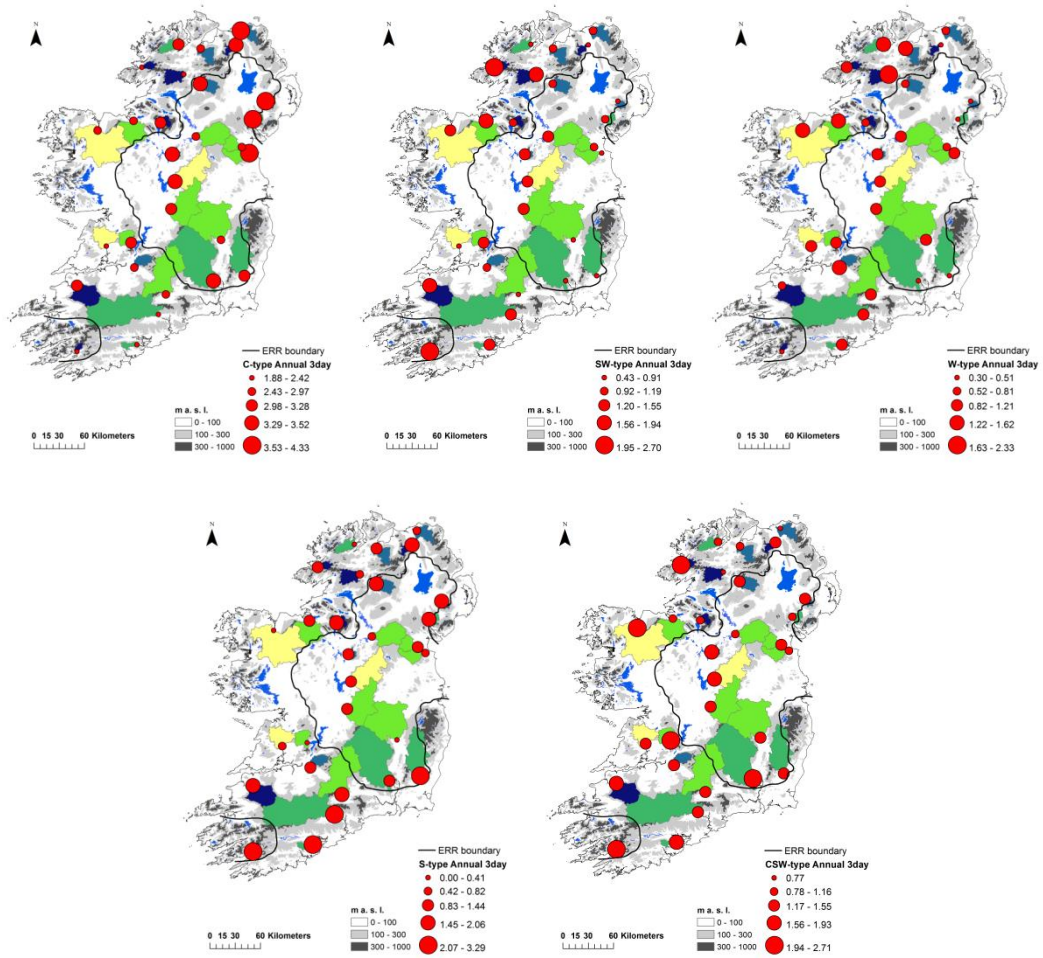


Figure 5.5: Flood loadings for each LWT and ERR for a.) annual, b.) winter half year, and c.) summer half year. Black lines are average flood loadings for the Island of Ireland (IoI), dark blue Coastal & Upland ERR (CU), and light blue Inland & East ERR (IE). Grey lines are flood loadings for individual stations and dashed red line represents when a LWT has a loading equal to the expected frequency (i.e. flood loading = 1); values above (below) are flood rich (poor).



**Figure 5.6: Spatial distribution of flood loadings for individual catchments for the top 5 LWTs associated with 75 % of POT3 floods. Circles increase (decrease) in size for catchments with greater (lower) flood loadings. Catchments are coloured according to RBMED (as in Fig. 4.1).**

only 9 floods were reported on the 08<sup>th</sup>, 10 on the 09<sup>th</sup>, and 4 on the 10<sup>th</sup>. If only the largest number of floods being reported for a single day was used to define multi-catchment flood events then this event would have been reported to affect just 34 % of the network, and therefore the spatial extent of this event been greatly underestimated.

Out of the top 10 most widespread floods, 5 occurred under a C-type, 2 under a W-type, 2 under a CS-type, and 1 under a CNW-type. The flood on the 08/01/2005 also had almost 80 % of the network reporting a POT3 (within a 3 day window). Figure 5.7 and Figure 5.8 shows a more detailed assessment of the atmospheric conditions within the 3 day window of one of the most widespread floods recorded between 1978-2009 on the 08/01/2005 using MSLP and Total Column Water (TCW) at 12:00 UTC (same

time MSLP from LWT catalogue) from the ERA-Interim reanalysis product (Dee et al., 2011). A positive North Atlantic Oscillation like dipole is apparent (NAO for the month of January 2005 was +1.85 using the index of Jones et al. (1997)), with a low pressure centre near Iceland and high pressure over southwest Europe (Fig. 5.7) and was recorded as a W-type in the LWT catalogue on the 07<sup>th</sup> and 08<sup>th</sup>, and a SW-type on the 09<sup>th</sup>. When examining the atmospheric water vapour component during the time of this event (depicted using TCW) two Atmospheric River-like patterns were apparent on the 07<sup>th</sup> and 09<sup>th</sup>, but not the 08<sup>th</sup> (Fig. 5.8). Allan et al. (2015) also detected the Atmospheric River on the 7<sup>th</sup> using more formal methods. Nevertheless, only 3 floods were recorded on the 07<sup>th</sup>, whereas 13 were recorded on the 08<sup>th</sup> (where no water vapour was advected over Iol at 12:00 UTC), and 7 on the 09<sup>th</sup>. This further supports the need for a multi-day window to be used when considering both the spatial flood extent from any single storm system and classification of the flood-producing circulation pattern. Only considering atmospheric conditions at a single point in time on the concurrent day of a flood may lead to misleading results.

**Table 5.1: Top 10 floods with largest spatial extent (% catchments from  $n = 29$ ) from stations reporting a POT3 flood within a 3 day window. ‘Date’ is the date of the centre day where in most cases the majority of floods were recorded. LWT and G are the Lamb Weather Type and G-index associated with floods over each 3 day window. Bold are very severe gales ( $G > 50$ ), underlined are severe gales ( $G > 40$ ), and Italics are gales ( $G > 30$ ).**

Rank	% catchments	LWT - 1	G - 1	LWT 0	G 0	LWT + 1	G + 1	Date	Season
1	79	W	33.6	W	<u>45.5</u>	SW	33	08/01/2005	WH
2	79	C	36.6	C	<u>46.2</u>	AN	21.6	09/12/2007	WH
3	76	CW	<b>56.6</b>	C	<b>63.5</b>	CN	38.6	20/12/1982	WH
4	69	SE	36.6	C	32	C	29.1	28/12/1978	WH
5	69	CSW	<u>38.6</u>	CNW	<b>53.8</b>	W	15.4	01/02/1983	WH
6	69	S	22.4	CS	<b>51.1</b>	W	11.7	10/03/1995	WH
7	66	CW	29.6	W	<u>41.3</u>	NW	38.5	22/12/1991	WH
8	66	CS	26.2	CS	19.6	C	30.3	17/08/2008	SH
9	62	SW	22.6	C	30.6	W	37.9	07/02/1990	WH
10	62	C	38.8	C	33	CW	30.2	09/12/2000	WH

### 5.4.3 Reconstructed annual and seasonal flood occurrence

The F-Index is based on the frequency of flood rich LWTs, so if a particular year has a higher than normal frequency of flood rich LWTs the F-index will be greater than normal. C- and SW-types contribute most weight to the F-index as these both occur

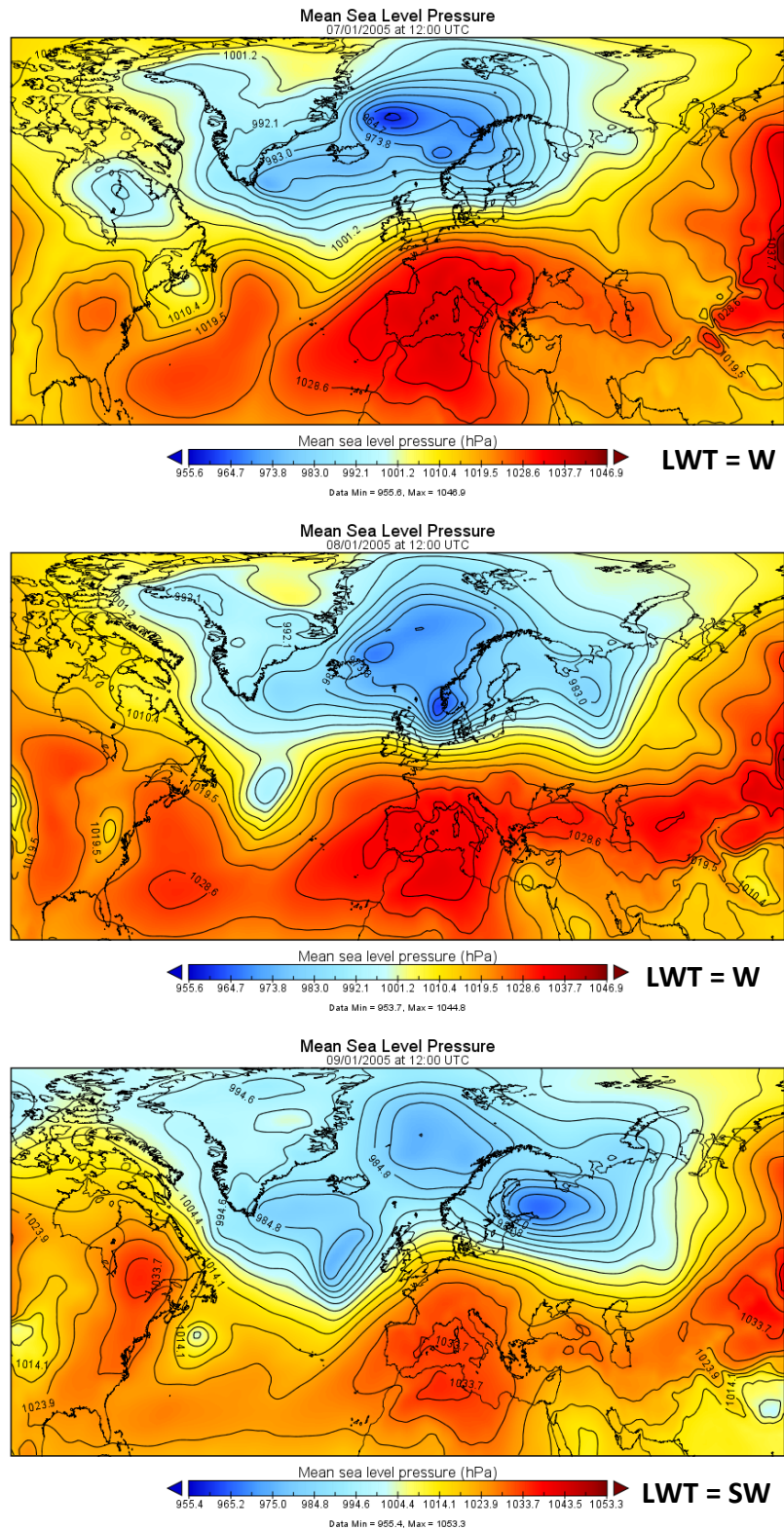


**Figure 5.7: Mean Sea Level Pressure (MSLP) fields (in hPa) at 12:00 UTC from ERA-Interim reanalysis at  $0.75^\circ \times 0.75^\circ$  resolution on the day before, day of (08/01/2005), and day after the most widespread flooding across the Island of Ireland (almost 80 % of catchments).**

often and have relatively large flood loadings. Table 5.2 shows correlations between annual, winter and summer F-Indices and average number of active POTs across the

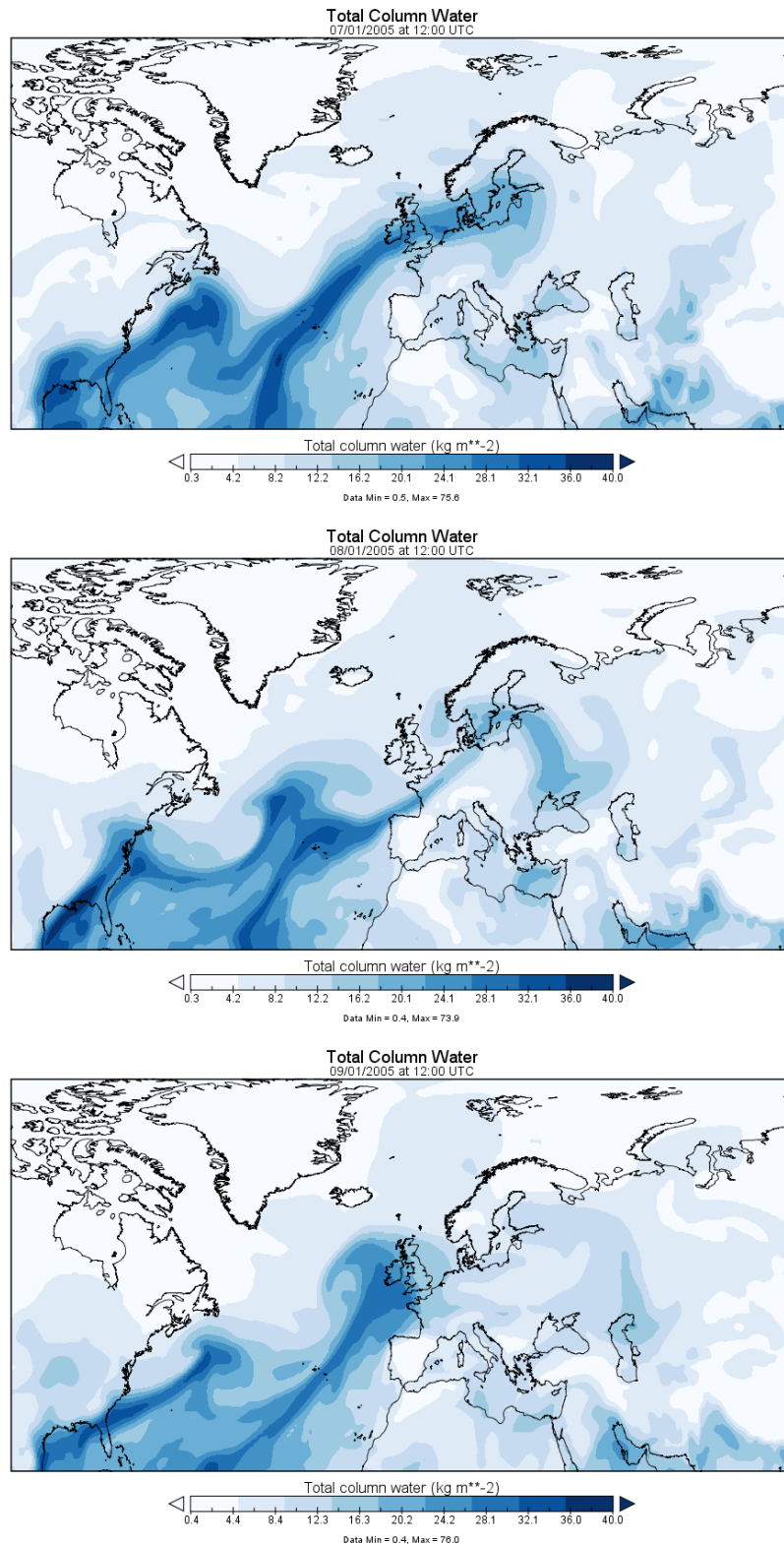


**Figure 5.8: Total Column Water (TCW) fields (in  $\text{kg m}^{-2}$ ) at 12:00 UTC from ERA-Interim reanalysis at  $0.75^\circ \times 0.75^\circ$  resolution on the day before, day of (08/01/2005), and day after the most widespread flooding across the Island of Ireland (almost 80 % of catchments).**

network during the evaluation period (1956-1977) and calibration period (1978-2009) for both the day 0 and 3 day method of classification. The annual F-Index is most skilful

in reproducing observed annual POT occurrence using the 3 day method (Fig. 5.9a) with a strong positive statistically significant correlation coefficient ( $\rho = 0.64$ ) compared to the day 0 method of  $\rho = 0.55$  (also statistically significant). The winter F-index is more strongly correlated with winter POT occurrence ( $\rho = 0.41$  for 3 day, significant) than using the annual F-Index for predicting observed winter POTs ( $\rho = 0.32$  for 3 day, non-significant) during calibration, but not for evaluation where correlations are not statistically significant for either day 0 and 3 day methods (Fig. 5.9b). The summer F-Index (Fig. 5.9c) has stronger correlations with summer POT occurrence than the annual F-Index during both calibration ( $\rho = 0.42$ , significant) and evaluation ( $\rho = 0.5$ , significant). In general, the F-Index shows moderate skill in reproducing observed POT occurrence with a higher number of POTs, on average, with higher F-Index values, but has better skill at annual than seasonal time-scale.

**Table 5.2: Flood Index evaluation and calibration based on Pearson correlation. Bold are statistically significant at the 5 % level with a null hypothesis of  $\rho = 0$ .**

	Evaluation (1956-1977)			Calibration (1978-2009)		
	Annual POTs	Winter POTs	Summer POTs	Annual POTs	Winter POTs	Summer POTs
Annual F-Index lol (day 0)	<b>0.55</b>	<b>0.48</b>	<b>0.45</b>	<b>0.53</b>	0.30	0.21
Annual F-Index lol (3 day)	<b>0.64</b>	<b>0.57</b>	<b>0.48</b>	<b>0.55</b>	0.32	0.21
Winter F-Index lol (day 0)	0.23	0.22	0.14	<b>0.36</b>	<b>0.47</b>	-0.16
Winter F-Index lol (3 day)	0.27	0.28	0.14	0.32	<b>0.41</b>	-0.14
Summer F-Index lol (day 0)	<b>0.48</b>	0.35	<b>0.50</b>	<b>0.39</b>	-0.04	<b>0.46</b>
Summer F-Index lol (3 day)	<b>0.50</b>	0.37	<b>0.50</b>	<b>0.47</b>	0.06	<b>0.42</b>

The flood loadings calibrated over the 1978-2009 period were then applied to LWT frequencies at an annual and seasonal scale using the 3 day method over water years 1872-2015 providing a 144-year long series of reconstructed flood occurrence (Figures 5.10-5.12) for lol and the two sub-regions. The F-Indices were standardised by their long term mean and standard deviation so that values above (below) 0 are indicative of greater (lower) than average flood incidence. LOESS is applied to reveal decadal-scale variability (using a 15-year span).

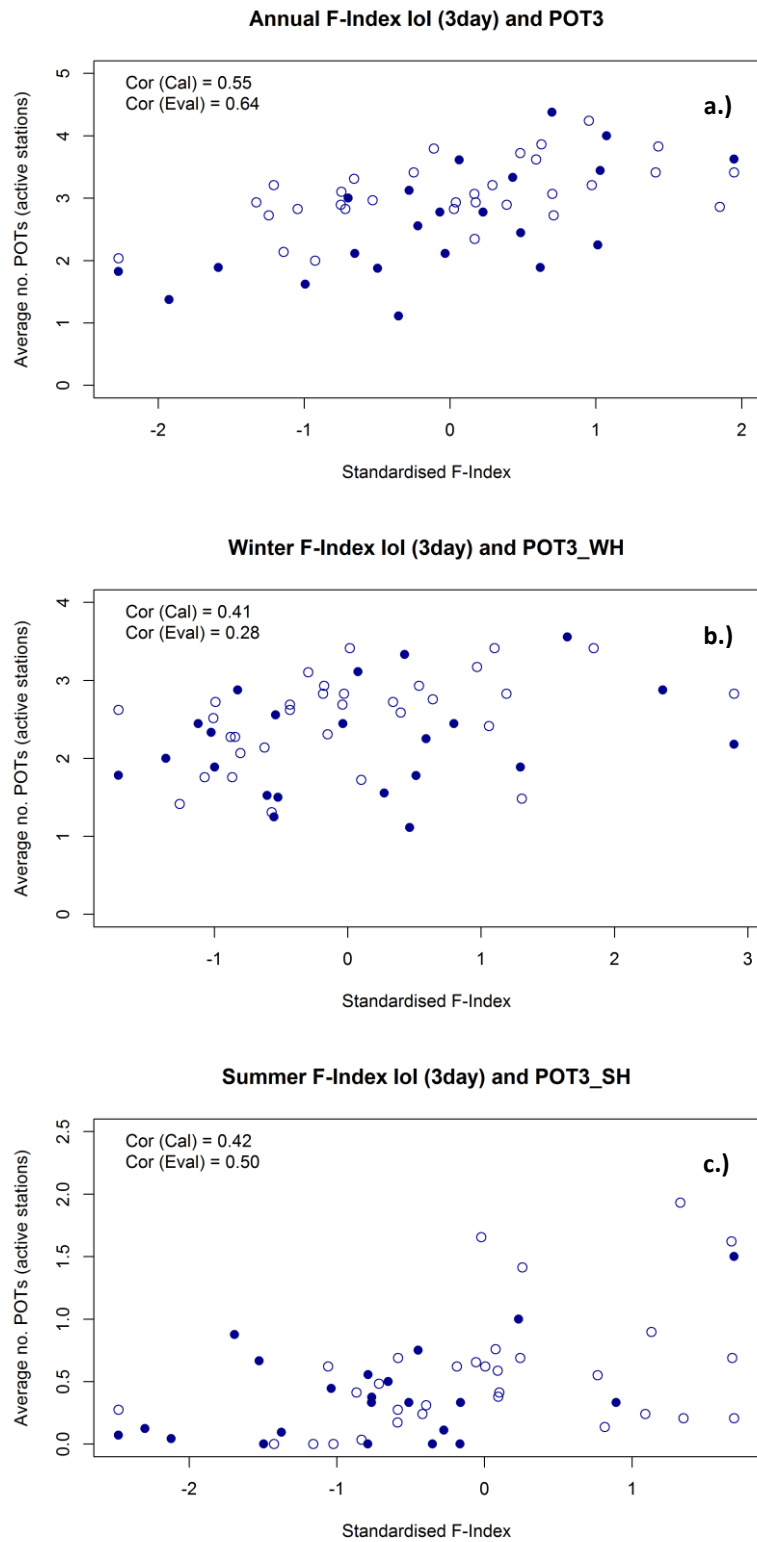


**Figure 5.9: Annual (a.), winter (b.), and summer (c.) relationships between F-index and average number of observed POTs per active station per year. Open circles show data used during calibration (1978-2009) with solid circles during evaluation (1956-1977).**

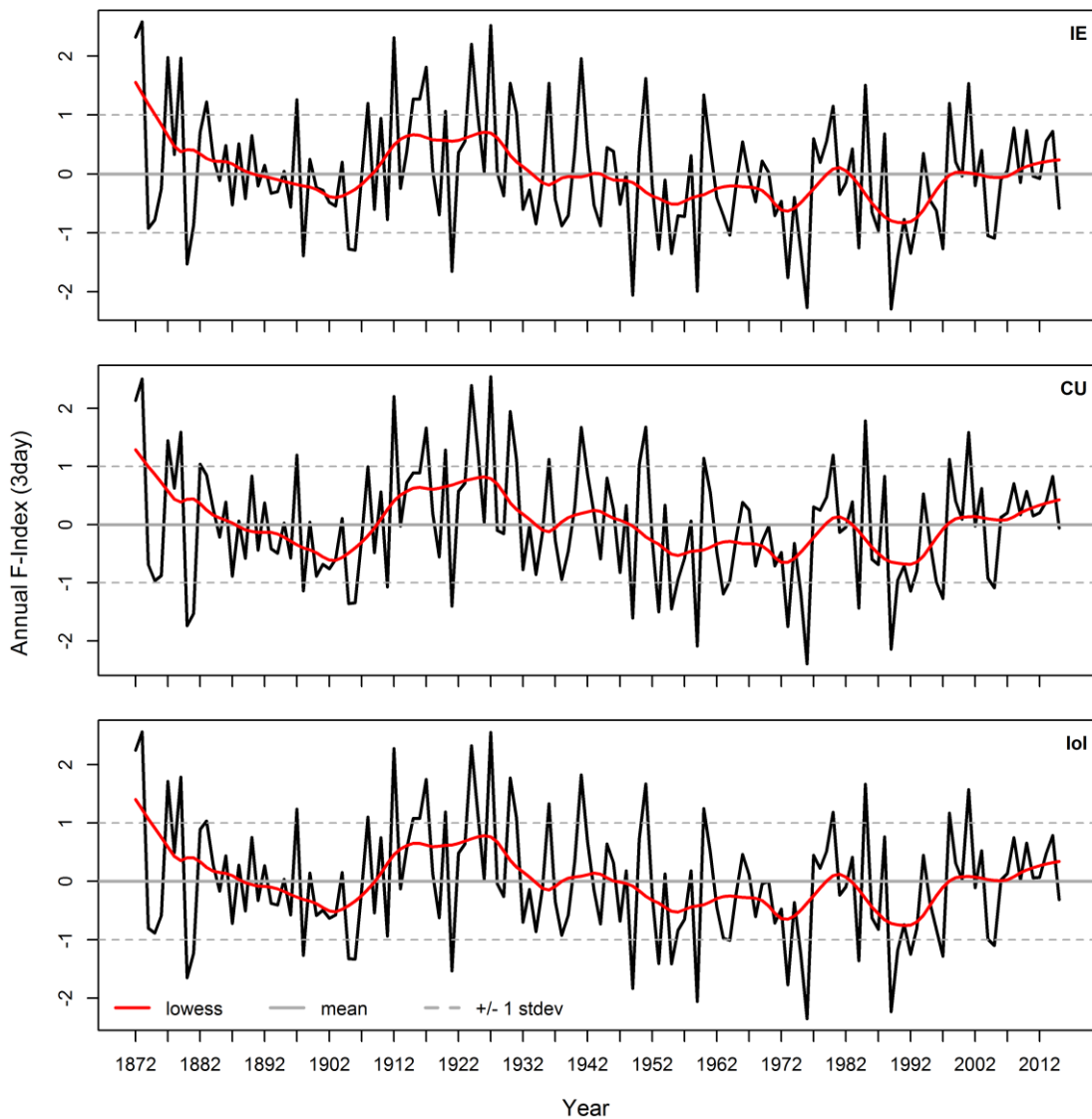


**Figure 5.10: Annual F-Index using annual 1978-2009 flood loadings for ERR-IE (top), ERR-CU (middle), and lol (bottom) applied to yearly LWT frequencies from 1872-2015 (water years), forming a 144-year flood reconstruction (black line). The F-Index has been standardised by its long-term mean and standard deviation. Red line is LOESS smoothed with a span = 15 years. Values above (below) 0 are rich (poor) with +/- 1 standard deviation as dashed grey line.**

Four flood rich periods (where the F-Index is above 0 for a sustained period of time) are acknowledged: 1.) 1870s to 1890s; 2.) late-1900s to mid-1930s, 3.) short spell in the 1980s, and 4.) late-1990s onwards. The two earlier flood rich periods are more extensive than the 1980s and current flood rich period. There is little notable difference between the F-Index at the scale of lol and sub-regional, suggesting that periods with sustained flood-favourable conditions, in general, affect the entire Island.

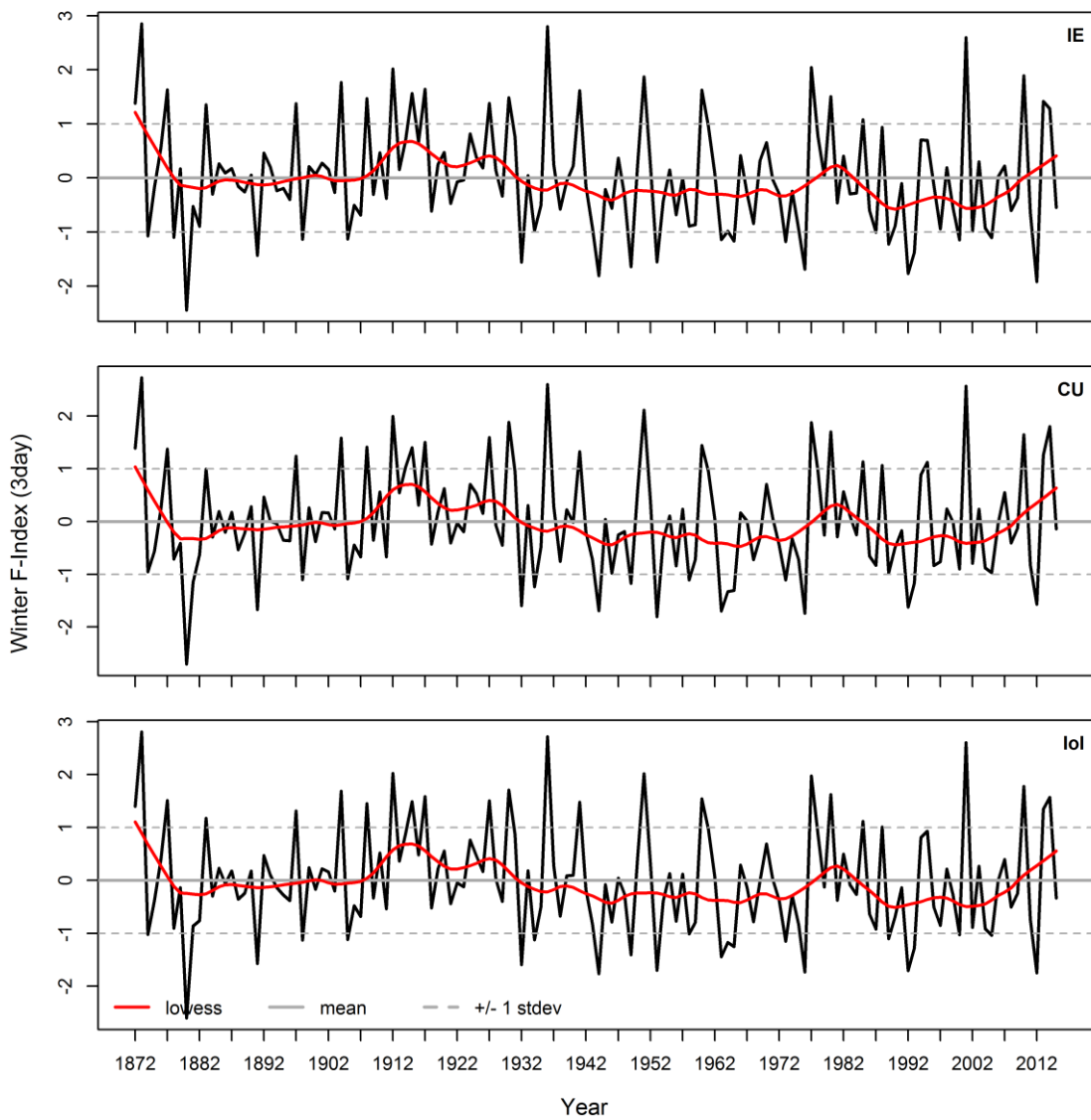


**Figure 5.11: As for Figure 5.10 but for the winter half year.**

When disaggregating to a seasonal scale, the same four flood rich periods emerge with some differences: In winter the 1870s to 1890s is more confined to pre-1880s, the 1980s is more pronounced, and the most recent flood rich period is only apparent since the mid-2000s. In summer the 1870s to 1890s lasted longer than for winter, the 1980s is not as pronounced, while the most recent period is flood rich in the 1990s and early 2000s with a flood quiescent period during summer since 2012.

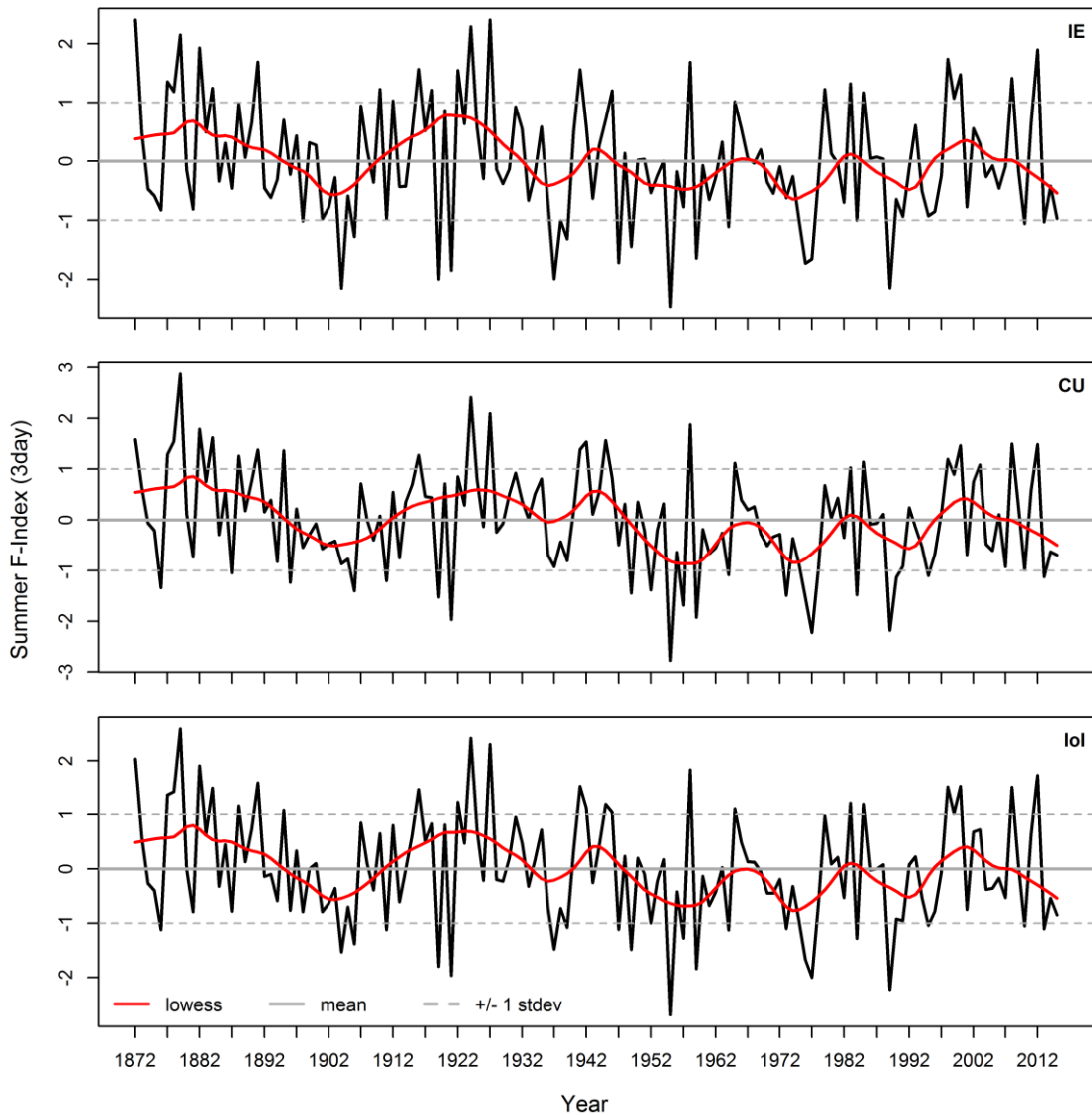


Figure 5.12: As for Figure 5.10 but for the summer half year.

#### 5.4.4 Large-scale climate links

Focus on links between large-scale climate and LWTs and flood indices is for the winter half year as this is when baroclinic activity is greatest due to the larger temperature gradient between cold polar regions and the warmer mid-latitudes, and thus is most appropriate for analyses involving the NAO – the most important mode of large-scale decadal climate variability in the Euro-Atlantic domain.

Correlations between DJF NAO and flood indices over water years 1978-2009 are shown in Figure 5.13. There are no statistically significant correlations with flood frequency at the annual-scale (POT3) but 17 % of stations have statistically significant correlations with winter flood frequency (POT3\_WH) with strongest values in ERR-CU,

particularly for catchments in the northwest. Correlations are much stronger for multi-day maximum streamflow magnitudes; MAX10 has 35 % of stations with statistically significant positive correlations compared to 10 % for annual maximum (AMAX). Again, a clear spatial pattern emerges with strongest positive NAO-flood relationships in the west and northwest with some negative correlations along the eastern seaboard. Almost 90 % of stations reported positive correlations with the NAO for PQ10 (a high flow prevalence measure) with 45 % of stations being statistically significant. Nearly a quarter of stations show statistically significant positive association with NAO and high flow duration, meaning when the NAO is in a positive phase high flow periods above the 10<sup>th</sup> percentile tend to last longer which could be a sign of more favourable antecedent conditions for flood generation.

MAX10 and PQ10 are most strongly related to positive phases of the NAO in areas in the west and northwest where catchment wetness tends to be highest (see distribution of the FLATWET Physical Catchment Descriptor in Fig. 4.1). The strength of NAO-MAX10 and NAO-PQ10 correlations themselves are strongly positively correlated with FLATWET ( $\rho = 0.56$  and  $0.59$ , respectively); Areas with lower FLATWET values are more strongly *negatively* correlated with the NAO, while catchments with higher FLATWET values are more strongly *positively* correlated with the NAO, suggesting that antecedent catchment characteristics (wetter soils) might be important. Only areas of the country that have the longest proportion of time with wet soils show strong positive associations with the NAO. For example, St34001 (Moy in Mayo) has the highest correlation with the NAO for PQ10 ( $\rho = 0.67$ ) and also has the largest FLATWET value (0.73, i.e. catchment typically wet 73 % of the time). Nied et al. (2014) show that soil moisture state within a catchment is a key variable of pre-event catchment conditions, where floods tend to be initiated by overall high soil moisture content. There are no statistically significant correlations between strength of NAO-MAX10 or NAO-PQ10 correlations and catchment flashiness (RBMED) or catchment altitude (ALTBAR). Therefore, the strongest influence of the NAO appears to be for wetter catchments and not necessarily those most strongly influenced by orography (e.g. ERR-SW) nor those which are more/less flashy.

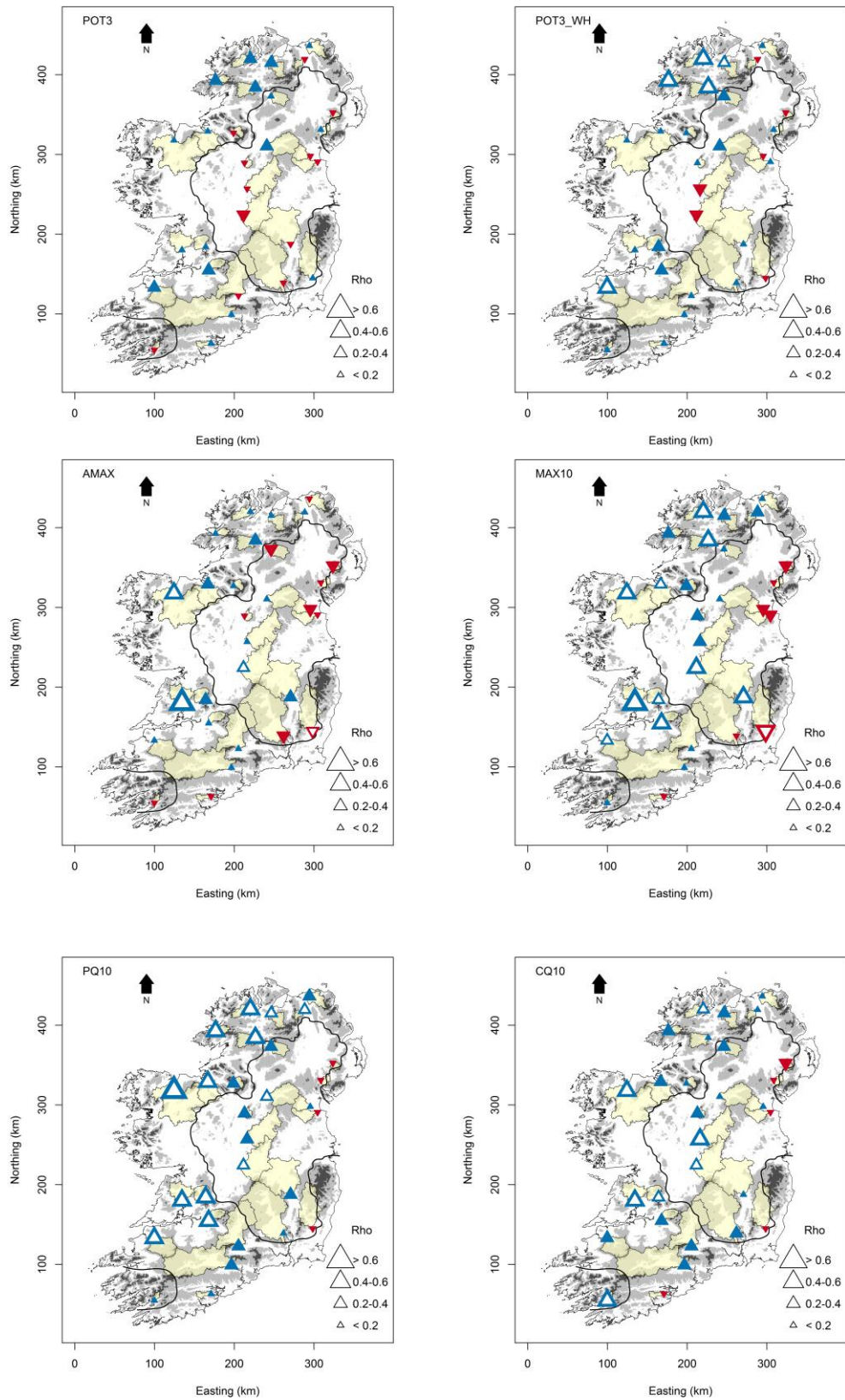


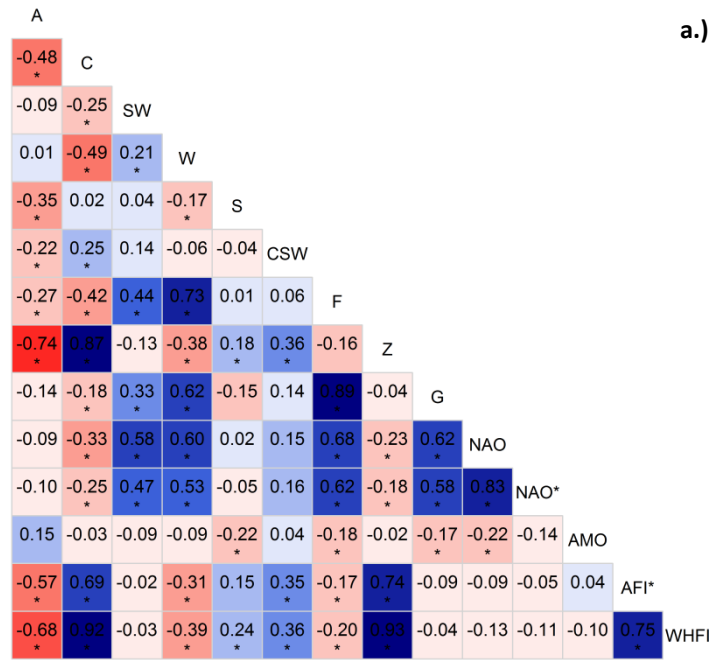
**Figure 5.13: Correlations between DJF NAO and flood indices over water years 1978-2009. Size of positive (blue triangles) and negative (red triangles) correlations are shown according to strength (Rho is the Pearson correlation  $\rho$ ) with statistically significant correlations (at the 5 % level) as inner white triangles.**

While several strong relationships between the NAO and flood indices have been shown, just 32 years of record was used to establish these relationships, limited by streamflow availability further back in time. Instead, the covariability of each of the top 5 winter flood-producing LWTs (C, SW, W, S, and CSW) and the DJF NAO (and ONDJFM version, denoted by NAO\*) as well as the average winter half year AMO (ONDJFM) is examined. Pearson correlations between each variable is shown in the correlograms (Fig. 5.14a) with LOESS smoothed (15 year span) time-series (to filter high frequency variability) in Figure 5.14b. Several other variables are included in an attempt to uncover relationships, including: annual and winter F-Index, A-type, F, Z, and G, which brings the total to 14 variables. Many relationships between these variables are rudimentary and already established from previous literature (e.g., Burt et al., 2015) but are presented here for comparability under the same study design.

The DJF NAO is strongly positively correlated with winter half year W- and SW-type frequency ( $\rho = 0.6$  and  $\rho = 0.58$ , respectively). This is supported by strong positive correlations between NAO and F and G ( $\rho = 0.68$  and  $\rho = 0.62$ , respectively), meaning positive phases of the NAO lead to increased frequency of important westerly flood-producing LWTs (W- and SW- types which together account for 25 % of winter floods), with increased mean atmospheric flow (F) and a higher gale index (G). The NAO shows statistically significant negative correlation with C-type frequency ( $\rho = -0.33$ ), also found by Matthews et al. (2015) in BI using a different cyclone identification method. This is also reflected in the statistically significant negative correlation between C- and W-types ( $\rho = -0.49$ ). The A-type, used here as an indication of winter atmospheric blocking frequency over BI, is also negatively correlated with C-type frequency ( $\rho = -0.48$ ), so winters with low incidents of blocking (pure anticyclonic type) have more cyclonic systems passing across the BI domain.

In order to reveal appropriate correlations between the AMO and other variables, noisy short-term variability is filtered using Loess smoothing with a span of 15 years (Fig. 5.14b). The AMO is negatively correlated with the NAO ( $\rho = -0.43$ ); the most positive NAO phases occur during AMO cold phases. The relationship between the AMO and A-type is statistically significant and positive ( $\rho = 0.39$ ), so increased (decreased) blocking occurs during warm (cold) North Atlantic SST anomalies.

### Correlogram 1872-2015 WY



### Correlogram 1872-2015 WY (loess smoothed, span = 15 years)

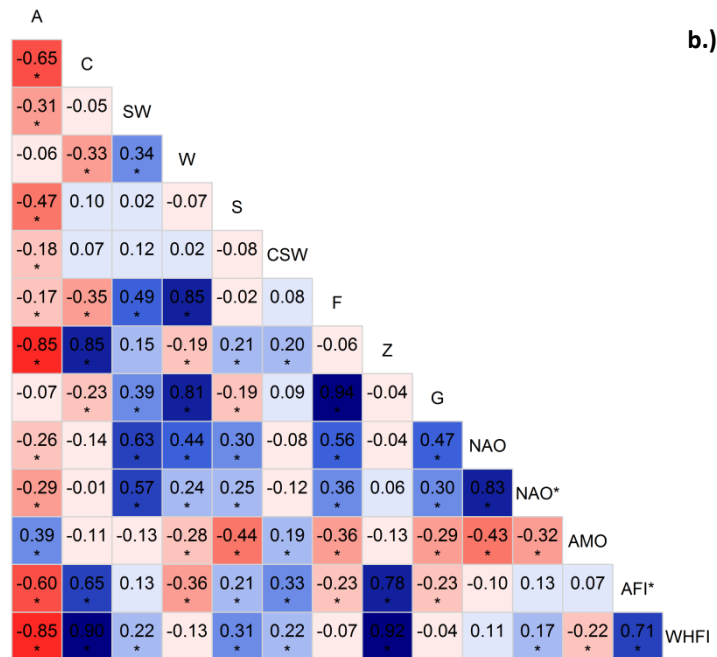
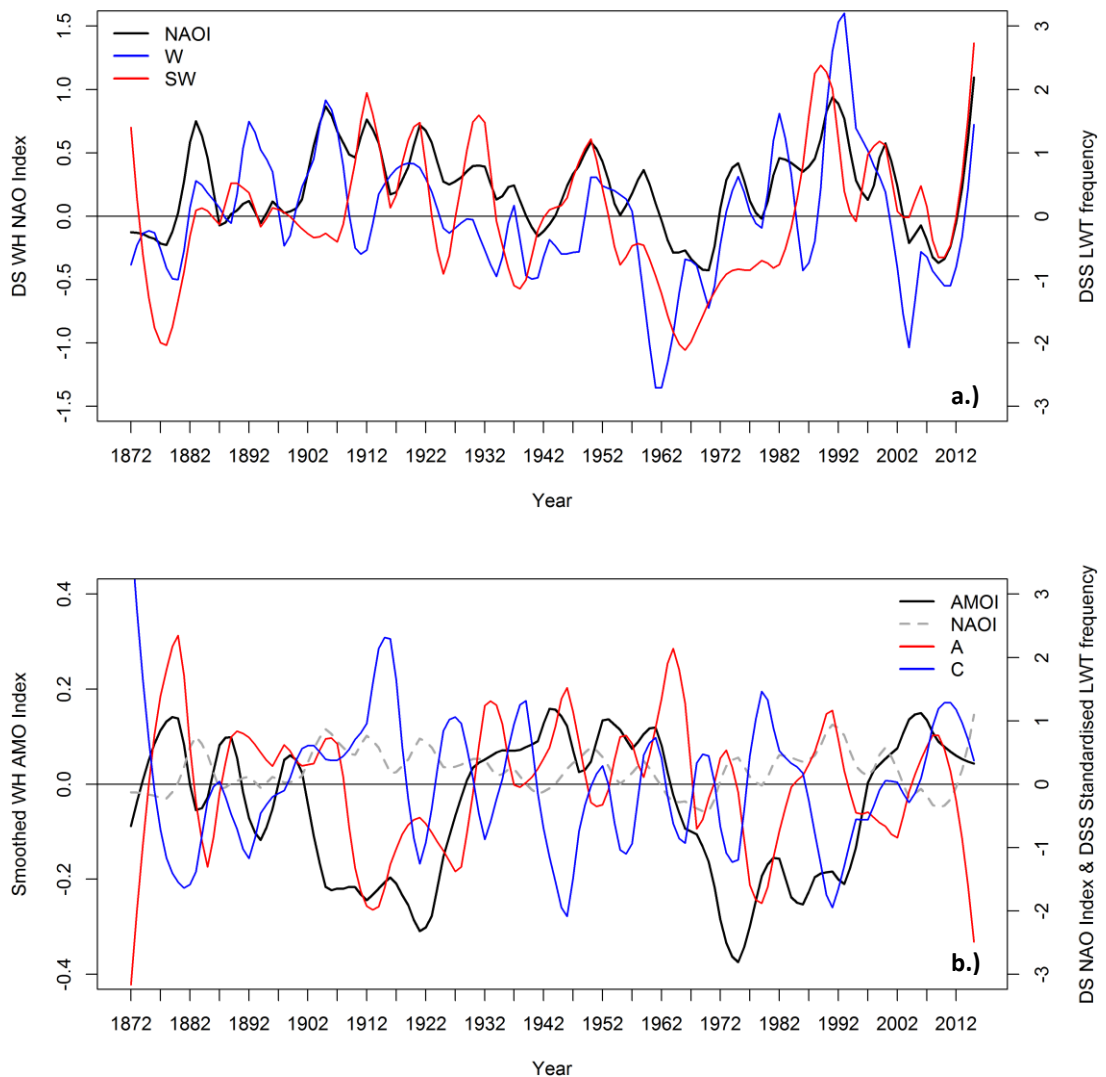


Figure 5.14: Pearson correlations between synoptic (LWT variables), large-scale climate indices (NAO and AMO), and annual (AFI) and winter (WHFI) F-Index variables (a.). The same time-series are Loess smoothed with 15 year span in (b.). Blue (red) represents positive (negative) correlations with those statistically significant and the 5 % level denoted with a star. All variables are for the winter half year except for NAO\* (DJF) and AFI\* (Oct to Sep).



**Figure 5.15: Detrended and smoothed (DS) winter half year NAO and detrended, standardised, and smoothed (DSS) W- and SW-type frequency (a.). Smoothed AMO (already detrended) with units °C, DS winter half year NAO, and DSS A- and C-type frequency (b.). Linear detrending was performed with trend estimated using the Theil-Sen Approach (Section 4.4.1), standardisation by long-term mean and standard deviation, and smoothing by Loess with span = 15 years. All series cover water years 1872-2015.**

Figure 5.15 shows the temporal covariability of a selection of these relationships with those most related to the NAO on the top panel and AMO on the bottom. It is clear that the W- and SW-type frequencies follow that of the NAO well with persistent positive anomalies during a persistent positive NAO. Notable above average periods are 1.) early 1900s to mid-1930s, 2.) 1970s to late-1990s, and 3.) from 2010 to present. W-Type frequency reached a peak over the 1872-2015 period in 1990 with over 20 % of all winter half year days reporting a W-type (double the average). In Figure 5.15b, the two AMO cold phases coincide with abnormally low prevalence of blocking

anticyclones over the BI region. Persistent periods of above average C-type frequency occur during AMO cold phases. For example, from around 1910 to 1920 positive C-type anomalies, while not statistically correlated with the AMO, occur simultaneously with a cold AMO phase and persistent negative A-type anomalies. Similarly, C-type anomalies are below normal during the 1940s while the AMO is in a warm phase and A-types are more frequent.

## 5.5 Discussion

### 5.5.1 Objective 5.1: Which synoptic weather types are associated with floods at the annual and seasonal scale?

The purpose of this chapter was to explore the synoptic and large-scale climate drivers of floods over a multi-decadal time-scale for the Island of Ireland. As mentioned in the introduction to this chapter, several studies have shown that floods in particular regions around Europe are actually associated with only a few atmospheric circulation patterns. Taking a synoptic climatology approach, results show that just 5 out of 27 LWTs are associated with 75 % of POT3 flood events across Iol. Four of the 5 most important LWTs in Britain are also the most important in Iol with the C-type (characterised by high atmospheric vorticity, Z) most dominant, as was the case in Pattinson and Lane (2012) and WQ2013. However, the S-type (7 % of floods) is found to be more important for floods in Iol than in Britain. This is in agreement with Sweeney and O'Hare (1992) and Perry and Mayes (1998) who find that when maritime tropical air masses come heavily laden with moisture from a southerly direction (S-type) this can accompany very heavy precipitation when the air mass is forced over the mountains of Cork/Kerry in the south of Iol. In fact, Sweeney (1985) finds that while cyclonic types produce a fairly even distribution of high precipitation totals across Ireland (although highest in the northeast, as found here in relation to largest flood loadings (> 3) in this part of the Island (Fig. 5.6)), highest precipitation receipts at the daily resolution are associated with southerly airflows along the southern seaboard. This is supported here with flood loadings (> 2.5) for four catchments in the south.

Westerly (W- and SW-types) circulation does not have as strong an influence on precipitation in Ireland compared to western Scotland, but purely westerly airflow is connected with high rainfall totals in the west and northwest, with areas in the

southwest affected by a more southwesterly flow direction (Sweeney and O'Hare, 1992). The geographically confined influence of the westerly type in this part of the Island is simply due to the proximity of these areas to depression centres at their most active stages of development (Sweeney, 1985). While the W-type is not flood rich at the scale of IoI when the expected frequency is considered, it does have high flood loadings (between 1.5 and 2.5) in smaller scales confined mainly to catchments in the west and northwest, which is consistent with findings from LWT-precipitation studies.

Petrow et al. (2009) found that the WZ-type (West wind, cyclonic in the Grosswetterlagen catalogue) was responsible for the majority of winter floods in Germany, but found that synoptic drivers of summer floods were different in southern Germany (most notably the TRM-type, Trough Central Europe). Results here show that floods in IoI are mainly driven by cyclonic circulation (> 40 %) in both winter and summer, with only few seasonal differences, namely: LWTs with a westerly (southerly) component more important in winter (summer). The dominance of C-types has also been identified by WQ2013 who find this type is associated with 30 % of floods in Britain between 1961-2000. This is comparable here if the day 0 approach is used (34 %), but as has been highlighted above, using a 3 day window within which to classify the flood-producing LWT increases the dominance of the C-types. It was found in many cases that taking the atmospheric condition on the concurrent day of a flood event does not capture the actual flood-producing atmospheric system. The three day method used here makes use of the Jenkinson Gale Index that is a measure of the intensity of atmospheric circulation. While it is acknowledged that the most intense circulation pattern may not always be responsible for generating floods (as seen in Fig. 5.8), it is better able to take account of flood-producing storms that occur before or after the day of the flood (i.e., plausible that the storm is captured at 12:00 UTC the following day instead if the rainfall responsible for the flow peak is dumped on the catchment later in the day). This was shown to slightly improve on the day 0 (concurrent day) used by WQ2013 resulting in stronger correlations between the F-Index and observed POT occurrence during evaluation (Table 5.2).

The use of the 3 day window was also necessary for examining the spatial extent of flooding across the entire network. If only the largest number of floods on any single day was considered, the true extent of widespread flooding would be underestimated

(by almost 50 % for the case of the flood on the 09/12/2007). Further work could be done making use of multi-day water vapour concentrations in the atmosphere (available from many reanalysis products), perhaps using accumulated totals instead of 'snapshots' in time, to better characterise the timing of the advected moisture to the region. ARs have been shown to be related to the most extreme floods (e.g. Lavers et al., 2011) but whether this approach applies for moderate floods, and even during summer has yet to be investigated in terms of improving synoptic classification of floods in Ireland. Further, investigation into the use of daily precipitation data from the network established in Chapter 3 to more accurately identify the timing of flood-producing precipitation receipt within a catchment should be undertaken. Although, a concern is that a mismatch in measurement (i.e. rainfall at 09:00 UTC and streamflow at 12:00 UTC) could be an issue and difficult to resolve in the absence of sub-daily precipitation records.

### **5.5.2 Objective 5.2: Reconstruction of flood occurrence for earlier periods**

At an annual scale the F-Index showed moderate skill in reproducing observed POT occurrence but less so when disaggregated to a seasonal scale. Rather than evidence for a long-term gradual increase in flood frequency, with the benefit of a 144-year time-series the F-Index simply reveals flood rich and poor periods due to temporal variation in yearly frequency of flood related LWTs. Four flood rich periods are identified that are consistent with Pattison and Lane (2012) and WQ2013: 1.) 1870s to 1890s; 2.) late-1900s to mid-1930s; a short spell in the 1980s, and 4.) late-1990s onwards. These findings help to contextualise trend results from studies based on shorter records, such as the detected increases in flood indices in Chapter 4. It is shown here the most recent period (where the majority of streamflow time-series end) is flood rich, whereas the 1960s and 1970s were relatively flood poor (where the majority of streamflow time-series start), therefore increasing trends would clearly dominate and could lead to misleading conclusions. Also, earlier flood rich periods, lasting even longer than the current, must be taken into account when interpreting trends.

Concerns over stationarity of climate-streamflow linkages when applied outside calibration have been raised by WQ2103 and are echoed here. Cyclones have been

shown to be a prominent feature in the flood hydroclimatology of Iol. Cyclone frequency is expected to change from year-to-year, depending on favourable atmospheric conditions (e.g. low incidence of atmospheric blocking), and this is accounted for within the F-Index. However, changing intensity of cyclones is not. For example, Matthews et al. (2015) examined the cyclone climatology of the BI domain and found a strong increasing trend in winter cyclone intensity (December to February) between 1871 and 2012. More work could be done to examine if this has an influence on extrapolation of the F-Index to periods outside calibration.

Although the F-Index was reasonably skilful at the annual-scale, overall skill was not improved from disaggregation to the seasonal-scale. The winter and summer F-Index did produce stronger correlations with observed seasonal POTs during calibration (and evaluation for summer), but correlation between the annual F-Index and annual POTs was still stronger ( $\rho = 0.64$ ) during evaluation. A possible explanation for the reduced winter F-Index skill is the limited length of available observed records. There is a notable gap in station density around the north and northeast (where the C-type has highest weighting) for longer record stations used for evaluation (1956-1977). As C-type frequency dominates the F-index, especially in winter (Fig. 5.14b), the use of these stations for independent evaluation may be perceived as a reduction in skill. It also highlights the potential to improve the F-Index skill if a more targeted sub-regional index was developed to capture more subtle regional synoptic influences. While it is argued that lumping the F-Index per ERR makes better physical sense than say for local authority boundaries, it is still relatively coarse. Additionally, LWTs could be derived from the new higher resolution long-term ERA-20C reanalysis product (Poli et al., 2013) at a sub-regional scale (Jones et al., 2014b) to test if enhanced links to regional floods could be established.

### **5.5.3 Objective 5.3: Investigating relationships with large-scale climate drivers**

Correlation between NAO and flood indices (over water years 1978-2009) was strongest for MAX10 and PQ10 than for more extreme flood indices (AMAX or POT), and was largely confined to the west and northwest. This was also found by Svensson et al. (2015) for the UK and they provide evidence of skilful seasonal forecasting of floods in catchments showing appropriately strong NAO links. They also find that there

is no/weak NAO relationship in the southeast of the UK. This is consistent with findings here for IoI with catchments in ERR-IE weakly negatively correlated with the NAO. However, this is in contrast with Kiely (1999) who used the Boyne catchment in the east of Ireland (within ERR-IE) as an exemplar of a NAO-streamflow link and concluded that such climatic changes have implications for flood management. It appears from this analysis that this is only the case in the western half of the Island.

Three possible reasons are offered to why particular catchments were more strongly related to the NAO: 1.) catchments with flashy responses (more impermeable geology) have stronger relationships to large-scale climate than those that have low flashiness due to larger size and/or more permeable geology (Lavers et al., 2010b); 2.) catchments with stronger antecedent conditions (i.e., higher soil moisture content) would trigger floods more often from receiving above average inputs of precipitation; and 3.) catchments in areas more exposed, geographically, to the track of westerly airflow will experience stronger NAO links (e.g. Sweeney (1985) for precipitation). The first possibility does not appear to be the case for IoI. The top three catchments with the highest NAO correlations ( $\rho > 0.5$ ) have instead a low median flashiness index (RBMED) ( $< 0.2$ ). These findings also do not support the theory of 'double orographic enhancement' (Burt and Howden, 2013) which states that as precipitation increases with altitude it is amplified when the NAO is positive, and thus catchments at higher altitude are expected to be more strongly correlated with the NAO than low elevation sites, particularly in winter. The highest NAO-flood correlations here were actually for lower elevation catchments (ALTBAR  $< 100$  m a. s. l.). This suggests that catchments most exposed to the NAO (and hence moisture laden westerly airflow) have stronger links to the NAO than those with particular catchment characteristics such as high flashiness (permeability) or high elevation (orographic effects), supporting Sweeney (1985). Moreover, there was also an influence of catchment wetness (FLATWET) suggesting that antecedent conditions might be important; whereby areas with highest soil moisture are pre-conditioned be more responsive to the influence of the NAO. However, it is difficult to separate these two hypotheses as catchments in the west and northwest might have a higher FLATWET in the first place because they are more exposed to the influence of the NAO. This highlights complex interplay between climate and hydrology. A note of caution is due here since the sample of catchment

characteristics (such as elevation and geology) is much less extensive in Ireland than in Britain. Nevertheless, these working hypotheses could be tested across both Ireland and UK under a standard experimental design.

Over the longer-term flood-producing LWTs themselves show evidence of decadal-scale variability. W- and SW-types become more frequent during the positive phase of the NAO due to increased strength of atmospheric flow (F) from a westerly direction. These two types have been shown to be responsible for ~ 25 % of floods in Ireland (over water years 1978 to 2009) so a strongly positive NAO will more strongly favour these circulation patterns hence increasing the likelihood of flooding in west and northwest catchments. Variability in C-types frequency (which dominates the F-Index variability) have shown distinct periods of above average cyclone frequency – termed flood rich periods. Cyclone frequency is strongly anti-correlated with frequency from atmospheric blocking form anticyclones (high pressure) in the BI domain (depicted here using A-type frequency). Periods with an anomalously low frequency of A-types correspond with those with higher than normal C-types (and hence F-Index), the period from early-1900s to 1920s being a particularly notable example. This close coupling between increasing cyclonic conditions (low pressure) at the expense of anticyclonic (high pressure) is a natural redistribution of atmospheric mass that has been shown elsewhere to create more favourable flood/drought conditions through teleconnections (Trenberth et al., 2014). A-type frequency is positively related to the AMO and negatively related to the NAO. When the AMO is in a cool phase (NAO positive phase) lowest A-type frequencies occur, while highest A-type frequency occurs during warm phases of the AMO (weak/negative NAO phase). This relationship has been found elsewhere. A warm phase AMO is associated with a more negative phase of the NAO (Smith et al., 2014) and hence increased incidence of atmospheric blocking in the BI domain in winter months (Häkkinen et al., 2011), thereby impeding entry of rain-bearing storm systems.

Increasing understanding of the synoptic and large-scale climate drivers of floods makes it possible to say *why* variability and change was detected in Chapter 4. A change in the frequency or intensity of these flood-producing systems would result in a non-stationary flood response. For example, the detected increase in winter cyclone intensity by Matthews et al. (2015) is certainly consistent with changes in extreme

precipitation magnitude and intensity (Chapter 4), and is in-line with what would be expected as the atmosphere warms globally (Trenberth, 2003; IPCC, 2013). In addition, the current 'cold blob' in the North Atlantic stands out as an anomaly during an exceptionally warm 2015 due to a markedly strong El Niño. This has been attributed to a weakening of the Atlantic Meridional Overturning Circulation (AMOC) which is at its weakest in the past millennium (Rahmstorf et al., 2015) and is consistent with an influx of freshwater from Greenland diluting sea water. This condition in the Atlantic has been shown to intensify and extend the North Atlantic storm track in the vicinity of BI, thereby impacting storminess (Woollings et al., 2012). Natural variability of ocean-atmosphere dynamics over multi-decadal time-scales, and plausible alteration of these dynamics due to effects of anthropogenic climate change, clearly has a considerable role in determining flood propensity in BI. Accordingly, this exploratory analysis suggests there may be some influence of the AMO on flood frequency that warrants further investigation to better quantify its influence and disentangle the chain of causality in more detail.

## 5.6 Chapter summary

Given the shortcomings of streamflow record length in Chapter 4 for understanding the long-term changes in flooding, Chapter 5 first set out to identify the synoptic drivers of flooding at the annual and seasonal scale (Chapter Objective 5.1) so that flood occurrence could be reconstructed back to 1872 using an objective weather classification scheme (Chapter Objective 5.2). Results show that only a few circulation patterns are related to floods in Iol and are seasonally similar, with the role of extratropical cyclones on flood hydroclimatology particularly prominent. Linkages with large-scale climate indices were established (Chapter Objective 5.3) and highlighted, (i) the NAO is only strongly positively correlated with flood indices in catchments in the west and northwest, with evidence of decadal-scale variability within westerly and south-westerly flood-producing LWTs time-series following that of the NAO, and (ii) a tentative link between the AMO and floods was outlined. Atlantic SSTs have been shown to modulate incidence of atmospheric blocking over the BI domain and hence is anti-correlated with cyclone frequency.

It was found that the NAO did not appear to have a strong influence on catchments in the Inland and East (ERR-IE) region. However, Kiely (1999) used the Boyne catchment in the east of Ireland as an exemplar of the impact of the NAO on streamflow concluding that NAO positive phases would have implications for flood risk management. This is inconsistent with what is found here. Further, the Boyne catchment has been subject to one of the most extensive arterial drainage schemes in Ireland during the mid-1970s and thus cannot be considered 'near natural'. Establishing the driver(s) of change in such catchments is a challenge but is tackled in Chapter 6 in the advancement of catchment-scale attribution of change.

## 6 Attribution of Detected Changes in Streamflow Using Multiple Working Hypotheses

---

### 6.1 Introduction

There has been a proliferation of studies assessing changes in observed hydrological series (whether gradual trend, abrupt change or more complex forms) at the catchment scale (e.g. Villarini et al., 2009; Burn et al., 2010; Petrone et al., 2010; Stahl et al., 2010; Hannaford and Buys, 2012; Murphy et al., 2013a) and also Chapter 4 in this thesis. While statistical detection of change is an important scientific endeavour, attribution of change (i.e. determining the most likely cause(s)) is fundamental to developing appropriate management responses and long-term adaptation strategies. In pursuit of evidence-based decision making, water managers need to not only better understand how but why hydrological change is happening. Without rigorous attribution, detection studies can be of limited use for planning and could even lead to mal-adaptation, thereby increasing risks to society and the environment, or wasting limited economic resources.

Merz et al. (2012) claim that most studies of statistically detected change in floods fall into the category of 'soft' attribution: they typically employ qualitative reasoning and/or correlation based techniques to show consistency between changes detected and typically a single driver (e.g. climatic change) with little effort to reliably quantify the assumed cause-effect relationship, and even less effort to falsify alternative candidate drivers. In calling for increased rigour in attribution, they suggest a framework of 'hard' attribution based on evidence of consistency (effect of an identified driver(s) translated into observed change), inconsistency (observed change is inconsistent with alternative drivers) and provision of a statement of confidence (strength of attribution statement with acknowledgment of data and methodological limitations). The authors outline many potential drivers of change that affect river systems and catchments at different scales. These range from natural and anthropogenic climate variability and change, internal human induced modifications within the catchment system (such as urbanisation and deforestation) to disturbances to the river channel itself from river training or reduction of channel length. Since

multiple factors may be acting in parallel and interact with each other, they call for approaches that investigate multiple, rather than single drivers of change.

Without considering the entire signal of change, some studies have begun to include a wider set of factors for attribution. For example, Jia et al. (2012) employed a fingerprint based method to attribute observed changes in water resource amounts in the Hai catchment, China to local human activity, rather than climate variability. Vorogushyn and Merz (2013) showed that an important contribution to detected increasing trends in observed flood time-series along the Rhine is attributable to extensive river training. Fenicia et al. (2009) used a rainfall-runoff modelling approach to re-examine an anomalous model overestimation in the River Meuse rainfall-runoff behaviour between 1930 and 1965 and hypothesised that land-use and land management changes rather than climate change (as suggested by previous studies) were the likely responsible drivers. Within the Upper Mississippi River Basin, despite extensive evidence of land-use/land-cover change, Frans et al. (2013) attribute increases in runoff to growing regional precipitation, amplified by artificial field drainage. Hundecha and Merz (2012) use ensemble simulations to assess the relative importance of meteorological drivers in accounting for detected changes in flooding for catchments in Germany showing that detected trends in extreme streamflow were attributable to changes in precipitation.

Hydrological modelling based approaches have been widely used for change detection and attribution (e.g. Schreider et al., 2002; Andréassian et al., 2003; Seibert and McDonnell, 2010; Gebrehiwot et al., 2013). The creation of a 'virtual control catchment' (Andréassian et al., 2003) is possible by calibrating rainfall-runoff models before a known internal disturbance (such as forest cover change, urbanisation, river engineering, dam construction) to reconstruct streamflow throughout the period of interest, driven by observed climate inputs as if the internal change had not occurred. Any divergence between reconstructed and observed streamflow can then be attributed to an internal disturbance rather than a change in climate, with the premise that the model(s) fully capture catchment behaviour. Use of models to isolate internal disturbances from external climate driven changes can help to decipher the nature of change and therefore contribute to a better understanding of processes of change.

Most attribution studies to date have been limited to one or two drivers of change. In moving towards more rigorous attribution through systematic examination of known drivers in explaining the full signal of change, the Method of Multiple Working Hypotheses (MMWH) offers an established approach in which to develop and test hypotheses of change (Chamberlin, 1890). MMWH involves development, prior to the analysis, of several hypotheses that might explain the phenomenon being observed, while explicitly recognising the possibility that more than one hypothesis may be simultaneously valid. This increases the likelihood of uncovering potential interactions and synergies among hypotheses. The method requires an open-minded assessment of plausible explanations of the phenomenon under study, including the possibility that none are correct and that some new explanation may emerge given further research and/or additional data. Many studies have highlighted the utility of MMWH (e.g. Platt, 1964; Raup and Chamberlin, 1995; Elliott and Brook, 2007) and in the context of hydrological change it is asserted here to have the potential to provide a more systematic approach to attribution.

In practical application of MMWH there will be a certain level of subjectivity in the initial selection of hypotheses as well as data limitations in quantitatively assessing drivers. However, these drawbacks should not discourage attempts to assess a larger set of potential causes of hydrological change as knowledge of drivers can be reasonably gained in many cases. Additionally, MMWH is more systematic and holistic than traditional approaches to attribution where the consideration of a single (or limited) driver of change can lead to confirmation bias. Nonetheless, only a few studies in hydrology have employed MMWH, such as Clark et al. (2011) who advocates MMWH in attaining more scientifically defensible and operationally reliable hydrological models.

In combining MMWH and the framework proposed by Merz et al. (2012), this chapter revisits an earlier study that attributed an abrupt change (change point) in daily streamflow records of the Boyne catchment in east Ireland to climatic change (Kiely, 1999). Using flow series derived from the gauging station at Slane Castle for 1941-1995, Kiely (1999) found a statistically significant upward change point (increase in flow after change point) in annual (1978,  $p = 0.004$ ) (Fig. 6.1) and March (1976,  $p = 0.001$ ) mean flows. Additionally, on a national scale an increase in March, October and

annual precipitation was found to occur after 1975, most noticeably in west Ireland (Kiely, 1999). The change point in both variables was attributed to a shift to more positive phase of the North Atlantic Oscillation (NAO) since the mid-1970s, resulting in stronger mid-latitude westerlies, with increased precipitation over Ireland, and higher mean annual and March streamflow.

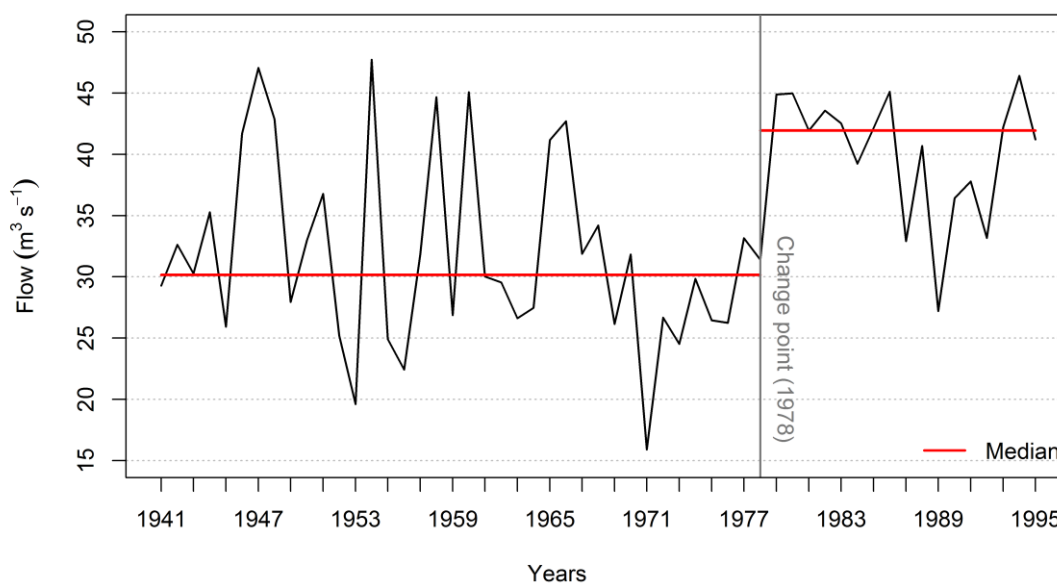


**Figure 6.1: Observed annual mean flows in the Boyne for 1941-1995. Solid red line is the median of the period before and after the 1978 change point detected by Kiely (1999).**

Given the importance to understanding the drivers of change at the catchment scale, for both improving knowledge of hydroclimatic processes and practical management of flood risk, this chapter aims to demonstrate the value of the hydroclimatic perspective in advancement of more rigorous attribution of change using the Boyne catchment as a case study (**Thesis Objective 4**). More specifically, the single driver analysis of Kiely (1999) is extended by investigating multiple factors of external and internal change. Using MMWH a preliminary assessment of consistency with the observed change point is undertaken based on process understanding, available information on potential drivers and meta-data. From this screening, hypotheses about the causes of change are formulated and assessed in more detail. To isolate hypothesised internal and external (climatic) drivers of change, streamflow is reconstructed using a suite of conceptual rainfall-runoff models (CRR). Statistical tests

for evidence of both monotonic trends and change points are employed to explore signatures of change from hypothesised drivers using a comparative analysis between reconstructed and observed streamflow and precipitation.

Accordingly, Section 6.2 provides detail on the case study catchment and presents a preliminary assessment of the potential drivers of change within the Boyne using MMWH. Section 6.3 outlines the methods and data used to decipher the nature of change. The results are presented in Section 6.4 and discussed in Section 6.5 in light of advancing more rigorous attribution within the discipline.

## **6.2 Study area and hypotheses of hydrological change**

### **6.2.1 The Boyne catchment**

The study area is the Boyne catchment at Slane Castle streamflow gauging station (latitude: 53.706870° N, longitude: 6.562389° W) (Fig. 6.2). The Boyne is located in east Ireland and has annual average total precipitation of 897 mm (1952-2009). The catchment area is 2460 km<sup>2</sup> and main channel length is 94 km. Topography is predominantly flat to undulating lowland with elevation ranging between 16 m and 338 m. Soil and land-use data were obtained from the Irish Environmental Protection Agency (EPA). Land-use was calculated using the 2006 European Union Coordination of Information on the Environment (CORINE) dataset and consists mainly of agricultural pastures (87 %) with approximately 1.5 % forest and urban area. The catchment is classified as 'essentially rural' (Institute of Hydrology, 1999). More than 35 % of the Boyne is comprised of poorly drained soils (mainly Basin Peats and Gleys).

### **6.2.2 Overview of potential drivers of hydrological change**

The observed streamflow behaviour in the Boyne – a large upward change-point – narrows the choice of plausible drivers. Most land-use changes develop gradually over decades to centuries whereas alterations to the river channel by engineering works would be visible as an abrupt change (Merz et al., 2012). Climate variables can also have an effect across multiple time-scales. Anthropogenic climate change is expected to unfold as a gradual intensification of the hydrological cycle over decadal time-scales (Huntington, 2006; Durack et al. 2012), whereas recurrent patterns of large-scale atmospheric variability such as the NAO can manifest as an abrupt change (Kiely, 1999)

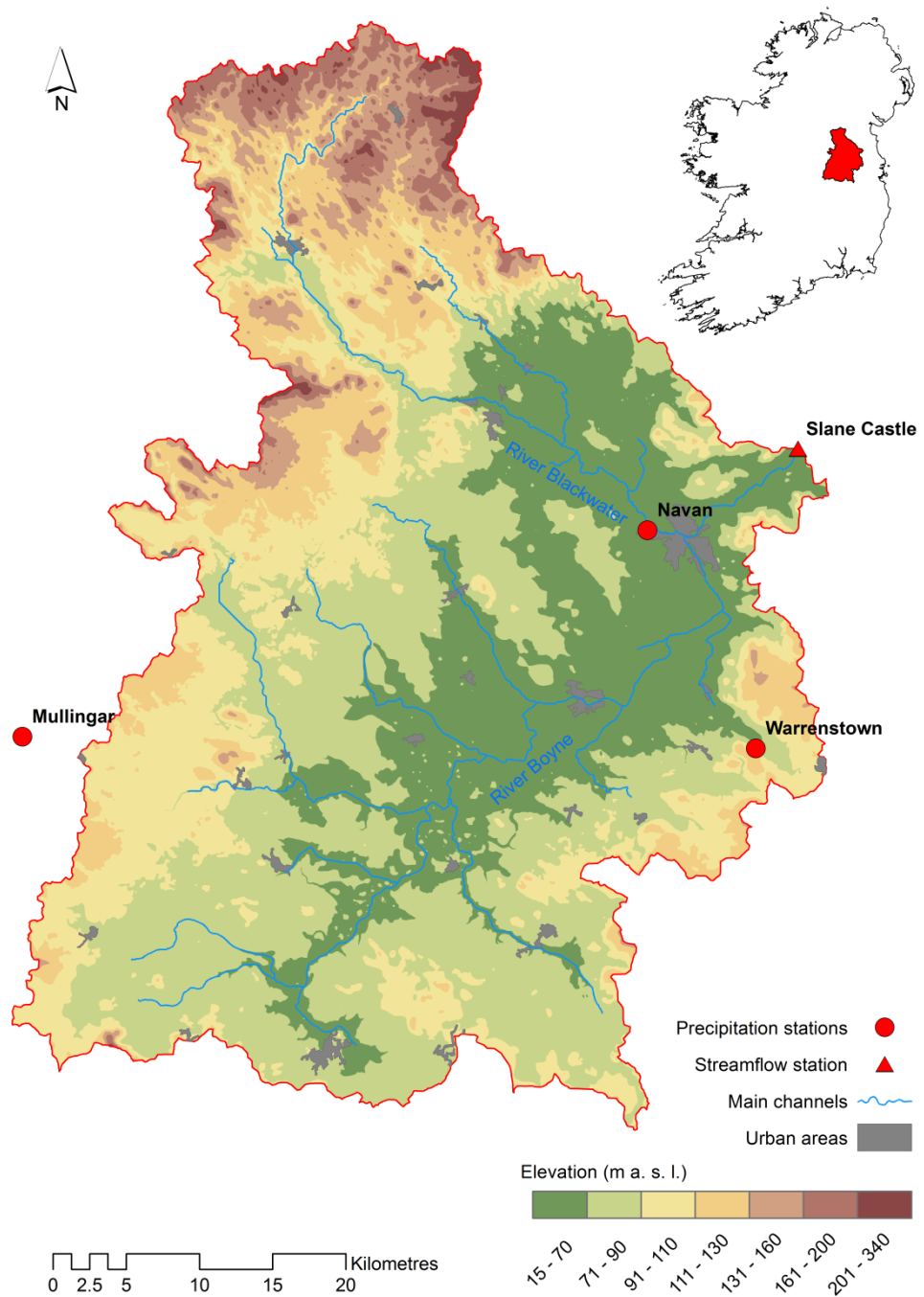


**Figure 6.2: Boyne catchment showing major urban areas, streamflow and precipitation stations.**

in shorter records. If potential drivers of change are occurring in concert and over similar time-scales then their relative contributions need to be deconstructed.

Using MMWH, possible explanations for the change points detected by Kiely (1999) were derived. Eleven working hypotheses (WHs) (Table 6.1) are based on potential internal and external (climate) drivers of change, together with combinations of drivers where potential synergies (WH 10) are apparent. There is also an acceptance that

other factors not yet known/accounted for could be contributing to or counteracting change (WH 11). Each WH was subject to an assessment of consistency with the detected change based on previous literature, expert consultation, and analysis of available qualitative and quantitative data. Potentially important drivers selected for further quantitative analysis are described below.

Some hypotheses of change were relatively straightforward to reject such as WH 2 (Water abstractions/diversions) which is both inconsistent with the direction of detected change and has limited influence volumetrically on the natural flow regime. Contemporary surface water abstraction within the Boyne catchment upstream from Slane Castle is ~ 8 % of the 1952-2009 Q95 (flow equalled or exceeded for 95 % of the time) as estimated by the EPA (2009) and is therefore considered too insignificant to impact the natural flow regime (Bradford and Marsh, 2003). Change in Potential Evapotranspiration (PET) (WH 9) was also assessed using estimated PET derived for Dublin airport which is the closest synoptic station (38 km south-east of Slane Castle streamflow gauging station) with data covering the period of study. PET was eliminated as no statistically significant gradual or abrupt changes in annual or monthly total PET were found using the methods described in Section 6.3.3. The quality and consistency of hydrometric data at Slane Castle gauging station was examined through consultation with responsible hydrometric personnel. The station changed ownership from the Irish Electricity Supply Board (ESB) to the Office of Public Works (OPW) on the 25<sup>th</sup> of February 1977, which also coincided with metrication of measurements. Archived paper streamflow charts before and after 1977 were examined for inconsistencies in measurement and data collection methods along with historical and current rating curves for this station. For the period of record the gauge is deemed of high quality for high and mean flows and fair for low flows according to OPW quality ratings. The station location and measurement method (automatic gauge) have remained the same throughout. Inconsistent/poor quality streamflow data (WH 1) was therefore ruled an unlikely explanation of the observed change point.

WH 3 to 5 (treated water discharges, urbanisation and forest cover and management change) were not selected for further analysis due to their assumed second-order influence. An increase in treated water discharges (WH 3) is known to occur around the mid-1970s due to discharge of groundwater into the River Boyne from a zinc and

Working hypotheses	Potential influence / time-scale	Additional information	Decision and justification
1. Inconsistent/poor quality streamflow data.	Data values post (pre) mid 1970s artificially higher (lower). Effect can be abrupt.	Checks were made to ensure data at Slane Castle gauging station was of good consistent quality. Hydrometric experts responsible for gauge were consulted and archives analysed.	No evidence of inconsistent measurements from consultation with OPW hydrometric division.
2. Water abstractions/diversions.	Reduction in flow quantity. Effect can be both gradual and abrupt.	The estimated water abstraction impact does not exceed 10% of Q95 therefore the flow regime can be classed as natural. In addition, the potential impact is inconsistent with direction of change. No known diversions.	Logical / quantitative assessment.
3. Treated water discharges.	Increased flow quantity. Effect can be abrupt.	Potentially consistent with direction of change. Largest known discharge is from pumping groundwater from Tara Mines clear water pond in Navan into surface water of the River Boyne. Discharges limited to a dilution rate of 1% (EPA, 2012).	<i>Volume of discharged water from Tara Mines too small to have significant impact. Other possible notable discharges unknown.</i>
4. Urbanisation.	More flashy rainfall-runoff response. Effect likely gradual.	Potentially consistent with direction of change. ~1.5 % of catchment urbanised, essentially rural according to Institute of Hydrology (1999) definition.	<i>Urbanisation unlikely important but cannot be completely ruled out.</i>
5. Forest cover and management change.	Increased flow by reduction of evaporation with declining forest cover. Effect likely gradual.	Potentially consistent with direction of change. ~1.5% of total catchment area is covered in forest.	<i>Limited area of forest cover. Unlikely to have an important effect but cannot be completely ruled out.</i>
6. Arterial drainage.	Increases discharge capacity of channel; increases flood peaks; increases flashiness. Effect can be abrupt.	Over 60% of the Boyne channel network was subject to arterial drainage where the channel bed was deepened and widened (in some instances by up to 3 metres) between 1969 and 1986.	<b>Evidence of widespread installation of arterial drainage, merits further analysis.</b>
7. Agricultural land-use and management change.	Multiple influences. Drainage of land increases transmission of water to the channel. Effect can be both gradual and abrupt.	Potentially consistent with direction of change. Majority of land cover is agricultural pasture (87%). Government initiatives to install field drainage consistent with timing of change.	<b>Evidence of widespread installation of field drainage, merits further analysis.</b>
8. Changes in precipitation.	Increase in precipitation quantity translates into increased streamflow. Effect can be both gradual and abrupt.	Consistent with direction of change. The NAO index changed from a negative to positive phase during the mid-1970s.	<b>Increases in precipitation linked to changes in NAO in the 1970s; well documented in literature.</b>
9. Changes in Potential Evapotranspiration (PET).	Decrease in PET increases runoff. Effect can be both gradual and abrupt.	Daily PET data was analysed to assess if an abrupt decrease occurred that could possibly contribute to the change point.	No change in PET that could explain the Boyne change point.
10. Multiple drivers/synergetic effects.	Multiple influences, working together or against each other. Complex mix of gradual and abrupt.	Given the integrating properties of streamflow the potential for synergistic interaction of multiple drivers is high. WH 6, 7 and 8 could all contribute to increase in streamflow.	<b>Potential for interaction between combination of field and arterial drainage and changes in precipitation.</b>
11. Other drivers.	Unknown.	The identification of other potential driver(s) of change is limited to current knowledge/data availability. Future research may expose other factors that could further refine hypotheses of change.	<i>Lack of current knowledge of other potential drivers but cannot be ruled out.</i>

**Table 6.1: Working hypotheses (WHs) for drivers of change in the Boyne catchment. The table provides an overview of potential influence of each WH and a preliminary assessment and justification for inclusion/exclusion in further investigation (Roman = not analysed further; *Italic* = not analysed further but justification based on limited evidence; **Bold** = Warrants further investigation).**

lead mine 2 km west of the town of Navan. The contribution to flow is limited to a dilution rate of 1 % (EPA, 2012) hence can be effectively ruled out as having a major influence on streamflow.

The impact of land-use changes are difficult to assess at the scale of the Boyne catchment. In spite of this, it is a local phenomenon so the impact is assumed to decrease with increasing catchment size (Blöschl et al., 2007). However, it is important to consider the position of land-use change within the catchment as well as total extent of disturbances. The town of Navan (Fig. 6.2) is the largest in the catchment (spatial extent 9.13 km<sup>2</sup> in 2006) and is situated 10 km upstream of the Slane Castle gauging station. While the population of the Navan urban area decreased slightly (5.6 %) from 4,367 people between 1971 and 1981, the population immediately surrounding the town centre almost doubled from 5,907 to 11,136 people over the same period (Meath County Council, 2009). Navan also experienced a similar expansion in population between 1996 and 2002 but streamflow at Slane Castle shows no evidence of change during this period. Hence, an increase in population leading to likely urban expansion in the 1970s was deduced not to have had an important influence, although it is acknowledged that the effects of the two periods of urban expansion might be different with regard to their influences on the hydrological system. Forest cover (WH 5) accounts for only ~1.5 % of catchment land-use (in 2006), with change in management practices unlikely to cause a magnitude of change in streamflow consistent with that detected.

#### **6.2.2.1 Arterial and field drainage**

Both WH 6 (arterial drainage) and WH 7, (agricultural land-use and management change) were identified as plausible drivers of change. Arterial drainage (WH 6) has been widely installed in Ireland and involved the artificial widening and deepening of main river channels and important tributaries to improve their discharge conveyance. O'Kelly (1955) noted that following arterial works peak flows were raised to about three times pre-drainage values and that both the time to peak and the duration of flood hydrographs were greatly shortened following implementation in the adjacent Brosna catchment. Similar responses in flood peaks have been reported elsewhere (e.g. Bree and Cunnane, 1979; Bailey and Bree, 1981; Lynn, 1981). Likewise, Wilcock

and Wilcock (1995) examined the impacts of arterial drainage on the River Maine in Northern Ireland and found systematic increases in high flows. Similarly, Bhattarai and O'Connor (2004), studying the Brosna catchment with the benefit of additional data, confirm the effects of arterial drainage reported by previous research.

The Boyne catchment has experienced widespread arterial drainage with over 60 % of the river network affected during the period 1969-1986 (OPW, 2014). The Boyne scheme represents the largest investment in arterial drainage in Ireland at a cost of 8.6 m Irish Pounds at the time (equivalent of EU 10.9 m without accounting for inflation) and employed 1000 people at peak (OPW arterial drainage archives). Figure 6.3 shows the extent and timing of completion of arterial drainage works and the cumulative length of network excavated for major watercourses in the catchment based on information derived from hard copy archives held by OPW. Most works on channels

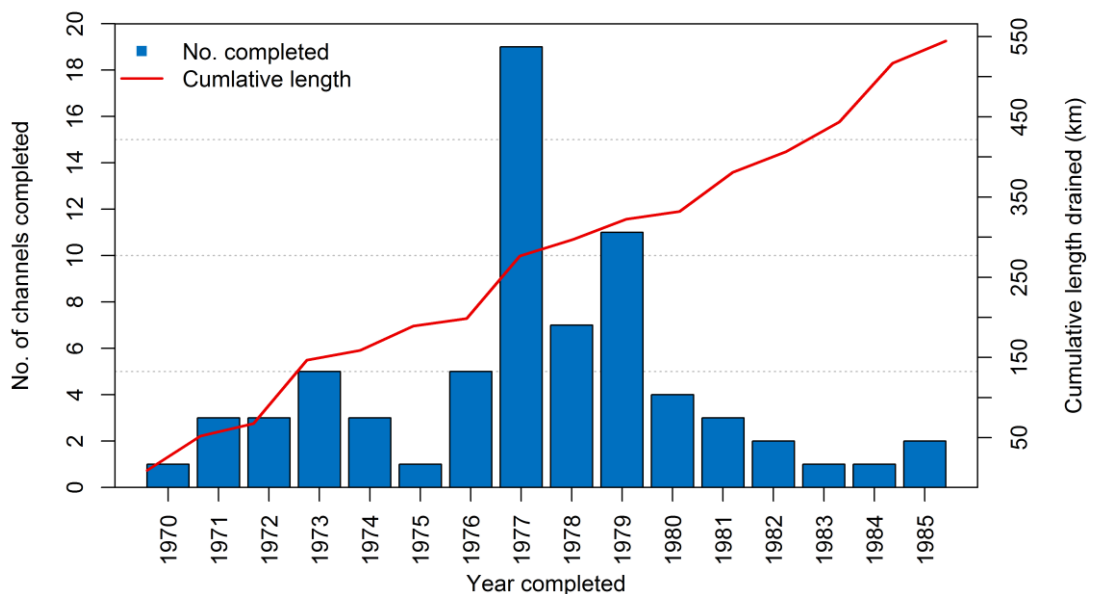


**Figure 6.3: Number of major watercourses per year in which arterial drainage was completed in the Boyne. The cumulative length (km) completed is shown by the red line.**

were completed between 1977 and 1979 with large increases in the length of channel (km) in which drainage works were completed in 1973, 1977 and when the works at the largest tributary (the Blackwater) and the Boyne main channel were completed in 1983 and 1984 respectively.

The most important agricultural land-use and management change (WH 7) during the late 1970s and early 1980s was the implementation of field drainage. Field drainage involves the installation of pipes and ditches to remove surplus water from waterlogged agricultural lands resulting in reduced transmission time of water to river channels. Little research has been reported in Ireland on the impact of field drainage on hydrological response, however, Burdon (1986) notes that field drainage appreciably increases winter and spring flows (wetter seasons) from drained lands. Drainage measures have been widely implemented in Ireland, under the Land Reclamation Project (1949) then superseded by the Farm Modernisation Scheme (1974) following Ireland's entry to the European Economic Community (EEC).

It is estimated that a large proportion (>30 %) of the Boyne catchment area has been subjected to field drainage (Burdon, 1986). However, exact figures are not available due to a lack of records on implementation, because the physical work of drainage was undertaken at a local scale by individual farmers. When field and arterial drainage measures were implemented they were intended to work in tandem, with the efficiency of field works reliant on the increased capacity of receiving river channels to convey additional runoff. Due to their close association, WH 6 and WH 7 are henceforth regarded as a single driver of change (drainage) in the further analysis.

#### **6.2.2.2 Precipitation regime**

Kiely (1999) originally linked the observed change point in streamflow in the Boyne to increases in precipitation driven by the NAO. Hence, WH 8 (changes in precipitation) is also included for further analysis. As introduced in Chapter 2 the NAO is the dominant mode of natural climate variability in the region (Hurrell and Van Loon, 1997; Wilby et al., 1997) with positive phases of the NAO index associated with increased westerly airflow and positioning of storm tracks over north-west Europe. The NAO influence in winter has subsequently been linked to extreme rainfalls (Maraun et al., 2011), winter runoff (Lai   and Hannah, 2010), high flows (Hannaford and Marsh, 2008), and enhanced orographic rainfall (Burt and Howden, 2013) in the British-Irish Isles. Similarly, Leahy and Kiely (2011) report an increase in March and October hourly rainfall in 1975 across Ireland, with a corresponding decrease in July rainfall. These changes are concurrent with a shift in the winter NAO index to a more positive phase.

They further note that annual totals and seasonal distributions of rainfall have changed most in the west and northwest of Ireland. Kingston et al. (2006) undertook a comprehensive review of the NAO and hydrological variables and found a positive correlation between winter NAO and streamflow for most of north-west Europe between 1961 and 1990. While the NAO-streamflow link appears well established, it is seen from Chapter 5 that it has stronger influence on catchments within ERR-CU than for ERR-IE, where the Boyne resides.

### **6.3 Data and Methods**

Four favoured hypotheses of change emerge from preliminary screening of WHs in Section 6.2: drainage (WHs 6 and 7 together); precipitation (WH 8); combined effects of drainage with precipitation (WH 10); or other unknown factors (WH 11). To obtain a better understanding of the influence of drainage on hydrological behaviour in the Boyne, rainfall-runoff models forced with climate variables (precipitation and PET) were used to simulate a control catchment using data before the known disturbance. Therefore unlike observed flows, reconstructed streamflow time-series are free from the effect of drainage. Statistical tests for both monotonic trend and change points were then employed to explore signatures of change in observed and reconstructed streamflow. The following sections describe the data and each step of the methodology.

#### **6.3.1 Hydroclimatic data**

Meteorological and streamflow data were obtained from Met Éireann and the OPW respectively. Daily data from three precipitation stations were averaged to produce catchment area precipitation (see Fig. 6.2, red points and Table 6.2). Data for Navan and Mullingar were not available post 2003, so data from Warrenstown was used to extend the catchment average to 2009. Raw data for Warrenstown slightly underestimates the 1952-2003 catchment average hence monthly correction factors were applied to Warrenstown from 2004-2009 following the method of Barker et al. (2004). Here, correction factors were calculated for each month by dividing the sum of monthly total precipitation from the 1952-2003 catchment average by the sum of the total monthly precipitation from Warrenstown over the same period (Table 2.2). These correction factors were then applied to daily Warrenstown data from 2004-2009 and

merged with the 1952-2003 catchment average to create an extended catchment precipitation series of 58 years. Daily streamflow data for the Boyne at Slane Castle (Fig. 6.2, red triangle) were obtained for the period 1952-2009. Slane Castle is a velocity-area gauging station automated in 1940 with a weir acting as a control. This is one of the longest, highest quality (stable rating) records in Ireland with less than 1 % missing data.

**Table 6.2: Stations and correction factors used to obtain catchment average precipitation.**

Station	Station name	Period	m .a. s. l.											
2531	Navan	1952-2003	52											
2922	Mullingar	1952-2003	101											
2931	Warrenstown	1952-2009	90											
Correction factor	Jan	Feb	Mar	Apr	May	Jun	Jul	Aug	Sep	Oct	Nov	Dec		
	1.038	1.039	1.032	1.019	1.018	1.003	1.062	1.001	1.029	1.021	1.031	1.014		

### 6.3.2 Hydrological modelling

Conceptual Rainfall-Runoff (CRR) models were employed to reconstruct daily mean flows. Using the pre-drainage period (pre-1970) to train models allows the simulation of streamflow series as if there are no impacts of drainage. All CRR models are subject to uncertainties stemming from input data, parameter, and model structure uncertainty. It is well known that different combinations of plausible parameter sets within a hydrological model structure can simulate the observed flow to a similar extent – the concept of equifinality (Beven and Binley, 1992). The same concept also applies to model structure, with a number of studies highlighting the utility of multi-model ensembles in simulating change in catchments (Butts et al., 2004; Wilby, 2005; Bastola et al., 2011), while Clark et al. (2008) highlight the challenges of identifying appropriate model structures.

To reconstruct streamflow, three structurally different hydrological models were chosen, each of which have been applied to the Boyne before (Murphy et al., 2006, 2011; Bastola et al., 2011, 2012; Hall and Murphy, 2011; Bastola and Murphy, 2013).

These models are HYSIM (Manley, 1978), NAM (Madsen, 2000) and HyMOD (Boyle, 2001). While all three models are lumped, they differ in complexity as defined by the number of parameters requiring calibration and the way in which spatial heterogeneity of the catchment is represented. HYSIM and NAM describe catchment hydrology using a group of conceptual elements. HyMOD is a variable contributing area model, with spatial variability modelled using a probability distribution function. All three models employ a single linear reservoir to represent groundwater.

Each model was calibrated using streamflow data prior to widespread drainage and then used to simulate streamflow for the full period 1952-2009. The time periods for calibration and evaluation were 1952-1959 and 1960-1969 respectively, with one year used for model spin up to stabilise state variables. No weights were applied to individual model structures or parameter sets. All models were forced with catchment average precipitation and PET data. Latin Hypercube Sampling (LHS) with a uniform distribution was used to generate 500 parameter sets for each model structure. Three objective functions were employed to identify behavioural parameter sets (i.e., those deemed to acceptably simulate observed pre-drainage flow): the Nash-Sutcliffe Efficiency (NSE) (Nash and Sutcliffe, 1970); Percent Bias (PBIAS) (e.g., Gupta et al., 1999); and the Mean Absolute Error (MAE) (e.g., Dawson and Wilby, 2001). NSE is a measure of the goodness-of-fit to the 1:1 line when the observed flow is plotted against modelled flow (Moriasi et al., 2007). The closer the NSE is to 1, the higher the accuracy of the hydrological model. PBIAS measures the average tendency of the modelled flow series to be larger or smaller than the observed flow expressed as percentage. Positive (negative) PBIAS values mean reconstructed flow over (under)-estimated observed flow values. MAE provides the average magnitude of the residuals. Behavioural parameter sets were defined as those achieving  $NSE \geq 0.75$ ,  $PBIAS \leq |10|$  and  $MAE < \frac{1}{2}$  multiplied by standard deviation of observed streamflow for that period. These thresholds ensure that unsatisfactory models are not classed as behavioural (Moriasi et al., 2007). Only parameter sets that were found to be behavioural for both calibration and evaluation periods were used for reconstructing flows.

### 6.3.3 Trend and change point analysis

#### 6.3.3.1 Hydrological and precipitation indicators

Observed precipitation, observed streamflow, and reconstructed streamflow series were analysed for evidence of monotonic trends and change points. Fifteen hydrological and 15 precipitation indicators were extracted for the period 1952-2009. These were:

- Annual mean flow (AMF)
- Annual 90<sup>th</sup> percentile of daily mean flow (Q10)
- Annual Richards-Baker hydrological flashiness index (RB)
- Monthly mean flow, January to December
- Total annual precipitation (TAP)
- Annual 90<sup>th</sup> percentile of daily precipitation totals (P10)
- Annual coefficient of variation (CV) of daily precipitation totals (PCV)
- Total monthly precipitation, January to December

The RB index, as introduced in Chapter 4, computes variations in flow relative to total flow and provides a useful characterisation of the way a catchment translates precipitation into streamflow (Baker et al., 2004). Q10 and P10 are high flow/precipitation indicators defined as the flow/precipitation equalled or exceeded for 10 % of the time (i.e. 90<sup>th</sup> percentile) during each year in the period 1952-2009. Hydrological and precipitation indicators were calculated in  $\text{m}^3 \text{s}^{-1}$  and mm over period of time, respectively, except for the RB index and PCV which are dimensionless. PCV is the standard deviation divided by the mean daily precipitation totals for each year and tests for evidence of changing precipitation variability. To aid comparison between hydrological and climatological indicators, as well as with the results obtained by Kiely (1999) all indicators were derived for the calendar year (1<sup>st</sup> January to 31<sup>st</sup> December).

#### 6.3.3.2 Tests for change detection

As in Chapter 4, evidence for monotonic trends was assessed using the Mann-Kendall test (MK) (Mann, 1945; Kendall, 1975), a non-parametric rank-based method that is widely applied in analyses of streamflow (e.g. Hannaford and Marsh 2008; Villarini et al., 2011b; Murphy et al., 2013a) and precipitation (e.g. Villarini et al., 2011a;

Guerreiro et al., 2014). The standardized MK statistic (MKZs) follows the standard normal distribution with a mean of zero and variance of one. A positive (negative) value of MKZs indicates an increasing (decreasing) trend. Statistical significance was evaluated with probability of Type I error set at the 5 % significance level. A two tailed MK test was chosen, hence the null hypothesis of no trend (increasing or decreasing) is rejected when  $|MKZs| > 1.96$ .

The Pettitt (1979) statistic was used to identify a single change point and is extensively employed in both hydrological and precipitation change detection studies (e.g. Kiely, 1999; Zhang et al., 2008; Villarini et al., 2011a, b; Gao et al., 2011; Guerreiro et al., 2014). The Pettitt test is non-parametric and relative to other tests is less sensitive to outliers and skewed data (Pettitt, 1979). The null hypothesis (no step change in time-series) against the alternative (an upward or downward change point in a given year) is tested at the 5 % significance level.

Both change detection tests require data to be independent (i.e. free from serial correlation) as positive serial correlation increases the likelihood of Type 1 errors or incorrect rejection of a true null hypothesis (Kulkarni and von Storch, 1995). All indicators were, therefore, checked for positive lag-1 serial correlation at the 5 % level using the autocorrelation function (ACF). The existence of a trend influences the correct estimate of serial correlation (Yue et al., 2002). Therefore to avoid the possibility of detecting significant serial correlation, when in fact none may exist, original time-series were detrended to form a ‘trend-removed’ *residual* series before the ACF was applied. The linear trend,  $b$ , used to detrend the original time-series was estimated using the robust Theil-Sen approach (TSA; Theil, 1950; Sen, 1968). This is the median of all pairwise slopes in the time-series:

$$b = \text{Median} \left( \frac{X_j - X_i}{j - i} \right) \forall i < j$$

**Equation 6.1**

where  $X_i$  and  $X_j$  are sequential data values of the time-series in the years  $i$  and  $j$ . The TSA is more suitable for use with hydroclimatic data compared to linear regression as it

is a robust non-parametric method that is less sensitive to outliers (Helsel and Hirsch, 2002).

Pre-whitening was used to remove statistically significant positive lag-1 serial correlation from time-series. The conventional pre-whitening approach (Kulkarni and von Storch, 1995) was however found to artificially remove part of the magnitude of the trend hence a modified Trend Free Pre-Whitening (TFPW) technique was applied (Yue et al., 2002). This has been implemented before to deal with serially correlated data when using the Mann-Kendall (e.g. Yue et al., 2002; Petrow and Merz, 2009) and Pettitt test (e.g. Busuioc and von Storch, 1996; Zhang et al., 2008). Steps involved with the TFPW procedure are described in detail by Yue et al. (2002). In summary, the trend is first removed, the lag-1 positive serial correlation is removed, then the trend is added back to the time-series producing a blended TFPW time-series including the original trend but without serial correlation. Trend tests were only applied to the TFPW time-series when significant serial correlation existed; otherwise they were applied to the original time-series.

Over reliance on statistical significance is reduced by presenting the actual MKZs statistic values and the Pettitt test p-values to help interpret relative differences between signatures of change in observed and reconstructed indicators, rather than relying entirely on statistical significance relative to arbitrary p-value thresholds.

## **6.4 Results**

### **6.4.1 Hydrological modelling**

Model calibration and evaluation yielded 328 out of 1500 model simulations deemed to be behavioural (HYSIM 151, HyMOD 113 and NAM 64). Figure 6.4 compares the performance of the three models in simulating daily mean flows during calibration (1952-1959), evaluation (1960-1969) and for the period with known disturbance, post 1970 (1970-2009). During calibration, median NSE values for each model range between 0.82 (NAM) and 0.87 (HYSIM), with the maximum NSE value of 0.92 returned for both HYSIM and HyMOD. Similarly high objective function scores are returned for the evaluation period. However, there is a large reduction in the performance of each model for the post 1970 simulation period, resulting in median NSE scores of all

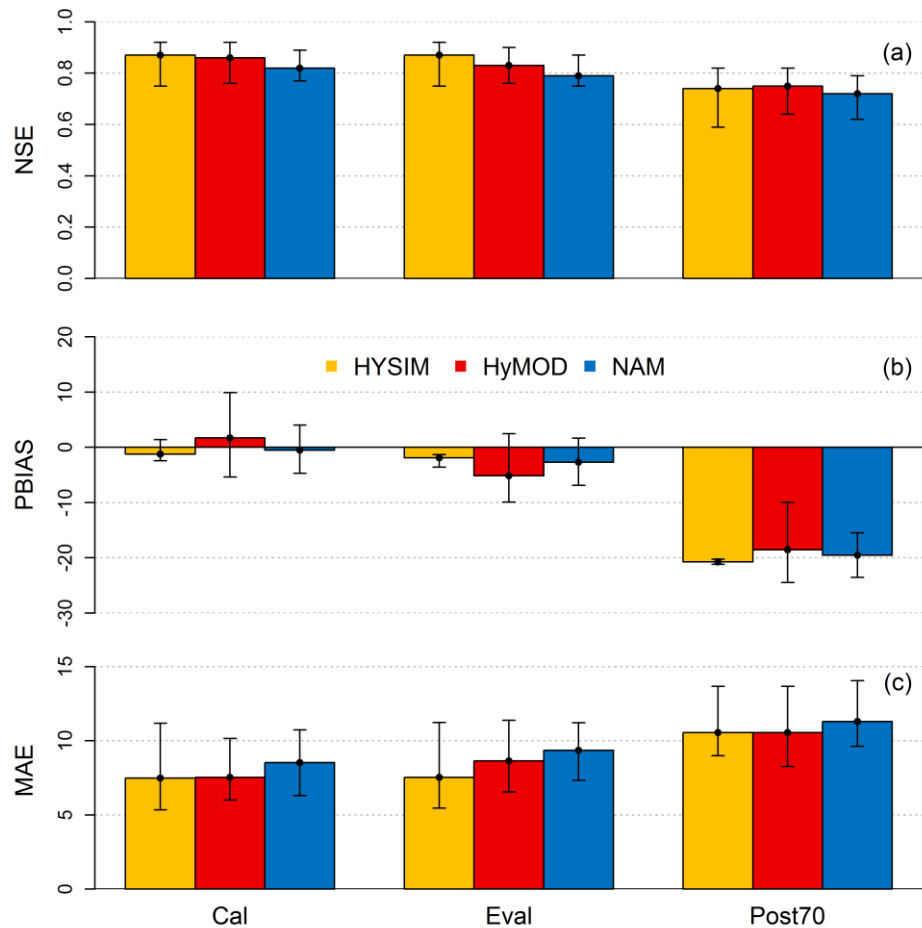


**Figure 6.4: Objective functions (a) NSE, (b) PBIAS and (c) MAE for HYSIM, HyMOD and NAM for calibration (Cal: 1952-1959), evaluation (Eval: 1960-1969) and post 1970 (Post70: 1970-2009) periods. Each bar represents the median score for behavioural simulations with error bars giving the maximum and minimum range.**

reconstructed flows ranging from 0.72 (NAM) to 0.74 (HYSIM). There are also large differences apparent between the reconstructed and observed PBIAS in the post 1970 period, with differences of the order of 20 %. Similarly, MAE values show a large increase post 1970 compared with model training periods. There is a strong degree of consistency between the three models used in all simulation periods despite the differences in model structure and complexity. Overall, during the post 1970 period, all reconstructed flows show a large discrepancy compared with observed flows. This is evident in lower NSE values, increased PBIAS and higher MAE. Differences in model performance evidenced by PBIAS and MAE suggest that the discrepancy between reconstructed and observed flows for the post drainage period is volumetric in nature.

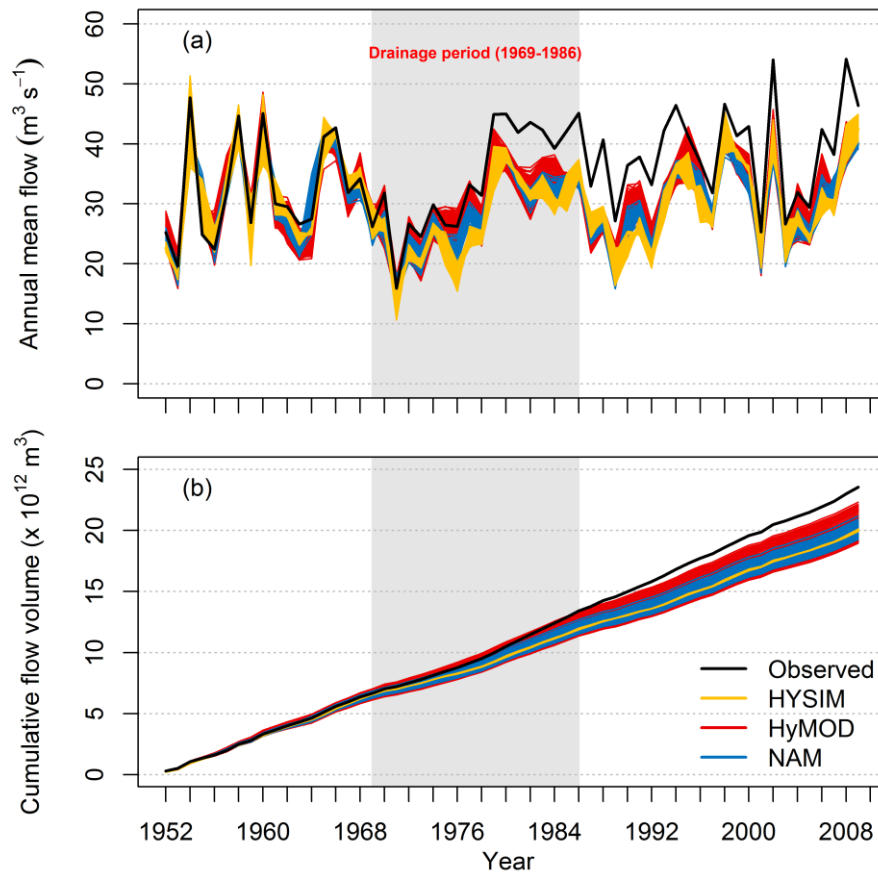


**Figure 6.5: Annual (a) mean and (b) cumulative volume of reconstructed and observed flow for 1952-2009. The period of drainage works is shown by the shaded grey area. Behavioural simulations for each model structure are colour coded.**

Figure 6.5 compares time-series of observed and reconstructed annual flows. Figure 6.5a shows close agreement between observed and reconstructed flows for both the calibration and evaluation periods with annual mean observed flows well bounded by simulations. After 1970, reconstructed and observed mean flows start to diverge. Largest divergence occurs from the late 1970s onwards, after which none of the simulations capture the observations. Despite the large deviation, the pattern of inter-annual variability between the observed and reconstructed flows remains similar, again emphasising the volumetric nature of the discrepancy. This deviation is also apparent from the cumulative flow volume plot (Figure 6.5b) where a point of inflection in the late 1970s becomes noticeable, after which a large deviation in the volume of flows occurs. The cumulative volume of flows for the full observed series is 17.6 % higher than the median of the reconstructed time-series. For all simulations the

cumulative volume underestimation ranges from 5.5 % to 24.2 % for the reconstructed flow.

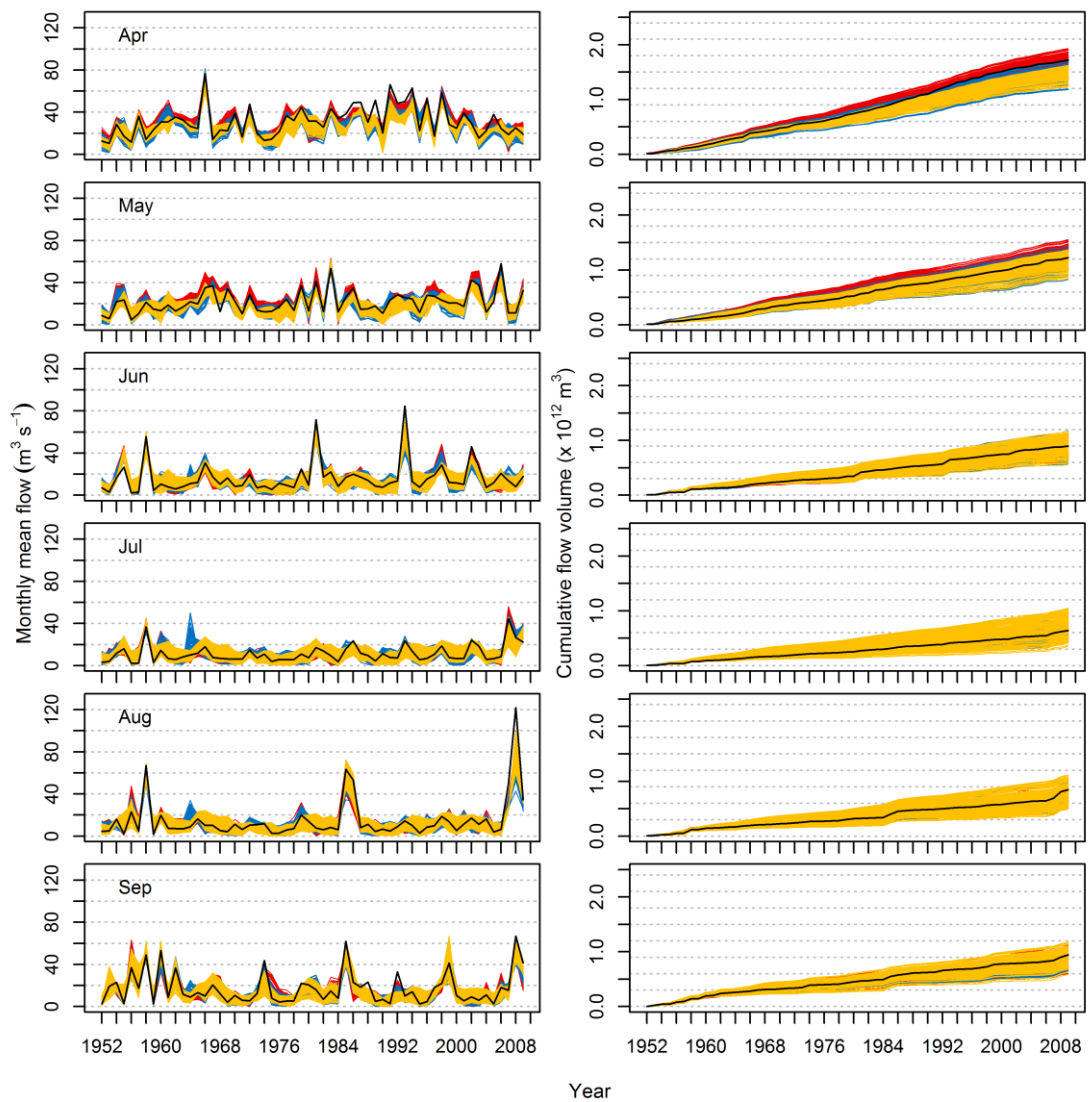


**Figure 6.6: Monthly (left) mean and (right) cumulative volume of reconstructed and observed flow for 1952-2009 for the summer half year (April to September). Colour code as in Fig. 6.5.**

Figures 6.6 and 6.7 display time-series of monthly mean flow and cumulative flow volume for the summer (dry) half year (April to September) and winter (wet) half year (October to March) respectively. Greatest divergence between observed and reconstructed flows is apparent for months within the winter half year. Conversely, within the summer half year only April shows any substantial evidence of divergence. Observed series lie near the centre of the reconstructed flows for other summer months.

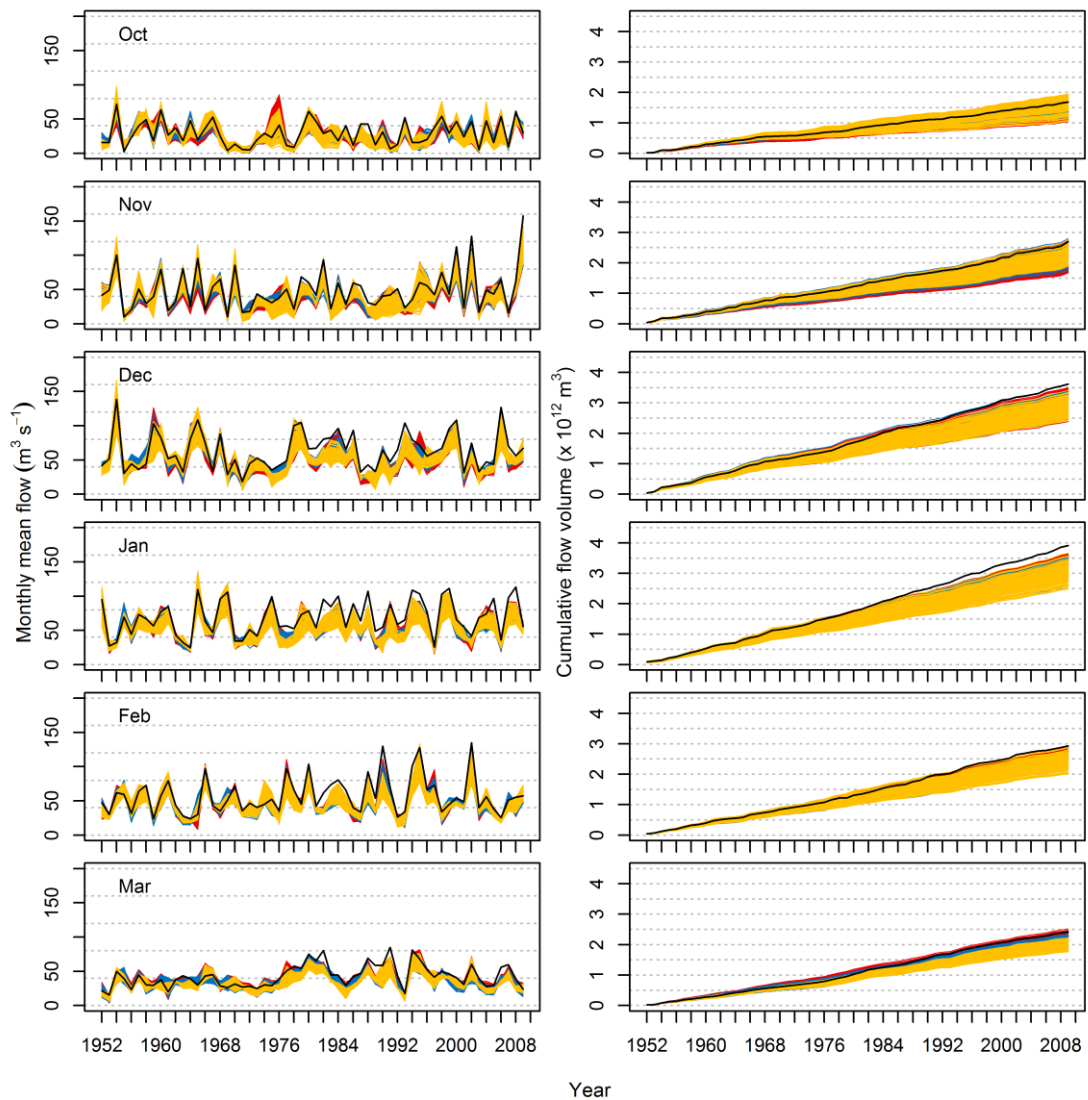


**Figure 6.7: As in Fig. 6.6 but for the winter half year (October to March).**

Reconstructions for months within the winter half year again show good agreement with observed monthly mean flow for the calibration and evaluation periods (Figure 6.7 left). However, for the post drainage period a large divergence is evident, particularly from the cumulative flow volume plots (Figure 6.7 right) where the observed series lies at the very upper bounds or outside reconstructed flows in the majority of months (particularly during December, January and February). The magnitude of divergence in winter half year months highlight their dominant contribution to the divergence evident in the annual observed flow.

## 6.4.2 Trend and change point analysis

In total 15 observed precipitation, 15 observed streamflow and 4920 reconstructed streamflow series (i.e. 15 indicators by 328 reconstructed series) were generated for further analysis for the period 1952-2009. Use of the term 'significant' below refers to changes at  $p = 0.05$  level.

### 6.4.2.1 Serial correlation

When analysing observed indicators for serial correlation only March and August mean flows show significant positive lag-1 serial correlation. This is also reflected in the reconstructed flow series with 81 % and 79 % of reconstructed simulations for March and August mean flow exhibiting serial correlation respectively. Four other reconstructed indicators have a smaller degree of significant serial correlation, AMF (33 % of the reconstructed series), and to a lesser extent in the RB index (3 %), September (5 %) and June (2 %) mean flow reconstructions. No precipitation indicators were significantly serially correlated. For observed streamflow indicators with significant serial correlation MK and Pettitt tests were applied to both original and TFPW time-series for comparison.

### 6.4.2.2 Monotonic trend

Results from the monotonic trend analysis for the period 1952-2009 using the MK test are presented in Figure 6.8. Observed indicators consistently show larger MKZs values than reconstructed. Observed AMF shows a significant increasing monotonic trend with the strongest positive MKZs value (3.1) in the analysis. None of the reconstructed AMF time-series or observed annual total precipitation show significant trends. Similarly, observed Q10 shows a significant increasing trend (MKZs 2.6), while P10 shows a non-significant increasing trend (MKZs 0.85). The median MKZs for reconstructed Q10 is 1.14, with one reconstructed Q10 series showing a barely significant trend (MKZs 1.97). A near significant increasing trend is found for the observed RB index (MKZs 1.93) with none of the reconstructed data or PCV (MKZs 1.58) exhibiting a significant trend.

All observed monthly mean flow indicators show increasing monotonic trends over the period 1952-2009 with significant trends for January, March, June, and July. When

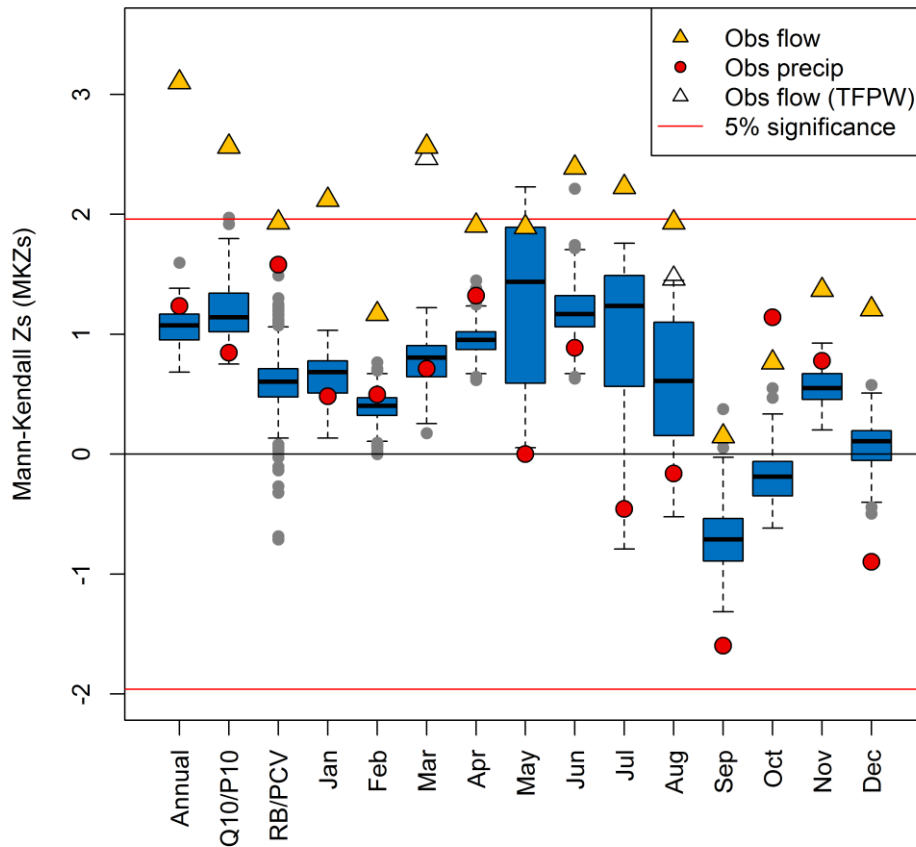


**Figure 6.8: Mann-Kendall tests for monotonic trend in precipitation and flow indicators. MKZs values above (below) 5% significance line ( $|MKZs| > 1.96$ ) indicate significant increasing (decreasing) trends. Boxplots summarise MKZs values for 328 reconstructed time-series with the black line representing the median, box the interquartile range (IQR), whiskers extend to the most extreme data point which is no more than 1.5 times the IQR from the box, and grey circles are outliers beyond this range.**

serial correlation is accounted for the strength of trends in March and August reduces. For the reconstructed monthly flow indicators the majority of the series reveal non-significant increasing trends with the exception of September and October which show non-significant decreasing trends. Only in May is there evidence of several significant trends in reconstructed series with 16 % showing significant increasing trends. For reconstructed June mean flows, one model from 328 behavioural simulations shows a significant increasing trend. Observed precipitation did not reveal significant trends in any of the 15 indicators with the relative strength of trends being much weaker than observed flow for corresponding metrics.

### 6.4.2.3 Change point

Results from the Pettitt change point test are presented in Figure 6.9 for selected indicators. For all identified change points the time-series increase after the stated change point year. A significant change point is found in 1978 ( $p < 0.001$ ) in observed AMF. Observed TAP and 85 % of reconstructed AMF series reveal non-significant change points also in 1978. For the remaining 15 % of reconstructed AMF series non-significant change points are shown for 1993. Observed annual Q10 also shows a significant upward change point in 1978 ( $p = 0.004$ ) with 61 % of models showing a non-significant change point for the same year, the remaining simulations show non-significant change points in different years. For P10 there is a non-significant ( $p = 0.12$ ) change point in 1977. A significant change point in 1982 ( $p = 0.014$ ) is found for the observed RB index with no significant changes in the reconstructed RB series for that year and several non-significant change points in other parts of the reconstructed series. In addition, there is a non-significant change in PCV in 2002 ( $p = 0.098$ ).

For monthly indicators observed January mean flow shows a non-significant ( $p = 0.086$ ) change point in 1978. In January, 31 % of reconstructed flows also show non-significant change points for the same year. However, there is a large difference in the strength of changes with reconstructed series having median  $p = 0.558$ . January precipitation shows a non-significant change point in 1964 ( $p = 0.7$ ). In March, a significant change point is detected in both observed mean flow (TFPW series,  $p = 0.0012$ ) and total precipitation ( $p = 0.044$ ) in 1975 with 7 % of reconstructed time-series having a change point in 1976. The March total is the only precipitation indicator with a significant change point.

Serial correlation has a large influence on results for March mean flows. Before serial correlation was accounted for the change point in observations occurred one year later in 1976 ( $p < 0.001$ ) while 85 % of reconstructed series showed a significant change point between 1975 and 1977. Despite the large reduction in the number of reconstructed series showing a significant change point after application of TFPW, the relative difference between observed and reconstructed p-values around the mid-1970s is the closest of all the indicators shown in Figure 6.9. Other statistically significant change points (not shown) occurred in observed monthly mean flow in April

(1976), June (1978) and July (1978). For reconstructed April and June mean flows less than 3 % of simulations show significant changes in the same year, with none reproducing a significant change in 1978 for July.

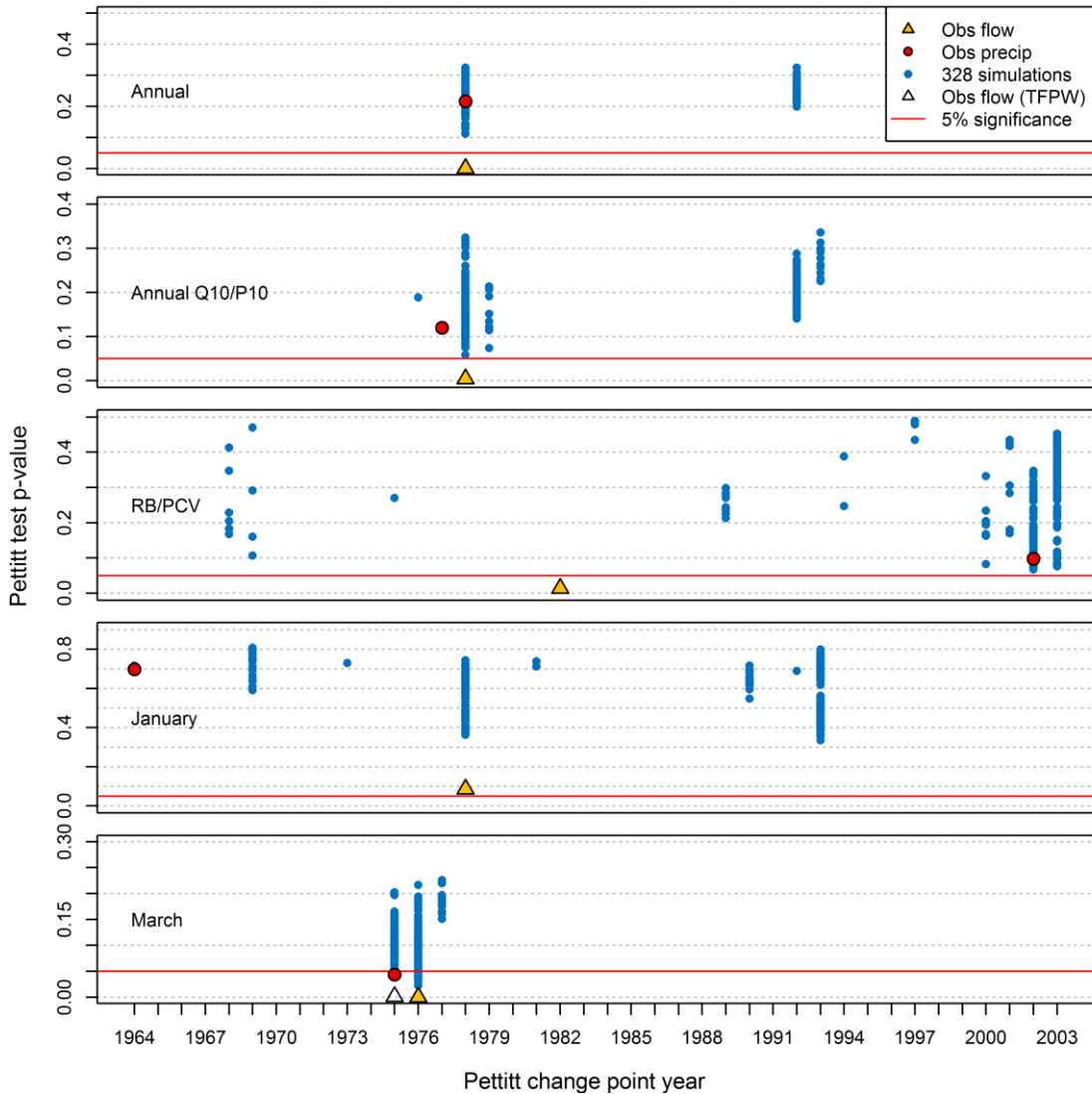


Figure 6.9: Pettitt test for change points in selected indicators. Solid red lines represent the threshold for significant change points at the 5 % level with p-values below (above) indicating a significant (non-significant) change point for corresponding year of change on the x-axis.

## 6.5 Discussion

### 6.5.1 Attribution of change in Boyne streamflow

Following a preliminary assessment of multiple potential drivers of hydrological change, the contribution of climate (WH 8 precipitation) and internal factors (WH 6 and 7 drainage) to the detected mid-1970s change point in Boyne streamflow were

explored. Reconstructed flows obtained from behavioural simulations from three structurally different CRR models do not show the trend and change point found in observed AMF in 1978 when only climate variability is considered. While this discrepancy is particularly evident for high flows (Q10) and during winter months (Figure 6.7, right) there is some evidence of statistically significant changes in observed June and July mean streamflow. However, a statistically significant change in summer (i.e. low flows) contributes little to the large detected change point in observed AMF (see Figure 6.6, right). Additionally, there is no evidence of a trend or change point in TAP, P10 or precipitation totals in winter months. While it is important to test for both gradual and abrupt changes, given that different drivers have effects at different time-scales, it is clear from visual inspection of time-series (Figures 6.1, 6.5 and 6.10) that the observed change in Boyne streamflow is abrupt and therefore detected trends are an artefact of change points rather than real gradual linear changes. This further supports the assumption that drivers with longer-term gradual or linear effects are less important in this context.

Given that reconstructed flows contain precipitation as a key forcing variable it is therefore unlikely that changes in flow observations are driven entirely by a change in precipitation (WH 8). The observed RB index was found to increase post 1982 while the PCV (coefficient of variation of daily precipitation) did not change significantly. Changes in RB index have been previously linked to human disturbance within catchments (e.g. Baker et al., 2004; Holko et al., 2011). An increase in flashiness is consistent with the effects of drainage, where there is an acceleration of the response to rainfall with flood peaks of increased intensity (Lynn, 1981).

However, the influence of precipitation change cannot be completely discounted. A significant (5 % level) change point in 1975 was detected in March for both observed mean flow and precipitation totals, with reconstructed series showing evidence of a change around the same time. This is further supported by visual inspection of the time-series for observed and reconstructed March mean flows in Figure 6.10. The plot shows the median of observed and reconstructed time-series before and after 1975. Evident is the close agreement between series before the change point, while an increase in the median of March mean flows is apparent after 1975 in both observed and reconstructed flows. Of note, however, is the larger change in observations which

can be interpreted as a combined influence, of similar magnitude, from drainage and precipitation. This is consistent with the hypothesis of increased March precipitation after 1975 being magnified by an altered rainfall-runoff response of the catchment following drainage which also increases flashiness.

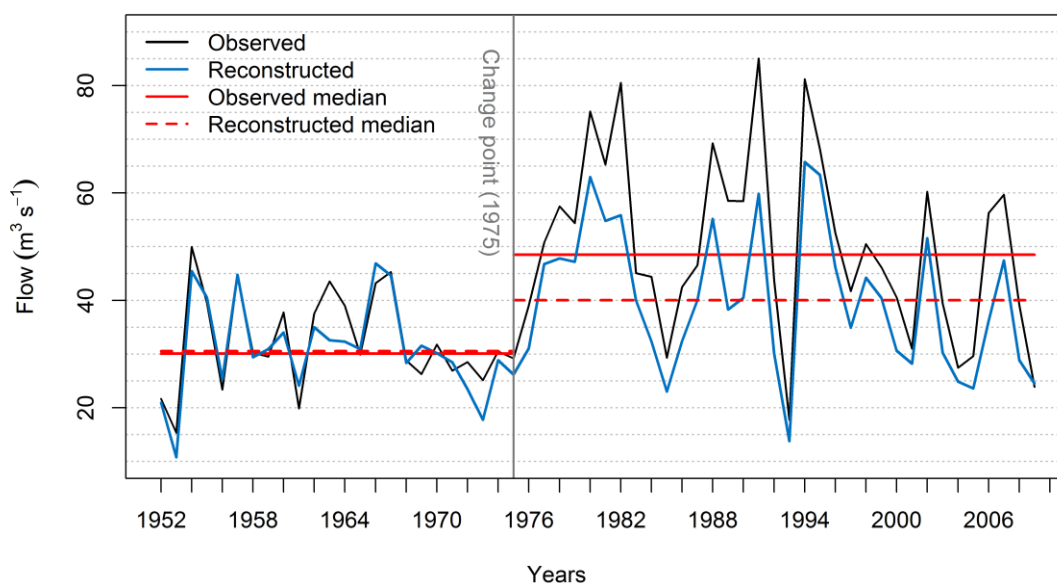


**Figure 6.10: Observed and median of 328 reconstructed series for March mean flow. Solid red line is the observed median flow before (1952-1975) and after (1976-2009) the detected change point; dash red is the reconstructed median flow for the same periods.**

In light of these findings, it is unlikely that observed changes in the flow regime of the Boyne are driven solely by changes in precipitation as a result of a shift in the NAO index from a negative to positive phase in the mid-1970s. While detection of the change point in annual and March observed mean flow by Kiely (1999) is confirmed here, attribution of change is different. Here it is asserted that the dominant driver of change in observed AMF and Q10 is arterial and field drainage (WH 6 and 7). Data on the extent and timing of arterial drainage show that the majority of dredging in major channels was completed between the late 1970s and early 1980s thereby facilitating widespread field drainage. Differences in response between observed and reconstructed flows are consistent with current understanding of the impact of drainage, with largest divergence evident in wetter months. Results for March suggest that there is an influence from both internal and climatic drivers of change, by which drainage magnifies the signal of the mid-1970s abrupt change in precipitation.

Therefore, in line with WH 10 (multiple drivers/synergetic effects) it is postulated that the attribution of abrupt change evident in observations is driven predominantly by drainage at the annual and high flow scale and in March by comparable contributions of both drainage and precipitation change. Future work should examine whether change in March precipitation is most strongly linked to a change in the NAO or other regional-scale atmospheric circulation.

### **6.5.2 Confidence in attribution**

To qualify this explanation for hydrological change in the Boyne a critical examination of uncertainties and assumptions in the methodology is required (after Merz et al., 2012). While the approach used here accommodates uncertainties from rainfall-runoff model structure and parameters, it is assumed that the simulations reflect the full hydrological response of the catchment. Model inter-comparison tests (e.g. Reed et al., 2004; Duan et al., 2006) indicate a wide range of simulations when many different model structures are forced with the same input. In this chapter only when all three models are combined is the full range of observed flows in the pre-drainage series (calibration and evaluation period) captured. This highlights the importance of considering multiple model structures and signals potential benefits from applying generic model structures such as the Framework for Understanding Structural Errors (FUSE; Clark et al., 2008) in detection and attribution studies.

Positive serial correlation has a large influence on the statistical significance of results. There are several ways of dealing with this. Here, pre-whitening (TFPW) before application of statistical tests was applied; but block bootstrapping has also been used (e.g. Önöz and Bayazit, 2012; Murphy et al., 2013a). The large reduction in the number of statistically significant change points in reconstructed March mean flows reported above also occurred when block bootstrapping was applied (not shown). The influence of serial correlation on statistical change detection is particularly important when using reconstructed time-series given the high degree of serial correlation that can be introduced by soil moisture accounting algorithms or 'memory' of CRR models (Evin et al., 2013). However, of greater importance in this approach is the relative difference in the statistics derived from observed and reconstructed series, rather than significance based on arbitrary p-value thresholds.

There is unavoidable subjectivity in identification of potential working hypotheses and exclusion of some WHs from detailed assessment (Table 6.1). Substantial effort was made to include all plausible drivers of change. MMWH also accepts that other currently unknown factors (WH 11) may emerge as important drivers of change given further research, recognising attribution as an iterative process. Furthermore not all drivers can be quantitatively analysed and excluded on that basis. Here, treated water discharges (WH 3), urbanisation (WH 4), and forest cover and management change (WH 5) were considered second order influences based on available data and the nature of change in streamflow observations. Although the scale of land-use change, such as urban and forest cover, is modest and unlikely to be influential in a catchment of this size (Blöschl et al., 2007), there is little data to quantify such impacts in the Boyne. There is also no control case for large catchments compared to small experimental watersheds, where a paired catchment approach can be used to examine impacts of land-use changes (Hewlett, 1982; Brown et al., 2005).

### **6.5.3 Towards more rigorous attribution**

A detected change in streamflow is the integrated response to all drivers, climate and internal, natural and human induced. This makes attribution of hydrological change inherently challenging. However, it is demonstrated that valuable insights can emerge from application of MMWH which enables systematic consideration of multiple drivers, helping to postulate new hypotheses and importantly highlighting weaknesses in current understanding, while still acknowledging the possibility of unknown drivers. Ideally, an attribution study will establish whether change is driven by climate and/or internal disturbances, as management responses to the detected driver could be very different. Here, this was achieved with the aid of hydrological simulation. It was also shown that human disturbance can have larger impacts on the hydrological system than climate at the catchment scale.

Even for the Boyne, where relatively rich data sources are available in comparison to other catchments, full confidence in attribution cannot be achieved. Conclusions are founded on an assessment of inconsistency, while hard attribution also requires evidence of consistency (Merz et al., 2012). Data were gathered for precipitation, PET, streamflow, the NAO, land-use, soil types, and supplemented with documentary

evidence from hydrometric and drainage archives. In pursuing evidence of consistency physically based models could be used to explicitly represent arterial and field drainage systems. However, the value-added by more complex modelling of artificial drainage at the scale of the Boyne is contingent on the availability of detailed data on the timing and location of local channel changes. Hard attribution is fundamentally problematic for historic changes where data can be more qualitative in nature. Hence rigorous attribution will require investment in monitoring change in catchments, beyond typical hydrological variables.

In agreement with Merz et al. (2012), advancement in attribution is an iterative process whereby revealing weaknesses in established hypotheses of change can lead to improved overall understanding of dominant drivers of change. In this chapter coupled interactions and feedbacks between human and natural components of the catchment system are apparent. For example, the economic imperative for increased agricultural productivity was the main motivation for implementing drainage, facilitated through structural funds available by the accession of Ireland to the EEC. In the face of such complexity MMWH offers a formal structure within which to build and refine hypotheses of change.

## 6.6 Chapter summary

Attributing changes in streamflow to climate drivers cannot take place without reference to other human induced catchment disturbances. This chapter revisited an attributed change point in observed streamflow in the Boyne (Kiely, 1999) using MMWH and the Merz et al. (2012) attribution framework. Evidence of consistency and inconsistency with the detected change was systematically examined given a set of credible external and internal drivers. Changes in precipitation and a combination of arterial and field drainage, as well as possible synergistic effects were brought forward for further analysis. CRR models were employed to reconstruct streamflow in the absence of drainage while statistical tests were used to detect monotonic trends and change points in reconstructed and observed flows.

Results show that climate variability is not the only possible driver of hydrological change in the Boyne. Arterial drainage and the simultaneous onset of field drainage in the 1970s and early 1980s were inferred to be the predominant driver of change in

observed annual mean and high flows. Wetter, winter months contribute most to the large 1978 change point found in annual and high flows. However, a change in precipitation regime is also reflected in March mean flow with observed and reconstructed runoff showing a contemporaneous upward change point in 1975 of similar magnitude to the effects of drainage. This new explanation posits that multiple drivers acting simultaneously were responsible for observed changes in Boyne streamflow, but detectable in different aspects of the flow regime.

This chapter shows the range of data types needed for rigorous attribution, especially where substantial human modifications to catchments may be involved. The Method of Multiple Working Hypotheses compels the researcher to review all plausible drivers of change, thus avoiding confirmation bias, in addition to identifying key weakness in current understanding of change within a catchment. A key weakness here was the limited information and data availability on the impact of urbanisation and forest cover change on hydrological behaviour. These knowledge gaps create opportunities for future research. Attribution of hydrological change is a challenging task but understanding the interplay and co-evolution of human and natural hydrological dynamics (Sivapalan et al., 2012) is essential to the discipline (Montanari et al., 2013). It is of great societal importance that signals of human disturbance and natural and anthropogenic climate change within the hydrological system are detected and properly attributed so that effective management responses are invoked.

This chapter has demonstrated the value of application of the hydroclimatic perspective to the attribution problem using the Boyne catchment as a case study therefore completing Thesis Objective 4. In the next chapter, the main findings from each chapter are discussed.

## 7 Discussion, Conclusions, and Future Work

---

### 7.1 Introduction

The core aim of this thesis was to explore spatio-temporal changes in physical flood hazard on the Island of Ireland taking a hydroclimatic perspective to better understand *how* (detection) and *why* (attribution) floods have changed over multi-decadal time-scales. Thesis objectives were set out in Chapter 1 from 4 key research gaps identified in Chapter 2:

- **Thesis Objective 1:** Classify extreme rainfall regions for the Island of Ireland to explore the fundamental climatology of extreme precipitation (Chapter 3).
- **Thesis Objective 2:** Assess spatio-temporal changes in extreme precipitation and floods for a number of characteristics (Chapter 4).
- **Thesis Objective 3:** Explore the relationship between large-scale atmospheric circulation and variability and change in floods (Chapter 5).
- **Thesis Objective 4:** Advance approaches in attributing drivers of change at the catchment scale by considering both external and internal drivers of change under a multiple working hypotheses framework (Chapter 6).

These objectives could only be undertaken once 2 key **thesis data objectives** were completed:

- **Thesis Data Objective 1:** Establish a network of station-based precipitation observations appropriate for the analysis of extreme precipitation (Chapter 3).
- **Thesis Data Objective 2:** Extract a flood Peaks-Over-Threshold database from near natural catchments for the Island of Ireland appropriate for the analysis of changes in flood frequency (Chapter 4).

This final chapter draws conclusions on the research undertaken, discusses limitations, and identifies areas for further research.

## 7.2 Summary of main research findings

### 7.2.1 Thesis Objective 1: Extreme Rainfall Regions (Chapter 3)

Classification of Extreme Rainfall Regions (ERRs) (**Thesis Objective 1**) reflecting similar extreme precipitation characteristics was needed to simplify local weather for improving physical interpretation of climate-flood links in Chapters 4 and 5. First, a station-based dataset of precipitation observations was compiled that was deemed suitable for examination of extremes; that is, balancing the highest spatial resolution available, against the longest temporal resolution available, without compromising data quality. A final set of 126 precipitation stations for both Ireland and Northern Ireland for use in classification of ERRs was identified (**Thesis Data Objective 1**). A set of 17 variables describing 5 key extreme precipitation characteristics (Magnitude, variance, extreme value tail behaviour, timing, and persistence) and physiographic properties (height and distance to coast) were reduced into four rotated principal components (PCs) using Principal Component Analysis (PCA). Cluster Analysis was undertaken using the k-means algorithm to objectively identify 3 ERRs with distinct extreme precipitation climatologies. The first PC accounted for 53 % of the variability in the original dataset with near uniform direction, mainly reflecting extreme precipitation magnitude, suggesting a relatively simple extreme precipitation regime. The remaining 3 PCs only explained ~ 10 % of the variance each but did have an influence in the final delineation of ERR boundaries, particularly the influence of elevation and coast, and extreme precipitation and wet-day spell length were considered, most notably in the north of the Island. After a rigorous sensitivity analysis, 3 ERRs were considered appropriate for IoI. These ERRs were then used to better interpret spatio-temporal changes in extreme precipitation in Chapter 4 and for grouping the developed flood-Index in Chapter 5 into more physically relevant regions, instead of political or agency boundaries which is often done.

### 7.2.2 Thesis Objective 2: Detection of Spatio-temporal changes in extremes (Chapter 4)

Anthropogenic greenhouse gas induced climate change is expected to intensify the hydrological cycle leading to increased frequency and severity of precipitation extremes, and hence increasing the physical hazard component of flood risk. This

chapter, for the first time, assessed if there are statistically discernible changes in both extreme precipitation and flood time-series across the Island of Ireland (**Thesis Objective 2**). Much effort was dedicated to ensuring use of the best available station-based datasets and ensuring best possible spatio-temporal coverage. Only catchments that are considered 'near natural' were used so that any detected change can be attributed (with more confidence) to climatic drivers, rather than human modification within the catchment. A new flood Peaks-Over-Threshold (POT) database was developed to facilitate the assessment of flood frequency (**Thesis Data Objective 2**).

The Mann-Kendall test for monotonic trend was applied for exploring signatures of change in indices relating to the magnitude, duration, and intensity of extremes and logistic regression was employed for assessment of changes in frequency indices. Results show evidence of robust increasing changes in extreme precipitation indices for the periods investigated. Over 80 % of stations show increases in maximum 5-day precipitation (RX5day), a flood relevant indicator, with 22 % of those statistically significant at the 5 % level. The magnitude of increases in precipitation intensity (SDII) is within the range of what is expected with observed atmospheric warming (6.98 % with an interquartile range of 2.67 % and 16.99 % between 1956 and 2009). Despite the small size of the Island of Ireland in relation to the Atlantic Ocean, many extreme precipitation indices show most pronounced increases in the southwest (ERR-SW) and within the coastal and upland Extreme Rainfall Region (ERR-CU) indicating changes in maritime air masses that interact with the Atlantic facing topography.

For floods, while shorter time-series showed predominantly increasing trends, when longer records were considered, conclusions on floods are less certain than those for precipitation due to the more limited availability of long record stations. Caution is required in making inferences about the drivers (causes) of these changes. Although results are broadly in-line with climate change, time-series revealed large decadal-scale variability coherent across the entire Island for both precipitation and streamflow series. This provides compelling evidence that changes are indeed climate-driven but that the role of Decadal Climate Variability (DCV) is considerable.

### 7.2.3 Thesis Objective 3: Synoptic and Large-scale drivers of floods (Chapter 5)

Chapter 4 shows that the influence of natural large-scale climate variability can dominate signals in observed flood records expressed as periods of enhanced/reduced flooding. This is problematic for assessing trends in flood time-series as observed data are often too short and hence detected changes reflect a snap-shot of climate variability rather than evidence of long-term climate change. This Chapter used an objective weather classification scheme to reconstruct the atmospheric drivers of flood occurrence across the Island of Ireland since 1872, and explored further linkages with large-scale climate (**Thesis Objective 3**). Synoptic drivers show modest skill in reproducing observed Peaks-Over-Threshold (POT) floods at the annual-scale, but are not as skilful at the seasonal-scale. Four flood rich periods were identified: 1.) 1870s to 1890s; 2.) late-1900s to mid-1930s, 3.) a short spell in the 1980s, and 4.) late-1990s onwards. It was found that just 5 weather types could account for 75 % of annual floods, cyclonic being most dominant with important contributions from westerly (during winter) and southerly (during summer) types. Remarkably, the most widespread floods can affect up to 80 % of the network during a large event, highlighting the importance of considering the entire Island, rather than just small groups or individual catchments when assessing the large-scale drivers of floods.

The North Atlantic Oscillation was shown to be positively correlated with high flows and floods. For flood frequency, this relationship is only evident in the west and north west, but evidence of an NAO influence in other parts of the Island were more evident for high flow indices that describe catchment wetness. An exploratory analysis of the role of Atlantic sea surface temperature anomalies, expressed as the AMO, on modulating flood-producing weather types was also undertaken. The AMO was found to be positively correlated with anticyclones over the British-Irish Isles domain, meaning these blocking high pressure systems occur less frequently during AMO cool phases. This is supported by a negative correlation between AMO-NAO. Persistent periods of low anticyclonic frequency tend to coincided with prolonged periods of higher than normal cyclonic types, and are identified as a contributing factor to prolonged flood rich periods. However, much more research into this tentative link is needed, but if confirmed could have important implications for understanding long-term variability of flood propensity.

#### 7.2.4 Thesis Objective 4: Attribution of detected changes in streamflow (Chapter 6)

Chapter 5 shows statistically significant links between large-scale climate indices and streamflow over decadal time-scales. However identifying the dominant driving mechanism(s) of detected changes in streamflow (i.e., attribution) at the catchment scale is a challenging task due to the confounding influence of human disturbance such as land-use changes, water abstractions, and river engineering.

This Chapter addresses this challenge by examining the utility of the multiple working hypotheses framework in moving towards more rigorous attribution of changes using the Boyne catchment in the east of Ireland as a case study (**Thesis Objective 4**). Previous research in this catchment found that a large upward change point in streamflow during the mid-1970s corresponded with a shift in the NAO towards a more positive phase, bringing increased precipitation, and hence increased risk of flooding. Here, the single driver analysis is extended to include multiple factors causing change, both climate driven and internal to the catchment, to establish relative contributions. Rainfall-runoff models were employed to reconstruct streamflow to isolate the effect of climate, taking account of both model structure and parameter uncertainty. The Mann-Kendall test for monotonic trend and Pettitt change point test were applied to explore signatures of change.

Results show that the detected increase in annual mean and high flows was not predominantly driven by changes in precipitation as a result of a shift in the NAO index. Rather it is asserted that the dominant driver of change was arterial drainage and the simultaneous onset of agricultural field drainage in the 1970s and early 1980s. It is also demonstrated that attribution can be more complex at different time-scales with multiple drivers acting simultaneously. This study emphasises the amount and range of data types needed for rigorous attribution, especially when substantial human modifications to catchments may be involved. In fact, it was shown that human disturbance can have larger impacts on the hydrological system than climate at the catchment scale. In the face of such complexity, the use of this systematic hypothesis testing framework, combined with hydrological modelling, helps to avoid confirmation bias and improves overall understanding of dominant drivers of change.

### 7.3 Synthesis of cross-cutting themes

This research has many important implications. Floods are already one of the most costly natural hazards to society and theory suggests they will increase in frequency and severity with a warming climate. However, as revealed here, the climate-flood link is not straightforward and in 'real world' catchments is often the result of the complex interplay of decadal climate variability, local hydrology, and human disturbance internal to catchments. This is a real challenge for both detection and attribution of anthropogenic climate change signals throughout Europe where there is limited land area that has not been affected by human activities to some extent. The dominant role of decadal climate variability and the tendency for floods to cluster into periods of persistent occurrence mean that floods can no longer be seen as random local events occurring within stationary hydroclimatic conditions. Such a realisation requires building on multi-disciplinary approaches as employed here that start with viewing floods within their large-scale climatic and long-term context. While each chapter provides a discussion of main findings, limitations and prospects for future work, the following sections identify cross-cutting issues from across the body of work undertaken here.

#### 7.3.1 The importance of observations

The largest barrier to progress in this area for Ireland has been the lack of quality assured long-term station-based datasets. Each of the 4 core chapters depended on good quality long-term precipitation and/or streamflow data that was fit-for-purpose for the assessment of extremes. The raw data across the entire climatological network for Ireland has only recently become available for research through work completed during the meteorological analysis component of Ireland's Flood Studies Update (Fitzgerald, 2007) and subsequent work of Walsh (2012a) and Walsh (2012b). However, the output from these studies was a daily 1 km gridded precipitation grid. While a valuable product for many applications, it was not considered optimal for the assessment of precipitation extremes. Therefore this thesis scrutinised the raw station based precipitation data behind this product as well as including data from Northern Ireland to derive a network of pre-processed (i.e., quality controlled and infilled) stations covering the Island of Ireland at a high, evenly distributed, spatial density (126 stations) with suitable length (minimum 38 years; maximum 71 years). While methods

used here are robust (within reason) to stations with possible inhomogeneities as identified in Section 4.5.3 (e.g., St2635, Derryhillagh) it is recommended that a full network homogenisation is undertaken at the daily time-scale when appropriate international standards are established, and that any associated metadata be made available to end users. Additionally, daily precipitation data pre-1941 is available for several stations in Ireland in hard copy records. Digitisation of this data would be of great benefit to the research community for assessment of longer-term changes.

This study is the first to use streamflow data from the Irish Reference Network (IRN) for flood analysis. It is recognised that Reference Hydrometric Networks (RHNs) such as the IRN are live networks so they need constant updating when new information becomes available or issues in the current version are identified. This thesis has identified a non-nested subset of 29 IRN stations most suitable for the analysis of high flows and floods. There are however some recommendations for the next round of IRN development: 1.) there are a number of gaps in network coverage particularly in the west and east, and for longer records (pre-1978) the north of the country is not represented. Additionally, the southwest Extreme Rainfall Region (ERR) has only one catchment within its boundaries, future network reviews should give priority to finding potential candidate catchments here given its important hydroclimatic location; 2.) The original infilling of streamflow (Murphy et al., 2013b) used a single conceptual hydrological model driven with observed inputs of precipitation and PET. However, the new precipitation dataset identified here, with much improved spatial coverage, could be used in combination with multiple hydrological models to give more accurate results along with associated uncertainty estimates.

While most extreme precipitation and flood indices used here were straightforward to extract following standard international guidance (e.g., ETCCDI indices) the flood Peaks-Over-Threshold (POT) database needed much more consideration. It was found that fully automatic implementation of the derived POT extraction algorithm could lead to misleading results. Knowledge of the physical characteristics of each catchment was necessary as heavily groundwater dominated catchments have such dampened response that it was not possible to extract 3 independent peaks, on average, per year. However, by accounting for this, the new POT database developed here allows for much richer analyses of floods beyond just the assessment of magnitude. This data is

available for other researchers and it is hoped that it will provide the basis for further improving knowledge of floods in Ireland.

Two thirds of time during this three year study was spent developing these observed datasets, but the effort was worth it. The central conclusions of this thesis are all based on the reliability of these data. Basic hydroclimatic data are the foundation of studies tracking emerging patterns of change and for evaluating climate and hydrological models, so have much wider application. The derivation of these datasets is thus a major contribution of this thesis.

### 7.3.2 Scale considerations

A key theme throughout this thesis has been the importance of scale. *Spatial scale* ranged from global (influence of anthropogenic climate change) → North Atlantic basin (role of decadal climate variability) → Island of Ireland (understanding impacts on surface variables) → Extreme Rainfall Regions (regional climatology of extreme precipitation) → sub-regional impacts (flood-producing weather types have more subtle signals) → individual catchment scale (where many drivers both climatic and internal interact in complex ways). While the synoptic and large-scale drivers of floods (Chapter 5) had a detectable influence on the island as a whole; there were many more subtle differences that were uncovered. For example, the NAO has been shown to modulate physical flood risk, with strongest links for western areas, whereas, cyclonic systems from a southerly direction are more important for understanding flood change in the south.

Second, the *data resolution* and *time-scale* of extreme precipitation and flood indices was crucial. Robust increasing trends were detected in point-based extreme precipitation records. However, increases in precipitation extremes in studies using observed gridded products (e.g., Casanueva et al., 2014) did not appear to reveal such strong trends over a similar time-period using the same metric (R95pTOT). This suggests that part of the signal may be concealed due to aggregation within such products. Therefore, this resolution mismatch has potential wider implications for detection of changes in precipitation extremes that warrants further investigation under a more standard study design and on a seasonal basis.

Throughout this thesis effort was made to consider the seasonal *time-scales* of extreme precipitation and floods. This has certainly improved physical interpretation of driving processes. For example, the delivery of maximum precipitation in each of the three ERRs is different. ERR-SW receives maximum precipitation in late November while a large fraction (27 %) of stations within ERR-IE receive maximum precipitation in late summer / early autumn (between 17<sup>th</sup> of August to 17<sup>th</sup> of September). Matthews et al. (2015) found that peak storminess (cyclone frequency  $\times$  cyclone intensity) in BI (British-Irish Isles) occurs in late November with a secondary peak in late summer / early autumn indicating that the climatology of precipitation extremes is driven by the cyclone climatology of BI. Additionally, from the outset it was assumed that most floods occurred during the winter half year, but this has never been formally quantified for Ireland. Here it was shown that a substantial fraction (18 %) of floods occur during the summer half year. Overall, the drivers of floods in summer are similar to those in winter (cyclonic types), but with moisture laden air masses from southerly directions more important. Interestingly, there was a diverse spread in the contribution of summer floods to the total flood count for individual catchments. It was expected that summer floods would be more prevalent for catchments within ERR-IE given the greater influence of convective summer rainfall, and earlier extreme precipitation seasonality. However, the fraction of summer floods to total was positively correlated to streamflow flashiness. Precipitation during a summer storm is much less likely to cause a flood event in a groundwater dominated catchment, whereas up to almost 30 % of floods in the most flashy basins (located in the north and southwest) occur during the summer half year.

*Temporal* scale was shown to be perhaps one of the foremost factors in this thesis. It has been well documented that the NAO dramatically transitioned from a predominantly negative phase during late-1950s and 1960s, to an anomalously positive phase until the mid-1990s. This transition has been linked to changes in regional surface climate such as increased occurrence of heavy precipitation in the UK (e.g., Osborn, 2006). This time-period also corresponds with the expansion of the precipitation and streamflow network in Ireland and the UK. For example, precipitation deficits of the mid-1970s led to severe hydrological drought in Ireland and the UK and motivated an expansion of the hydrometric network, thus 'hard wiring' an overall

positive trend into the network when time-series up to the recent wet period are examined (Murphy et al., 2013a). Clearly, results from trend analyses on observed records (precipitation and streamflow) from this period would reveal mainly changes due to a particularly dominant period of natural climate variability rather than evidence of long-term climate change. A key contribution of this thesis was placing these short term trends in their longer-term context by reconstructing the atmospheric drivers of floods over a 144-year time-period (F-Index). Instead, four distinct flood rich periods were identified providing evidence that floods cluster in time when long-enough records are evaluated (confirming Fig. 2.5 in Chapter 2).

### 7.3.3 From Detection to Attribution

Application of statistical change *Detection* in Chapter 4 found evidence of an increase in extreme precipitation magnitude, frequency, duration, and intensity, consistent with an intensification of the hydrological cycle due to climate change. Natural decadal climate variability has undoubtedly played a role (i.e., changing frequency of extratropical cyclones), but the increasing trends are robust to changing period of record. While longer streamflow records also show increased trends in flood indices, this result is hampered by the limited spatial extent (just 8 catchments) for longer records. During the shorter time-period (1978-2009) where good spatial coverage was achieved, there were spatial patterns to trends in flood indices that were inconsistent with changes in precipitation. This suggests (i) a more complex climate-flood relationship than climate-precipitation, likely due to the added complexity of varying catchment characteristics (Laizé and Hannah, 2010) and/or (ii) the drivers of changes in flood variables is not uniform at the scale of the Island of Ireland. Therein lays the key limitation of detection only studies. Without an understanding of the drivers, little can be concluded about future changes. Attribution on the other hand is concerned with establishing the most likely drivers of detected changes.

As outlined in Chapter 2 and 6, Merz et al. (2012) proposed two categories of attribution: 'soft' attribution which establishes drivers that are shown to be consistent with the detected change, and 'hard' attribution that takes a hypotheses based approach and aims to also prove inconsistency with other plausible drivers. Hydroclimatic links established in Chapter 5 (i.e., between NAO, AMO, LWTs, and flood

indices) can only be regarded as ‘soft’ attribution as no formal attribution framework was applied. Still, the use of streamflow from RHNs and multiple-lines of evidence linking both synoptic and large-scale drivers to flood occurrence improves on previous research in Ireland and gives additional confidence to and greater understanding of the atmospheric drivers of floods.

More of a challenge is the pursuit of ‘hard’ attribution, as demonstrated in Chapter 6, in the face of complex hydroclimatic interactions and even for the Boyne case study where rich data are available, this was not attainable. Uncertainty in current methods (i.e., hydrological modelling) and lack of historic data were key limitations. Alternatively, it was argued that ‘hard’ attribution should be seen as the highest standard, but is rarely (if ever) possible in practical application. Instead, this thesis proposes that in the face of such complexity a multiple working hypotheses approach can lead to improved attribution by forcing researchers to, at least, consider a wider set of plausible drivers of change. In the case of the Boyne this has led to an improved attribution of the detected mid-1970s change in streamflow. It is also advocated that attribution be viewed as an iterative process and even the newly proposed hypothesis of change in the Boyne, arterial and field drainage, should be challenged in future when new data and methods become available. This process of finding weaknesses in current hypotheses (e.g., Popper, 1963) will surely lead to the advancement in knowledge of drivers of hydroclimatic change, and can make a contribution to advancing the IAHS scientific decade (Montanari et al., 2013).

## **7.4 Priorities for future work**

Discussion of limitations and future work has taken place throughout this thesis within the relevant core chapters. However, the two most promising and significant areas for further work identified within this thesis are developed in more detail here.

### **7.4.1 Seasonal hydrological forecasting**

Despite the large degree of (unpredictable) internal variability in the vicinity of the British-Irish Isles, this thesis has provided evidence of links between synoptic and large-scale climate drivers and flooding that could be exploited in dynamic flood risk management strategies (Fig. 2.7 in Chapter 2). Most notable was the strong

relationship between the NAO and flood indices identified in Chapter 5. It was found that positive NAO phases are associated with increased flood potential in the winter half year, particularly for the west and northwest of the Island, and have also been linked with increased probability of Atmospheric Rivers (from a southwesterly direction) by Lavers and Villarini (2013b).

The floods of November 2009 and November and December 2015 emphasise the need for increased knowledge of heightened flood risk at lead times of weeks to months so that organisations responsible for managing flood risk (such as the Office of Public Works and local county councils, hydropower companies, and flood managers) can be better prepared. This was highlighted during the 2009 flood when reservoir levels at Inniscarra dam were maintained at an inappropriately high level in advance of heavy precipitation thus requiring a rapid release of water to prevent dam failure which consequently exacerbated the flood inundation downstream in Cork city.

Skilful seasonal flow forecasts are determined by two major contributing factors – initial moisture conditions within the catchment and future climate (for monthly to seasonal forecasts) (Nied et al., 2014). In groundwater dominated catchments flow persistence means that knowledge of the previous month streamflow can be a good predictor of the following month as demonstrated in the southeast of England by Svensson (2014). However, in the west and northwest of Ireland many catchments do not have large groundwater components and so persistence will not be an important contributor. Much of the reason why seasonal precipitation forecasts for the Euro-Atlantic sector have been unsuccessful in the past is the inability to predict the NAO. However, the very recent success of forecasting models in capturing the NAO have the potential to make key aspects of winter climatology predictable months in advance (Scaife et al., 2014). Using the new UK Met Office seasonal forecast system Global Seasonal forecast System 5 (GloSea5), which incorporates the improved NAO predictability, Svensson et al. (2015) have demonstrated significant skill in predicting the frequency of winter high flow events, using a Peaks-Over-Threshold approach, which has the potential to feed into dynamic flood risk management.

Of course, any seasonal forecasting system must take account of the various uncertainties and production of ensemble forecasting will be necessary. However,

recent research in Ireland has already made good progress in this area (Bastola et al., 2011). In addition, more work is needed to uncover more fully tentative links between Atlantic SSTs (AMO) and occurrence of atmospheric blocking. While the anticyclonic LWT was used here as a measure of blocking, more sophisticated metrics have been used (e.g. Greenland Blocking Index (Fang, 2004) in Hanna et al. (2015); the Blocking Index of Tibaldi and Molteni (1990) and the British-Irish Isles Blocking Frequency (BIBF) by Matthews et al. (2015)). The interplay between cyclone frequency and intensity and blocking episodes, and their respective dynamics will be critical for future understanding of how extreme precipitation and floods will change, and has the potential to reduce uncertainty in future projections of climate change (Feser et al., 2015).

Finally, an operational seasonal forecasting system founded on improved understanding of hydroclimatic links has application beyond just flooding. It was shown in Chapter 5 that sustained flood rich periods were preceded by and followed flood poor periods. This highlights that the drivers of wetter than normal and dryer than normal conditions are related. Given that the most pronounced droughts in this part of the world are often initiated by prolonged periods of dry winters (Marsh et al., 2007) the F-Index might provide a good indication of drought potential. Persistent drought periods on the Island of Ireland (Wilby et al., 2015) match the F-Index flood poor periods remarkably well: 1.) 1886-1888; 2.) 1892-1894; 3.) 1905-1907; 4.) 1951-1953; 5.) 1962-1964; 6) 1970-1973; and 7.) 1974-1976. This shows that hydrological extremes of floods and droughts are connected through large-scale organisation of atmospheric circulation and thus allows for future research to exploit such links.

#### **7.4.2 Long-term projections of flood risk**

The current modelling chain for deriving future flood hazard under climate change is typically as follows (Merz et al., 2014): emissions scenarios → General circulation models (GCM) → downscaling (usually with the need for bias correction) → hydrological impact models → flood frequency analysis. The cascade of uncertainty in such an approach is such that even the direction of change of future impacts can be uncertain (Murphy et al., 2011). Instead, an augmented model chain (Merz et al., 2014) can be used to supplement traditional approaches. For example, precipitation is

inherently difficult to simulate correctly in global and regional climate models due to their relatively coarse resolution (typically 60-300 km and 10-50 km respectively) (Kendon et al., 2014). However, other variables such as MSLP or atmospheric moisture, that have been directly linked with floods (e.g., flood-producing LWTs in Chapter 5) can be simulated more reliably in GCMs and therefore could be used to assess future changes in the flood-producing atmospheric conditions directly (Lavers et al., 2013; Delgado et al., 2014). For example, Åström et al. (2015) apply a modified LWT scheme for examining relationships between flood-producing atmospheric circulation and flood events for a city in Denmark. They assessed the change in future flood-producing atmospheric circulation frequency using regional climate models and found an increase in the frequency of westerlies. However, they state that there are deficiencies in representation of atmospheric circulation within climate models which adds uncertainty. Hence, future work could assess how well current generation climate models (i.e. regional climate models, and global climate models in CMIP5; Taylor et al., 2012) reproduce observed flood-producing LWTs as a means of model scrutiny and development.

## 7.5 Final Remarks

This thesis has contributed significantly to the advancement of flood hydroclimatology for the Island of Ireland. The derivation and refinement of observed precipitation and streamflow datasets is fundamental to all hydroclimatic research, whether it be detection of climate-driven changes, attribution of drivers of change, or for evaluation of future hydrological and climate modelling efforts. Description of change is in itself important; it was found here that the current flood rich period is not unprecedented when placed in context of longer term variability. Even more important is exploration of the processes regulating these flood rich and poor periods. It was shown that flood propensity on the Island of Ireland is modulated by large-scale atmospheric circulation, which in itself is only a single component in a dynamically coupled ocean-atmosphere-cryosphere system. While atmospheric water vapour will increase in a warming world due to thermodynamics, whether this will result in increased flood risk is dependent on changes in extreme precipitation delivery mechanisms, particularly extratropical cyclones, which themselves are modulated by large-scale natural climate variability on decadal to multi-decadal time-scales. Only with increased knowledge of the response

of these delivery mechanisms to both variability and change, combined with better understanding of catchment response, can robust and skilful medium- (seasonal) and long-term (climate change) projections be produced. This thesis has made the first steps in this regard for Ireland and will thus contribute to the realisation of operational products to provide more sophisticated management of flood risk with significant benefit to society. At the catchment scale, where management of hydroclimatology ultimately takes place, this work also puts forth an integrated methodology for better deciphering drivers of change. Implementation of the method of multiple working hypotheses increases strength of attribution and will lead to better, evidence based, decision making in adapting to hydroclimatic variability and change. Finally, the data and code (R programming language) developed during this thesis is available upon request ([shaun.harrigan@nuim.ie](mailto:shaun.harrigan@nuim.ie)).

## References

- Agel, L., Barlow, M., Qian, J.-H., Colby, F., Douglas, E. and Eichler, T.: Climatology of Daily Precipitation and Extreme Precipitation Events in the Northeast United States, *J. Hydrometeorol.*, 16(6), 2537–2557, doi:10.1175/JHM-D-14-0147.1, 2015.
- Alexander, L. V. and Jones, P. D.: Updated Precipitation Series for the U.K. and Discussion of Recent Extremes, *Atmospheric Science Letters*, 1(2), 142–150, doi:10.1006/asle.2001.0025, 2001.
- Alexander, L. V., Zhang, X., Peterson, T. C., Caesar, J., Gleason, B., Klein Tank, A. M. G., Haylock, M., Collins, D., Trewin, B., Rahimzadeh, F., Tagipour, A., Rupa Kumar, K., Revadekar, J., Griffiths, G., Vincent, L., Stephenson, D. B., Burn, J., Aguilar, E., Brunet, M., Taylor, M., New, M., Zhai, P., Rusticucci, M. and Vazquez-Aguirre, J. L.: Global observed changes in daily climate extremes of temperature and precipitation, *J. Geophys. Res.*, 111(D5), D05109, doi:10.1029/2005JD006290, 2006.
- Allan, R. P. and Liepert, B. G.: Anticipated changes in the global atmospheric water cycle, *Environ. Res. Lett.*, 5(2), 025201, doi:10.1088/1748-9326/5/2/025201, 2010.
- Allan, R. P., Lavers, D. A. and Champion, A. J.: Diagnosing links between atmospheric moisture and extreme daily precipitation over the UK, *Int. J. Climatol.*, Early View, doi:10.1002/joc.4547, 2015.
- Andréassian, V., Parent, E. and Michel, C.: A distribution-free test to detect gradual changes in watershed behavior, *Water Resources Research*, 39(9), doi:10.1029/2003WR002081, 2003.
- Åström, H. I. a., Sunyer, M., Madsen, H., Rosbjerg, D. and Arnbjerg-Nielsen, K.: Explanatory analysis of the relationship between atmospheric circulation and occurrence of flood generating events in a coastal city, *Hydrol. Process.*, Early View, doi:10.1002/hyp.10767, 2015.
- Bailey, A. D. and Bree, T.: Effect of improved land drainage on river flow, In: *Flood Studies Report - five Years on, Manchester*, 131-142, 1981.
- Baker, D. B., Richards, R. P., Loftus, T. T. and Kramer, J. W.: A New Flashiness Index: Characteristics and Applications to Midwestern Rivers and Streams, *JAWRA Journal of the American Water Resources Association*, 40(2), 503–522, doi:10.1111/j.1752-1688.2004.tb01046.x, 2004.
- Bárdossy, A. and Filiz, F.: Identification of flood producing atmospheric circulation patterns, *Journal of Hydrology*, 313(1–2), 48–57, doi:10.1016/j.jhydrol.2005.02.006, 2005.
- Barker, P. A., Wilby, R. L., and Borrows, J.: A 200-year precipitation index for the central English Lake District, *Hydrolog. Sci. J.*, 49, 769-785, 2004.

- Bastola, S. and Murphy, C.: Sensitivity of the performance of a conceptual rainfall-runoff model to the temporal sampling of calibration data, *Hydrology Res.*, 44, 484-494, 2013.
- Bastola, S., Murphy, C. and Sweeney, J.: The role of hydrological modelling uncertainties in climate change impact assessments of Irish river catchments, *Advances in Water Resources*, 34(5), 562–576, doi:10.1016/j.advwatres.2011.01.008, 2011.
- Bastola, S., Murphy, C., and Fealy, R.: Generating probabilistic estimates of hydrological response for Irish catchments using a weather generator and probabilistic climate change scenarios, *Hydrol. Process.*, 26, 2307-2321, doi:10.1002/hyp.8349, 2012.
- Bayliss, A. C. and Jones, R. C.: Peaks-over-threshold flood database: summary statistics and seasonality. Report 121, Institute of Hydrology, Wallingford, UK, 1993.
- Beven, K. and Binley, A.: The future of distributed models: Model calibration and uncertainty prediction, *Hydrol. Process.*, 6, 279-298, doi:10.1002/hyp.3360060305, 1992.
- Bhattacharai, K. and O'Connor, K.: The effects over time of an arterial drainage scheme on the rainfall-runoff transformation in the Brosna catchment, *Physics and Chemistry of the Earth, Parts A/B/C*, 29(11–12), 787–794, doi:10.1016/j.pce.2004.05.006, 2004.
- Black, A. R. and Werritty, A.: Seasonality of flooding: a case study of North Britain, *Journal of Hydrology*, 195(1–4), 1–25, doi:10.1016/S0022-1694(96)03264-7, 1997.
- Blöschl, G., Ardoin-Bardin, S., Bonell, M., Dorninger, M., Goodrich, D., Gutknecht, D., Matamoros, D., Merz, B., Shand, P. and Szolgay, J.: At what scales do climate variability and land cover change impact on flooding and low flows?, *Hydrological Processes*, 21(9), 1241–1247, doi:10.1002/hyp.6669, 2007.
- Boyle, D. P.: Multicriteria calibration of hydrological models, Ph.D. Thesis, University of Arizona, USA, 2001.
- Bradford, R. B. and Marsh, T. J.: Defining a network of benchmark catchments for the UK, *Proceedings of the Institution of Civil Engineers - Water and Maritime Engineering*, 156, 109–116, doi:10.1680/wame.2003.156.2.109, 2003.
- Bree, T. and Cunnane, C.: Evaluating the effects of arterial drainage on river flood discharges, Annex 1, Office of the Public Works, Ireland, 1979.
- Brown, A. E., Zhang, L., McMahon, T. A., Western, A. W., and Vertessy, R. A.: A review of paired catchment studies for determining changes in water yield resulting from alterations in vegetation, *J. Hydrol.*, 310, 28-61, 2005.
- Brunsdon, C. and Comber, L.: An introduction to R for spatial analysis and mapping, Sage, London, 2015.

- Burdon, D. J.: Hydrogeological Aspects Drainage in Ireland of Agricultural Drainage in Ireland, *Environ. Geol. Water S.*, 9, 41-65, 1986.
- Burn, D. H. and Hag Elnur, M. A.: Detection of hydrologic trends and variability, *Journal of Hydrology*, 255(1-4), 107-122, doi:10.1016/S0022-1694(01)00514-5, 2002.
- Burn, D. H., Sharif, M. and Zhang, K.: Detection of trends in hydrological extremes for Canadian watersheds, *Hydrological Processes*, 24(13), 1781-1790, doi:10.1002/hyp.7625, 2010.
- Burt, T. P. and Howden, N. J. K.: North Atlantic Oscillation amplifies orographic precipitation and river flow in upland Britain, *Water Resources Research*, 49(6), 3504-3515, doi:10.1002/wrcr.20297, 2013.
- Burt, T. P., Jones, P. D. and Howden, N. J. K.: An analysis of rainfall across the British Isles in the 1870s, *Int. J. Climatol.*, 35(10), 2934-2947, doi:10.1002/joc.4184, 2015.
- Busuioc, A. and Storch, H. V.: Changes in the winter precipitation in Romania and its relation to the large-scale circulation, *Tellus A*, 48(4), 538-552, doi:10.1034/j.1600-0870.1996.t01-3-00004.x, 1996.
- Butts, M. B., Payne, J. T., Kristensen, M., and Madsen, H.: An evaluation of the impact of model structure on hydrological modelling uncertainty for streamflow simulation, *J. Hydrol.*, 298, 242-266, 2004.
- Cane, M. A.: EL Nino, *Annual Review of Earth and Planetary Sciences*, 14(1), 43-70, doi:10.1146/annurev.ea.14.050186.000355, 1986.
- Casanueva, A., Rodríguez-Puebla, C., Frías, M. D. and González-Reviriego, N.: Variability of extreme precipitation over Europe and its relationships with teleconnection patterns, *Hydrol. Earth Syst. Sci.*, 18(2), 709-725, doi:10.5194/hess-18-709-2014, 2014.
- CEH: Centre for Ecology & Hydrology North West floods – Hydrological update, Available: <http://www.ceh.ac.uk/news-and-media/blogs/north-west-floods-hydrological-update> (last accessed: 8<sup>th</sup> December 2015), 2015.
- Chamberlin, T. C.: The Method of Multiple Working Hypotheses, *Science (old series)*, 15(366), 92-96, doi:10.1126/science.ns-15.366.92, 1890.
- Chou, C., Neelin, J. D., Chen, C.-A. and Tu, J.-Y.: Evaluating the “Rich-Get-Richer” Mechanism in Tropical Precipitation Change under Global Warming, *J. Climate*, 22(8), 1982-2005, doi:10.1175/2008JCLI2471.1, 2009.
- Christensen, J.H., K. Krishna Kumar, E. Aldrian, S.-I. An, I.F.A. Cavalcanti, M. de Castro, W. Dong, P. Goswami, A. Hall, J.K. Kanyanga, A. Kitoh, J. Kossin, N.-C. Lau, J. Renwick, D.B. Stephenson, S.-P. Xie and T. Zhou: Climate Phenomena and their Relevance for Future Regional Climate Change. In: *Climate Change 2013: The Physical Science Basis. Contribution of Working Group I to the Fifth Assessment Report of the Intergovernmental Panel on Climate Change* [Stocker, T.F., D. Qin, G.-K. Plattner, M. Tignor, S.K. Allen, J. Boschung, A. Nauels, Y. Xia, V. Bex and P.M. Midgley (eds.)].

Cambridge University Press, Cambridge, United Kingdom and New York, NY, USA, 2013.

Clark, M. P., Slater, A. G., Rupp, D. E., Woods, R. A., Vrugt, J. A., Gupta, H. V., Wagener, T. and Hay, L. E.: Framework for Understanding Structural Errors (FUSE): A modular framework to diagnose differences between hydrological models, *Water Resources Research*, 44(12), doi:10.1029/2007WR006735, 2008.

Clark, M. P., Kavetski, D., and Fenicia, F.: Pursuing the method of multiple working hypotheses for hydrological modeling, *Water Resour. Res.*, 47, W09301, doi:10.1029/2010WR009827, 2011.

Clarke, R. T.: On the (mis)use of statistical methods in hydro-climatological research, *Hydrological Sciences Journal*, 55(2), 139–144, doi:10.1080/02626661003616819, 2010.

Cohn, T. A. and Lins, H. F.: Nature's style: Naturally trendy, *Geophysical Research Letters*, 32(23), L23402, doi:10.1029/2005GL024476, 2005.

Coles, S.: An introduction to statistical modelling of extreme values, Springer-Verlag London, 2001.

Collins, M., R. Knutti, J. Arblaster, J.-L. Dufresne, T. Fichet, P. Friedlingstein, X. Gao, W.J. Gutowski, T. Johns, G. Krinner, M. Shongwe, C. Tebaldi, A.J. Weaver and M. Wehner: Long-term Climate Change: Projections, Commitments and Irreversibility. In: *Climate Change 2013: The Physical Science Basis. Contribution of Working Group I to the Fifth Assessment Report of the Intergovernmental Panel on Climate Change* [Stocker, T.F., D. Qin, G.-K. Plattner, M. Tignor, S.K. Allen, J. Boschung, A. Nauels, Y. Xia, V. Bex and P.M. Midgley (eds.)]. Cambridge University Press, Cambridge, United Kingdom and New York, NY, USA, 2013.

Compo, G. P., Whitaker, J. S., Sardeshmukh, P. D., Matsui, N., Allan, R. J., Yin, X., Gleason, B. E., Vose, R. S., Rutledge, G., Bessemoulin, P., Brönnimann, S., Brunet, M., Crouthamel, R. I., Grant, A. N., Groisman, P. Y., Jones, P. D., Kruk, M. C., Kruger, A. C., Marshall, G. J., Maugeri, M., Mok, H. Y., Nordli, Ø., Ross, T. F., Trigo, R. M., Wang, X. L., Woodruff, S. D. and Worley, S. J.: The Twentieth Century Reanalysis Project, *Q.J.R. Meteorol. Soc.*, 137(654), 1–28, doi:10.1002/qj.776, 2011.

Cunderlik, J. M., Ouarda, T. B. M. J. and Bobée, B.: Determination of flood seasonality from hydrological records, *Hydrological Sciences Journal*, 49(3), 511–526, doi:10.1623/hysj.49.3.511.54351, 2004.

Dacre, H. F., Clark, P. A., Martinez-Alvarado, O., Stringer, M. A. and Lavers, D. A.: How Do Atmospheric Rivers Form?, *Bull. Amer. Meteor. Soc.*, 96(8), 1243–1255, doi:10.1175/BAMS-D-14-00031.1, 2015.

Dales, M. Y. and Reed, D. W.: Regional flood and storm hazard assessment, Institute of Hydrology, Wallingford, Oxfordshire., 1989.

Dawson, C. W. and Wilby, R. L.: Hydrological modelling using artificial neural networks, *Prog. Phys. Geog.*, 25, 80-108, 2001.

Dee, D. P., Uppala, S. M., Simmons, A. J., Berrisford, P., Poli, P., Kobayashi, S., Andrae, U., Balmaseda, M. A., Balsamo, G., Bauer, P., Bechtold, P., Beljaars, A. C. M., van de Berg, L., Bidlot, J., Bormann, N., Delsol, C., Dragani, R., Fuentes, M., Geer, A. J., Haimberger, L., Healy, S. B., Hersbach, H., Hólm, E. V., Isaksen, L., Kållberg, P., Köhler, M., Matricardi, M., McNally, A. P., Monge-Sanz, B. M., Morcrette, J.-J., Park, B.-K., Peubey, C., de Rosnay, P., Tavolato, C., Thépaut, J.-N. and Vitart, F.: The ERA-Interim reanalysis: configuration and performance of the data assimilation system, *Q.J.R. Meteorol. Soc.*, 137(656), 553–597, doi:10.1002/qj.828, 2011.

Delgado, J. M., Merz, B. and Apel, H.: Projecting flood hazard under climate change: an alternative approach to model chains, *Nat. Hazards Earth Syst. Sci.*, 14(6), 1579–1589, doi:10.5194/nhess-14-1579-2014, 2014.

Deser, C., Knutti, R., Solomon, S. and Phillips, A. S.: Communication of the role of natural variability in future North American climate, *Nature Clim. Change*, 2(11), 775–779, doi:10.1038/nclimate1562, 2012.

Di Baldassarre, G., Kooy, M., Kemerink, J. S. and Brandimarte, L.: Towards understanding the dynamic behaviour of floodplains as human-water systems, *Hydrol. Earth Syst. Sci.*, 17(8), 3235–3244, doi:10.5194/hess-17-3235-2013, 2013.

Donat, M. G., Alexander, L. V., Yang, H., Durre, I., Vose, R., Dunn, R. J. H., Willett, K. M., Aguilar, E., Brunet, M., Caesar, J., Hewitson, B., Jack, C., Klein Tank, A. M. G., Kruger, A. C., Marengo, J., Peterson, T. C., Renom, M., Oria Rojas, C., Rusticucci, M., Salinger, J., Elrayah, A. S., Sekele, S. S., Srivastava, A. K., Trewin, B., Villarroya, C., Vincent, L. A., Zhai, P., Zhang, X. and Kitching, S.: Updated analyses of temperature and precipitation extreme indices since the beginning of the twentieth century: The HadEX2 dataset, *J. Geophys. Res. Atmos.*, 118(5), 2098–2118, doi:10.1002/jgrd.50150, 2013.

Douglas, E. M., Vogel, R. M. and Kroll, C. N.: Trends in floods and low flows in the United States: impact of spatial correlation, *Journal of Hydrology*, 240(1–2), 90–105, doi:10.1016/S0022-1694(00)00336-X, 2000.

Duan, Q., Schaake, J., Andréassian, V., Franks, S., Goteti, G., Gupta, H. V., Gusev, Y. M., Habets, F., Hall, A., Hay, L., Hogue, T., Huang, M., Leavesley, G., Liang, X., Nasonova, O. N., Noilhan, J., Oudin, L., Sorooshian, S., Wagener, T., and Wood, E. F.: Model Parameter Estimation Experiment (MOPEX): An overview of science strategy and major results from the second and third workshops, *J. Hydrol.*, 320, 3–17, doi:10.1016/j.jhydrol.2005.07.031, 2006.

Duckstein, L., Bárdossy, A. and Bogárdi, I.: Linkage between the occurrence of daily atmospheric circulation patterns and floods: an Arizona case study, *Journal of Hydrology*, 143(3–4), 413–428, doi:10.1016/0022-1694(93)90202-K, 1993.

Durack, P. J., Wijffels, S. E. and Matear, R. J.: Ocean Salinities Reveal Strong Global Water Cycle Intensification During 1950 to 2000, *Science*, 336(6080), 455–458, doi:10.1126/science.1212222, 2012.

Elliott, L. P. and Brook, B. W.: Revisiting Chamberlin: Multiple Working Hypotheses for the 21st Century, *BioScience*, 57(7), 608–614, doi:10.1641/B570708, 2007.

Enfield, D. B., Mestas-Nuñez, A. M. and Trimble, P. J.: The Atlantic Multidecadal Oscillation and its relation to rainfall and river flows in the continental U.S., *Geophys. Res. Lett.*, 28(10), 2077–2080, doi:10.1029/2000GL012745, 2001.

EPA: The Provision and Quality of Drinking Water in Ireland – A Report for the Years 2007–2008, Environmental Protection Agency (EPA), Johnstown Castle, Wexford, Ireland, 2009.

EPA: Integrated Pollution Prevention and Control (IPCC) Licence no. P0516-03 for Boliden Tara Mines Limited, Environmental Protection Agency (EPA), Johnstown Castle, Wexford, Ireland, 2012.

Evin, G., Kavetski, D., Thyer, M., and Kuczera, G.: Pitfalls and improvements in the joint inference of heteroscedasticity and autocorrelation in hydrological model calibration, *Water Resour. Res.*, 49, 4518-4524, doi:10.1002/wrcr.20284, 2013.

Fang Z. F.: Statistical relationship between the northern hemisphere sea ice and atmospheric circulation during wintertime. In *Observation, Theory and Modeling of Atmospheric Variability*. World Scientific Series on Meteorology of East Asia, Zhu X (ed). World Scientific Publishing Company: Singapore, 131–141, 2004.

Fenicia, F., Savenije, H. H. G. and Avdeeva, Y.: Anomaly in the rainfall-runoff behaviour of the Meuse catchment. Climate, land-use, or land-use management?, *Hydrol. Earth Syst. Sci.*, 13(9), 1727–1737, doi:10.5194/hess-13-1727-2009, 2009.

Feser, F., Barcikowska, M., Krueger, O., Schenk, F., Weisse, R. and Xia, L.: Storminess over the North Atlantic and northwestern Europe—A review, *Q.J.R. Meteorol. Soc.*, 141(687), 350–382, doi:10.1002/qj.2364, 2015.

Fischer, E. M., Beyerle, U. and Knutti, R.: Robust spatially aggregated projections of climate extremes, *Nature Clim. Change*, 3(12), 1033–1038, doi:10.1038/nclimate2051, 2013.

Fitzgerald D. L.: Estimation of Point Rainfall Frequencies. Met Éireann Technical Note 61, MetÉireann, Glasnevin Hill, Dublin 9, Ireland, 2007.

Fowler, H. J. and Kilsby, C. G.: Implications of changes in seasonal and annual extreme rainfall, *Geophys. Res. Lett.*, 30(13), 1720, doi:10.1029/2003GL017327, 2003.

Fowler, H. J. and Wilby, R. L.: Detecting changes in seasonal precipitation extremes using regional climate model projections: Implications for managing fluvial flood risk, *Water Resour. Res.*, 46(3), W03525, doi:10.1029/2008WR007636, 2010.

Fraedrich, K.: European grosswetter during the warm and cold extremes of the El Niño/Southern Oscillation, *Int. J. Climatol.*, 10(1), 21–31, doi:10.1002/joc.3370100104, 1990.

Frans, C., Istanbuluoglu, E., Mishra, V., Munoz-Arriola, F. and Lettenmaier, D. P.: Are climatic or land cover changes the dominant cause of runoff trends in the Upper Mississippi River Basin?, *Geophysical Research Letters*, 40(6), 1104–1110, doi:10.1002/grl.50262, 2013.

- Frei, C. and Schär, C.: Detection Probability of Trends in Rare Events: Theory and Application to Heavy Precipitation in the Alpine Region, *J. Climate*, 14(7), 1568–1584, doi:10.1175/1520-0442(2001)014<1568:DPOTIR>2.0.CO;2, 2001.
- Gao, P., Mu, X.-M., Wang, F. and Li, R.: Changes in streamflow and sediment discharge and the response to human activities in the middle reaches of the Yellow River, *Hydrol. Earth Syst. Sci.*, 15(1), 1–10, doi:10.5194/hess-15-1-2011, 2011.
- Garner, G., Van Loon, A. F., Prudhomme, C. and Hannah, D. M.: Hydroclimatology of extreme river flows, *Freshw Biol*, Early View, doi:10.1111/fwb.12667, 2015.
- Gebrehiwot, S. G., Seibert, J., Gärdenäs, A. I., Mellander, P.-E. and Bishop, K.: Hydrological change detection using modeling: Half a century of runoff from four rivers in the Blue Nile Basin, *Water Resources Research*, 49(6), 3842–3851, doi:10.1002/wrcr.20319, 2013.
- Gilleland, E. and Katz, R. W.: New Software to Analyze How Extremes Change Over Time, *Eos Trans. AGU*, 92(2), 13–14, doi:10.1029/2011EO020001, 2011.
- Gimeno, L., Nieto, R., Vázquez, M. and Lavers, D. A.: Atmospheric rivers: a mini-review, *Front. Earth Sci*, 2, 2, doi:10.3389/feart.2014.00002, 2014.
- Gregory, J. M., Jones, P. D. and Wigley, T. M. L.: Precipitation in Britain: An analysis of area-average data updated to 1989, *Int. J. Climatol.*, 11(3), 331–345, doi:10.1002/joc.3370110308, 1991.
- Greve, P. and Seneviratne, S. I.: Assessment of future changes in water availability and aridity, *Geophys. Res. Lett.*, 2015GL064127, doi:10.1002/2015GL064127, 2015.
- Greve, P., Orłowsky, B., Mueller, B., Sheffield, J., Reichstein, M. and Seneviratne, S. I.: Global assessment of trends in wetting and drying over land, *Nature Geosci*, 7(10), 716–721, doi:10.1038/ngeo2247, 2014.
- Groisman, P. Y., Karl, T. R., Easterling, D. R., Knight, R. W., Jamason, P. F., Hennessey, K. J., Suppiah, R., Page, C. M., Wibig, J., Fortuniak, K., Razuvaev, V. N., Douglas, A., Førland, E. and Zhai, P.-M.: Changes in the Probability of Heavy Precipitation: Important Indicators of Climatic Change, *Climatic Change*, 42(1), 243–283, doi:10.1023/A:1005432803188, 1999.
- Guerreiro, S. B., Kilsby, C. G. and Serinaldi, F.: Analysis of time variation of rainfall in transnational basins in Iberia: abrupt changes or trends?, *International Journal of Climatology*, 34(1), 114–133, doi:10.1002/joc.3669, 2014.
- Gupta, H. V., Sorooshian, S., and Yapo, P. O.: Status of automatic calibration for hydrologic models: Comparison with multilevel expert calibration, *J. Hydrol. Eng.*, 4, 135-143, 1999.
- Häkkinen, S., Rhines, P. B. and Worthen, D. L.: Atmospheric Blocking and Atlantic Multidecadal Ocean Variability, *Science*, 334(6056), 655–659, doi:10.1126/science.1205683, 2011.

Hall, J. and Murphy, C.: Robust adaptation assessment - climate change and water supply, *International Journal of Climate Change Strategies and Management*, 3, 302–319, 2011.

Hall, J., Arheimer, B., Borga, M., Brázdil, R., Claps, P., Kiss, A., Kjeldsen, T. R., Kriauciūnienė, J., Kundzewicz, Z. W., Lang, M., Llasat, M. C., Macdonald, N., McIntyre, N., Mediero, L., Merz, B., Merz, R., Molnar, P., Montanari, A., Neuhold, C., Parajka, J., Perdigão, R. A. P., Plavcová, L., Rogger, M., Salinas, J. L., Sauquet, E., Schär, C., Szolgay, J., Viglione, A. and Blöschl, G.: Understanding flood regime changes in Europe: a state-of-the-art assessment, *Hydrol. Earth Syst. Sci.*, 18(7), 2735–2772, doi:10.5194/hess-18-2735-2014, 2014.

Hanna, E., Cropper, T. E., Jones, P. D., Scaife, A. A. and Allan, R.: Recent seasonal asymmetric changes in the NAO (a marked summer decline and increased winter variability) and associated changes in the AO and Greenland Blocking Index, *Int. J. Climatol*, 35(9), 2540–2554, doi:10.1002/joc.4157, 2015.

Hannaford, J. and Buys, G.: Trends in seasonal river flow regimes in the UK, *Journal of Hydrology*, 475, 158–174, doi:10.1016/j.jhydrol.2012.09.044, 2012.

Hannaford, J. and Marsh, T. J.: An assessment of trends in UK runoff and low flows using a network of undisturbed catchments, *International Journal of Climatology*, 26(9), 1237–1253, doi:10.1002/joc.1303, 2006.

Hannaford, J. and Marsh, T. J.: High-flow and flood trends in a network of undisturbed catchments in the UK, *International Journal of Climatology*, 28(10), 1325–1338, doi:10.1002/joc.1643, 2008.

Hannaford, J., Buys, G., Stahl, K. and Tallaksen, L. M.: The influence of decadal-scale variability on trends in long European streamflow records, *Hydrol. Earth Syst. Sci.*, 17(7), 2717–2733, doi:10.5194/hess-17-2717-2013, 2013.

Harrigan, S., Murphy, C., Hall, J., Wilby, R. L. and Sweeney, J.: Attribution of detected changes in streamflow using multiple working hypotheses, *Hydrol. Earth Syst. Sci.*, 18(5), 1935–1952, doi:10.5194/hess-18-1935-2014, 2014.

Hartmann, D.L., A.M.G. Klein Tank, M. Rusticucci, L.V. Alexander, S. Brönnimann, Y. Charabi, F.J. Dentener, E.J. Dlugokencky, D.R. Easterling, A. Kaplan, B.J. Soden, P.W. Thorne, M. Wild and P.M. Zhai, 2013: Observations: Atmosphere and Surface. In: *Climate Change 2013: The Physical Science Basis. Contribution of Working Group I to the Fifth Assessment Report of the Intergovernmental Panel on Climate Change* [Stocker, T.F., D. Qin, G.-K. Plattner, M. Tignor, S.K. Allen, J. Boschung, A. Nauels, Y. Xia, V. Bex and P.M. Midgley (eds.)]. Cambridge University Press, Cambridge, United Kingdom and New York, NY, USA.

Hawcroft, M. K., Shaffrey, L. C., Hodges, K. I. and Dacre, H. F.: How much Northern Hemisphere precipitation is associated with extratropical cyclones?, *Geophys. Res. Lett.*, 39(24), L24809, doi:10.1029/2012GL053866, 2012.

Hawkins, E. and Sutton, R.: The potential to narrow uncertainty in projections of regional precipitation change, *Clim Dyn*, 37(1-2), 407–418, doi:10.1007/s00382-010-0810-6, 2011.

Haylock, M. R., Hofstra, N., Klein Tank, A. M. G., Klok, E. J., Jones, P. D. and New, M.: A European daily high-resolution gridded data set of surface temperature and precipitation for 1950–2006, *J. Geophys. Res.*, 113(D20), D20119, doi:10.1029/2008JD010201, 2008.

Hegerl, G. C., Zwiers, F. W., Stott, P. A. and Kharin, V. V.: Detectability of Anthropogenic Changes in Annual Temperature and Precipitation Extremes, *J. Climate*, 17(19), 3683–3700, doi:10.1175/1520-0442(2004)017<3683:DOACIA>2.0.CO;2, 2004.

Hegerl, G. C., Black, E., Allan, R. P., Ingram, W. J., Polson, D., Trenberth, K. E., Chadwick, R. S., Arkin, P. A., Sarojini, B. B., Becker, A., Dai, A., Durack, P. J., Easterling, D., Fowler, H. J., Kendon, E. J., Huffman, G. J., Liu, C., Marsh, R., New, M., Osborn, T. J., Skliris, N., Stott, P. A., Vidale, P.-L., Wijffels, S. E., Wilcox, L. J., Willett, K. M. and Zhang, X.: Challenges in Quantifying Changes in the Global Water Cycle, *Bull. Amer. Meteor. Soc.*, 96(7), 1097–1115, doi:10.1175/BAMS-D-13-00212.1, 2015.

Held, I. M. and Soden, B. J.: Robust Responses of the Hydrological Cycle to Global Warming, *J. Climate*, 19(21), 5686–5699, doi:10.1175/JCLI3990.1, 2006.

Helsel, D. R. and Hirsch, R. M.: Statistical methods in water resources, *Techniques of water-resources investigations*, Book 4, chapter A3, [http://pubs.usgs.gov/twri/twri4a3/html/pdf\\_new.html](http://pubs.usgs.gov/twri/twri4a3/html/pdf_new.html), last access: 23 September 2013, US Geological Survey, 522pp., 2002.

Hess, P., and Brezowsky, H.: *Katalog der Großwetterlagen Europa*, Ber. Dt. Wetterd. in der US-Zone 33, 1952.

Hewlett, J. D., *Principles of Forest Hydrology*, University of Georgia Press, Athens, 1982.

Hirabayashi, Y., Mahendran, R., Koirala, S., Konoshima, L., Yamazaki, D., Watanabe, S., Kim, H. and Kanae, S.: Global flood risk under climate change, *Nature Clim. Change*, 3(9), 816–821, doi:10.1038/nclimate1911, 2013.

Hirschboeck, K. K.: Flood hydroclimatology, in: *Flood geomorphology*, edited by: Baker, V. R., Kochel, R. C., and Pattern, P. C., Wiley, New York, 27–49, 1988.

Holko, L., Parajka, J., Kostka, Z., Škoda, P. and Blöschl, G.: Flashiness of mountain streams in Slovakia and Austria, *Journal of Hydrology*, 405(3–4), 392–401, doi:10.1016/j.jhydrol.2011.05.038, 2011.

HOME (2013) Homepage of the COST Action ES0601 – Advances in Homogenisation Methods of Climate Series: An Integrated Approach (HOME). <http://www.homogenisation.org> (last accessed 24 October 2015).

Hundechea, Y. and Merz, B.: Exploring the relationship between changes in climate and floods using a model-based analysis, *Water Resources Research*, 48(4), W04512, doi:10.1029/2011WR010527, 2012.

Huntington, T. G.: Evidence for intensification of the global water cycle: Review and synthesis, *Journal of Hydrology*, 319(1–4), 83–95, doi:10.1016/j.jhydrol.2005.07.003, 2006.

Hurrell, J. W.: Decadal Trends in the North Atlantic Oscillation: Regional Temperatures and Precipitation, *Science*, 269(5224), 676–679, doi:10.1126/science.269.5224.676, 1995.

Hurrell, J. W. and Van Loon, H.: Decadal variations in climate associated with the North Atlantic Oscillation, *Climatic Change*, 36(3-4), 301–326, doi:10.1023/A:1005314315270, 1997.

Huth, R.: Arctic or North Atlantic Oscillation? Arguments based on the principal component analysis methodology, *Theor. Appl. Climatol.*, 89(1-2), 1–8, doi:10.1007/s00704-006-0257-1, 2007.

Huth, R., Beck, C., Philipp, A., Demuzere, M., Ustrnul, Z., Cahynová, M., Kyselý, J. and Tveito, O. E.: Classifications of Atmospheric Circulation Patterns, *Annals of the New York Academy of Sciences*, 1146(1), 105–152, doi:10.1196/annals.1446.019, 2008.

Institute of Hydrology: Flood Studies Report (five volumes), Centre for Ecology & Hydrology, Wallingford, UK, 1975.

Institute of Hydrology: Flood Estimation Handbook (five volumes), Centre for Ecology & Hydrology, Wallingford, UK, 1999.

IPCC: Summary for Policymakers. In: *Managing the Risks of Extreme Events and Disasters to Advance Climate Change Adaptation* [Field, C.B., V. Barros, T.F. Stocker, D. Qin, D.J. Dokken, K.L. Ebi, M.D. Mastrandrea, K.J. Mach, G.-K. Plattner, S.K. Allen, M. Tignor, and P.M. Midgley (eds.)]. A Special Report of Working Groups I and II of the Intergovernmental Panel on Climate Change. Cambridge University Press, Cambridge, UK, and New York, NY, USA, pp. 3-21, 2012.

IPCC: Summary for Policymakers. In: *Climate Change 2013: The Physical Science Basis. Contribution of Working Group I to the Fifth Assessment Report of the Intergovernmental Panel on Climate Change* [Stocker, T.F., D. Qin, G.-K. Plattner, M. Tignor, S.K. Allen, J. Boschung, A. Nauels, Y. Xia, V. Bex and P.M. Midgley (eds.)]. Cambridge University Press, Cambridge, United Kingdom and New York, NY, USA, 2013

Jenkinson, A.F. and Collison, F.P.: An initial climatology of gales over the North Sea. Synoptic Climatology Branch Memorandum No. 62, Meteorological Office, Bracknell, 1977.

Jia, Y., Ding, X., Wang, H., Zhou, Z., Qiu, Y., and Niu, C.: Attribution of water resources evolution in the highly water-stressed Hai River Basin of China, *Water Resour. Res.*, 48, W02513, doi:10.1029/2010WR009275, 2012.

Jolliffe, I. T.: Principal component analysis: A beginner's guide — I. Introduction and application, *Weather*, 45(10), 375–382, doi:10.1002/j.1477-8696.1990.tb05558.x, 1990.

Jolliffe, I. T.: Principal component analysis: A beginner's guide — II. Pitfalls, myths and extensions, *Weather*, 48(8), 246–253, doi:10.1002/j.1477-8696.1993.tb05899.x, 1993.

Jones, M. R., Fowler, H. J., Kilsby, C. G. and Blenkinsop, S.: An assessment of changes in seasonal and annual extreme rainfall in the UK between 1961 and 2009, *Int. J. Climatol.*, 33(5), 1178–1194, doi:10.1002/joc.3503, 2013a.

Jones, M. R., Blenkinsop, S., Fowler, H. J. and Kilsby, C. G.: Objective classification of extreme rainfall regions for the UK and updated estimates of trends in regional extreme rainfall, *Int. J. Climatol.*, 34(3), 751–765, doi:10.1002/joc.3720, 2014a.

Jones, P. D., Hulme, M. and Briffa, K. R.: A comparison of Lamb circulation types with an objective classification scheme, *Int. J. Climatol.*, 13(6), 655–663, doi:10.1002/joc.3370130606, 1993.

Jones, P. D., Jonsson, T. and Wheeler, D.: Extension to the North Atlantic oscillation using early instrumental pressure observations from Gibraltar and south-west Iceland, *Int. J. Climatol.*, 17(13), 1433–1450, doi:10.1002/(SICI)1097-0088(19971115)17:13<1433::AID-JOC203>3.0.CO;2-P, 1997.

Jones, P. D., Lister, D. H., Osborn, T. J., Harpham, C., Salmon, M. and Morice, C. P.: Hemispheric and large-scale land-surface air temperature variations: An extensive revision and an update to 2010, *J. Geophys. Res.*, 117(D5), D05127, doi:10.1029/2011JD017139, 2012.

Jones, P. D., Harpham, C. and Briffa, K. R.: Lamb weather types derived from reanalysis products, *Int. J. Climatol.*, 33(5), 1129–1139, doi:10.1002/joc.3498, 2013b.

Jones, P. D., Osborn, T. J., Harpham, C. and Briffa, K. R.: The development of Lamb weather types: from subjective analysis of weather charts to objective approaches using reanalyses, *Weather*, 69(5), 128–132, doi:10.1002/wea.2255, 2014b.

Kalnay, E., Kanamitsu, M., Kistler, R., Collins, W., Deaven, D., Gandin, L., Iredell, M., Saha, S., White, G., Woollen, J., Zhu, Y., Leetmaa, A., Reynolds, R., Chelliah, M., Ebisuzaki, W., Higgins, W., Janowiak, J., Mo, K. C., Ropelewski, C., Wang, J., Jenne, R. and Joseph, D.: The NCEP/NCAR 40-Year Reanalysis Project, *Bull. Amer. Meteor. Soc.*, 77(3), 437–471, doi:10.1175/1520-0477(1996)077<0437:TNYRP>2.0.CO;2, 1996.

Kendall, M. G.: Rank correlation methods, Charles Griffin, London, 1975.

Kendon, E. J., Roberts, N. M., Fowler, H. J., Roberts, M. J., Chan, S. C. and Senior, C. A.: Heavier summer downpours with climate change revealed by weather forecast resolution model, *Nature Clim. Change*, 4(7), 570–576, doi:10.1038/nclimate2258, 2014.

Kiely, G.: Climate change in Ireland from precipitation and streamflow observations, *Advances in Water Resources*, 23(2), 141–151, doi:10.1016/S0309-1708(99)00018-4, 1999.

Kilmartin, R. F.: Hydroclimatology – a needed cross-discipline. In “Improved Hydrologic Forecasting – Why and how”, Proc. Eng. Found. Conf., 1979, pp. 160-198. P. Am. Soc. Civ. Eng., New York, 1980.

Kingston, D. G., Lawler, D. M. and McGregor, G. R.: Linkages between atmospheric circulation, climate and streamflow in the northern North Atlantic: research prospects, *Progress in Physical Geography*, 30(2), 143–174, doi:10.1191/0309133306pp471ra, 2006.

Kulkarni, A. and von Storch, H.: Monte Carlo experiments on the effect of serial correlation on the Mann–Kendall test of trend, *Meteorol. Z.*, 4, 82-85, 1995.

Kundzewicz, Z. W., Kanae, S., Seneviratne, S. I., Handmer, J., Nicholls, N., Peduzzi, P., Mechler, R., Bouwer, L. M., Arnell, N., Mach, K., Muir-Wood, R., Brakenridge, G. R., Kron, W., Benito, G., Honda, Y., Takahashi, K. and Sherstyukov, B.: Flood risk and climate change: global and regional perspectives, *Hydrological Sciences Journal*, 1–28, doi:10.1080/02626667.2013.857411, 2013.

Küttel, M., Xoplaki, E., Gallego, D., Luterbacher, J., García-Herrera, R., Allan, R., Barriendos, M., Jones, P. D., Wheeler, D. and Wanner, H.: The importance of ship log data: reconstructing North Atlantic, European and Mediterranean sea level pressure fields back to 1750, *Clim Dyn*, 34(7-8), 1115–1128, doi:10.1007/s00382-009-0577-9, 2009.

Labat, D., Goddérís, Y., Probst, J. L. and Guyot, J. L.: Evidence for global runoff increase related to climate warming, *Advances in Water Resources*, 27(6), 631–642, doi:10.1016/j.advwatres.2004.02.020, 2004.

Laizé, C. L. R. and Hannah, D. M.: Modification of climate–river flow associations by basin properties, *Journal of Hydrology*, 389(1–2), 186–204, doi:10.1016/j.jhydrol.2010.05.048, 2010.

Lamb H.H.: British Isles weather types and a register of daily sequence of circulation patterns 1861–1971. Geophysical Memoir 116, HMSO, London, 1972.

Langbein W.G.: Hydroclimate. In *The Encyclopedia of Atmospheric Sciences Astrogeology*. (Fairbridge, R. W. (eds.)). pp. 447–451. Reinhold, New York, 1967.

Lavers, D. A., Prudhomme, C. and Hannah, D. M.: Large-scale climatic influences on precipitation and discharge for a British river basin, *Hydrol. Process.*, 24(18), 2555–2563, doi:10.1002/hyp.7668, 2010a.

Lavers, D., Prudhomme, C. and Hannah, D. M.: Large-scale climate, precipitation and British river flows: Identifying hydroclimatological connections and dynamics, *Journal of Hydrology*, 395(3–4), 242–255, doi:10.1016/j.jhydrol.2010.10.036, 2010b.

Lavers, D. A. and Villarini, G.: Atmospheric Rivers and Flooding over the Central United States, *Journal of Climate*, 26(20), 7829–7836, doi:10.1175/JCLI-D-13-00212.1, 2013a.

Lavers, D. A. and Villarini, G.: The nexus between atmospheric rivers and extreme precipitation across Europe, *Geophysical Research Letters*, 40(12), 3259–3264, doi:10.1002/grl.50636, 2013b.

Lavers, D. A., Allan, R. P., Wood, E. F., Villarini, G., Brayshaw, D. J. and Wade, A. J.: Winter floods in Britain are connected to atmospheric rivers, *Geophysical Research Letters*, 38(23), L23803, doi:10.1029/2011GL049783, 2011.

Lavers, D. A., Villarini, G., Allan, R. P., Wood, E. F. and Wade, A. J.: The detection of atmospheric rivers in atmospheric reanalyses and their links to British winter floods and the large-scale climatic circulation, *Journal of Geophysical Research: Atmospheres*, 117(D20), doi:10.1029/2012JD018027, 2012.

Lavers, D. A., Allan, R. P., Villarini, G., Lloyd-Hughes, B., Brayshaw, D. J. and Wade, A. J.: Future changes in atmospheric rivers and their implications for winter flooding in Britain, *Environ. Res. Lett.*, 8(3), 034010, doi:10.1088/1748-9326/8/3/034010, 2013.

Leahy, P. G. and Kiely, G.: Short Duration Rainfall Extremes in Ireland: Influence of Climatic Variability, *Water Resour Manage*, 25(3), 987–1003, doi:10.1007/s11269-010-9737-2, 2011.

Legates, D. R., Lins, H. F. and McCabe, G. J.: Comments on “Evidence for global runoff increase related to climate warming” by Labat et al., *Advances in Water Resources*, 28(12), 1310–1315, doi:10.1016/j.advwatres.2005.04.006, 2005.

Lins, H. F. and Slack, J. R.: Streamflow trends in the United States, *Geophys. Res. Lett.*, 26(2), 227–230, doi:10.1029/1998GL900291, 1999.

Logue, J. J.: Regional variations in the annual cycle of rainfall in Ireland as revealed by principal component analysis, *J. Climatol.*, 4(6), 597–607, doi:10.1002/joc.3370040604, 1984.

Lynn, M. A.: Estimating flood magnitude/return period relationships and the effect of catchment drainage, Office of the Public Works, Hydrology Unit Report Dublin, 1981.

Macdonald, N., Phillips, I. D. and Mayle, G.: Spatial and temporal variability of flood seasonality in Wales, *Hydrological Processes*, 24(13), 1806–1820, doi:10.1002/hyp.7618, 2010.

Madsen, H.: Automatic calibration of a conceptual rainfall-runoff model using multiple objectives, *J. Hydrol.*, 235, 276–288, 2000.

Mallakpour, I. and Villarini, G.: The changing nature of flooding across the central United States, *Nature Clim. Change*, advance online publication, doi:10.1038/nclimate2516, 2015.

Manley, R. E.: Simulation of flows in ungauged basins, *Hydrolog. Sci. J.*, 23, 85–101, 1978.

- Mann, H. B.: Nonparametric Tests Against Trend, *Econometrica*, 13(3), 245–259, doi:10.2307/1907187, 1945.
- Maraun, D., Osborn, T. J. and Gillett, N. P.: United Kingdom daily precipitation intensity: improved early data, error estimates and an update from 2000 to 2006, *Int. J. Climatol.*, 28(6), 833–842, doi:10.1002/joc.1672, 2008.
- Maraun, D., Osborn, T. J., and Rust, H. W.: The influence of synoptic airflow on UK daily precipitation extremes. Part I: Observed spatio-temporal relationships, *Clim. Dynam.*, 36, 261–275, doi:10.1007/s00382-009-0710-9, 2011.
- Marsh, T. J. and Hannaford, J.: (eds.) UK Hydrometric Register, Hydrological data UK series. Centre for Ecology & Hydrology. 210 pp, 2008.
- Marsh, T. J, Cole, G. and Wilby, R. L.: Major droughts in England and Wales, 1800–2006, *Weather*, 62(4), 87–93, doi:10.1002/wea.67, 2007.
- Matthews, T., Murphy, C., Wilby, R. L. and Harrigan, S.: A cyclone climatology of the British-Irish Isles 1871–2012, *Int. J. Climatol.*, Early View, doi:10.1002/joc.4425, 2015.
- Mayes, W. m., Walsh, C. I., Bathurst, J. c., Kilsby, C. g., Quinn, P. f., Wilkinson, M. e., Daugherty, A. j. and O’Connell, P. e.: Monitoring a flood event in a densely instrumented catchment, the Upper Eden, Cumbria, UK, *Water and Environment Journal*, 20(4), 217–226, doi:10.1111/j.1747-6593.2005.00006.x, 2006.
- McCarthy, G. D., Gleeson, E. and Walsh, S.: The influence of ocean variations on the climate of Ireland, *Weather*, 70(8), 242–245, doi:10.1002/wea.2543, 2015b.
- McCarthy, G. D., Haigh, I. D., Hirschi, J. J.-M., Grist, J. P. and Smeed, D. A.: Ocean impact on decadal Atlantic climate variability revealed by sea-level observations, *Nature*, 521(7553), 508–510, doi:10.1038/nature14491, 2015a.
- McCullagh, P., and Nelder, J. A.: Generalized linear models, 2<sup>nd</sup> Edition, 532 pp., 31, Chapman and Hall/CRC, 1989
- McElwain, L. and Sweeney, J.: Key meteorological indicators of climate change in Ireland. Johnstown Castle, Wexford, Ireland: Environmental Protection Agency, 2007.
- McIlveen, R.: Fundamentals of Weather and Climate, 2nd Edition, Oxford University Press, Oxford, 2010. evelopment Plan 2009–2015, Navan, Ireland, 2009.
- Meath County Council: Navan Development Plan 2009–2015, Navan, Ireland, 2009.
- Merz, B., Vorogushyn, S., Uhlemann, S., Delgado, J. and Hundedcha, Y.: HESS Opinions “More efforts and scientific rigour are needed to attribute trends in flood time series,” *Hydrol. Earth Syst. Sci.*, 16(5), 1379–1387, doi:10.5194/hess-16-1379-2012, 2012.
- Merz, B., Aerts, J., Arnbjerg-Nielsen, K., Baldi, M., Becker, A., Bichet, A., Blöschl, G., Bouwer, L. M., Brauer, A., Cioffi, F., Delgado, J. M., Gocht, M., Guzzetti, F., Harrigan, S., Hirschboeck, K., Kilsby, C., Kron, W., Kwon, H.-H., Lall, U., Merz, R., Nissen, K., Salvatti, P., Swierczynski, T., Ulbrich, U., Viglione, A., Ward, P. J., Weiler, M., Wilhelm, B. and

Nied, M.: Floods and climate: emerging perspectives for flood risk assessment and management, *Nat. Hazards Earth Syst. Sci.*, 14(7), 1921–1942, doi:10.5194/nhess-14-1921-2014, 2014.

Merz, R. and Blöschl, G.: A process typology of regional floods, *Water Resour. Res.*, 39(12), 1340, doi:10.1029/2002WR001952, 2003.

Milly, P. C. D., Wetherald, R. T., Dunne, K. A. and Delworth, T. L.: Increasing risk of great floods in a changing climate, *Nature*, 415(6871), 514–517, doi:10.1038/415514a, 2002.

Milly, P. C. D., Betancourt, J., Falkenmark, M., Hirsch, R. M., Kundzewicz, Z. W., Lettenmaier, D. P. and Stouffer, R. J.: Stationarity Is Dead: Whither Water Management?, *Science*, 319(5863), 573–574, doi:10.1126/science.1151915, 2008.

Milly, P. C. D., Betancourt, J., Falkenmark, M., Hirsch, R. M., Kundzewicz, Z. W., Lettenmaier, D. P., Stouffer, R. J., Dettinger, M. D. and Krysanova, V.: On Critiques of “Stationarity is Dead: Whither Water Management?,” *Water Resour. Res.*, doi:10.1002/2015WR017408, 2015.

Montanari, A., Young, G., Savenije, H. H. G., Hughes, D., Wagener, T., Ren, L. L., Koutsoyiannis, D., Cudennec, C., Toth, E., Grimaldi, S., Blöschl, G., Sivapalan, M., Beven, K., Gupta, H., Hipsey, M., Schaefli, B., Arheimer, B., Boegh, E., Schymanski, S. J., Di Baldassarre, G., Yu, B., Hubert, P., Huang, Y., Schumann, A., Post, D. A., Srinivasan, V., Harman, C., Thompson, S., Rogger, M., Viglione, A., McMillan, H., Characklis, G., Pang, Z. and Belyaev, V.: “Panta Rhei—Everything Flows”: Change in hydrology and society—The IAHS Scientific Decade 2013–2022, *Hydrological Sciences Journal*, 58(6), 1256–1275, doi:10.1080/02626667.2013.809088, 2013.

Moriasi, D. N., Arnold, J. G., Van Liew, M. W., Binger, R. L., Harmel, R. D., and Veith, T. L.: Model evaluation guidelines for systematic quantification of accuracy in watershed simulations, *Transactions of the ASABE*, 50, 885-900, 2007.

Murphy, C., Fealy, R., Charlton, R., and Sweeney, J.: The reliability of an ‘off-the-shelf’ conceptual rainfall runoff model for use in climate impact assessment: uncertainty quantification using Latin hypercube sampling, *Area*, 38, 65-78, doi:10.1111/j.1475-4762.2006.00656.x, 2006.

Murphy, C., Bastola, S., Hall, J., Harrigan, S., Murphy, N. and Holman, C.: Against a “wait and see” approach in adapting to climate change, *Irish Geography*, 44(1), 81–95, doi:10.1080/00750778.2011.615707, 2011.

Murphy, C., Harrigan, S., Hall, J. and Wilby, R. L.: Climate-driven trends in mean and high flows from a network of reference stations in Ireland, *Hydrological Sciences Journal*, 58(4), 755–772, doi:10.1080/02626667.2013.782407, 2013a.

Murphy, C., Harrigan, S., Hall, J. and Wilby, R.L.: HydroDetect: The Identification and Assessment of Climate Change indicators from an Irish Reference Network of River Flow Stations. Environmental Protection Agency, Ireland, pp 89, ISBN 978-1-84095-507-1, 2013b.

Nash, J. E. and Sutcliffe, J. V.: River Flow Forecasting through Conceptual Models Part 1 - A Discussion of Principles, *J. Hydrol.*, 10, 282-290, 1970.

Nicholls, N.: commentary and analysis: The Insignificance of Significance Testing, *Bull. Amer. Meteor. Soc.*, 82(5), 981–986, doi:10.1175/1520-0477(2001)082<0981:CAATIO>2.3.CO;2, 2001.

Noone, S., Murphy, C., Coll, J., Matthews, T., Mullan, D., Wilby, R. L. and Walsh, S.: Homogenization and analysis of an expanded long-term monthly rainfall network for the Island of Ireland (1850–2010), *Int. J. Climatol.*, Early View, doi:10.1002/joc.4522, 2015.

O’Kelly, J. J.: The employment of Unit Hydrographs to determine the flows of Irish arterial drainage channels, in: *Proceedings of the Institution of Civil Engineers (London)*, 4, 365-412, 1955.

Önöz, B. and Bayazit, M.: Block bootstrap for Mann-Kendall trend test of serially dependent data, *Hydrol. Process.*, 26, 3552-3560, doi:10.1002/hyp.8438, 2012.

OPW: Flood Studies Update, Technical Research Report, (six volumes), Office of Public Works (OPW), Trim, Ireland, 2014.

Osborn, T. J.: Recent variations in the winter North Atlantic Oscillation, *Weather*, 61(12), 353–355, doi:10.1256/wea.190.06, 2006.

Osborn, T. J., Briffa, K. R., Tett, S. F. B., Jones, P. D. and Trigo, R. M.: Evaluation of the North Atlantic Oscillation as simulated by a coupled climate model, *Climate Dynamics*, 15(9), 685–702, doi:10.1007/s003820050310, 1999.

Osborn, T. J., Hulme, M., Jones, P. D. and Basnett, T. A.: Observed trends in the daily intensity of United Kingdom precipitation, *Int. J. Climatol.*, 20(4), 347–364, doi:10.1002/(SICI)1097-0088(20000330)20:4<347::AID-JOC475>3.0.CO;2-C, 2000.

Pattison, I. and Lane, S. N.: The relationship between Lamb weather types and long-term changes in flood frequency, River Eden, UK, *Int. J. Climatol.*, 32(13), 1971–1989, doi:10.1002/joc.2415, 2012.

Perry, A. and Mayes, J.: The Lamb weather type catalogue, *Weather*, 53(7), 222–229, doi:10.1002/j.1477-8696.1998.tb06387.x, 1998.

Petrow, T. and Merz, B.: Trends in flood magnitude, frequency and seasonality in Germany in the period 1951–2002, *Journal of Hydrology*, 371(1–4), 129–141, doi:10.1016/j.jhydrol.2009.03.024, 2009.

Petrow, T., Zimmer, J. and Merz, B.: Changes in the flood hazard in Germany through changing frequency and persistence of circulation patterns, *Nat. Hazards Earth Syst. Sci.*, 9(4), 1409–1423, doi:10.5194/nhess-9-1409-2009, 2009.

Petrone, K. C., Hughes, J. D., Van Niel, T. G., and Silberstein, R. P.: Streamflow decline in southwestern Australia, 1950-2008, *Geophys. Res. Lett.*, 37, L11401, doi:10.1029/2010GL043102, 2010.

Pettitt, A. N.: A Non-Parametric Approach to the Change-Point Problem, *J. Roy. Stat. Soc. C-App.*, 28, 126-135, 1979.

Platt, J. R.: Strong Inference, *Science*, 146(3642), 347–353, doi:10.1126/science.146.3642.347, 1964.

Poli, P., Hersbach, D. Tan, D. Dee, J.-N. Thépaut, A. Simmons, C. Peubey, P. Laloyaux, T. Komori, P. Berrisford, R. Dragani, Y. Trémolet, E. Holm, M. Bonavita, L. Isaksen and Fisher, M.: The data assimilation system and initial performance evaluation of the ECMWF pilot reanalysis of the 20th-century assimilating surface observations only (ERA-20C). ERA Report Series no. 14, ECMWF, 59 pp, 2013.

Popper, K.: *Conjectures and Refutations*, London: Routledge and Keagan Paul, 1963, pp. 33 39; from Theodore Schick, ed., *Readings in the Philosophy of Science*, Mountain View, CA: Mayfield Publishing Company, 2000, pp. 9-13, 1963.

Prosdocimi, I., Kjeldsen, T. R. and Svensson, C.: Non-stationarity in annual and seasonal series of peak flow and precipitation in the UK, *Nat. Hazards Earth Syst. Sci.*, 14(5), 1125–1144, doi:10.5194/nhess-14-1125-2014, 2014.

Prudhomme, C. and Geneviev, M.: Can atmospheric circulation be linked to flooding in Europe?, *Hydrol. Process.*, 25(7), 1180–1190, doi:10.1002/hyp.7879, 2011.

Prudhomme, C., Giuntoli, I., Robinson, E. L., Clark, D. B., Arnell, N. W., Dankers, R., Fekete, B. M., Franssen, W., Gerten, D., Gosling, S. N., Hagemann, S., Hannah, D. M., Kim, H., Masaki, Y., Satoh, Y., Stacke, T., Wada, Y. and Wisser, D.: Hydrological droughts in the 21st century, hotspots and uncertainties from a global multimodel ensemble experiment, *PNAS*, 111(9), 3262–3267, doi:10.1073/pnas.1222473110, 2014.

Rahmstorf, S., Box, J. E., Feulner, G., Mann, M. E., Robinson, A., Rutherford, S. and Schaffernicht, E. J.: Exceptional twentieth-century slowdown in Atlantic Ocean overturning circulation, *Nature Clim. Change*, 5(5), 475–480, doi:10.1038/nclimate2554, 2015.

Ramos, A. M., Barriopedro, D. and Dutra, E.: Circulation weather types as a tool in atmospheric, climate, and environmental research, *Front. Environ. Sci.*, 3, 44, doi:10.3389/fenvs.2015.00044, 2015.

Rasmusson, E. M. and Wallace, J. M.: Meteorological Aspects of the El Niño/Southern Oscillation, *Science*, 222(4629), 1195–1202, doi:10.1126/science.222.4629.1195, 1983.

Raup, D. C. and Chamberlin, T. C.: The Method of Multiple Working Hypotheses, *The Journal of Geology*, 103(3), 349–354, 1995.

Reed, S., Koren, V., Smith, M., Zhang, Z., Moreda, F., Seo, D.-J., and DMIP Participants: Overall distributed model intercomparison project results, *J. Hydrol.*, 298, 27-60, 2004.

Ropelewski, C. F. and Jones, P. D.: An Extension of the Tahiti–Darwin Southern Oscillation Index, *Mon. Wea. Rev.*, 115(9), 2161–2165, doi:10.1175/1520-0493(1987)115<2161:AEOTTS>2.0.CO;2, 1987.

Scaife, A. A., Arribas, A., Blockley, E., Brookshaw, A., Clark, R. T., Dunstone, N., Eade, R., Fereday, D., Folland, C. K., Gordon, M., Hermanson, L., Knight, J. R., Lea, D. J., MaLachlan, C., Maidens, A., Martin, M., Peterson, A. K., Smith, D., Vellinga, M., Wallace, E., Waters, J. and Williams, A.: Skillful long-range prediction of European and North American winters, *Geophys. Res. Lett.*, 41(7), 2014GL059637, doi:10.1002/2014GL059637, 2014.

Schreider, S. Y., Jakeman, A. J., Letcher, R. A., Nathan, R. J., Neal, B. P., and Beavis, S. G.: Detecting changes in streamflow response to changes in non-climatic catchment conditions: Farm dam development in the Murray-Darling basin, Australia, *J. Hydrol.*, 262, 84-98, 2002.

Seibert, J. and McDonnell, J. J.: Land-cover impacts on streamflow: a change-detection modelling approach that incorporates parameter uncertainty, *Hydrological Sciences Journal*, 55(3), 316–332, doi:10.1080/02626661003683264, 2010.

Sen, P. K.: Estimates of the regression coefficient based on Kendall's tau, *J. Am. Stat. Assoc.*, 63, 1379-1389, 1968.

Seneviratne, S.I., Nicholls, D. Easterling, C.M. Goodess, S. Kanae, J. Kossin, Y. Luo, J. Marengo, K. McInnes, M. Rahimi, M. Reichstein, A. Sorteberg, C. Vera, and X. Zhang: Changes in climate extremes and their impacts on the natural physical environment. In: *Managing the Risks of Extreme Events and Disasters to Advance Climate Change Adaptation* [Field, C.B., V. Barros, T.F. Stocker, D. Qin, D.J. Dokken, K.L. Ebi, M.D. Mastrandrea, K.J. Mach, G.-K. Plattner, S.K. Allen, M. Tignor, and P.M. Midgley (eds.)]. A Special Report of Working Groups I and II of the Intergovernmental Panel on Climate Change (IPCC). Cambridge University Press, Cambridge, UK, and New York, NY, USA, pp. 109-230, 2012.

Sheridan, T.: Analysis of trends at some Irish rainfall stations. Dublin, Ireland: Met Éireann Technical Report 59, 2001.

Sivapalan, M., Savenije, H. H. G., and Blöschl, G.: Socio-hydrology: A new science of people and water, *Hydrol. Process.*, 26, 1270-1276, doi:10.1002/hyp.8426, 2012.

Smith, D. M., Scaife, A. A., Eade, R. and Knight, J. R.: Seasonal to decadal prediction of the winter North Atlantic Oscillation: emerging capability and future prospects, *Q.J.R. Meteorol. Soc.*, Early View, doi:10.1002/qj.2479, 2014.

Stahl, K., Hisdal, H., Hannaford, J., Tallaksen, L. M., van Lanen, H. A. J., Sauquet, E., Demuth, S., Fendekova, M. and Jódar, J.: Streamflow trends in Europe: evidence from a dataset of near-natural catchments, *Hydrol. Earth Syst. Sci.*, 14(12), 2367–2382, doi:10.5194/hess-14-2367-2010, 2010.

Stahl, K., Tallaksen, L. M., Hannaford, J. and van Lanen, H. A. J.: Filling the white space on maps of European runoff trends: estimates from a multi-model ensemble, *Hydrol. Earth Syst. Sci.*, 16(7), 2035–2047, doi:10.5194/hess-16-2035-2012, 2012.

Sutton, R. T. and Dong, B.: Atlantic Ocean influence on a shift in European climate in the 1990s, *Nature Geosci*, 5(11), 788–792, doi:10.1038/ngeo1595, 2012.

Svensson, C.: Seasonal river flow forecasts for the United Kingdom using persistence and historical analogues, *Hydrological Sciences Journal*, Early View, doi:10.1080/02626667.2014.992788, 2014.

Svensson, C., Kundzewicz, W. Z. and Maurer, T.: Trend detection in river flow series: 2. Flood and low-flow index series, *Hydrological Sciences Journal*, 50(5), 811–824, doi:10.1623/hysj.2005.50.5.811, 2005.

Svensson, C., Brookshaw, A., Scaife, A. A., Bell, V. A., Mackay, J. D., Jackson, C. R., Hannaford, J., Davies, H. N., Arribas, A. and Stanley, S.: Long-range forecasts of UK winter hydrology, *Environ. Res. Lett.*, 10(6), 064006, doi:10.1088/1748-9326/10/6/064006, 2015.

Sweeney, J.: Regional weather and climates of the British Isles – Part 6: Ireland, *Weather*, 69(1), 20–27, doi:10.1002/wea.2230, 2014.

Sweeney, J. C.: The Changing Synoptic Origins of Irish Precipitation, *Transactions of the Institute of British Geographers*, 10(4), 467–480, doi:10.2307/621892, 1985.

Sweeney, J. C. and O'Hare, G. P.: Geographical Variations in Precipitation Yields and Circulation Types in Britain and Ireland, *Transactions of the Institute of British Geographers*, 17(4), 448–463, doi:10.2307/622710, 1992.

Taylor, K. E., Stouffer, R. J. and Meehl, G. A.: An Overview of CMIP5 and the Experiment Design, *Bull. Amer. Meteor. Soc.*, 93(4), 485–498, doi:10.1175/BAMS-D-11-00094.1, 2012.

Theil, H.: A Rank-invariant Method of Linear and Polynomial Regression Analysis, I., *Nederlands Akad. Wetensch. Proc.*, 53, 386–392, 1950.

Tibaldi, S. and Molteni, F.: On the operational predictability of blocking, *Tellus A*, 42(3) [online] Available from: <http://www.tellusa.net/index.php/tellusa/article/view/11882> (Accessed 17 December 2015), 1990.

Toreti, A., Kuglitsch, F. G., Xoplaki, E., Della-Marta, P. M., Aguilar, E., Prohom, M. and Luterbacher, J.: A note on the use of the standard normal homogeneity test to detect inhomogeneities in climatic time series, *Int. J. Climatol.*, 31(4), 630–632, doi:10.1002/joc.2088, 2011.

Trenberth, K. E.: Changes in precipitation with climate change, *Clim Res*, 47(1-2), 123–138, 2011.

Trenberth, K. E.: Signal Versus Noise in the Southern Oscillation, *Mon. Wea. Rev.*, 112(2), 326–332, doi:10.1175/1520-0493(1984)112<0326:SVNITS>2.0.CO;2, 1984.

Trenberth, K. E.: The Definition of El Niño, *Bull. Amer. Meteor. Soc.*, 78(12), 2771–2777, doi:10.1175/1520-0477(1997)078<2771:TDOENO>2.0.CO;2, 1997.

Trenberth, K. E.: Atmospheric Moisture Residence Times and Cycling: Implications for Rainfall Rates and Climate Change, *Climatic Change*, 39(4), 667–694, doi:10.1023/A:1005319109110, 1998.

Trenberth, K. E.: Conceptual Framework for Changes of Extremes of the Hydrological Cycle with Climate Change, *Climatic Change*, 42(1), 327–339, doi:10.1023/A:1005488920935, 1999.

Trenberth, K. E. and Shea, D. J.: Atlantic hurricanes and natural variability in 2005, *Geophys. Res. Lett.*, 33(12), L12704, doi:10.1029/2006GL026894, 2006.

Trenberth, K. E., Dai, A., Rasmussen, R. M. and Parsons, D. B.: The Changing Character of Precipitation, *Bull. Amer. Meteor. Soc.*, 84(9), 1205–1217, doi:10.1175/BAMS-84-9-1205, 2003.

Trenberth, K. E., P. D. Jones, P. Ambenje, R. Bojariu, D. Easterling, A. Klein Tank, D. Parker, F. Rahimzadeh, J.A. Renwick, M. Rusticucci, B. Soden and P. Zhai: Observations: Surface and Atmospheric Climate Change. In: *Climate Change 2007: The Physical Science Basis. Contribution of Working Group I to the Fourth Assessment Report of the Intergovernmental Panel on Climate Change* [Solomon, S., D. Qin, M. Manning, Z. Chen, M. Marquis, K.B. Averyt, M. Tignor and H.L. Miller (eds.)]. Cambridge University Press, Cambridge, United Kingdom and New York, NY, USA, 2007.

Trenberth, K. E., Dai, A., van der Schrier, G., Jones, P. D., Barichivich, J., Briffa, K. R. and Sheffield, J.: Global warming and changes in drought, *Nature Clim. Change*, 4(1), 17–22, doi:10.1038/nclimate2067, 2014.

UNISDR: *Global Assessment Report on Disaster Risk Reduction 2013, From Shared Risk to Shared Value: the Business Case for Disaster Risk Reduction*, United Nations International Strategy for Disaster Reduction Secretariat, Geneva, 2013.

van der Ent, R. J., Savenije, H. H. G., Schaefli, B. and Steele-Dunne, S. C.: Origin and fate of atmospheric moisture over continents, *Water Resour. Res.*, 46(9), W09525, doi:10.1029/2010WR009127, 2010.

van Oldenborgh, G. J., Otto, F. E. L., Haustein, K. and Cullen, H.: Climate change increases the probability of heavy rains like those of storm Desmond in the UK – an event attribution study in near-real time, *Hydrol. Earth Syst. Sci. Discuss.*, 12(12), 13197–13216, doi:10.5194/hessd-12-13197-2015, 2015.

Villarini, G., Serinaldi, F., Smith, J. A. and Krajewski, W. F.: On the stationarity of annual flood peaks in the continental United States during the 20th century, *Water Resources Research*, 45(8), W08417, doi:10.1029/2008WR007645, 2009.

Villarini, G., Smith, J. A., Baeck, M. L., Vitolo, R., Stephenson, D. B. and Krajewski, W. F.: On the frequency of heavy rainfall for the Midwest of the United States, *Journal of Hydrology*, 400(1–2), 103–120, doi:10.1016/j.jhydrol.2011.01.027, 2011a.

Villarini, G., Smith, J. A., Serinaldi, F. and Ntelekos, A. A.: Analyses of seasonal and annual maximum daily discharge records for central Europe, *Journal of Hydrology*, 399(3–4), 299–312, doi:10.1016/j.jhydrol.2011.01.007, 2011b.

Vorogushyn, S. and Merz, B.: Flood trends along the Rhine: the role of river training, *Hydrol. Earth Syst. Sci.*, 17(10), 3871–3884, doi:10.5194/hess-17-3871-2013, 2013.

- Walsh, S.: New Long-term rainfall averages for Ireland, Tullamore, Ireland, 3–12, 2012a.
- Walsh, S.: A Summary of Climate Averages 1981–2010 for Ireland, Climatological Note, 14, Dublin, 2012b.
- Wang, X. L., Feng, Y., Compo, G. P., Swail, V. R., Zwiers, F. W., Allan, R. J. and Sardeshmukh, P. D.: Trends and low frequency variability of extra-tropical cyclone activity in the ensemble of twentieth century reanalysis, *Clim Dyn*, 40(11-12), 2775–2800, doi:10.1007/s00382-012-1450-9, 2013.
- Ward, P. J., Jongman, B., Kumm, M., Dettinger, M. D., Weiland, F. C. S. and Winsemius, H. C.: Strong influence of El Niño Southern Oscillation on flood risk around the world, *PNAS*, 201409822, doi:10.1073/pnas.1409822111, 2014.
- Westra, S., Alexander, L. V. and Zwiers, F. W.: Global Increasing Trends in Annual Maximum Daily Precipitation, *J. Climate*, 26(11), 3904–3918, doi:10.1175/JCLI-D-12-00502.1, 2013.
- Westra, S., Fowler, H. J., Evans, J. P., Alexander, L. V., Berg, P., Johnson, F., Kendon, E. J., Lenderink, G. and Roberts, N. M.: Future changes to the intensity and frequency of short-duration extreme rainfall, *Rev. Geophys.*, 52(3), 2014RG000464, doi:10.1002/2014RG000464, 2014.
- Whitfield, P. H., Burn, D. H., Hannaford, J., Higgins, H., Hodgkins, G. A., Marsh, T. and Looser, U.: Reference hydrologic networks I. The status and potential future directions of national reference hydrologic networks for detecting trends, *Hydrological Sciences Journal*, 57(8), 1562–1579, doi:10.1080/02626667.2012.728706, 2012.
- Wigley, T. M. L., Lough, J. M. and Jones, P. D.: Spatial patterns of precipitation in England and Wales and a revised, homogeneous England and Wales precipitation series, *J. Climatol.*, 4(1), 1–25, doi:10.1002/joc.3370040102, 1984.
- Wilby, R. L.: Evidence of enso in the synoptic climate of the British Isles since 1880, *Weather*, 48(8), 234–239, doi:10.1002/j.1477-8696.1993.tb05897.x, 1993.
- Wilby, R. L.: Uncertainty in water resource model parameters used for climate change impact assessment, *Hydrological Processes*, 19(16), 3201–3219, doi:10.1002/hyp.5819, 2005.
- Wilby, R. L., O'Hare, G., and Barnsley, N.: The North Atlantic Oscillation and British Isles climate variability, 1865-1996, *Weather*, 52, 266-276, doi:10.1002/j.1477-8696.1997.tb06323.x, 1997.
- Wilby, R. L.: When and where might climate change be detectable in UK river flows?, *Geophys. Res. Lett.*, 33(19), L19407, doi:10.1029/2006GL027552, 2006.
- Wilby, R. L. and Quinn, N. W.: Reconstructing multi-decadal variations in fluvial flood risk using atmospheric circulation patterns, *Journal of Hydrology*, 487, 109–121, doi:10.1016/j.jhydrol.2013.02.038, 2013.

Wilby, R. L., O'Hare, G., and Barnsley, N.: The North Atlantic Oscillation and British Isles climate variability, 1865-1996, *Weather*, 52, 266-276, doi:10.1002/j.1477-8696.1997.tb06323.x, 1997.

Wilby, R. L., Wigley, T. M. L., Conway, D., Jones, P. D., Hewitson, B. C., Main, J. and Wilks, D. S.: Statistical downscaling of general circulation model output: A comparison of methods, *Water Resour. Res.*, 34(11), 2995–3008, doi:10.1029/98WR02577, 1998.

Wilby, R. L., Fowler, H. J., and Donovan, B.: Detecting changes in winter precipitation extremes and fluvial flood risk. In: Beven, K. and Hall, J. (eds.). *Applied uncertainty analysis for flood risk management*, Imperial College Press, London, pp. 578-604, 2014.

Wilby, R. L., Noone, S., Murphy, C., Matthews, T., Harrigan, S. and Broderick, C.: An evaluation of persistent meteorological drought using a homogeneous Island of Ireland precipitation network, *Int. J. Climatol.*, Early View, doi:10.1002/joc.4523, 2015.

Wilcock, D. and Wilcock, F.: Modelling the hydrological impacts of channelization on streamflow characteristics in a Northern Ireland catchment, in: *Modelling and Management of Sustainable Basin-Scale Water Resource Systems*, IAHS Publication No. 231, 41-48, 1995.

Wilks, D. S.: *Statistical methods in the atmospheric sciences*, 3<sup>rd</sup> Edition, Academic Press, 2011.

Woollings, T.: Dynamical influences on European climate: an uncertain future, *Philosophical Transactions of the Royal Society of London A: Mathematical, Physical and Engineering Sciences*, 368(1924), 3733–3756, doi:10.1098/rsta.2010.0040, 2010.

Woollings, T., Gregory, J. M., Pinto, J. G., Reyers, M. and Brayshaw, D. J.: Response of the North Atlantic storm track to climate change shaped by ocean-atmosphere coupling, *Nature Geoscience*, 5(5), 313–317, doi:10.1038/ngeo1438, 2012.

Yue, S. and Wang, C. Y.: Regional streamflow trend detection with consideration of both temporal and spatial correlation, *Int. J. Climatol.*, 22(8), 933–946, doi:10.1002/joc.781, 2002.

Yue, S., Pilon, P., Phinney, B. and Cavadias, G.: The influence of autocorrelation on the ability to detect trend in hydrological series, *Hydrological Processes*, 16(9), 1807–1829, doi:10.1002/hyp.1095, 2002.

Zehe, E. and Sivapalan, M.: Threshold behaviour in hydrological systems as (human) geo-ecosystems: manifestations, controls, implications, *Hydrology and Earth System Sciences*, 13(7), 1273–1297, doi:10.5194/hess-13-1273-2009, 2009.

Zhang, S., Lu, X. X., Higgitt, D. L., Chen, C.-T. A., Han, J. and Sun, H.: Recent changes of water discharge and sediment load in the Zhujiang (Pearl River) Basin, China, *Global and Planetary Change*, 60(3–4), 365–380, doi:10.1016/j.gloplacha.2007.04.003, 2008.

Zhang, X., Harvey, K. D., Hogg, W. D. and Yuzyk, T. R.: Trends in Canadian streamflow, *Water Resour. Res.*, 37(4), 987–998, doi:10.1029/2000WR900357, 2001.

Zhang, X., Alexander, L., Hegerl, G. C., Jones, P. D., Tank, A. K., Peterson, T. C., Trewin, B. and Zwiers, F. W.: Indices for monitoring changes in extremes based on daily temperature and precipitation data, *WIREs Clim Change*, 2(6), 851–870, doi:10.1002/wcc.147, 2011.

Zhu, Y. and Newell, R. E.: Atmospheric rivers and bombs, *Geophys. Res. Lett.*, 21(18), 1999–2002, doi:10.1029/94GL01710, 1994.

## Appendix I

**Appendix I: Details of precipitation stations removed (added) from clusters (gaps) in Section 3.2.**

Station	Station name	height	Start Year	End Year	Length	Percent missing	Notes
<b>Gap 1</b>							
1435	LOUGH FEA	225	1966	2000	35	5.867	C-list, Very difficult to find station in Sperrin Mountain area. This is a modified C-list station. i.e. Had too much data missing between 2001 and 2008 (21 % missing). However, 1966 to 2000 was used and bridged instead.
16284	UPPERLANDS	68	1961	2000	40	1.225	C-list
16208	CAPPAGH RESR	173	1961	2010	50	3.340	B-list
1551	EDENFEL	89	1872	2014	143	7.119	B-list
16534	PORTORA SLUICE	46	1963	2013	51	6.577	B-list
1544	BARONS COURT	132	1892	2014	123	10.387	C-list
<b>Gap 2</b>							
1452	ALRNAHINCH FILTERS	213	1966	2008	43	1.393	C-list, misses out on B-list by 1 year at end. Good anchor station on Northern coast.
<b>Gap 3</b>							
4131	BAILIEBORO (LEITER)	155	1974	2012	39	0	B-list, but misses out on A-list by 1 year at start.
4037	LOUGH GOWNA (GLENBROOK)	91	1974	2008	35	0	C-list, but misses out on B-list by 1 year at end.
2922	Mullingar II	101	1973	2007	35	0	C-list, misses out on B-list by 2 years at end.
4531	NAVAN (TARA MINES)	52	1987	2012	26	0.304	C-list
<b>Gap 4</b>							
4914	EMO COURT	91	1975	2000	26	4.436	C-list, important station in this gap.
5414	CASTLEDERMOT KILKEA HOUSE	85	1984	2012	29	0.854	C-list
4615	BOOLAVOGUE KNOCKAVOCCA	73	1988	2012	25	1.653	C-list
5214	COOLGREANY CASTLEWARREN	262	1983	2012	30	1.116	C-list
3613	Kilkenny	65	1958	2007	50	0	C-list, but missed out in B-list by 2 years at end.
4213	PARKNAHOWN CULLAHILL	110	1982	2012	31	2.424	C-list, but missed out in B-list by 2 years at start.
<b>Gap 5</b>							
4811	PATRICKSWELL (DOONEEN)	27	1982	2012	31	0	C-list
5306	MOUNT RUSSELL	195	1985	2012	28	0.294	C-list

4911	CASTLEMAHON W.W.	58	1983	2011	29	2.758	C-list
1510	LYREACRUMPANE (REENAGOWN)	187	1948	2009	62	1.986	B-list
1909	DINGLE (BAILE NA NGALL)	36	1985	2012	28	3.275	C-list
2010	LISTOWEL (INCH)	15	1956	2011	56	8.406	B-list, Missed A-list as too much missing.
<b>Gap 6</b>							
2121	GORT (DERRYBRIEN II)	155	1982	2012	30	0.556	C-list
1718	CARRON	134	1975	2012	38	0.216	B-list, Just missed out on A-list by 2 years at start.
<b>Gap 7</b>							
1128	LOUGHGLINN	98	1945	2012	68	6.288	B-list, Just missed A-list by a few % missing.
2727	Claremorris	69	1944	2007	64	0.387	C-list, Just missed B-list by 2 years at end.
4227	CORNAMONA	30	1969	2009	41	0.595	B-list
9827	M.MAAM (MT.RINAVORE)	389	1983	2012	30	0.274	C-list
1926	KILLADOON	46	1985	2012	28	0	C-list
<b>Minor Gaps</b>							
545	Malin Head (manual)	22	1957	2009	53	0	B-List
1043	LETTERKENNY (DROMORE)	20	1971	2012	42	5.099	B-list, Just missed out on A-list by < 1% missing.
<b>Cluster 1</b>							
1491	SILENT VALLEY	129	1961	2013	53	0.782	A-list; removed.
1338	OMEATH	12	1944	2012	69	3.113	A-list; removed.
9938	M.DUNDALK (BALLYMAKELLETT)	232	1941	2012	72	2.783	A-list; removed.
<b>Cluster 2</b>							
1823	DUBLIN (GLASNEVIN)	21	1941	2012	72	0	A-list; removed.
3923	DUBLIN (MERRION SQUARE)	13	1948	2012	65	0	A-list; removed.
7523	DUBLIN (SIMMONSCOURT)	9	1973	2011	39	1.65	A-list; removed.
3723	Casement	91	1954	2012	59	0	A-list; removed.
5623	GLENASMOLE (SUPT'S LODGE)	152	1960	2012	53	0.946	A-list; removed.
5523	GLENASMOLE (CASTLEKELLY)	183	1960	2011	52	1.741	A-list; removed.
19723	M.SALLY GAP	462	1944	2012	69	4.89	A-list; removed.
820	MONEYSTOWN	207	1949	2012	64	1.919	A-list; removed.
2415	GLEN IMAAL (FOR.STN.)	213	1952	2012	61	0	A-list; removed.
3823	BALLYMORE EUSTACE D.C.W.W.	172	1945	2012	68	3.289	A-list; removed.
<b>Cluster 3</b>							

1605	GLENVICKEE (CARAGH RIVER AREA)	128	1950	2011	62	4.466	A-list; removed.
1705	CLOONE LAKE (CARAGH RIVER AREA)	122	1950	2012	63	1.175	A-list; removed.
9303	M.CUMMERAGH NO.3	543	1943	2012	70	4.353	A-list; removed.
9403	M.CUMMERAGH NO.4	494	1943	2012	70	4.392	A-list; removed.
9503	M.CUMMERAGH NO.5	396	1943	2012	70	4.388	A-list; removed.
703	WATERVILLE OCTIVE NO.9	110	1943	2012	70	0.705	A-list; removed.
9103	M.CUMMERAGH NO.1	305	1943	2012	70	2.599	A-list; removed.
3804	MACROOM (RENANIRREE)	198	1960	2012	53	0.461	A-list; removed.
9904	M.INCHIGEELAGH (PIPE HILL)	299	1949	2012	64	2.983	A-list; removed.
3004	BALLINGEARY (VOC.SCH.)	91	1949	2012	64	1.947	A-list; removed.
<b>Minor Clusters</b>							
2435	KEENAGH BEG	91	1945	2012	68	0.124	A-list; removed.
3237	BALLYSHANNON (CHERRYMOUNT)	30	1955	2012	58	0.285	A-list; removed.
944	CREESLOUGH (CARROWNAMADDY)	88	1948	2011	63	3.878	A-list; removed.
1519	MEELICK (VICTORIA LOCK)	39	1941	2012	72	0.567	A-list; removed.
1929	ATHLONE O.P.W.	37	1941	2012	72	3.023	A-list; removed.

## Appendix II

**Appendix II: Precipitation stations used in the analysis categorised by their Network: (A) used in Extreme Rainfall Regions and trend analysis, and (GAP) used only for Extreme Rainfall Regions), and Organisation (Org.): Met Éireann (IRE) or UK Met Office (UK), with a number of metadata as discussed in Section 3.2: height is in m a. s. l., and distance to coast (coast) and nearest neighbour are in km.**

Station	Network	Station name	Easting	Northing	Org.	ERR	Start Year	End Year	Percent Missing	height	Coast	Nearest neighbour
108	A	Foulkesmills (Longraigue)	284187	118337	IRE	CU	1941	2012	0.0	71	4.9	11.9
201	A	Glengarriff (Innacullin)	93200	54700	IRE	SW	1941	2012	0.5	7	0.0	16.6
305	A	Valentia_Observatory (Manual)	45799	78549	IRE	SW	1941	2011	0.0	24	0.3	19.1
417	A	Inagh (Mt.Callan)	116500	177500	IRE	CU	1941	2012	4.1	122	11.3	23.5
441	A	Glenties_Hatchery	181510	393730	IRE	CU	1941	2012	0.3	44	5.6	24.3
518	A	Shannon_Airport	137900	160300	IRE	CU	1941	2012	0.0	15	0.1	19.7
532	A	Dublin_Airport	316900	243400	IRE	IE	1941	2012	0.0	71	4.8	10.0
538	A	Dundalk (Annaskeagh W.W.)	308015	312670	IRE	IE	1941	2012	0.1	61	2.5	26.3
542	A	Greencastle	264600	440800	IRE	CU	1949	2012	1.2	53	0.7	23.3
545	GAP	Malin Head (Manual)	241900	458600	IRE	CU	1957	2009	0.0	22	0.2	28.8
603	A	Kenmare (Derreen)	77100	58900	IRE	SW	1941	2012	0.3	24	0.1	16.6
639	A	Monaghan (Castleshane)	272160	332480	IRE	IE	1972	2012	0.2	94	38.4	16.9
705	A	Killorglin (Callinafercy)	77900	99400	IRE	CU	1941	2012	0.8	14	0.3	21.2
706	A	Mallow (Hazelwood)	155600	104500	IRE	CU	1941	2012	0.0	94	34.3	16.3
833	A	Newport (Furnace)	96700	298100	IRE	CU	1960	2012	0.0	14	2.2	17.1
844	A	Creeslough (Brockagh)	201400	425600	IRE	CU	1949	2012	0.5	119	7.7	11.0
1020	A	Arklow W.W.	322128	173028	IRE	CU	1950	2012	0.5	34	3.3	25.6
1024	A	Roundwood (Filter Beds)	321523	201207	IRE	CU	1943	2012	1.1	195	9.6	9.8
1034	A	Belmullet(Manual)	69100	332900	IRE	CU	1957	2011	0.0	9	0.2	37.8
1042	A	Pettigo (Lough Derg)	209110	373145	IRE	CU	1953	2012	1.1	146	15.9	18.8
1043	GAP	Letterkenny (Dromore)	220600	410970	IRE	CU	1971	2012	5.1	20	0.5	15.3
1128	GAP	Loughglinn	163400	286000	IRE	IE	1945	2012	6.3	98	42.9	12.9

1143	A	Termon (Goldrum)	212300	423800	IRE	CU	1973	2012	4.1	152	7.0	11.0
1205	A	Castleisland (Coom)	107400	109900	IRE	CU	1945	2012	1.5	157	20.8	13.1
1218	A	Tulla	148900	180100	IRE	CU	1944	2012	0.7	61	12.8	22.7
1225	A	Costelloe Fishery	97500	226700	IRE	CU	1961	2012	0.0	12	0.2	15.7
1242	A	Stranorlar (Cavan Lower)	217525	395245	IRE	CU	1965	2012	3.5	27	15.9	16.0
1406	A	Kanturk (Voc.Sch.)	138400	103300	IRE	CU	1945	2011	3.5	104	41.5	17.2
1420	A	Glenmacnass	311790	202275	IRE	CU	1966	2012	0.2	238	19.4	9.8
1425	A	Cloosh (For.Stn.)	110700	235200	IRE	CU	1964	2012	0.3	101	13.1	15.7
1435	GAP	Lough Fea	276407.7	386513.7	UK	CU	1966	2000	5.9	225	39.5	20.6
1452	GAP	Altnahinch Filters	311529.9	423657.3	UK	CU	1966	2008	1.4	213	13.0	27.0
1489	A	Hillsborough	325031.6	357708.7	UK	IE	1961	2014	0.4	116	24.1	21.6
1504	A	Rathduff G.S.	159800	84800	IRE	CU	1943	2012	4.5	138	14.3	10.9
1510	GAP	Lyreacrumpane (Reenagown)	97300	118200	IRE	CU	1948	2009	2.0	187	13.4	13.1
1529	A	Drumsna (Albert Lock)	2.00E+05	295800	IRE	IE	1941	2012	0.9	45	47.5	11.0
1530	A	Armagh	287827.3	345676.2	UK	IE	1853	2013	0.0	62	31.0	20.5
1544	GAP	Barons Court	237249.4	383207.7	UK	CU	1892	2014	10.4	132	32.7	15.0
1551	GAP	Edenfel	246398.7	371324.3	UK	IE	1872	2014	7.1	89	45.3	15.0
1563	A	Lough Navar Forest	206465	354487.1	UK	CU	1962	2014	2.2	126	20.3	18.1
1603	A	Kilgarvan (Gortnaboul)	100800	73100	IRE	SW	1970	2012	0.2	34	6.7	13.6
1641	A	Crolly (Filter Works)	184000	417900	IRE	CU	1973	2012	0.0	91	3.5	19.0
1718	GAP	Carron	127700	198200	IRE	CU	1975	2012	0.2	134	10.3	23.5
1719	A	Banagher (Canal Hse.)	200400	216000	IRE	IE	1943	2012	0.2	37	58.8	17.4
1723	A	Dublin (Phoenix Park)	310000	236100	IRE	IE	1941	2011	0.0	49	7.7	10.0
1729	A	Drumshanbo	196000	312500	IRE	IE	1941	2012	2.1	54	33.9	12.8
1819	A	Portumna O.P.W.	187200	204600	IRE	IE	1941	2012	0.3	35	47.6	17.4
1829	A	Dromod (Ruskey)	205300	286200	IRE	IE	1941	2012	2.7	42	58.1	11.0
1909	GAP	Dingle (Baile Na Ngall)	38600	108400	IRE	CU	1985	2012	3.3	36	0.3	30.7

1923	A	Glenasmole D.C.W.W.	309000	222200	IRE	CU	1941	2012	0.7	158	13.9	13.9
1926	GAP	Killadoon	75370	271270	IRE	CU	1985	2012	0.0	46	1.3	21.4
1936	A	Dromahair (Market St.)	180600	331500	IRE	CU	1961	2012	2.1	27	12.3	24.5
2010	GAP	Listowel (Inch)	95600	136400	IRE	CU	1956	2011	8.4	15	3.5	18.3
2037	A	Cuilcagh Mtns.	213000	324100	IRE	CU	1945	2012	1.3	290	45.2	7.2
2038	A	Carrickmacross (Dunoge)	281736	303601	IRE	IE	1959	2012	0.0	88	23.7	17.6
2115	A	Hacketstown (Voc.Sch.)	297500	179900	IRE	IE	1950	2012	0.0	189	28.7	24.3
2121	GAP	Gort (Derrybrien li)	159700	201900	IRE	CU	1983	2012	0.6	155	23.1	24.3
2227	A	Carndolla	133500	239500	IRE	CU	1942	2012	4.4	24	13.7	14.6
2237	A	Ballyshannon (Cathleen'S Fall)	188660	361120	IRE	CU	1946	2012	0.0	38	1.3	19.0
2335	A	Eskeragh	104300	319000	IRE	CU	1945	2012	0.0	85	18.2	9.9
2604	A	Ballyvourney (Clountycarty)	121000	71500	IRE	SW	1949	2012	0.0	152	26.8	10.5
2635	A	Derryhillagh	108800	310200	IRE	CU	1945	2012	0.5	104	18.0	9.9
2638	A	Ardee (Boharnamoe)	294194	290338	IRE	IE	1969	2012	0.4	31	14.3	18.2
2727	GAP	Claremorris	134500	273900	IRE	CU	1944	2007	0.4	69	37.7	25.4
2731	A	Ballivor (Hill Of Down)	264400	254100	IRE	IE	1952	2012	4.0	81	54.8	21.9
2802	A	Kinsale (Voc.Sch.)	163300	50800	IRE	CU	1953	2012	4.6	43	0.8	15.7
2804	A	Donoughmore	149200	82100	IRE	CU	1949	2012	0.8	200	19.0	10.9
2922	GAP	Mullingar li	242000	254300	IRE	IE	1973	2007	0.0	101	76.5	17.7
2931	A	Warrenstown	292155	253585	IRE	IE	1952	2012	0.0	90	27.5	16.6
3035	A	Castlebar (Burren)	114000	297000	IRE	CU	1953	2012	3.7	137	15.5	12.1
3037	A	Swanlinbar	219400	327500	IRE	CU	1943	2011	3.7	69	46.6	7.2
3127	A	Glenamaddy (Gortnagier)	162900	261600	IRE	IE	1945	2012	0.5	84	44.4	24.4
3135	A	Cloonacool (Lough Easkey)	144600	320700	IRE	CU	1953	2012	0.4	204	13.5	19.2
3205	A	Killarney (Muckcross Hse.)	97200	86200	IRE	SW	1969	2012	0.0	58	14.7	13.6
3335	A	Straide	126100	297900	IRE	CU	1964	2012	0.2	21	20.9	12.1
3402	A	Sherkin Island	100800	25800	IRE	CU	1973	2012	0.4	18	0.1	29.9

3431	A	Derrygreenagh	249300	238200	IRE	IE	1956	2012	0.3	90	68.4	17.7
3513	A	Slieve Bloom Mtns.(Nealstown)	219900	193600	IRE	IE	1954	2012	0.0	219	70.0	24.4
3604	A	Carrigadrohid (Gen.Stn.)	140500	72000	IRE	CU	1954	2012	0.1	67	19.9	13.3
3612	A	Ballymacarbery G.S.	219300	112800	IRE	CU	1944	2012	3.2	59	16.7	12.6
3613	GAP	Kilkenny	249400	157400	IRE	IE	1958	2007	0.0	65	23.7	11.3
3637	A	Newbliss (Drumshannon)	257465	324225	IRE	IE	1972	2012	2.2	137	50.1	16.9
3704	A	Inishcarra (Gen.Stn.)	154500	72200	IRE	CU	1954	2012	0.3	24	10.5	11.2
3735	A	Ballina (Shanaghy)	125600	318300	IRE	CU	1970	2012	1.7	24	1.0	18.7
3904	A	Cork_Airport	166500	66200	IRE	CU	1962	2012	0.0	155	5.0	13.4
3927	A	Galway (Univ.Coll.)	129000	225600	IRE	CU	1966	2011	0.0	14	0.9	14.6
3937	A	Aughnasheelan (Miskawn)	208500	315100	IRE	CU	1972	2012	1.0	155	44.1	10.1
4006	A	Knockanore	207500	89100	IRE	CU	1965	2012	0.0	122	1.5	5.3
4037	GAP	Lough Gowna (Glenbrook)	231200	292100	IRE	IE	1974	2008	0.0	91	74.5	26.6
4106	A	Youghal (Glendine W.W.)	206400	83900	IRE	CU	1965	2012	0.5	107	1.7	5.3
4112	A	Drangan (Moanvurrin)	228500	142200	IRE	IE	1963	2011	0.3	122	25.2	18.2
4129	A	Lecarrow	196900	254900	IRE	IE	1953	2012	0.1	47	65.8	20.4
4131	GAP	Bailieboro (Leiter)	264900	298500	IRE	IE	1974	2012	0.0	155	41.2	17.6
4213	GAP	Parknahown Cullahill	234300	173900	IRE	IE	1982	2012	2.4	110	46.0	22.4
4227	GAP	Cornamona	104800	253000	IRE	CU	1969	2009	0.6	30	14.7	13.6
4514	A	John F. Kennedy Park	272282	118921	IRE	CU	1966	2012	0.0	70	2.9	11.9
4531	GAP	Navan (Tara Mines)	284700	268400	IRE	IE	1987	2012	0.3	52	31.7	16.6
4615	GAP	Boolavogue Knockavocca	305073	146206	IRE	CU	1988	2012	1.7	73	14.8	31.8
4629	A	Athlone (Glynnwood)	210300	239500	IRE	IE	1963	2012	0.2	64	71.8	20.4
4729	A	Coolavin	166600	298500	IRE	IE	1964	2011	0.0	61	30.7	12.9
4811	GAP	Patrickswell (Dooneen)	154500	149600	IRE	CU	1982	2012	0.0	27	6.3	19.7
4819	A	Silvermines Mtns.(Curreeny)	190100	164700	IRE	CU	1954	2012	0.4	312	31.9	15.6
4911	GAP	Castlemahon W.W.	131500	131200	IRE	CU	1983	2011	2.8	58	19.0	28.7

4914	GAP	Emo Court	254100	206300	IRE	IE	1975	2000	4.4	91	68.4	27.6
5012	A	Bansha (Aherlow W.W.)	191700	128400	IRE	CU	1956	2012	0.6	128	34.5	31.6
5214	GAP	Coolgreany Castlewarren	259600	162300	IRE	IE	1983	2012	1.1	262	24.1	11.3
5229	A	Boyle (Marian Rd.)	180000	302300	IRE	IE	1972	2012	0.4	62	30.4	13.9
5306	GAP	Mount Russell	161300	119800	IRE	CU	1985	2012	0.3	195	30.4	16.3
5323	A	Naas (C.B.S.)	289600	219500	IRE	IE	1956	2012	2.2	98	32.1	19.6
5414	GAP	Castledermot Kilkea House	274500	187700	IRE	IE	1984	2012	0.9	85	48.3	24.3
5512	A	Clonmel (Redmondstown)	223400	124700	IRE	CU	1963	2012	2.8	64	19.7	12.6
5819	A	Nenagh (Connolly Park)	187200	180000	IRE	IE	1972	2012	2.6	55	35.0	15.6
9005	A	M.Ballaghbeama Gap	75500	78300	IRE	SW	1950	2012	2.9	311	10.8	14.0
9203	A	M.Cummeragh No.2	63400	71200	IRE	SW	1943	2012	1.1	404	7.1	14.0
9704	A	M.Ballingeary (Tooreenaneen)	113100	64500	IRE	SW	1949	2012	0.3	323	16.4	10.6
9804	A	M.Ballyvourney (Knockacommeen)	116000	80700	IRE	SW	1949	2012	0.9	415	23.5	10.5
9827	GAP	M.Maam (Mt.Rinavore)	92100	258000	IRE	CU	1983	2012	0.3	389	5.8	13.6
16208	GAP	Cappagh Resr	268458.2	367520.6	UK	IE	1961	2010	3.3	173	54.9	20.6
16277	A	Toomebridge	298933.4	390600.6	UK	IE	1961	2013	2.4	15	37.8	18.2
16284	GAP	Upperlands	287670.2	404875.1	UK	IE	1961	2000	1.2	68	28.9	18.2
16295	A	Coleraine (Cutts)	285383	430288.7	UK	CU	1961	2013	1.2	3	3.5	23.3
16346	A	Ballycarry	344952.5	394937.5	UK	CU	1961	2014	0.9	61	1.4	20.7
16374	A	Belfast P Sta.	334992.6	376836.2	UK	IE	1961	2014	3.4	4	2.7	20.7
16478	A	Annalong Valley	335604.1	322521	UK	CU	1924	2013	1.1	130	2.5	29.3
16507	A	Crom Castle	235630.2	323977.6	UK	IE	1929	2014	1.4	58	61.1	16.6
16534	GAP	Portora Sluice	222136	345383.3	UK	IE	1963	2013	6.6	46	38.3	18.1

*This page is intentionally left blank*